

# **Process-Based Characterization and Typology of Runoff Events in Germany**

**Dissertation**

**zur Erlangung des  
Doktorgrades der Naturwissenschaften (Dr. rer. nat)**

**Der  
Naturwissenschaftlichen Fakultät III  
Agrar- und Ernährungswissenschaften, Geowissenschaften und Informatik  
der Martin-Luther-Universität  
Halle-Wittenberg**

vorgelegt  
von Frau Larisa Tarasova  
geb. am 29.06.1990 in Kalinin



**1. Gutachter:**

Prof. Dr. Ralf Merz

**2. Gutachter:**

Prof. Dr. Jan Seibert

**Tag der Verteidigung:**

15.12.2020



## Acknowledgments

This cumulative thesis was developed at the Department Catchment Hydrology, Helmholtz Centre for Environmental Research (UFZ), Halle (Saale) within the Research Group FOR 2416 "SPAcE-Time Dynamics of Extreme Floods (SPATE)" funded by the German Research Foundation (DFG). Their financial support is gratefully acknowledged.

First and foremost I would like to thank Prof. Dr. Ralf Merz for his scientific guidance, thoughtful advises and constant encouragement that were and remain invaluable and inspirational for my work. I am greatly indebted to him for being my supervisor and mentor over the past five years and teaching me a great deal, for always having answers to my endless questions, for keeping me on track with important tasks, but also for providing me with the freedom to pursue and work on my own ideas and for always listening and considering my opinion in discussions. My thanks also goes to Dr. Stefano Basso for his constant support, help and encouragement, but more importantly for being a critical voice in our discussions and, of course, for countless hours he spent improving my writing.

I am also most grateful to my collaborators Dr. Alberto Viglione, Dr. Dadiyorto Wendi, Dr. Rohini Kumar, Dr. Matthias Zink and Dr. Carine Poncelet for their valuable contributions that helped me to develop this thesis. I thank student assistants Réne Zahl and Andrea Domin for their assistance in data preparation. I would also like to thank Lina Stein for all the discussion we had and the ideas we shared, I have enjoyed greatly doing my PhD along with her.

My thanks goes to all members of the SPATE Research Group for always stimulating interesting scientific discussions that further fostered my research ideas. I am also most grateful to my colleagues and friends at the UFZ and especially at the Department of Catchment Hydrology for providing nurturing research environment and for their personal support.

A very special thanks goes to my partner Martin, my family and my friends for taking care of me and believing in me, for their support and encouragement and most importantly for always being by my side in good and bad times.



*Моей семье*





---

## Summary

Runoff events are fundamental hydrological elements that define quantity and quality of water delivered to the streams and play an imperative role in shaping riverine environments. Singular large runoff events (i.e., flood events) have tremendous socio-economical consequences. In a changing world accurate predictions of runoff events are crucial for management of future water resources and flood hazard. Understanding of processes that control runoff event generation and dynamics can strengthen the robustness of such predictions. The objective of this thesis is to provide a deeper understanding on large scale controls of spatial patterns and temporal dynamics of runoff event characteristics and to develop a framework for event characterization and classification that is able to distinguish events governed by different runoff generation processes.

In the first part of this thesis an automated event separation procedure was devised that includes existing time-series-based base flow separation, runoff event identification, rainfall attribution and a novel iterative procedure for refinement of single-peak components of multiple-peak events. This procedure allowed consistent event isolation from continuous hydro-meteorological time series in a wide range of German catchments across different landscape and climatic regions. The analysis of event-to-event variability of runoff event characteristics based on more than 220,000 events revealed regions with dominance of different runoff generation mechanisms. The seasonality of event characteristics highlighted the importance of snowmelt contribution and the seasonal variations of water balance components. Non-stationarity of event characteristics (i.e., their long-term trends) emphasized the role of modifications of the intra-annual seasonality wetness conditions rather than of the total precipitation amount.

In the second part of this thesis the analysis of spatial distribution of runoff event characteristics revealed relatively clear regional patterns due to the dominance of climatic controls at regional scale. Subsurface properties (i.e., catchment storage) played also a considerable role for the prediction of event runoff response. Best performing variable selection method based on the Self-Organizing Maps identified soil depth, hydraulic permeability and frequency, size and seasonality of wet spells as relevant catchment descriptors for prediction of spatial patterns and regionalized values of runoff event characteristics. Linking temporal dynamics of runoff event characteristics and their spatial controls with hypothesized runoff generation mechanisms and the concept of threshold processes in catchments provided the basis for deriving archetypes of distinct catchment behaviors in Germany. The identified controls of event runoff response and hydrologically-homogeneous regions might provide useful information for selecting relevant physical catchment descriptors for various hydrological applications.

Finally, in the third part of this thesis a new process-based framework for characterizing runoff events and deriving event typologies was developed in this study. The indicators of the proposed framework categorize runoff events based on space-time dynamics of observed precipitation and simulated snowmelt and soil moisture and their mutual interactions within catchments. A rigorous uncertainty analysis showed that the indicators of the framework are robust and regionally consistent. Dimensionless covariance- and ratio-based indicators used in the framework reduces classification uncertainty compared to commonly used indicators relying on absolute values of metrics such as rainfall volume, duration or intensity and allow consistent classification of runoff events of various magnitudes and recurrences. The validation procedure based on cross recurrence plots showed that the event typology derived in this thesis is able to stratify events with distinct hydrograph dynamics in most of study catchments, even though streamflow was not directly used for classification. This indicates that the derived event typology effectively captures first-order controls of event runoff response in a wide variety of catchments.

Consistent national data sets of isolated and classified runoff events and their event characteristics produced in this study are a valuable source of information for advancing data-driven approaches in the context of comparative hydrology in Germany. Moreover, the developed event characterization framework can be further applied for understanding regional differences of runoff and flood events and detect temporal changes of the dominant processes. Similarly, it could be applied for disentangling the variability of solutes and particulates exports from catchments during different runoff event conditions, thus providing additional insights on variability of water quality metrics

observed in streams.

This thesis consists of three peer-reviewed papers published in the ISI-listed journals.

**Keywords** Rainfall-runoff events, events separation, event characteristics, runoff coefficient, temporal dynamics, catchment descriptors, regional patterns, event classification, event typology, runoff generation mechanisms

---

## Zusammenfassung

Abflussereignisse sind wesentliche hydrologische Elemente, die Menge und Qualität des Abflusses bestimmen und eine wichtige Rolle für die Entwicklung der aquatischen Ökosysteme spielen. Einzelne singuläre Ereignisse, wie z.B. große Hochwasserereignisse können enorme wirtschaftliche und gesellschaftliche Folgen haben. Zuverlässigere Vorhersagen von Abflussereignissen in einer sich schnell verändernden Welt sind daher entscheidend für das nachhaltige Management zukünftiger Wasserressourcen und des Hochwasserrisikos. Das Ziel dieser Dissertation ist die Entwicklung einer Methode zur großräumigen Analyse und Charakterisierung von Niederschlags-Abflussereignissen als Grundlage für ein verbessertes Verständnis für die regionale Variabilität und Dynamik der Abflussbildung und ihrer kontrollierenden Prozesse.

Der erste Teil dieser Dissertation beinhaltet die Entwicklung eines Verfahrens zur automatischen Separation von Niederschlags-Abflussereignissen aus kontinuierlichen hydro-meteorologischen Zeitreihen. Das Verfahren besteht aus einer Basisabflussabtrennung, der Bestimmung von Anfangs- und Endpunkten von Abflussereignissen, der Ermittlung der zugehörigen Ereignisniederschläge und einem neuen iterativen Ansatz zur Verbesserung der Separation bei Ereignissen mit mehreren Abflussscheiteln. Im Fokus der Entwicklung des Verfahrens stand die automatische Anwendung und Übertragbarkeit auf viele Einzugsgebiete mit unterschiedlichen Landschafts- und Klimabedingungen. Das Verfahren wurde an 185 deutschen Einzugsgebieten entwickelt und getestet.

Für die über 220 000, mit Hilfe der Methode, separierten Einzelereignisse wurden Ereignisindikatoren für die Niederschlags-Abflussdynamik berechnet. Die Analyse der Variabilität dieser Indikatoren zeigt deutlich die unterschiedliche Bedeutung verschiedener Abflussbildungsmechanismen in einzelnen Regionen Deutschlands. Die Bedeutung von Schneeschmelze und der jahreszeitlichen Schwankungen der Wasserbilanzkomponenten spiegelt sich in der saisonalen Schwankung von den Ereignisindikatoren wieder. Langjährige Trends in den Ereignisindikatoren werden mehr durch veränderte saisonale Dynamik der Bodenfeuchte hervorgerufen als durch Trends im Jahresniederschlag.

Im zweiten Teil der Dissertation werden die räumlichen Muster der Ereignisindikatoren untersucht und in Zusammenhang mit Klima- und Landschaftscharakteristiken in Deutschland gesetzt. Die Ereignisindikatoren zeigen deutliche regionale Muster, die den dominanten Einfluss des Klimas auf die regionalen Unterschiede im Abflussgeschehen erkennen lassen. Die regionale Variabilität der Abflussbildung ist auch stark durch die Hydrogeologie geprägt. Mit Hilfe von Self-Organising Maps konnten Bodentiefe, hydraulische Durchlässigkeit, durchschnittliche Häufigkeit, Größe und Saisonalität von Niederschlagsphasen als die maßgeblichen Einzugsgebietscharakteristiken für die Vorhersagbarkeit der Ereignisindikatoren identifiziert werden. Es konnten so Archetypen von Einzugsgebieten in Deutschland herausgearbeitet werden, die regional unterschiedliche Zusammenhänge von Klima- und Landschaftsbedingungen auf die Abflussbildung aufzeigen.

Im dritten Teil dieser Dissertation wurde ein neues prozess-basiertes Klassifikationssystem für Niederschlags-Abflussereignisse entwickelt, das gegenüber existierenden Ereignisklassifikationen in der hydrologischen Literatur folgende Innovationen aufzeigt: a) Mit Hilfe des Verfahrens wurden alle Niederschlags-Abflussereignisse und nicht nur Extreme, wie z.B. Hochwasserereignisse, klassifiziert; b) Das Verfahren berücksichtigt die raum-zeitliche Dynamik und die Interaktion von Niederschlag, Bodenfeuchte und Schneebedeckung innerhalb von Einzugsgebieten und kann somit das Zusammenwirken dieser hydrologischen Größen bei der Abflusentstehung besser beschreiben; c) Die Klassifikation beruht auf dimensionslosen Indikatoren, wie z.B. Verhältnisse und Kovarianzen und kann somit besser auf andere Untersuchungsgebiete und Ereignisse unterschiedlichster Größe übertragen werden; d) Das Verfahren basiert auf einem hierarchischen Ansatz, so dass flexibel unterschiedliche Dynamiken von Niederschlag, Schneebedeckung und Bodenfeuchte erfasst werden können. In einer umfassenden Unsicherheitsanalyse erwiesen sich die gewählten Ansätze als robust und regional konsistent. Die Validierung mit Hilfe der Recurrence Plots Analyse zeigte, dass die entwickelte Klassifikation in der Lage ist, zwischen Ereignissen unterschiedlicher Abflussdynamik zu unterscheiden, obwohl die Abflussdaten für die Klassifizierung nicht direkt benutzt wurden. Dies bestätigt, dass das Klassifikationsverfahren die wesentlichen Ähnlichkeiten und Unterschiede in der Abflusentstehung zwischen Gebieten gut erfassen kann.

Auf Basis des entwickelten Ansatzes konnten zum ersten Mal deutschlandweit alle Niederschlag-Abflussereignisse konsistent in hydrologische Prozesstypen eingeteilt werden. Mit Hilfe dieser Prozesstypen lassen sich nun regionale Dynamiken in der Abflussbildung besser erklären und die dominanten Treiber der zeitlichen Änderungen erfassen. Dies erlaubt neue daten-basierte regionale Prozessanalysen im Sinne der „Comparative Hydrology“ und öffnet neue Wege hin zu z.B. einer zuverlässigeren Vorhersage der Größe und Frequenz zukünftiger Hochwasserereignisse oder des Einflusses sich verändernder hydrologischer Prozesses auf den Stofftransport und -eintrag von Einzugsgebieten.

Diese Dissertation besteht aus drei peer-reviewed Artikeln, die bereits in ISI-gelisteten Journals veröffentlicht wurden.

**Keywords** Niederschlag-Abfluss Ereignisse, Ereignisabtrennung, Abflussbeiwert, Abflussbildung, Ereignistypen, Ereignis-Klassifizierung

---

# Contents

<b>Summary</b>	<b>i</b>
<b>Zusammenfassung</b>	<b>iii</b>
<b>List of Acronyms</b>	<b>vii</b>
<b>List of Figures</b>	<b>ix</b>
<b>List of Tables</b>	<b>xv</b>
<b>1 Introduction</b>	<b>1</b>
<b>2 Exploring Controls on Rainfall-Runoff Events: Time Series-Based Event Separation and Temporal Dynamics of Event Runoff Response in Germany</b>	<b>5</b>
2.1 Introduction . . . . .	6
2.2 Data . . . . .	7
2.3 Methods . . . . .	9
2.3.1 Time-series-based identification of runoff events . . . . .	9
2.3.1.1 Base flow separation . . . . .	10
2.3.1.2 Runoff event identification . . . . .	10
2.3.1.3 Attribution of rainfall/ snowmelt events . . . . .	10
2.3.1.4 Refinement of multiple-peak events . . . . .	11
2.3.2 Temporal dynamics of event runoff response . . . . .	11
2.3.2.1 Event characteristics and possible drivers . . . . .	12
2.3.2.2 Event-to-event variability of event characteristics . . . . .	14
2.3.2.3 Seasonal variability of event characteristics . . . . .	14
2.3.2.4 Long-term variability of event characteristics . . . . .	14
2.4 Results . . . . .	14
2.4.1 Time-series-based event separation . . . . .	14
2.4.1.1 Performance of tested base flow separation methods . . . . .	14
2.4.1.2 Attribution of rainfall to runoff events and refinement of multiple-peak events . . . . .	16
2.4.2 Temporal dynamics of event runoff response . . . . .	16
2.4.2.1 Event-to-event variability of rainfall-runoff event characteristics . . . . .	16
2.4.2.2 Seasonality of event characteristics . . . . .	18
2.4.2.3 Long-term trends of event characteristics . . . . .	19
2.5 Discussion and Conclusions . . . . .	21
2.6 Supporting Information . . . . .	26
2.6.1 Test of the distribution equality . . . . .	26
2.6.2 Long-term trends of the event characteristics . . . . .	26
<b>3 Exploring Controls on Rainfall-Runoff Events: Regional Patterns and Spatial Controls of Event Characteristics in Germany</b>	<b>29</b>
3.1 Introduction . . . . .	30
3.2 Data and study area . . . . .	32
3.3 Methods . . . . .	34
3.3.1 Event characteristics as hydrological signatures . . . . .	34
3.3.2 Event separation . . . . .	35
3.3.3 Identifying regions of homogeneous event runoff response . . . . .	36
3.3.4 Linking event characteristics and catchment descriptors . . . . .	36
3.3.4.1 Correlation analysis . . . . .	36
3.3.4.2 Variable selection methods . . . . .	37
3.3.4.3 Performance of variable selection methods . . . . .	39

3.4	Results . . . . .	39
3.4.1	Event characteristics and their spatial patterns . . . . .	39
3.4.2	Regions with homogeneous event runoff response . . . . .	41
3.4.3	Linking event characteristics and catchment descriptors . . . . .	42
3.4.3.1	Correlation analysis . . . . .	42
3.4.3.2	Performance of variable selection methods and generic groups of CDs . . . . .	42
3.4.3.3	Dominant controls of event characteristics within homogenous regions . . . . .	44
3.5	Discussion and Conclusions . . . . .	45
3.5.1	Regions of homogeneous event runoff response . . . . .	45
3.5.2	Linking event characteristics and catchment descriptors . . . . .	46
3.5.3	Hydrological interpretation of the emerged regional pattern of event characteristics and their spatial controls . . . . .	46
3.5.4	Concluding remarks: event characteristics as hydrological signatures . . . . .	51
3.6	Supporting Information . . . . .	52
3.6.1	Adjusted Rand Index . . . . .	61
<b>4</b>	<b>A Process-Based Framework to Characterize and Classify Runoff Events: The Event Typology of Germany</b>	<b>62</b>
4.1	Introduction . . . . .	63
4.2	Data and study area . . . . .	64
4.3	Methods . . . . .	66
4.3.1	A process-based framework for characterization of runoff events . . . . .	66
4.3.2	Hierarchical event classification: the event typology of Germany . . . . .	70
4.3.3	Uncertainty analysis and robustness check of the proposed framework . . . . .	71
4.3.4	Validation of the derived event typology: similarity of hydrograph dynamics of event types . . . . .	72
4.3.5	Exemplary application of derived event typology in Germany . . . . .	74
4.4	Results and Discussion . . . . .	74
4.4.1	Uncertainty analysis and robustness check of the proposed framework . . . . .	74
4.4.2	Validation of the derived event typology: similarity of hydrograph dynamics of event types . . . . .	76
4.5	Exemplary application of event typology in Germany . . . . .	77
4.5.1	Spatial patterns of event types . . . . .	78
4.5.2	Seasonality of dominant event types . . . . .	79
4.5.3	Runoff characteristics of event types . . . . .	81
4.6	Conclusions and Outlook . . . . .	83
4.7	Supporting Information . . . . .	84
4.7.1	Rainfall-runoff event attribution in nested river networks . . . . .	84
4.7.2	Definition of the threshold for catchment wetness state . . . . .	84
4.7.3	Cross Recurrence Plots and Recurrence Quantification Analysis . . . . .	85
<b>5</b>	<b>Conclusions and Perspectives</b>	<b>87</b>
5.1	Conclusions . . . . .	87
5.2	Outlook . . . . .	88
	<b>References</b>	<b>92</b>
	<b>Eidesstattliche Erklärung</b>	<b>105</b>
	<b>Curriculum Vitae</b>	<b>107</b>

---

## Acronyms

- AIC** Akaike Information Criterion. 39
- ARI** Adjusted Rand Index. 39, 61
- BE** Backward Elimination. 38, 42, 43, 44, 46, 52, 53, 54, 55, 56, 57, 58, 59, 60, 61
- BfG** Federal Institute for Hydrology. 5, 62
- BGR** Federal Institute for Geosciences and Natural Resources. 33, 35, 55, 57, 58, 59, 61
- CD** catchment descriptor. 34, 36, 39, 42, 43, 44, 45, 46, 47
- CORINE** Coordination of Information on the Environment. 8, 29, 54, 55
- CRP** Cross Recurrence Plot. 72, 73, 85, 86, 88
- DET** determinism. 73, 76, 77, 86
- DWD** German Weather Service. 5, 29, 34, 35, 52, 53, 62, 65
- EEA** European Environmental Agency. 35, 54, 55
- EWA** European Water Archive. 29, 62
- GR6J** modèle du Génie Rural à 6 paramètres Journalier. 33
- GRDC** Global Runoff Data Centre. 5, 29, 62
- HBV** Hydrologiska Byråns Vattenbalansavdelning. 66
- HLUG** Hessian Agency for the Environment and Geology. 29, 62
- HWSD** Harmonized World Soil Dataset. 29, 35, 55, 56, 57
- IG** Information Gain. 37, 38, 42, 43, 44, 52, 53, 54, 55, 56, 57, 58, 59, 60, 61
- KGE** Kling-Gupta Efficiency. 33
- LANUV NRW** Office for Nature, Environment and Consumer Protection North Rhine-Westphalia. 29, 62
- LfU** Bavarian State Office of Environment. 5, 29, 62
- LHW** Saxony-Anhalt Office of Flood Protection and Water Management. 29, 62
- LUBW** Baden-Württemberg Office of Environment, Measurements and Environmental Protection. 29, 62
- LUGV** Brandenburg Office of Environment, Health and Consumer Protection. 29, 62
- LUWG** Rhineland Palatinate Office of Environment, Water Management and the Factory Inspectorate. 29, 62
- mHM** mesoscale Hydrological Model. 8, 13, 29, 34, 52, 62, 65, 66, 71
- MUV** Saarland Ministry for Environment and Consumer Protection. 29, 62

- NLWKN** Lower Saxony Office for Water Management, Coast Protection and Nature Protection. 29, 62
- nRMSE** normalized Root Mean Squared Error. 39
- PC** Principal Component. 38
- PCA** Principal Component Analysis. 38, 42, 43, 44, 52, 53, 54, 55, 56, 57, 58, 59, 60, 61
- REGNIE** Regionalisierte Niederschlagshöhen. 8, 13, 34, 52, 53, 65
- RQA** Recurrence Quantification Analysis. 73, 86
- SALTO** "The SAme Like The Others". 66, 71
- SMUL** Saxony State Office of Environment, Agriculture and Geology. 29, 62
- SOM** Self-Organizing Maps. 36, 39, 87
- SPATE** Space-Time Dynamics of Extreme Floods. 5, 29, 62
- SRTM** Shuttle Radar Topography Mission. 5, 29, 35, 53, 54
- TLUG** Thüringen State Office of Environment and Geology. 29, 62
- UFZ** Helmholtz Centre for Environmental Research. 5, 29, 62
- WSV** Water and Shipping Management of the Fed. Rep. 29, 62



---

## List of Figures

2.1	The study area is the whole of Germany, which is divided into four main landscape units (the North German Plain, Central Uplands, South German Scarplands and Alpine Foreland regions). The names of smaller natural regions of Germany are also indicated. 185 catchments where daily flows are not affected by anthropogenic modifications were selected based on data availability . . . . .	8
2.2	Summary of the event separation procedure. The River Kyll at Junkerath is used as an example to illustrate it: a) base flow separation and identification of runoff events (Chapters 2.3.1.1 and 2.3.1.2); b) attribution of rainfall events (Chapter 2.3.1.3) using median seasonal lag time ( <i>med.lag</i> ); c) refinement of multi-peak events (Chapter 2.3.1.4) using iterative adjustment of separation thresholds, which are portrayed in the inset of panel c and described in Table 2.1; d) updating the samples of single and multiple-peak events . . .	9
2.3	Base flow separation: a-c) results of the different base flow separation methods tested for three selected catchments. Zoom circles display base flow behavior at the beginning of potential runoff events (i.e., troughs); d) fraction of troughs identified by different base flow separation methods for all catchments in the data set; e) time delay (lag) determined by the argument of the maximum of the cross correlation between total and base flow for all catchments in the data set. The length of time delay characterizes how fast does base flow reacts to changes of total runoff. $R^2$ shows the averaged value of the cross correlation coefficient averaged for all catchments and characterizes the strength of relation between total and base flow. Boxplots represents all catchments in the data set (fine horizontal line: median; box: interquartile range defined as the difference between 75 <sup>th</sup> and 25 <sup>th</sup> percentile; whiskers: 1.5 times interquartile range beyond the box; crosses: outliers)	15
2.4	Performance of multiple-peak refinement procedure: a) subdivision among single-peak, multiple-peak and unattributed events before and after applying the multiple-peak refinement procedure to catchments of different natural regions. Although, refinement procedure does not directly affect the absolute number of unattributed events, its relative portion might change if total number of identified events is increased after multiple-peak events are refined into their single-peak components; b) quartiles of the distribution of runoff coefficients for unrefined multiple-peak events (obtained after base flow separation and rainfall attribution) and refined single-peak and multiple-peak events (obtained after applying also the multiple-peak refinement procedure) plotted against quartiles of the distribution of runoff coefficients for the reference group of single-peak events. p25 corresponds to a lower quartile (25 <sup>th</sup> percentile), p50 corresponds to median and p75 corresponds to the upper quartile (75 <sup>th</sup> percentile) of a cumulative probability function of event runoff coefficients . . . . .	17
2.5	Relationship between runoff event characteristics (event runoff coefficient $rc$ , time scale $ts$ , rise time $rt$ and normalized <i>peak</i> ) and both the rainfall/ snowmelt event volume ( $Pvol$ ) and the indicators of pre-event catchment state (antecedent soil moisture $sm$ and pre-event base flow $qbase$ ). Results for the Lippe River at Haltern and the Ems River at Einen are displayed . . . . .	18
2.6	Squared Spearman correlation coefficient ( $R^2$ ) between event characteristics (runoff coefficient $rc$ , time scale $ts$ , rise time $rt$ , normalized <i>peak</i> ) and both the properties of rainfall/ snowmelt events (volume $Pvol$ , max intensity $Pint$ ) and the indicators of pre-event catchment state (10-day antecedent rainfall $Pant10$ , pre-event soil moisture $sm$ and base flow $qbase$ ). Higher values of $R^2$ indicate stronger linear correlation between the two considered variables. Thin grey lines represent the borders of the four main landscape regions of Germany (from north to south): North German Plain, Central Uplands, South German Scarplands and Alpine Foreland. Catchments' borders are not shown for clarity . . . . .	19
2.7	Soil moisture as a non-linear control of event runoff coefficient: a) the average of event runoff coefficients corresponding to different soil moisture conditions is represented for selected catchments as an exponential function of soil moisture fitted to them. The lines were color-coded according to the sub-surface storage index (Norbiato et al., 2009) defined as the ratio between Q90 and Q50; b) the exponent parameter $b$ of the fitted exponential function plotted against the ratio between Q90 and Q50. Lower values of $b$ characterize a more gradual increase of event runoff coefficients with increasing antecedent soil moisture. Higher values indicate instead a rapid increase of event runoff coefficients. Error bars show the residual standard error of the exponential model for every catchment. The regression line represents the best fit of an error-weighted regression model between scaling exponent and sub-surface storage index; c) spatial pattern of the subsurface storage index in Germany. Thin grey lines represent the borders of the four main landscape regions of Germany (from north to south): North German Plain, Central Uplands, South German Scarplands and Alpine Foreland. Catchments' borders are not shown for clarity . . . . .	20

- 2.8 Seasonality of event characteristics ( $rc$ ,  $ts$ ,  $rt$ ,  $peak$ ) rainfall and snowmelt properties ( $Pvol$ ,  $Pint$ ,  $melt$ ), pre-event indicators ( $sm$ ) and hydro-climatic variables ( $P$ ,  $AI$ ). The seasonality was computed as seasonal deviation (%) from the mean annual value of the considered variable. For non-additive variables (aridity index  $AI$ ) the deviation (%) of the mean seasonal value from the mean annual value is shown. For additive variables (total precipitation  $P$ ) the deviation (%) of the cumulative (3 month) seasonal value from the average among the cumulative values for the four seasons is shown. Thin grey lines represent the borders of the four main landscape regions of Germany (from north to south): North German Plain, Central Uplands, South German Scarplands and Alpine Foreland. Catchments' borders are not shown for clarity . . . . . 21
- 2.9 Long-term changes of the event runoff coefficient. Seasonal trends of  $rc$  in the period 1951-2013 were plotted against seasonal trends of rainfall properties (volume of rainfall events  $Pvol$ , maximum intensity of rainfall events  $Pmax$ ) and hydro-climatic variables (total precipitation amount  $P$ , aridity index  $AI$ , soil moisture  $sm$ , contribution of snow melt  $melt$ ). Trends were quantified by means of the relative Sen's slope that can be interpreted as the mean change per year in percent of the long-term mean value of the considered variable. Each marker represents a catchment belonging to a specific natural region differentiated by color. The marker's shape indicates the relative change of land use in the catchment from 1990-2012. Color-coded ellipses represent 95% confidence interval of seasonal trends for each natural region. The number of catchments in each quadrant was recorded in the corner of respective quadrant and color-coded according to a specific natural region. The number of catchments with significant trends of event runoff coefficient ( $\alpha = 0.1$ ) was noted in brackets for each quadrant and color-coded according to a specific natural region. . 22
- 2.10 Long-term changes of the event time scale. Seasonal trends of  $ts$  in the period 1951-2013 were plotted against seasonal trends of rainfall properties (volume of rainfall events  $Pvol$ , maximum intensity of rainfall events  $Pmax$ ) and hydro-climatic variables (total precipitation amount  $P$ , aridity index  $AI$ , soil moisture  $sm$ , contribution of snow melt  $melt$ ). Trends were quantified by means of the relative Sen's slope that can be interpreted as the mean change per year in percent of the long-term mean value of the considered variable. Each marker represents a catchment belonging to a specific natural region differentiated by color. The marker's shape indicates the relative change of land use in the catchment from 1990-2012. Color-coded ellipses represent 95% confidence interval of seasonal trends for each natural region. The number of catchments in each quadrant was recorded in the corner of respective quadrant and color-coded according to a specific natural region. The number of catchments with significant trends of event runoff coefficient ( $\alpha = 0.1$ ) was noted in brackets for each quadrant and color-coded according to a specific natural region. . 23
- 2.11 Long-term changes of the event rise time. Seasonal trends of  $rt$  in the period 1951-2013 were plotted against seasonal trends of rainfall properties (volume of rainfall events  $Pvol$ , maximum intensity of rainfall events  $Pmax$ ) and hydro-climatic variables (total precipitation amount  $P$ , aridity index  $AI$ , soil moisture  $sm$ , contribution of snow melt  $melt$ ). Trends were quantified by means of the relative Sen's slope that can be interpreted as the mean change per year in percent of the long-term mean value of the considered variable. Each marker represents a catchment belonging to a specific natural region differentiated by color. The marker's shape indicates the relative change of land use in the catchment from 1990-2012. Color-coded ellipses represent 95% confidence interval of seasonal trends for each natural region. The number of catchments in each quadrant was recorded in the corner of respective quadrant and color-coded according to a specific natural region. The number of catchments with significant trends of event runoff coefficient ( $\alpha = 0.1$ ) was noted in brackets for each quadrant and color-coded according to a specific natural region. . 27
- 2.12 Long-term changes of the normalized event peak discharge. Seasonal trends of  $peak$  in the period 1951-2013 were plotted against seasonal trends of rainfall properties (volume of rainfall events  $Pvol$ , maximum intensity of rainfall events  $Pmax$ ) and hydro-climatic variables (total precipitation amount  $P$ , aridity index  $AI$ , soil moisture  $sm$ , contribution of snow melt  $melt$ ). Trends were quantified by means of the relative Sen's slope that can be interpreted as the mean change per year in percent of the long-term mean value of the considered variable. Each marker represents a catchment belonging to a specific natural region differentiated by color. The marker's shape indicates the relative change of land use in the catchment from 1990-2012. Color-coded ellipses represent 95% confidence interval of seasonal trends for each natural region. The number of catchments in each quadrant was recorded in the corner of respective quadrant and color-coded according to a specific natural region. The number of catchments with significant trends of event runoff coefficient ( $\alpha = 0.1$ ) was noted in brackets for each quadrant and color-coded according to a specific natural region. . 28

3.1	<p>Example of two contrasting catchments with different climatic conditions (<math>P</math> – annual precipitation, <math>E</math> – annual potential evaporation, physical characteristics (storage capacity, vegetation) (upper panel) and hydrological response (lower panel). The extents of pre-event saturated areas (dark blue areas) represent typical runoff generation conditions in each catchment. The hydrological response of each catchment is presented for two different rainfall events (middle panel). Each event can be described by the event characteristics <math>rc</math> (event runoff coefficient [-]), <math>ts</math> (event time scale [days]), <math>rt</math> (event rise time [-]) (lower panel) . . . . .</p>	30
3.2	<p>The study area is the whole of Germany, which is divided into four main landscape units (the North German Plain, Central Uplands, South German Scarplands and Alpine Foreland region). The names of smaller natural regions of Germany are also indicated. 401 catchments where daily flows are not affected by anthropogenic modifications were selected based on data availability. Elevation (a), mean annual precipitation (b), aquifer type (c) and land use (d) are indicated by the color of the background . . . . .</p>	33
3.3	<p>Flowchart of the methodology used to identify hydrologically-relevant catchment descriptors based on their predictive power and their ability to reproduce observed spatial patterns of event characteristics. TS – time series; CD – catchment descriptor; MLR – multiple-regression models . . . . .</p>	38
3.4	<p>Spatial distribution of event characteristics: metrics describing a-c) event runoff coefficients (<math>rc</math>), d-f) event time scale (<math>ts</math>), g-i) event rise time (<math>rt</math>) and j-k) fraction of multiple-peak events (<math>multi</math>) are displayed, together with the; l) main natural regions of Germany. The top row (a, d, g, j) displays the average (<math>mean</math>) of the respective event characteristics, the middle row (b, e, h, k) shows the ratio between summer and winter median values (<math>sum2win</math>), whereas the bottom row (c, f, i) shows the coefficient of variation (<math>cv</math>) of the considered event characteristic. Solid black lines represent the borders of the main natural regions of Germany (Figure 3.2a) . . . . .</p>	40
3.5	<p>Linking event characteristics and catchment descriptors (CDs) through catchment classification: a) reference classification obtained by using Self-Organizing Maps based on event characteristics (SOM.event); b) alternative classification based on the CDs selected by the BE method (SOM.BE); c) alternative classification using all CDs (SOM.ALL). The hexagonal topology of the output layer with cluster numbering is depicted in the top left corner of the figure. The bottom panel represents the hexagonal topology of the output layer with node weight vectors derived from normalized values of the original variables. Solid black lines represent the borders of the main natural regions of Germany (Figure 3.2a) . . . . .</p>	41
3.6	<p>Heatmap of the correlations among event characteristics and catchment descriptors (CDs). The CDs are color-coded according to their generic group. Only the principal CDs identified through the PCA are shown (for details refer to Chapter 3.3.4.2). A detailed description of the CDs is available in Table 3.10 . . . . .</p>	43
3.7	<p>Summary of the variable selection performance: a) classification performance based on cluster similarity evaluated by means of the ARI between the reference and alternative classifications. The numbers on the bars indicates the number of CDs selected for catchment classification; b) prediction performance of stepwise regression models (normalized root mean square error (nRMSE) of “leave-one-out” cross-validation procedure) for each event characteristic; c) prediction performance of cluster-specific stepwise regression models (nRMSE) for each event characteristic . . . . .</p>	44
3.8	<p>Contribution (%) of individual catchment descriptor CDs (selected through the BE method based on cluster similarity) to the significant Principal Components (PCs) of each cluster. The CDs that contributed above the average expected contribution were referred as the principal CDs (Razavi and Coulibaly, 2013). Cluster numbering refers to topology of the SOM output layer (see Figure 3.5). Hatched bars indicate the most informative explanatory descriptors defined as the variables most frequently selected by regression models for prediction of event characteristics within the cluster (Ssegane et al., 2012a) . . . . .</p>	45

- 3.9 Archetypical behaviors of catchments from the identified clusters (Figure 3.5a). The cumulative distribution function of event runoff coefficients for a representative catchment (Figure 3.10) of respective cluster (upper panel of each cluster) informs about runoff coefficients for “dry” and “wet” states (and thus on the extent of the variably and permanently saturated regions) and about the character of change between the states (i.e., distinct switch or gradual increase). Typical shapes of hydrographs and their variability and seasonality (middle panel) are derived from cumulative distributions of event time scales and rise times. Typical relationships between runoff event coefficient ( $rc$ ) and both volume of precipitation event ( $Pvol$ ) and antecedent soil moisture ( $sm$ ) are schematically represented as well (middle panel). Typical catchment properties are presented using CDs selected by the best-performing variable selection method. The thickness of the blue arrows indicates the relative importance of the hypothesized fluxes. The texture of the topsoil is represented based on the proportion of silt and clay. The thickness of the subsoil is related to the descriptor of soil depth. The presence of duplex subsoil structure with one of the horizons enriched with clay is inferred from the abundance of Luvisol soil type (*soil.ClayEnrich*). The permeability of the upper aquifer is derived from the two classes of the descriptor of hydraulic conductivity (*moderate* and *from moderate to low*) and from the presence of sandstone, which can be interpreted as an indicator of low conductivity. The presence of limestone is perceived as an indicator of possible karstification. Land cover is presented in terms of abundance of coniferous and mixed forests. The volume of precipitation events (symbolized by the size of clouds) is approximated as the mean volume of wet spells, while the frequency of the events (number of clouds) is derived from the median duration of dry spells. The seasonality of precipitation (relative sizes of snowflakes and flashes of lightning) is derived from the ratio between the mean volumes of summer and winter precipitation. General climatic conditions (i.e., precipitation and evaporation, represented with white arrows) are inferred from mean annual precipitation and dryness index. . . . . 48
- 3.10 Examples of event separation and rainfall attribution for the hydrological year 1999-2000. The six catchments shown exemplify the behaviors of the six clusters of catchments identified in Germany (Figure 3.5a). The colors used for the catchments’ names match those of the clusters in Figure 3.5a. . . . . 52
- 4.1 Study catchments (thin black outline) and four test river basins: the Sieg, Naab, Neckar and Weser Rivers. Grey points indicate location of gauging stations. Red lines indicate the borders of four main German natural regions: the North German Plain, Central Uplands, South German Scarplands and Alpine Forelands. 65
- 4.2 a) A multi-layer framework for process-based characterization and categorization of runoff events. Indicators and categorization thresholds used for each layer of the framework are summarized in Table 4.1; b) A decision tree to perform hierarchical classification of runoff events. The amount of possible combinations (i.e., event types) was reduced by lumping together hydrologically similar (i.e., by hypothesizing possible runoff generation processes at catchment scale that correspond to each type of runoff events, see Table 4.2) and rarely occurring combinations. . . . . 68
- 4.3 Cross recurrence plot (CRP) illustration for quantifying similarity of runoff dynamics between (a) event hydrographs (Event A and B). Top panels illustrate how two identical hydrographs with different time of occurrence (blue line and shaded area in top panel (a)) are compared in their 3-dimensional phase space where the axis correspond to the original hydrograph values separated by the time delay  $\tau$  and  $2\tau$  (top panel (b)) and CRP (top panel (c)). The bottom panels illustrate the same comparison, but for two hydrographs with different runoff dynamics. Any identical or similar piece of the phase space trajectory which falls within the distance range/radius ( $\varepsilon$ ) (displayed in yellow in the top panel) is converted into a diagonal line in the CRP. These diagonal lines thus summarize the similarity of runoff dynamics between the compared hydrographs. Two perfectly identical runoff dynamics (top) have a *DET* of 1, while dissimilar dynamics yield low *DET* values (in our example *DET* = 0). Portion of CRP shaded in red indicate the information loss resulted from the time delay embedding method. . . . . 73

4.4	<p>Quantification of input uncertainty and robustness of the characterization framework for four test river basins (75 catchments in total): the Sieg, Naab, Neckar and Weser Rivers. Categorization discrepancy (i.e., portion of all events that is differently categorized) was calculated for each layer of the framework (i.e., inducing event, temporal organization, spatial organization, space-time organization, wetness state and spatial interaction; see rows of the Figure). The portion of discrepancy may vary from 0 to 1. High discrepancy indicates that categorization results are highly sensitive to the specific choice of the tested feature (i.e., input data, thresholds or indicators). Different features were examined (see columns of the Figure): different precipitation (<i>productP</i>) and, temperature (<i>productT</i>) products, original spatial resolution of products upscaled by a factor of 2 (<i>resolution</i>), set of 100 different soil moisture and snow water equivalent realizations simulated by 100 equifinal parameter sets of the mHM model (<i>parameters</i>), simulations of soil moisture and snow water equivalent from the alternative SALTO model instead of the original mHM run (<i>model</i>). We performed the robustness test for thresholds (<i>thresholds</i>) by means of a Monte Carlo experiment, where values of thresholds were randomly sampled from distributions assigned to the respective indicators (see Table 4.1). We averaged the categorization discrepancy over 10,000 Monte Carlo runs. The grey background highlights categorization discrepancy when alternative indicators listed in Table 4.1 (<i>alternative indicators</i>) were used instead of the original indicators. The robustness test for their thresholds (<i>alternative indicators thresholds</i>) shows average categorization discrepancy of 10,000 Monte Carlo runs.</p>	75
4.5	<p>Matrix of intra-type and inter-type value of determinism (<i>DET</i>, see Chapter 4.3.4, 4.7.3 and Wendi et al. (2019)), which measures the similarity of hydrograph dynamics of event pair (<math>DET = 0</math> corresponds to a low similarity in the dynamics): a) mean and b) coefficient of variation of the average values of <math>DET_{inter}</math> and <math>DET_{intra}</math> for all catchments. The diagonal shows <math>DET_{intra}</math> (black outline), horizontal and vertical bars show <math>DET_{inter}</math>. Events of a certain type exhibit more similar runoff dynamics compared to other event types if the value on the diagonal is higher than the values of the corresponding horizontal and vertical bars (these conditions are indicated by hatched squares). The matrix of coefficient of variations shows the variability of <math>DET_{intra}</math> (diagonal values, black outline) and <math>DET_{inter}</math> (values on horizontal and vertical bars) in the set of study catchments. The hierarchical classification tree corresponds to the decision tree in Figure 4.2b. . . . .</p>	77
4.6	<p>Regional pattern of event type frequency in Germany: a) spatial distribution of six homogeneous clusters in terms of frequency of event types; b) frequency of event types per cluster for all events. . . . .</p>	78
4.7	<p>Seasonality of event types in Germany: a) dominant type (i.e., most frequent type in the season) and b) variability of event type occurrence for each season defined as coefficient of unalikeability (see Chapter 4.3.5 and Kader and Perry (2007)). This metric defines the portion of all event pairs in the season that are unlike. When one event type dominates in a certain season the value of the coefficient of unalikeability is close to 0. When several event types are equally dominant for a certain season the value of the coefficient increases towards the maximum value of 1. . . . .</p>	80
4.8	<p>Hydrological response of event types in terms of their runoff event characteristics (i.e., event runoff coefficient, time scale, rise time, peak discharge and volume): a) all events; b) events with <math>Q_{peak} &gt; Q_{75}</math>; c) events with <math>Q_{peak} &lt; Q_{75}</math>. Runoff event characteristics are standardized by scaling all events to zero mean (by subtracting the mean of the sample from the original values) and unit variance (by dividing them by the standard deviation) for each catchment to make them comparable. Legend shows color coding of event types that is also valid for Figure 4.9. . . . .</p>	81
4.9	<p>Precipitation properties of event types that were not used for event characterization (i.e., maximum precipitation intensity, total volume of precipitation event, duration of precipitation event): a) all events; b) events with <math>Q_{peak} &gt; Q_{75}</math>; c) events with <math>Q_{peak} &lt; Q_{75}</math>. Maximum precipitation intensity, total volume of rainfall and duration of precipitation events are standardized by scaling all events to zero mean (by subtracting the mean of the sample from the original values) and unit variance (by dividing them by the standard deviation) for each catchment to make them comparable. The color-coding of this Figure corresponds to the color key in Figure 4.8. . . . .</p>	82

4.10	Attribution of rainfall-runoff events at upstream and downstream locations on the example of the River Kyll: a) at the upstream location using seasonal median lag time as a searching distance; b) at the downstream location using seasonal median lag time as a searching distance from the starting point of local runoff event (black color; compared to the upstream location the first precipitation pulse does not contribute to the considered runoff event) and from the corrected starting that corresponds to the runoff event starting date at the upstream location date (red color; similar to the upstream location the first precipitation pulse contributes to the considered runoff event). . . . .	84
4.11	Soil moisture as non-linear control of event runoff coefficient: a) Relationship between the observed event runoff coefficients and pre-event soil moisture simulated by the mHM model on example of the Lippe at Haltern and Ems at Einen and the fitted exponential function as described in Tarasova et al. (2018b). Circles correspond to single-peak events. Crosses correspond to multiple-peak events; b) the average of the observed event runoff coefficients corresponding to different simulated soil moisture conditions is presented for selected catchments as an exponential function of simulated soil moisture fitted to them as described in Tarasova et al. (2018b). The lines are color coded according to subsurface storage index defined as the ratio between Q90 and Q50 (ratio between daily discharges which is exceeded 90% of the time and the median flow). The Figure is modified from Tarasova et al. (2018b) with the permission from Wiley. . . . .	85
5.1	Frequency of occurrence of different states within the first layer (i.e., <i>Inducing event</i> ) of event characterization framework proposed in Chapter 4.3.1. The frequency of occurrence is calculated as the ratio between the number of events attributed to each category of <i>Inducing event</i> (see Figure 4.2a and Table 4.1) and the number of all events in the sample. Three different event samples are considered: all events identified by event separation procedure; maximum annual floods (MAF); and flood events with the estimated return period of at least 30 years (HQ30). All three event samples were obtained from the continuous hydrometeorological time series for the period 1951-2013 (see data reported in Tarasova et al., 2018b) and classified according to the framework proposed by Tarasova et al. (2020). A similar procedure can be performed for other layers of the proposed framework (e.g., <i>Temporal organization</i> , <i>Space-time organization of inducing event</i> or <i>Wetness state</i> ) . . . . .	89
5.2	Event-type-based diagnostic of the SALTO hydrological model (Merz et al., 2020) using two different performance measures (Kling-Gupta Efficiency (KGE) and volumetric bias) calculated event-wise for two mesoscale catchments (a) the River Sülz at Hoffnungsthal, 224 km <sup>2</sup> and b) the River Freiburger Mulde at Berthelsdorf, 246 km <sup>2</sup> ) for the period 1979-2002. $KGE_{tot}$ refers to a value of KGE calculated for the whole study period without event stratification. Event types are assigned to the events according to the hierarchical classification tree derived in Chapter 4, Figure 4.2b . . . . .	90

---

## List of Tables

2.1	Separation thresholds and their initial and critical values . . . . .	12
2.2	Summary of rainfall-runoff event characteristics and indicators of pre-event catchment state used in this study . . . . .	13
3.1	Metadata of catchment descriptors (CDs) . . . . .	35
3.2	Summary of the rainfall-runoff event characteristics, the metrics used to describe them in this study and the generic groups of catchment descriptors that are supposed to control them	37
3.3	Summary of catchment descriptors (CDs) . . . . .	52
4.1	Indicators for each characterization layer and alternative indicators used for robustness check of the proposed characterization framework . . . . .	69
4.2	Event types and corresponding hypothesized runoff generation processes at catchment scale	70





---

# 1 Introduction

Robust predictions of the future streamflow behavior are imperative in a changing world (Milly et al., 2008). The goodness of these predictions depends largely on in-depth understanding of the governing physical processes of runoff generation at the catchment scale. In the recent decades the efforts to deepen this understanding led to establishment of multiple terrestrial research observatories in the world (Tetzlaff et al., 2017) and to increasing of the density of state observational networks (Bonell et al., 2006). The accumulated long term data has immense value as it provides an opportunity on one hand to observe the full range of possible runoff generation mechanisms and on the other hand to detect any possible changes in their occurrence. However, conversion of the accumulated data into the knowledge about the processes that generated these data remains a challenge (Babovic, 2005). Development of novel techniques to “squeeze” valuable information from the existing data sets provides a remarkable opportunity to obtain insightful process implications (Soulsby et al., 2008).

Such data-based approaches might have a high exploratory potential beyond existing concepts in catchment hydrology. Compared to the model-based approaches that investigate runoff generation mechanisms (e.g., Vivoni et al., 2007; Frei et al., 2010; Sinha et al., 2016; Ala-aho et al., 2017), data-based techniques are not constrained to the investigation of the processes that are explicitly represented in the model structure and avoid model-specific uncertainties.

One way to extract additional information on runoff generation mechanisms from widely available data is to view recorded continuous time series of streamflow as the series of distinct events of quick flow interrupted by the periods of base flow. Isolating these events from the continuous time series provides an opportunity to extract valuable short-term dynamics of streamflow (i.e., event hydrograph) that is an instructive metric of catchment response to the inducing meteorological events (Blöschl et al., 2013b).

Manually identified rainfall-runoff events for a long time were and still are the main study object of the studies that aim to decipher hydrological processes that govern their generation in a singular catchment (e.g., McDonnell, 1990; McGlynn et al., 2004; Tromp-Van Meerveld and McDonnell, 2006; Rinderer et al., 2016; Knapp et al., 2020). Automation of rainfall-runoff event separation from continuous hydro-meteorological time series together with recent developments in regional seamless hydrological modeling (Samaniego et al., 2010; Kumar et al., 2013; Mizukami et al., 2017; Merz et al., 2020) that provide consistent regional datasets of modelled internal catchment states (e.g., soil moisture, snow water equivalent) (Zink et al., 2017) offer novel opportunities to the data-driven analysis of hydrological processes at larger scales. The analyses of temporal and spatial variability of runoff event characteristics proved to be a valuable tool for understanding runoff generation processes and their climatic and physiographic controls at regional and national scale (e.g., Seibert et al., 2016; Merz and Blöschl, 2009a). Such multi-catchment studies are an important step towards learning hydrological similarities and differences across places and advancing comparative hydrology (Sivapalan, 2009).

Analysis of discrete events also provides an opportunity to identify and characterize their immediate hydro-climatic and hydro-meteorological drivers. This might be particularly of interest for singular large streamflow events (i.e., flood events) due to their destructive socio-economic impact and their changing risks in the future (Slater and Wilby, 2017). The emergence of these singular flood events from ordinary runoff events is still debated in hydrology (Rogger et al., 2012; Smith et al., 2018; Miniussi et al., 2020). The analysis of large samples of runoff events that include runoff events of various sizes and major flood events might shed a light on the uniqueness of the latter.

By the definition flood events as well as their observations are rare and are limited mostly to peak discharges in the past. Therefore, flood frequency analysis was long dominated by application of univariate extreme value statistics. Extreme value theory assumes that all flood observations in a catchment are homogeneous (Gumbel, 1941). In fact this is rarely the case (Merz and Blöschl, 2008a,b). Flood events can be non-identically distributed due to their various hydro-climatic and hydro-meteorological origins (e.g., Hirschboeck, 1987; Merz and Blöschl, 2003a) and be nonstationary due to long-term climatic variability (Alila and Mtiraoui, 2002). Therefore, this is of advantage

to only consider events that exhibit similar traits when comparing river floods in different periods or catchments (Blöschl et al., 2013a).

A classification of runoff events (and specifically of flood events) that arranges events according to their generation processes and mechanisms can provide a tool to derive homogeneous groups of events that are necessary for robust flood frequency analysis in a changing world. In fact several causative classifications of river flood events that adopt hydro-climatic, hydrological or hydrograph perspectives were developed in the past (Tarasova et al., 2019) and used to improve at-site and regional flood frequency estimates (Alila and Mtiraoui, 2002; Merz and Blöschl, 2008a,b), identify and quantify changes in flood generation mechanisms (Hirschboeck et al., 2000; Nied et al., 2014) and assists in deciphering changes even if clear trends in climatic forcing or catchment conditions are not observed (Hirschboeck, 2009; Keller et al., 2018).

Despite usefulness of the existing causative classifications of flood events, lack of the uncertainty analysis and validation procedures limits their reliability (Tarasova et al., 2019). Locally derived and site-specific criteria hamper transferability of these frameworks across different climatic regions (Stein et al., 2019). More diverse and quantitative multicriteria classifications that account for antecedent wetness state and space-time dynamics of precipitation events are needed to encompass the wide spectrum of possible generation mechanisms and foster wider and novel applications of event classification frameworks in hydrological science and practice (Tarasova et al., 2019).

This calls for the development of the reliable tools for event separation, characterization and classification that can be applied at large scale to a wide range of catchments and can provide automated isolation of discrete runoff events from the observed streamflow time series, characterize various aspects of event generation using concise, non-local and transferable indicators and classify events accordingly using robust approaches that are rigorously tested.

Coupling automated separation of runoff events with comprehensive and transferable process-based event classification framework provides an opportunity of extending classifications from flood events to all runoff events. This can put singular flood events into perspective of the full distribution of streamflow events and allow to track transformation of processes from small to large events. On the other hand, it can facilitate large scale analysis of runoff generation processes and provide a unique opportunity to detect possible changes in the relevance of the governing processes in time and space.

## Objectives

The general goal of this work is to provide a deeper understanding on large scale controls of runoff event characteristics and to develop a framework for event characterization and classification that is able to distinguish events governed by different runoff generation processes. This objective is pursued through the development of comprehensive tools that enables an automated analysis of runoff events in wide range of catchments and specifically includes three major steps: event separation of continuous hydro-meteorological time series; event characterization procedure that computes spatially and temporally-explicit indicators of precipitation event dynamics and their interaction with antecedent catchment states from gridded hydro-meteorological products and outputs of distributed hydrological models; and event classification that comprehensively combines derived event characteristics to stratify events generated by distinct runoff generation mechanisms. The developed approaches are especially designed to deal with large datasets and allow for automated application in wide range of mesoscale catchments across climatic and physiographic regions. The approaches take advantages of dense long-term hydro-meteorological observations and regional distributed hydrological simulations available in Germany and provides an example on how the conventional continuous observational and simulated data can be merged and comprehensively analyzed to provide more insights on the event dynamics at regional scale.

The specific research objectives of this thesis are:

- Development of an automated procedure to identify rainfall-runoff events that can be applied to a wide range of catchments encompassing different landscape and climatic regions
- Investigating temporal dynamics of the event runoff response and exploring large scale con-

trols of its temporal variability at different time scales

- Investigating emergent regional pattern of event characteristics and exploring their spatial controls
- Development of a new multi-layer framework for process-based characterization of runoff events that uses dimensionless indicators of space-time dynamics of precipitation events and their spatial interaction with antecedent catchment states described as snow cover, distribution of frozen soils and soil moisture content
- Deriving and testing the event typology for Germany that captures first order controls of event runoff response and runoff generation processes in a wide range of German catchments

## Innovations

The research presented in this thesis makes a novel contribution by Germany-wide analysis of runoff event characteristics and their large scale controls, and by developing the event typology for Germany that goes beyond existing approaches in several ways:

- a In contrast to past frameworks, all runoff events that are identified by the proposed event separation procedure are classified which allows to analyze the process transformation from small to larger events
- b Event types are derived using indicators of spatially and temporally distributed rainfall and soil moisture within the catchment. This goes beyond existing approaches that employ lumped indicators and are unable to examine runoff generation mechanisms within catchments in a distributed way
- c A new hierarchical classification scheme is developed in which meteorological forcing and catchment state are analyzed separately. This new methodological approach allows capturing a large number of different process combinations effectively.

The outcome of this research is a unique database of separated and classified runoff events of various sizes for a wide range of German catchments for several observational decades that can be further used to detect transformation of processes from small to large events and temporal changes in runoff generation mechanisms across different regions.

## Structure of dissertation

The outlined research is presented in this thesis as follows:

- Chapter 2 presents an automated event separation procedure that consists of available time-series-based base flow separation, runoff event identification, rainfall attribution and a novel iterative procedure for the adjustment of thresholds used to identify single-peak components of multiple-peak events. Temporal dynamics of event characteristics of separated events is analyzed at different time scales (i.e., event-to-event variability, seasonality and long-term trends) and their large scale controls are investigated.
- Chapter 3 investigates regional pattern and spatial controls of event characteristics in Germany. Multi-objective performances of various variable selection methods are used to identify hydrologically-relevant variables from a comprehensive set of catchment descriptors featuring climatic, topographical, geomorphological, hydrogeological, geological, soil and land use descriptors. The hydrological interpretation of the emergent regional event characteristics, their variability and seasonality provides insights on archetypical catchment behaviors.
- Chapter 4 present a new multi-layer process-based framework for characterization and classification of runoff events that uses dimensionless indicators of space-time dynamics of precipitation events and their spatial interaction with antecedent catchment states. A rigorous

uncertainty analysis of the developed indicators is performed by means of the Monte Carlo simulations. The ability of the event typology derived from the proposed characterization framework to stratify events that result in distinct hydrograph dynamics is tested using cross recurrence plots and recurrence quantification analysis of event hydrographs.

- Chapter 5 summarizes pivotal findings and conclusions. Future potential research perspectives that emerge from the findings of this thesis are also discussed.

Chapters 2-4 are formatted versions of the three peer-reviewed papers published in the ISI-listed journals.

---

## 2 Exploring Controls on Rainfall-Runoff Events: Time Series-Based Event Separation and Temporal Dynamics of Event Runoff Response in Germany

This Chapter presents a formatted version of the original paper: **Tarasova, L.**, Basso, S., Zink, M., and Merz, R. (2018). Exploring controls on rainfall-runoff events: 1. Time-series-based event separation and temporal dynamics of event runoff response in Germany. *Water Resources Research*, 54 (10), 7711–7732. <https://doi.org/10.1029/2018WR022587>, with permission from Wiley (Copyright 2018 Wiley).

**Own contribution:** The manuscript was drafted by Larisa Tarasova, who also devised the proposed event separation method, prepared the data, performed the analysis and interpreted the results under supervision of Stefano Basso and Ralf Merz. Matthias Zink has provided simulations of snowmelt and soil moisture for this study.

**Acknowledgement and Data:** The financial support of the German Research Foundation (“Deutsche Forschungsgemeinschaft”, DFG) in terms of the research group FOR 2416 “Space-Time Dynamics of Extreme Floods (SPATE)” and Helmholtz Centre for Environmental Research (UFZ) is gratefully acknowledged. We acknowledge detailed and constructive comments of Charles Luce, Beverley Wemple, Alberto Montanari and five anonymous reviewers, which greatly helped to improve original manuscript. Our thanks go to Carine Poncelet for help in data preparation. We are grateful to Luis Samaniego for providing simulations of mHM. The simulated soil moisture data is available at <http://www.ufz.de/index.php?en=41160>. For providing the discharge data for Germany, we are grateful to Bavarian State Office of Environment (LfU) (<https://www.gkd.bayern.de/de/fluesse/abfluss>) and Global Runoff Data Centre (GRDC) prepared by the Federal Institute for Hydrology (BfG) (<http://www.bafg.de/GRDC>). Climatic data can be obtained from the German Weather Service (DWD) (<ftp://ftp-cdc.dwd.de/pub/CDC/>). Digital elevation model can be retrieved from Shuttle Radar Topography Mission (SRTM) (<http://www.cgiar-csi.org/data/srtm-90m-digital-elevation-database-v4-1>). Land use data is available from Copernicus monitoring system (<http://land.copernicus.eu/pan-european/corine-land-cover>). Characteristics of separated runoff events for every streamflow gauge used in the analysis can be found in Data Set S1 at <https://agupubs.onlinelibrary.wiley.com/doi/full/10.1029/2018WR022587>

### Abstract

Analyzing a response of catchments to rainfall inputs allows for deeper insights on the mechanisms of runoff generation at catchment scale. In this study an automated time-series-based event separation procedure consisting of available base flow separation, runoff event identification and rainfall attribution methods and of a novel iterative procedure for the adjustment of thresholds used to identify single-peak components of multiple-peak events is proposed. Event runoff coefficient, time scale, rise time and peak discharge of more than 220,000 identified rainfall-runoff events are then used to analyze dynamics of event runoff response in 185 catchments at multiple temporal scales. In mountainous catchments with poor storage event runoff response is strongly controlled by the characteristics of rainfall and is generated by event-fed saturation or infiltration excess. A distinct switch between saturated and unsaturated states occurs in these catchments. A weak relation between rainfall and runoff event properties is instead observed in lowland and hilly catchments with substantial storage, where a gradual transformation between functioning states occurs and the response is driven by pre-event saturation. The seasonality of their event characteristics is governed by the contribution of snowmelt and the seasonality of the aridity index rather than of rainfall properties. Long-term changes of total precipitation amount alone do not explain season-specific long-term changes of event characteristics that are rather consistent with changes of seasonal indicators of the wetness state. The effects of land use changes are detectable only in a few cases and display themselves mostly in the characteristic response time of catchments.

## 2.1 Introduction

Streamflow time series can be regarded as a sequence of distinct runoff events separated by periods of base flow. This view is deemed useful for exploring hydrological processes and rainfall-runoff transformation at catchment scale (Seibert et al., 2016). In particular, linking event hydrographs to their rainfall triggers and to pre-event catchment wetness states can give insights on the role of hydrologic connectivity and subsurface stormflow (Graeff et al., 2012) and provide relevant information about runoff generation processes and their temporal dynamics (Blume et al., 2007). The variability of the event runoff response in time and among regions produces distinct patterns of water and nutrients delivery to river channels (Stieglitz et al., 2003; James, 2007). In addition, climate and land use changes can modify the relative importance and the mutual interactions of hydrological processes (Merz et al., 2011), thus altering the response of catchments to rainfall events. Therefore, detecting and attributing heterogeneity of events' characteristics is pivotal for flood protection and water quality management and constitutes a key issue to predict future hydrologic behaviors.

Although the concept of runoff events is widely used in hydrology and is probably a part of every hydrology textbook, there is no widely accepted approach, how to identify runoff events from continuous streamflow series. All the existing techniques to identify runoff events and link them to their triggers involve a base flow separation, identification of potential runoff (rainfall) events with their starting and ending points, and the attribution of rainfall to runoff events (or vice versa). However, applied methods and assumptions differ considerably and are often tailored to a specific catchment under study. For example, base flow separation has been previously realized by means of recursive filters (e.g., Chapman and Maxwell, 1996; Eckhardt, 2005), event-based recession analysis (Blume et al., 2007) or simple smoothing of time series (Institute of Hydrology, 1980). None of these methods delivers a "true" base flow (Su et al., 2016), but they are useful to identify runoff events when combined with additional separation thresholds (Hewlett and Hibbert, 1967). The search for potential rainfall-runoff events can be initiated from the identification of either runoff (Merz et al., 2006; Graeff et al., 2012; Rodríguez-Blanco et al., 2012; Mei and Anagnostou, 2015) or precipitation events (Koskelo et al., 2012; Seibert et al., 2016; Tang and Carey, 2017). In the latter case, critical rainfall depth (or intensity) and duration of dry spells are used as determinants (e.g., Graeff et al., 2012; Rodríguez-Blanco et al., 2012). The search for runoff events instead begins with the identification of the event peaks using criteria of minimum peak magnitude (e.g., ratios between quick and base flow or between peak flow and pre-event flow) (Norbiato et al., 2009). Runoff events are further defined by their beginning and end points (Mei and Anagnostou, 2015). While the beginning of a runoff event is relatively straightforward to identify, the choice of the end point is far more challenging, largely depends on the applied base flow separation method (Seibert et al., 2016) and often requires additional separation thresholds, such as the long-term base flow index (e.g., Mei and Anagnostou, 2015), or the ratio between quick and base flow at the end of the event (e.g., Merz et al., 2006). Separation thresholds like the time interval between two peaks (e.g., Graeff et al., 2012) or the ratio between two consecutive peak discharges (e.g., Sikorska et al., 2015) are also used to assess the independency of events and divide multiple-peak events into their single-peak components. These thresholds are usually selected to mimic an event separation a hydrologist would do manually for the catchments under study. Hence they are site-specific and have a limited transferability to catchments with contrasting event runoff response. Finally, rainfall events must be attributed to runoff events (or vice versa) in order to derive events' attributes and draw conclusions on the processes linking these two phenomena. Previously proposed attribution methods range from very simple approaches (like the integration of rainfall depths occurring during runoff events Capell et al. (2012)) to physically-based methods that consider the whole precipitation fallen within the average lag time of a basin (Mei and Anagnostou, 2015), to even more sophisticated procedures that take into account the characteristic rainfall time scale of a catchment (Merz et al., 2006).

Dimensionless variables, such as the event runoff coefficient and time scale (i.e., the ratio between volume and peak of each event (Gaál et al., 2012)), prove handy to describe events' attributes and analyze spatial and temporal differences exhibited by hydrological processes (Merz and Blöschl,

2009a,b; Seibert et al., 2016). Several studies correlated varying event runoff coefficients to sets of indicators, highlighting their dependence on event rainfall amounts (Merz et al., 2006; Blume et al., 2007), rainfall intensity (Blume et al., 2007; Graeff et al., 2012), volume of snowmelt Norbiato et al. (2009) and antecedent conditions of rainfall, flow and soil moisture (Merz et al., 2006; James, 2007; Rodríguez-Blanco et al., 2012; Graeff et al., 2012). Both event runoff coefficients and time scales exhibited seasonality due to seasonal variations of soil moisture and rainfall attributes (Merz and Blöschl, 2009a; Rodríguez-Blanco et al., 2012) and to the effect of snowmelt (Gaál et al., 2012). At long time scale their changes are often attributed to land use changes (e.g., urbanization, deforestation and wildfire), especially in small catchments (e.g., Andréassian et al., 2003; Martin et al., 2012; Trudeau and Richardson, 2015). However, changes of the climatic forcing (e.g., precipitation and temperature) might also affect the event runoff response (Sawicz et al., 2014; Dumanski et al., 2015; Ajami et al., 2017).

The majority of the referred literature studied only few catchments (with the noticeable exceptions of Merz et al. (2006) and Gaál et al. (2012)) and merely examined variability among events, despite the evidence of multi-scale (e.g., seasonal and long-term) variability of the runoff response. Existing multi-catchment comparative studies focused on annual floods (e.g., Gottschalk and Weingartner, 1998; Gaál et al., 2012) or on a few large events per year (Norbiato et al., 2009), and were confined to the climatically homogeneous alpine regions of Northern Italy, Switzerland and Austria. These limitations lead to fragmented information about the temporal dynamics of event runoff response and to contradictory results concerning its drivers. Moreover, the effect of changing climate forcing and land use on runoff event characteristics has not been quantitatively examined yet. Most of the cited studies also adopted event runoff identification techniques that are tailored to specific geographic areas, thus preventing the possibility to use their results to perform regional analyses of the runoff response across climatic gradients. An enabling prerequisite for a consistent large scale analysis of the attributes of runoff events is the availability of a simple method to identify them that could be automated and uniformly applied to diverse river basins and long time series of streamflow and rainfall (Hewlett and Hibbert, 1967).

The purpose of this study is twofold. First, we propose a procedure to automatically identify rainfall-runoff events that can be applied to a wide range of catchments across climatic and physiographic regions. To reach this goal, different base flow separation methods are tested and an optimal technique for subsequent identification of runoff events is selected. Rainfall attribution is performed using a simple physically-based method proposed by Mei and Anagnostou (2015), which accounts for the seasonal variability of rainfall events and is suitable also in case of snowmelt. A novel iterative procedure to objectively select separation thresholds used to distinguish between overlapping single-peak and multiple-peak events (called multiple-peak events refinement in the following) is proposed. The second goal is to analyze temporal dynamics (i.e., event-to-event variability, seasonality and long-term changes) of the event runoff response in a large number of catchments featuring varied climatic and morphological conditions (using the whole of Germany as case study). The comparison of these dynamics among themselves and with a set of explanatory variables aims to shed light on the drivers of the observed variability of runoff response at different time scales. The inter-catchment variability of event characteristics and its spatial patterns will be instead discussed in a companion paper (Tarasova et al., 2018a).

## 2.2 Data

Germany is located in a transition zone between a maritime climate in the west and a continental climate in the eastern part of the country. Precipitation is dominated by westerly circulation patterns, whose influence decreases from west to east. Spatial precipitation patterns are strongly affected by topography, which features lowlands in the North, the Alps in the South, and the Central Uplands in the middle part of Germany. German catchments mostly drain to the North Sea (e.g., the Rhine, the Weser and the Elbe Rivers), with the exception of the Danube that flows to the Black Sea. Figure 2.1 shows the main landscape regions of Germany and the outlets of the catchments selected for this study.

Water resources management has a long history in Germany. All catchments affected by flow

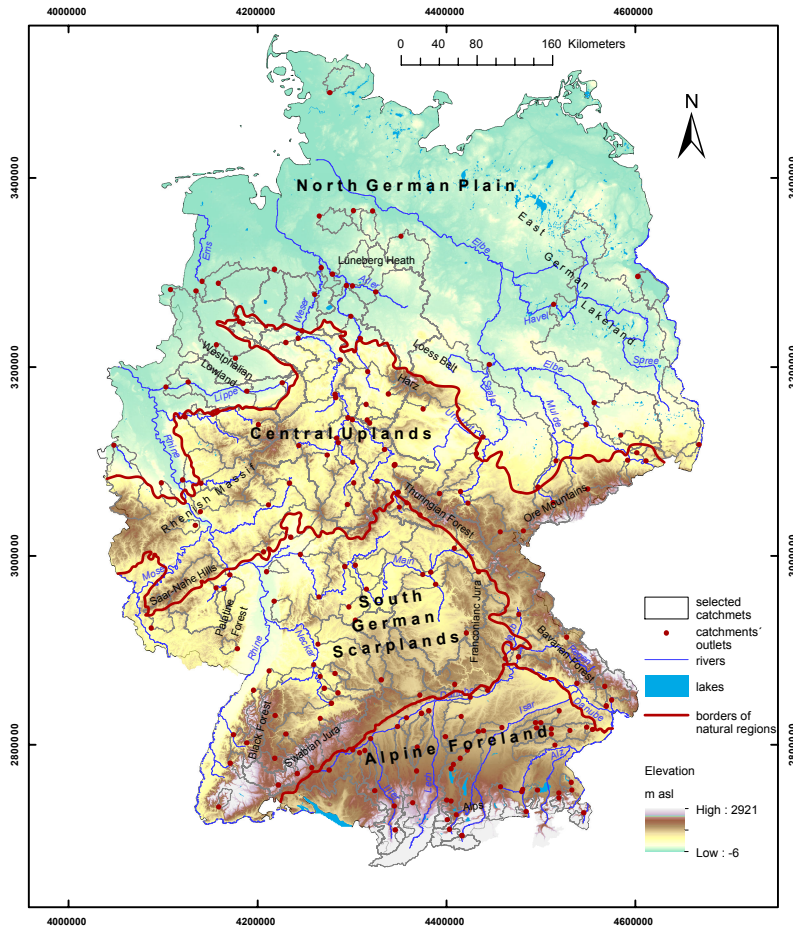


Figure 2.1: The study area is the whole of Germany, which is divided into four main landscape units (the North German Plain, Central Uplands, South German Scarplands and Alpine Foreland regions). The names of smaller natural regions of Germany are also indicated. 185 catchments where daily flows are not affected by anthropogenic modifications were selected based on data availability

disturbance due to large reservoirs or control gates (Lehner et al., 2011) were removed from the dataset in order to avoid confounding effects on event characteristics due to anthropogenic flow regulation. Moreover, catchments were removed from the dataset if visual examination revealed obvious diurnal flow disturbances. The preselection resulted in a set of 185 catchments with area ranging from 31 to 23,700 km<sup>2</sup> and median value equal to 516 km<sup>2</sup>. The length of the considered daily time series of streamflow and rainfall varies between 37 and 63 years, with a median value of 61 years.

Daily precipitation time series for each catchment were aggregated from the Regionalisierte Niederschlagshöhen (REGNIE) dataset provided by the German Weather Service (Rauthe et al., 2013). In this dataset, rainfall fields are estimated from point observations through multiple regression using elevation, aspect and location as explanatory variables. Residuals are interpolated by means of the Inverse Distance Weighting method and then accounted for (Rauthe et al., 2013). Daily temperature time series in the considered basins were generated from the German Weather Service observations by means of external drift kriging, using elevation as explanatory variable (Zink et al., 2017).

Catchment wetness conditions preceding runoff events were assessed by considering the soil moisture values simulated by the mesoscale Hydrological Model (mHM) (Samaniego et al., 2010; Kumar et al., 2013). Daily snowmelt and actual evapotranspiration were also simulated by using the mHM model (Zink et al., 2017). The evolution of land use in the study catchments was analyzed by using the change layers of “Coordination of Information on the Environment (CORINE)” dataset (<http://land.copernicus.eu/pan-european/corine-land-cover>), which are available for the periods 1990-2000, 2000-2006 and 2006-2012.



## 2.3 Methods

### 2.3.1 Time-series-based identification of runoff events

An event separation procedure consists of three main steps: base flow separation, identification of runoff events and attribution of rainfall events (Figure 2.2a-b). Base flow separation divides streamflow time series into quick and base flows. Quick flow episodes separated by periods of base flow are then identified as runoff events using additional separation thresholds (e.g., time interval between two peaks, ratio between two peak discharges) (Merz et al., 2006; Graeff et al., 2012; Sikorska et al., 2015). Finally, rainfall events are attributed to the identified runoff events. In this study, event separation is implemented through the above mentioned steps plus a novel iterative procedure for the adjustment of separation thresholds that allows for distinguishing between multiple-peak and single-peak overlapping events (Figure 2.2c, Chapter 2.3.1.4).

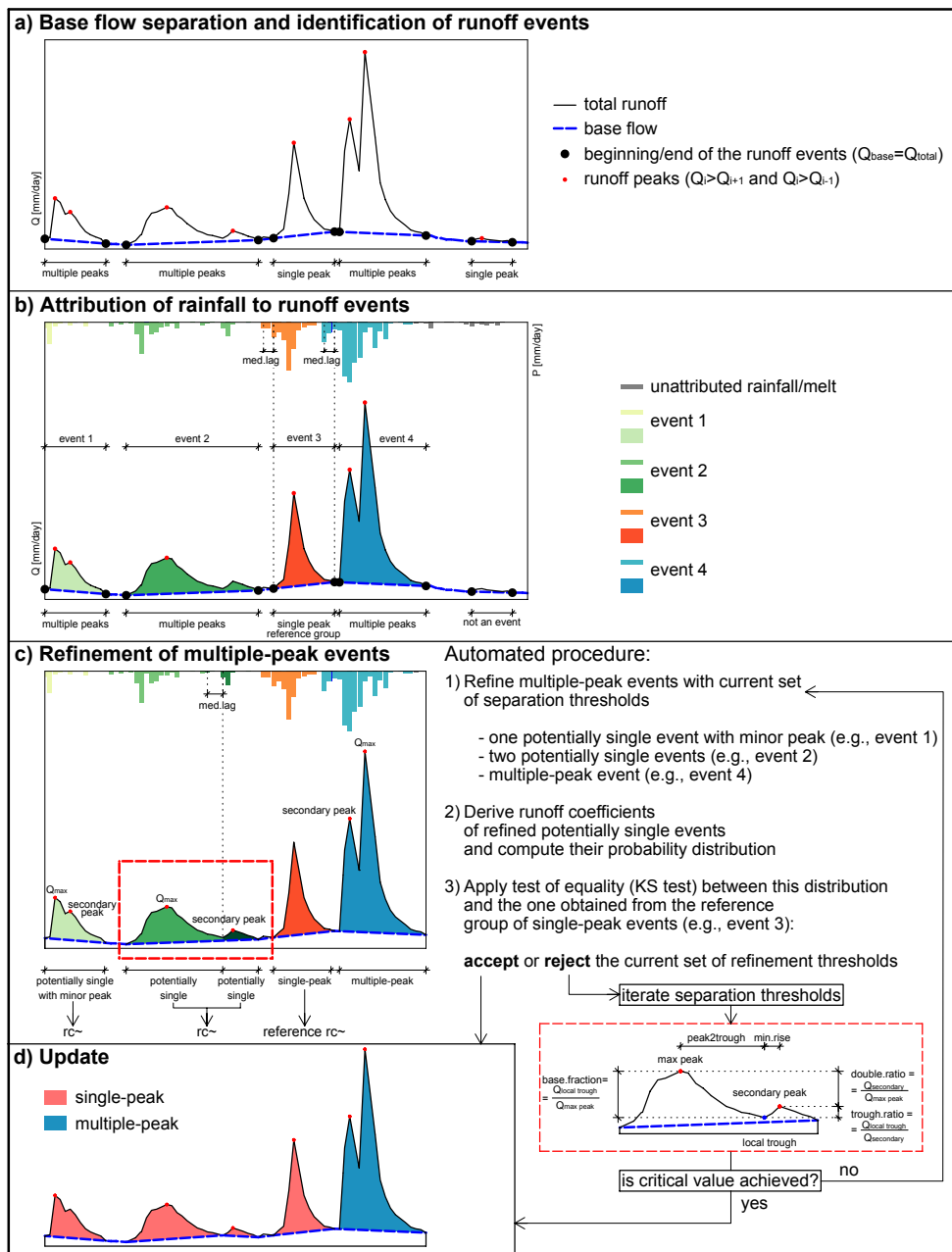


Figure 2.2: Summary of the event separation procedure. The River Kyll at Junkerath is used as an example to illustrate it: a) base flow separation and identification of runoff events (Chapters 2.3.1.1 and 2.3.1.2); b) attribution of rainfall events (Chapter 2.3.1.3) using median seasonal lag time (*med.lag*); c) refinement of multi-peak events (Chapter 2.3.1.4) using iterative adjustment of separation thresholds, which are portrayed in the inset of panel c and described in Table 2.1; d) updating the samples of single and multiple-peak events

**2.3.1.1 Base flow separation** Several techniques for base flow separation were tested in order to find the most suitable option to identify runoff events. In continuous streamflow time series, troughs (defined as the days  $i$  where  $Q_i < Q_{i-1}$  and  $Q_i < Q_{i+1}$ ) potentially correspond to the beginnings of runoff events (see e.g., the inset circles of Figure 2.3). To allow for separating consecutive runoff events, the estimated values of base flow should equal to total flow in correspondence to troughs. Therefore, base flow separation methods were assessed by comparing their ability to consistently match troughs across a set of basins. This is especially important for studies analyzing a large number of catchments, since biases may arise if the base flow separation method identifies troughs with varied reliability in different case studies. Additionally, we also performed time delay analysis calculating the maximum of the cross correlation function between total and base flow time series to examine the lag and the strength of relation between total and separated base flow time series. Only digital filters were tested due to their applicability to large datasets. More elaborated methods were instead discarded due to possible parameters' uncertainty in absence of "true" base flow data for calibration (Chapman, 1999). We have examined the following techniques:

- Three algorithms which assume that catchments behave as linear reservoirs. These techniques require the estimation one (i.e., recession constant) (Chapman and Maxwell, 1996) or two parameters (i.e., recession constant and maximum base flow index, *BFI<sub>max</sub>*) (Eckhardt, 2005). The recession constant was estimated from recession analysis as described in Vogel and Kroll (1992). *BFI<sub>max</sub>* was instead estimated as the ratio of  $Q_{90}$  to  $Q_{50}$  (Smakhtin, 2001), or by using the backward smoothing method proposed by Collischonn and Fan (2013);
- One algorithm based on the assumption of a non-linear relationship between storage and outflow, which requires the estimation of two parameters (Wittenberg, 1999). Parameters of the non-linear reservoir were estimated as suggested by Ye et al. (2014) and Berghuijs et al. (2016a);
- A non-parametric algorithm based solely on the analysis of streamflow time series Institute of Hydrology (1980); WMO (2008). In a first step the algorithm finds local minima within non-overlapping 5-days windows for the entire time series. In the following step, the extracted series of minima are examined to find turning points, which are empirically defined as the points that are smaller than 1.11 times their neighboring minima. Once all turning points have been found, the base flow hydrograph is reconstructed by linear interpolation between the points.

**2.3.1.2 Runoff event identification** After the separation of base flow, streamflow time series were screened to identify runoff events, which are characterized by their: peak, beginning and end points (Mei and Anagnostou, 2015). A peak occurs at day  $i$  if  $Q_i > Q_{i+1}$  and  $Q_i > Q_{i-1}$ . The event begins at the closest point in time before the peak when total runoff is equal to base flow before the peak, whereas it ends as soon as total runoff has fallen to the base flow level again (Figure 2.2a). The minimal duration of a runoff event was set equal to one day due to the daily temporal resolution of the available time series. To avoid the detection of false events caused by small runoff fluctuations, only events with peak discharge higher than 10% of the base flow were considered as potential events. This threshold was set as a trade-off between number of unattributed and total number of identified runoff events. Finally, runoff events with only one peak (see e.g., event 3 in Figure 2.2b) were aggregated into a reference group of single-peak events.

**2.3.1.3 Attribution of rainfall/ snowmelt events** A physically-based criterion, namely the median basin lag time (Mei and Anagnostou, 2015), was applied to identify beginning and end of rainfall and snowmelt events from daily time series and attribute them to runoff events. The basin lag time is the delay between rainfall and runoff generation and is largely independent from storm type (Bell and Om Kar, 1969). For simplicity we defined the basin lag times as the time between rainfall and flow peaks (Marchi et al., 2010). To account for differences between rainfall and snowmelt events we identified lag time for winter and summer periods separately (Mei and

Anagnostou, 2015). The seasonal median lag time was subsequently used to set a distance backwards from the starting point of the runoff event within which searching for rainfall. All rainfall/melting that has occurred within the basin lag time was assumed to contribute to the considered runoff event and was excluded from preceding events, unless it occurred during the rising limb of the latter (Figure 2.2b). Volume and maximum intensity of the attributed rainfall events were finally calculated. This step is required to determine event runoff coefficients.

**2.3.1.4 Refinement of multiple-peak events** Previous studies dealing with runoff event separation (e.g., Merz et al., 2006; Norbiato et al., 2009; Mei and Anagnostou, 2015; Sikorska et al., 2015) have shown that using base flow separation alone might lead to the identification of multiple-peak events that are merely artefacts arising from erroneous results of the base flow separation method. Therefore, additional separation thresholds are usually applied to identify single runoff events. In this study we devised a procedure to separate multiple-peak events into their single-peak components by using a set of iteratively adjusted refinement thresholds (see Table 2.1 for a description of them), chosen among those commonly used in the event separation studies cited in Chapter 2.1. The goal is to avoid subjective selection of separation thresholds and allow for applicability of the method to a wide range of catchments. The procedure (Figure 2.2c) comprises the following steps:

- i Thresholds are set to initial values chosen either from literature or based on their physical meanings;
- ii Every multiple-peak event is analyzed based on these thresholds, and results either in a main single event followed by minor peaks, or in two or more single events, or still in a multiple-peak event;
- iii Events identified as potentially single-peak events are grouped together and the frequency distribution of their runoff coefficients is compared to the distribution of runoff coefficients of reference single-peak events by means of a Kolmogorov-Smirnov test of equality (see Chapter 2.6.1 for details);
- iv If the two distributions differ, more conservative thresholds (i.e., resulting in fewer multiple-peak events being divided into their components) are chosen and the procedure is repeated from step 2.

The refinement proceeds iteratively until either all multiple-peak events are subdivided into their single-peak components or the critical threshold values are reached (Table 2.1). Once the critical values are reached, unrefined events are assigned to a group of multiple-peak events.

Although the lacking knowledge of the “true” multiple-peak events prevents us from a rigorous evaluation the proposed refinement procedure, its performance in terms of number of identified, attributed and refined events in catchments with different runoff regimes and belonging to different landscape regions has been analyzed, since consistent performances for a wide range of catchments are required for a comparative analysis of event characteristics.

## 2.3.2 Temporal dynamics of event runoff response

Based on the set of identified rainfall-runoff events we analyzed dynamics of event runoff response on multiple temporal scales: the variability among events (Chapter 2.3.2.2), seasonality (Chapter 2.3.2.3) and long-term changes (Chapter 2.3.2.4). Event runoff response was characterized by the set of event characteristics that provide an insight regarding catchment-scale runoff generation processes and their variability in time (Chapter 2.3.2.1). To understand controls of emergent variability we examined dynamics of hypothesized drivers and evaluated their consistency with event characteristics at each corresponding scale.

Table 2.1: Separation thresholds and their initial and critical values

Parameter	Description	Purpose	Initial value <sup>a</sup>	Increment <sup>b</sup>	Critical value <sup>c</sup>	Reference <sup>d</sup>
<i>peak2trough</i>	Min time interval in days between max peak and previous/next trough	Distinguishing separated events	3	1	10	Merz et al. (2006); Graeff et al. (2012); Sikorska et al. (2015)
<i>base.fraction</i>	Fraction of peak flow value at which total runoff is equal to base flow	Distinguishing separated events	0.20	-0.02	0.02	Rinderer et al. (2016); Sikorska et al. (2015)
<i>double.ratio</i>	Ratio between secondary peak discharge and max peak discharge	Distinguishing between multiple-peak and minor peaks on the limb of single-peak events	0.60	0.02	0.78	Sikorska et al. (2015)
<i>trough.ratio</i>	Ratio between local trough and secondary peak discharge	Distinguishing between multiple-peak and minor peaks on the limb of single-peak events	0.80	0.02	0.98	Merz et al. (2006); Rodríguez-Blanco et al. (2012); Graeff et al. (2012)
<i>min.rise</i>	Min length in days of the rising limb of secondary peaks	Distinguishing between multiple-peak and minor peaks on the limb of single-peak events	1	1	5	Sikorska et al. (2015)

<sup>a</sup> The initial values of thresholds were chosen either from literature (*peak2through*, *base.fraction*, *double.ratio*, *trough.ratio*) or set to the physical minimum (*min.rise*)

<sup>b</sup> After each iteration more conservative thresholds were chosen resulting in fewer multiple-peak events being refined. The increments of the thresholds were set to the time step size (1 day) for temporal thresholds and back-calculated using initial and critical values for fractional thresholds

<sup>c</sup> The critical values of thresholds were chosen either from literature (*peak2through*, *min.rise*, *double.ratio*) or set to the physical minimum (*base.fraction*, *trough.ratio*)

<sup>d</sup> References where similar criteria for event separation or refinement were used

**2.3.2.1 Event characteristics and possible drivers** Four diagnostic variables (called event characteristics in the following) of every identified rainfall-runoff event were computed to objectively quantify differences among them. The (i) event runoff coefficient ( $rc$ ) [dimensionless] is estimated as the ratio between the volume of the quick runoff component [mm] of a particular event and the respective rainfall and/or snowmelt event [mm]. It characterizes which portion of rainfall (snowmelt) is stored (including interception by vegetation, soil moisture accumulation and percolation into deeper layers) and which portion is instead released from the storages as event runoff. The (ii) runoff event time scale ( $ts$ ) [days] is the ratio between quick runoff volume [mm] and peak discharge [mm/day] (Gaál et al., 2012). The event time scale characterizes the shape of the hydrograph and the duration of an event. Shorter event time scales are expected when fast runoff generation processes prevail, while longer time scales is an indicator that slow runoff components contribute as well. For most rainfall-runoff events in humid climates as in Germany, one would expect a mixture of fast and slow runoff generation processes. An indicator of the relative importance of fast and slow runoff generation processes within one event is the event rise time. The (iii) event rise time ( $rt$ ) [dimensionless] characterizes the duration [days] from the beginning of the

event till the day when peak discharge is observed (Bell and Om Kar, 1969) normalized by the overall duration of the event in days. It shows how fast the peak is reached. During event with a mixture of runoff generation processes, but with a relative high contribution of fast processes one would expect earlier peaks (i.e., short event rise time), but also longer recession time, (i.e., longer event time scales). The (iv) normalized event peak discharge (*peak*) [dimensionless] is the maximum total discharge [mm/day] of the identified runoff event normalized by the long-term average flow (Q50) [mm/day] derived from observed discharge time series. The event peak provides information about the magnitude of a runoff event. Its normalized version allows for comparing of the magnitude of the peak deviation from the mean discharge in catchments with various flow conditions.

With the aim of understanding controls on characteristics of runoff events occurring at different times, we also analyzed several indicators describing rainfall/ snowmelt events (e.g., overall volume and maximum intensity) and pre-event wetness states (e.g., antecedent rainfall, soil moisture and base flow). Their metadata are summarized in Table 2.2.

Table 2.2: Summary of rainfall-runoff event characteristics and indicators of pre-event catchment state used in this study

	Description	Symbol	Unit	Data source
<b>Event characteristics</b>				
<i>Event runoff coefficient</i>	Ratio between the volumes of quick runoff and the attributed rainfall and snowmelt events ( <i>Pvol</i> )	<i>rc</i>	dimensionless	Event separation
<i>Event time scale</i>	Ratio between quick runoff volume [mm] and peak discharge [mm/day]	<i>ts</i>	days	Event separation
<i>Event rise time</i>	Duration [day] from the beginning of the event till the day when peak discharge was observed, normalized by the total duration [day] of the event	<i>rt</i>	dimensionless	Event separation
<i>Normalized event peak discharge</i>	Maximum event flow normalized by the long-term average flow (Q50)	<i>peak</i>	dimensionless	Event separation
<b>Rainfall/ snowmelt characteristics</b>				
<i>Rainfall and snowmelt event volume</i>	Sum of rainfall and snowmelt volumes contributing to a certain runoff event	<i>Pvol</i>	mm	REGNIE (Rauthe et al., 2013), mHM (Zink et al., 2017)
<i>Volume of snowmelt</i>	Integrated volume of the snowmelt contributing to a certain runoff event	<i>melt</i>	mm	mHM (Zink et al., 2017)
<i>Maximum intensity of rainfall event</i>	Max rainfall/ snowmelt intensity during the attributed event	<i>Pint</i>	mm/day	REGNIE (Rauthe et al., 2013)
<b>Indicators of pre-event catchment state</b>				
<i>Antecedent soil moisture</i>	Catchment average of the water content within the entire soil column in the day preceding the event	<i>sm</i>	mm	mHM (Zink et al., 2017)
<i>10-day antecedent rainfall and snowmelt</i>	10-day sum of rainfall and snowmelt before the attributed rainfall/ melting event	<i>Pant10</i>	mm	REGNIE (Rauthe et al., 2013)
<i>Base flow at the beginning of the event</i>	Base flow in the day preceding the runoff event	<i>qbase</i>	mm/day	Base flow separation (Institute of Hydrology, 1980)

**2.3.2.2 Event-to-event variability of event characteristics** To understand the role played by rainfall/ melting in determining runoff response characteristics we quantified the strength of their inter-relationships by using Spearman-rank correlation. A similar procedure was applied to study the effect of catchments' pre-event states on runoff generation processes.

To analyze regional differences in the event-to-event variability of runoff coefficients with increasing soil moisture, for every catchment we fitted an exponential function ( $rc = a * e^{sm*b}$ ) to the average runoff coefficient of events grouped by their antecedent soil moisture. The residual standard error was chosen as criterion to assess the quality of the fit. The dependency of the threshold behavior on the subsurface storage capacity was analyzed by comparing regional patterns of the scaling exponent  $b$  of the fitted function and of the ratio between Q90 and Q50 (ratio between the daily discharge which is exceeded 90% of the time and the median flow) (Norbiato et al., 2009).

**2.3.2.3 Seasonal variability of event characteristics** In this study, the year is divided into four seasons as suggested by Beurton and Thielen (2009) for German catchments: winter (December-February), spring (March-May), summer (June-August) and autumn (September-November). In order to provide insights concerning the seasonality of event characteristics, we have quantified the deviation of their mean seasonal values from their long-term (1951-2013) annual means. Seasonality of rainfall/ snowmelt and of the indicators of pre-event catchment state was also analyzed to link the detected seasonality of event characteristics to its drivers. In addition seasonal patterns of general hydro-climatic conditions, represented by means of continuous variables such as total precipitation and aridity index (Budyko, 1974) were also analyzed.

**2.3.2.4 Long-term variability of event characteristics** To detect possible changes of event characteristics in Germany in the period 1951-2013 we applied a non-parametric Mann-Kendall test (Kendall, 1975) on their mean seasonal values calculated for each year. The Mann-Kendall test is often used for detection of hydrological changes and was previously applied for trend analysis of water-balance-based runoff coefficients (Dumanski et al., 2015; Ajami et al., 2017), hydrological extremes (e.g., Petrow et al., 2009), as well as for analysis of hydro-climatic and water quality trends (e.g., Lutz et al., 2016). Data were corrected for serial correlation using trend-free pre-whitening procedure (Yue et al., 2002). The magnitude of the trend was finally determined by using the non-parametric Sen's slope estimator (Sen, 1968).

For the attribution of potential hydrological changes to their causes we also performed trend analysis on possible drivers of these changes, such as rainfall/ snowmelt properties and pre-event conditions. Additionally, to identify possible trends of the general climatic conditions in Germany we applied the Mann-Kendall test to time series of seasonal (cumulated or average) values of precipitation and aridity index. Finally, we analyzed available data on land use and land cover changes in Germany, with the aim of investigating the role played by local landscape conditions in determining hydrological trends. The overall land use change per catchment was estimated as the sum of the areas that changed land use during three available periods 1990-2000, 2000-2006 and 2006-2012.

## 2.4 Results

### 2.4.1 Time-series-based event separation

**2.4.1.1 Performance of tested base flow separation methods** Various base flow separation techniques were tested in this study with the goal of selecting a robust methodology for further event identification. Specifically, the parametric digital filter proposed by Chapman and Maxwell (1996), two versions of the filter introduced by Eckhardt (2005), the non-linear approach of (Wittenberg, 1999) and a non-parametric simple smoothing ((Institute of Hydrology, 1980) have been compared. In the absence of the "true base flow" as a reference for comparison, performances of the methods were assessed by their ability to unambiguously identify the beginning of potential runoff events (i.e., troughs; see the zoom circles in Figure 2.3a-c).

The digital filters of Chapman and Maxwell (1996) (Figure 2.3, light blue line) and Eckhardt

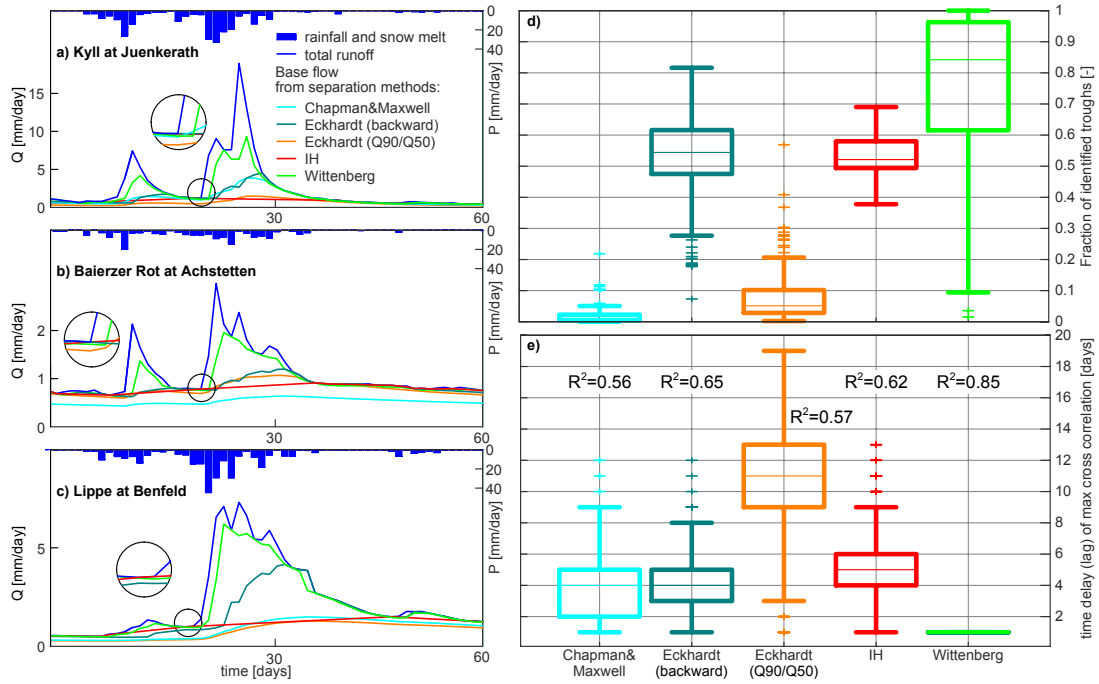


Figure 2.3: Base flow separation: a-c) results of the different base flow separation methods tested for three selected catchments. Zoom circles display base flow behavior at the beginning of potential runoff events (i.e., troughs); d) fraction of troughs identified by different base flow separation methods for all catchments in the data set; e) time delay (lag) determined by the argument of the maximum of the cross correlation between total and base flow for all catchments in the data set. The length of time delay characterizes how fast does base flow reacts to changes of total runoff.  $R^2$  shows the averaged value of the cross correlation coefficient averaged for all catchments and characterizes the strength of relation between total and base flow. Boxplots represents all catchments in the data set (fine horizontal line: median; box: interquartile range defined as the difference between 75<sup>th</sup> and 25<sup>th</sup> percentile; whiskers: 1.5 times interquartile range beyond the box; crosses: outliers)

(2005) (in the version where the parameter  $BFI_{max}$  is estimated as the ratio between Q90 and Q50 (Smakhtin, 2001); see Figure 2.3, orange line) consistently underestimated base flow, i.e., base flow is considerably below the observed streamflow, even during dry spells for most catchments. This is visible in the exemplifying hydrographs of Figure 2.3b-c, and becomes clear from the boxplots of Figure 2.3d, where the overall fraction of troughs identified by the tested base flow separation methods is shown. Because of their poor performances, using these two methods for event identification would require additional cut-off thresholds to set the starting points of events. Also time delay analysis of cross correlation (Figure 2.3e) shows that these two methods had the lowest correlation coefficient ( $R^2$ ) indicating poor relation between separated base flow and total runoff time series. An alternative version of the Eckhardt (2005) approach, where  $BFI_{max}$  is estimated by using a backward moving filter (Collischonn and Fan, 2013) (Figure 2.3, turquoise line) performed fairly well for mid-altitude catchments with fast runoff response, such as the one shown in Figure 2.3a. However, for other types of catchments (Figure 2.3c) the base flow contribution at the beginning of runoff events was underestimated, thus hampering the possibility to identify their starting points.

The non-linear filter of Wittenberg (1999) consistently overestimated base flow for most catchments (Figure 2.3a-c, green line). Time delay analysis shows that for all catchments the maximum of the cross correlation between base and total flow time series is at  $lag = 0$  (Figure 2.3e), meaning that base flow reacts immediately when total runoff changes. This result indicates that compared to other base flow separation methods (Figure 2.3e) this method failed to capture the variability of delay times expected in the diverse catchments in study data set. Although this method allows for identifying a large fraction of troughs on average, its performance strongly varies among catchments (Figure 2.3d). Moreover, for more than 20% of the catchments the estimation procedure resulted in implausible values of the exponent of the non-linear filter, thus hampering reliable base flow separation.

Despite its simplicity, the non-parametric simple smoothing method (Institute of Hydrology, 1980)

allowed for unambiguous identification of the beginning points of events (Figure 2.3a-c, zoomed circles) in a wide range of catchments. In particular, this method guaranteed the lowest variance of the fraction of identified troughs among catchments (Figure 2.3d), an especially important feature in view of studying and comparing runoff response in a large number of case studies. The cross correlation of base flow separated with this method and the range of identified delay times (Figure 2.3e) is comparable with the version of Eckhardt (2005) filter with parameters estimated as in Collischonn and Fan (2013). Therefore, Institute of Hydrology (1980) was finally chosen to implement the initial step (i.e., base flow separation) of the procedure used to identify rainfall-runoff events.

**2.4.1.2 Attribution of rainfall to runoff events and refinement of multiple-peak events** A total number of 222,353 events were identified from daily series of streamflow observed in 185 German catchments in the period from 1951 to 2013. The number of events for each catchment varied from 622 to 1779. No corresponding rainfall or melting events were found for 3082 runoff events, which have therefore been discarded (see unattributed events in Figure 2.4a). The application of the proposed iterative procedure for multiple-peak events refinement highlighted the possibility to extract from this group of events single-peak events whose distribution of runoff coefficients matched the distribution of the reference group of single-peak events (Figure 2.4b). At the same time, this distribution significantly differed from that of the remaining multiple-peak events (Figure 2.4b). This is true for 183 out of 185 analyzed catchments. For two nested sub-catchments (with area equal to 1193 and 1256 km<sup>2</sup>) of the Amper River (located in the Alpine Foreland region of Germany) no significant differences between runoff coefficients of single and multiple-peak events existed. This result can be explained by the fact that streamflow in this catchment is strongly dampened by passing through the Ammer Lake (which has an area of 47 km<sup>2</sup> and subtends a catchment area of 995 km<sup>2</sup>), thus resulting in very similar event runoff characteristics. The multiple-peak refinement procedure performed homogeneously for catchments belonging to different natural regions of Germany (Figure 2.4a). After its application 44.7% of all identified and attributed events were classified as multiple-peak events.

## 2.4.2 Temporal dynamics of event runoff response

The set of identified rainfall-runoff events was used to examine how rainfall/ snowmelt event properties and antecedent catchment wetness (described through soil moisture and base flow indicators) alter event runoff coefficient, time scale, rise time and normalized peak among the events and at seasonal and long-term time scales.

**2.4.2.1 Event-to-event variability of rainfall-runoff event characteristics** Typical event-to-event variations of the runoff response of German catchments are presented in Figure 2.5, where event characteristics (i.e., runoff coefficient, time scale, rise time, and normalized peak discharge) are plotted against several rainfall and pre-event wetness indicators for two selected catchments. The strength of these and other additional relationships in all studied catchments is summarized through the correlation maps displayed in Figure 2.6.

The event runoff coefficient ( $rc$ ) and the normalized peak discharge ( $peak$ ) exhibit similar relationships with rainfall properties and pre-event catchment state (Figure 2.5). The volume of rainfall ( $Pvol$ ) appears to be a stronger predictor of these two runoff event characteristics than rainfall intensity (Figure 2.5,  $rc-Pint$ ,  $peak-Pint$ ). The event peak discharge increases proportionally to the volume of rainfall in all study catchments (Figure 2.6,  $peak-Pvol$ ), whereas a strong relation of the latter variable with the event runoff coefficient is confined to the Central Uplands and South German Scarplands (Figure 2.6,  $rc-Pvol$ ). In smaller mountainous headwater catchments of these regions, where very intense rainfall events occur, correlation between runoff characteristics and rainfall intensity is strong as well (Figure 2.6,  $rc-Pint$ ,  $peak-Pint$ ).

Interestingly multiple-peak events (blue crosses in Figure 2.5, albeit exhibiting a similar behavior to single-peak events (red dots in Figure 2.5), reach higher values of runoff coefficient, normalized peak and time scale. For both types of events the time scale is strongly influenced by the underlying volume of rainfall and snowmelt ( $Pvol$ ). In fact, except for catchments belonging to the



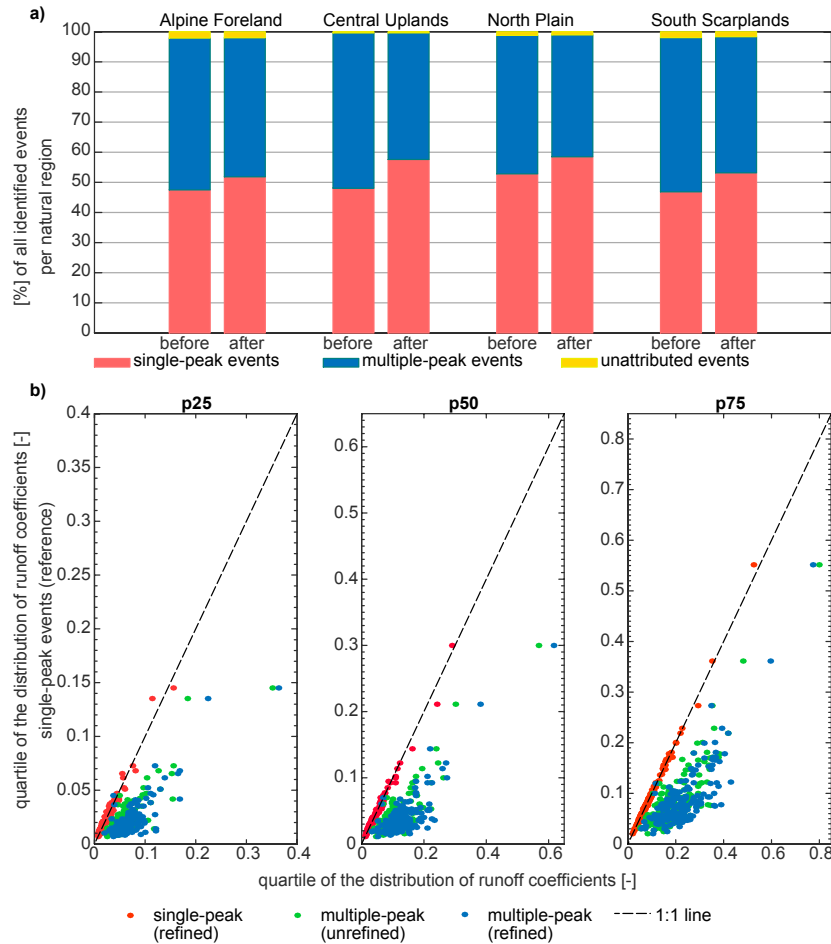


Figure 2.4: Performance of multiple-peak refinement procedure: a) subdivision among single-peak, multiple-peak and unattributed events before and after applying the multiple-peak refinement procedure to catchments of different natural regions. Although, refinement procedure does not directly affect the absolute number of unattributed events, its relative portion might change if total number of identified events is increased after multiple-peak events are refined into their single-peak components; b) quartiles of the distribution of runoff coefficients for unrefined multiple-peak events (obtained after base flow separation and rainfall attribution) and refined single-peak and multiple-peak events (obtained after applying also the multiple-peak refinement procedure) plotted against quartiles of the distribution of runoff coefficients for the reference group of single-peak events. p25 corresponds to a lower quartile (25<sup>th</sup> percentile), p50 corresponds to median and p75 corresponds to the upper quartile (75<sup>th</sup> percentile) of a cumulative probability function of event runoff coefficients

Alpine Foreland region, a strong correlation of the event time scale with this explanatory variable is observed for most catchments (Figure 2.6, *ts-Pvol*). The pre-event base flow rate only slightly affected the event time scale (Figure 2.5, *ts-qbase*), while it is a strong linear predictor of runoff coefficient and peak discharge, especially in the lowlands (Figure 2.6, *rc-qbase*, *peak-qbase*). On the contrary, antecedent rainfall during a period of 10-days shows no correlation with any of the examined event characteristics (Figure 2.6, *Pant10*). No clear relation is also observed between event rise time (*rt*) and the considered rainfall/ snowmelt and pre-event characteristics (see *rt* plots in Figures 2.5 and 2.6).

Figure 2.5 distinctly portrays the existence of a non-linear relation between event runoff coefficient and pre-event soil moisture. An exponential function was fitted in each catchment to the average value of runoff coefficients observed for different ranges of soil moisture (see Chapter 2.3.2.2 and Figure 2.7a). The relation between the scaling exponent of the fitted function and the ratio between Q90 and Q50 (the ratio between low and median flows) was then examined, in order to understand the role played by the subsurface storage of catchments (Figure 2.7). Catchments with large subsurface storage capacity (high Q90/Q50) tend to have lower scaling exponents  $b$  (Figure 2.7b), which reflect a gradual increase of the event runoff coefficient with increasing soil moisture content (Figure 2.7a). On the contrary, in the Central Uplands, South Scarplands and mountainous Alpine regions characterized by poor-developed soils runoff coefficients exhibit minor

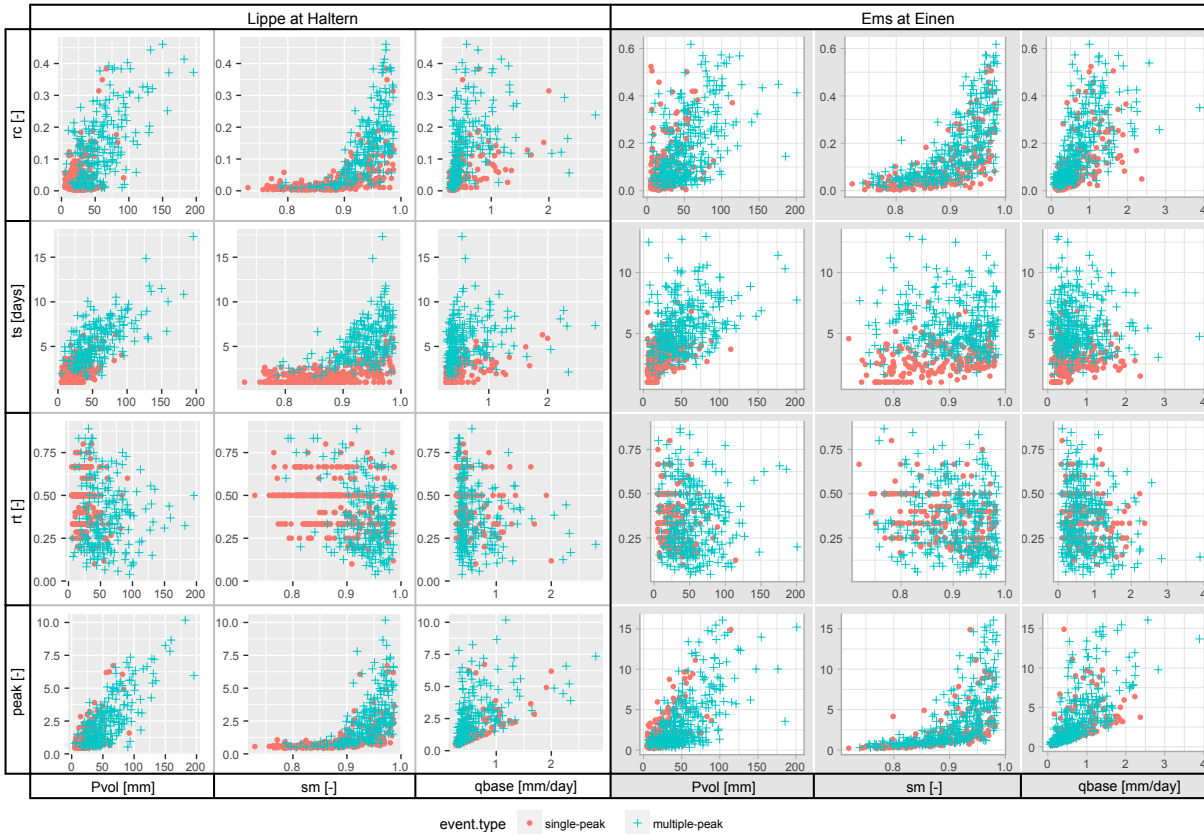


Figure 2.5: Relationship between runoff event characteristics (event runoff coefficient  $rc$ , time scale  $ts$ , rise time  $rt$  and normalized  $peak$ ) and both the rainfall/ snowmelt event volume ( $Pvol$ ) and the indicators of pre-event catchment state (antecedent soil moisture  $sm$  and pre-event base flow  $qbase$ ). Results for the Lippe River at Haltern and the Ems River at Eimen are displayed

variations up to a certain saturation threshold (different for each basin), strongly increasing in both value and variability once this threshold is crossed.

**2.4.2.2 Seasonality of event characteristics** Figure 2.8 shows deviations of the long-term seasonal means of event characteristics from their long-term annual averages, thus providing insights on the seasonality of runoff generation processes in Germany. Our results reveal strong seasonality of event runoff coefficient and normalized event peak for most catchments, with considerably higher values in winter and considerably lower values in summer (Figure 2.8,  $rc$ ,  $peak$ ). This seasonality is especially strong for western catchments where summer runoff coefficients are very low. On the contrary, catchments in the Alpine Foreland exhibit only weak seasonality of event runoff coefficient and normalized event peak. The seasonal pattern of these event characteristics seems to be inversely related to the seasonal values of the aridity index (Budyko, 1974) (Figure 2.8,  $AI$ ), while the seasonality of the soil moisture appears to be shifted (Figure 2.8,  $sm$ ).

Time scales of summer events are also considerably shorter than those of winter and spring events and follow the pattern of snowmelt contribution and soil moisture (Figure 2.8,  $ts$ ,  $sm$ ,  $melt$ ) with the exception of south-eastern catchments where the seasonality is low (Figure 2.8,  $ts$ ). Rise time of winter and spring events was slightly shorter than of summer and autumn events in most study catchments (Figure 2.8,  $rt$ ).

Volume and intensity of rainfall and snowmelt events show asymmetrical seasonal patterns in the Western, North-Eastern and Southern parts of Germany. The maximum of the total precipitation amount occurs in summer for the whole country (Figure 2.8,  $P$ ), but the amount of the runoff generating rainfall is apparently lower in this season than in winter and spring in the Western part (Figure 2.8,  $Pvol$ ), while in the North-Eastern and Southern parts summer events are more pronounced (Figure 2.8,  $Pvol$  and  $Pint$ ).

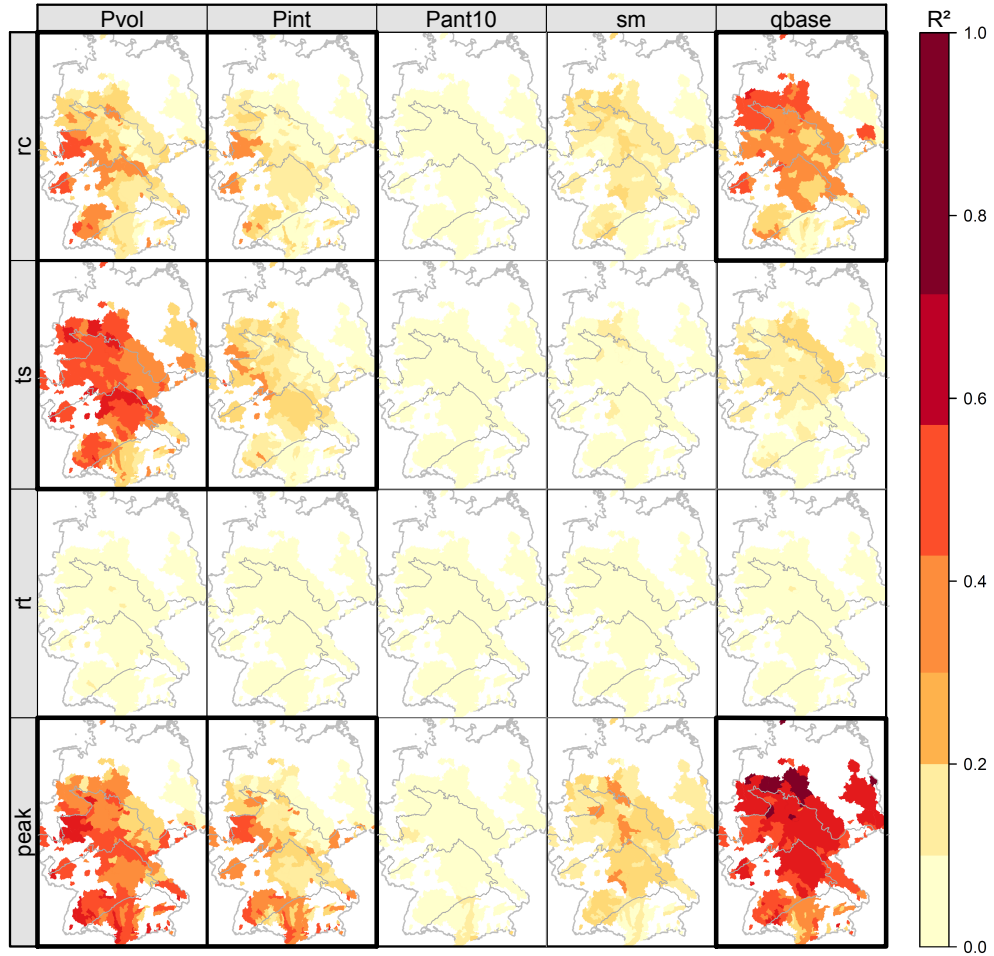


Figure 2.6: Squared Spearman correlation coefficient ( $R^2$ ) between event characteristics (runoff coefficient  $rc$ , time scale  $ts$ , rise time  $rt$ , normalized  $peak$ ) and both the properties of rainfall/ snowmelt events (volume  $Pvol$ , max intensity  $Pint$ ) and the indicators of pre-event catchment state (10-day antecedent rainfall  $Pant10$ , pre-event soil moisture  $sm$  and base flow  $qbase$ ). Higher values of  $R^2$  indicate stronger linear correlation between the two considered variables. Thin grey lines represent the borders of the four main landscape regions of Germany (from north to south): North German Plain, Central Uplands, South German Scarplands and Alpine Foreland. Catchments' borders are not shown for clarity

**2.4.2.3 Long-term trends of event characteristics** Changes of the event runoff response (in terms of event runoff coefficient  $rc$  and time scale  $ts$ ) and their relation with the long-term evolution of hydro-climatic characteristics and land use are analyzed in Figures 2.9 and 2.10. To emphasize the regional patterns the results are grouped according to the four major natural regions of Germany: North German Plain, Central Uplands, South German Scarplands and Alpine Foreland (respectively yellow, green, blue and red markers and ellipses in Figures 2.9 and 2.10). Evidences of consistency between detected changes of event characteristics and their possible drivers (Merz et al., 2012) are investigated by plotting the relative Sen's slope of long-term seasonal trends in event characteristics versus trends in hydro-climatic variables (total precipitation amount  $P$ , aridity index  $AI$ , soil moisture  $sm$ ), properties of rainfall (events' volume  $Pvol$  and maximum intensity  $Pmax$ ) and snowmelt contribution ( $melt$ ) (Figure 2.9-2.10). The relative Sen's slope can be interpreted as the mean change per year in percent of the long-term mean value of the considered variable within the analyzed period (1951-2013). If there is evidence of trend consistency between two variables the points in Figure 2.9-2.10 appear either in the top right and bottom left quadrants (if the variables are directly proportional), or in the two remaining quadrants (if the variables are inversely proportional). If points are dispersed along the  $y$ -axis but constrained within a limited range on the  $x$ -axis, there is no evidence of consistency in trends. The trends for event rise time  $rt$  and normalized event peak discharge  $peak$  are shown in the Supporting Information (see Chapter 2.6.2, Figures 2.11-2.12).

In summer most catchments exhibit decreases of normalized peaks (Figure 2.12,  $peak.summer$ )

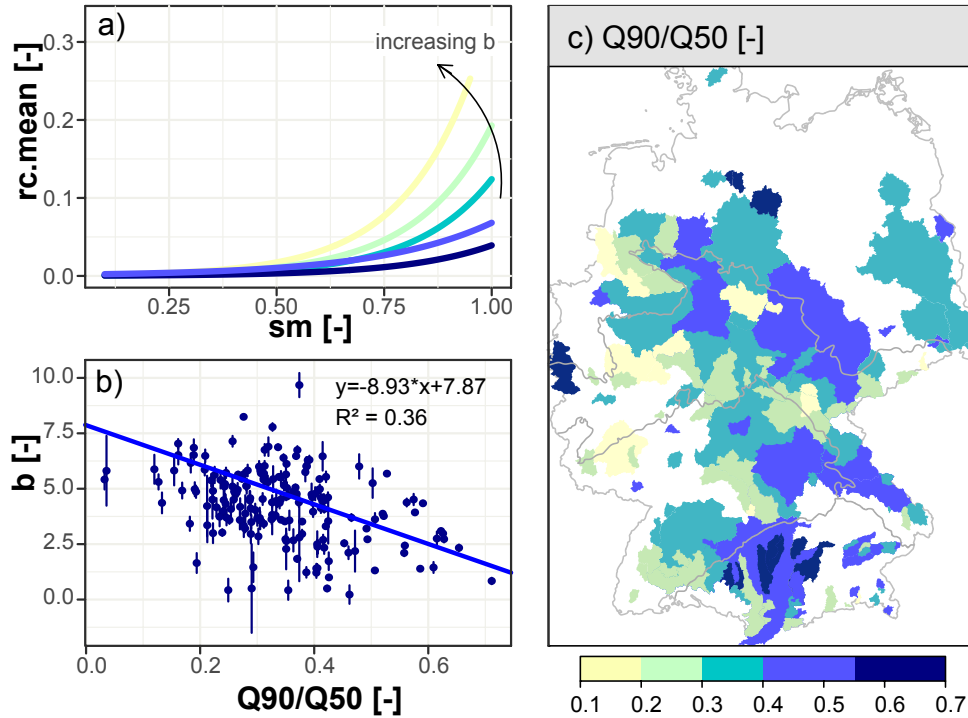


Figure 2.7: Soil moisture as a non-linear control of event runoff coefficient: a) the average of event runoff coefficients corresponding to different soil moisture conditions is represented for selected catchments as an exponential function of soil moisture fitted to them. The lines were color-coded according to the sub-surface storage index (Norbiato et al., 2009) defined as the ratio between Q90 and Q50; b) the exponent parameter  $b$  of the fitted exponential function plotted against the ratio between Q90 and Q50. Lower values of  $b$  characterize a more gradual increase of event runoff coefficients with increasing antecedent soil moisture. Higher values indicate instead a rapid increase of event runoff coefficients. Error bars show the residual standard error of the exponential model for every catchment. The regression line represents the best fit of an error-weighted regression model between scaling exponent and sub-surface storage index; c) spatial pattern of the subsurface storage index in Germany. Thin grey lines represent the borders of the four main landscape regions of Germany (from north to south): North German Plain, Central Uplands, South German Scarplands and Alpine Foreland. Catchments' borders are not shown for clarity

and runoff coefficients which are consistent with the decreasing volume of rainfall events and total amount of precipitation (Figure 2.9,  $rc.summer-Pvol$ ,  $rc.summer-P$ ). Smaller volumes of rainfall events and generally drier conditions (i.e., positive trends in aridity index) also influence flashiness and timing of runoff response, as shown by the negative trends of event time scale (Figure 2.10,  $ts.summer-AI$ ) and positive trends of rise time in all natural regions (Figure 2.11,  $rt.summer$ ). Although in autumn strong negative trends of soil moisture are observed (Figure 2.9,  $rc.autumn-sm$ ), an increase of event runoff coefficients and normalized event peak discharges occurs as the result of increasing volume of rainfall events (see Figure 2.9,  $rc.autumn-Pvol$  and Figure 2.12,  $peak.autumn-Pvol$ ). The situation is different only in the North German Plain, where most of the catchments show negative trends of runoff coefficient and normalized event peak discharge. Changes of characteristic response times are inhomogeneous within natural regions, but negative trends prevail (Figure 2.10, Figure 2.11).

Differently from the other seasons, conditions tend to get wetter in spring, as indicated by the respectively negative and positive trends of the aridity index and the soil moisture (Figure 2.9). Changes in the volume of rainfall events are consistent with trends in runoff coefficients (Figure 2.12,  $rc.spring-Pvol$ ) and normalized peak (Figure 2.12,  $peak.spring-Pvol$ ), except for the North Plain and the catchments of the Alpine Foreland, where considerable changes in the contribution of melting are detected (Figure 2.9,  $rc.spring-melt$ ; Figure 2.12,  $peak.spring-melt$ ).

Winter snowmelt contribution is shrinking in all catchments, while the total amount of precipitation and the volume of rainfall events mostly increase (Figure 2.9,  $rc.winter$ ). Consequently, normalized event peak discharges increase country-wide (Figure 2.12,  $peak.winter$ ). Observed changes in winter runoff coefficients are instead difficult to attribute (Figure 2.9,  $rc.winter$ ). Despite drier

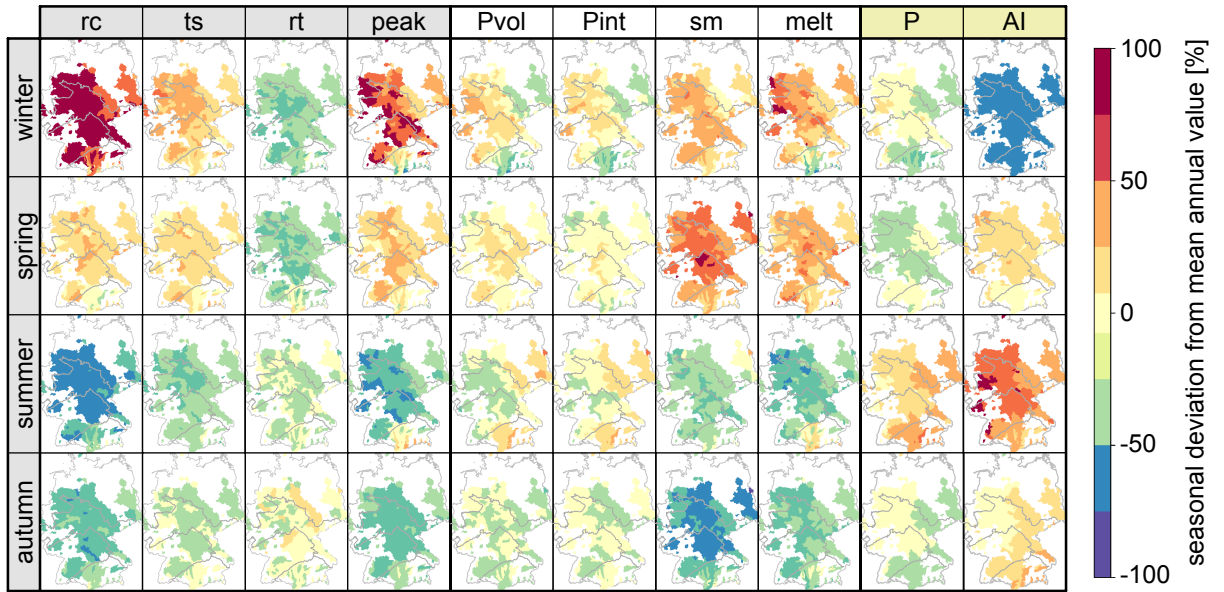


Figure 2.8: Seasonality of event characteristics (*rc*, *ts*, *rt*, *peak*) rainfall and snowmelt properties (*Pvol*, *Pint*, *melt*), pre-vent indicators (*sm*) and hydro-climatic variables (*P*, *AI*). The seasonality was computed as seasonal deviation (%) from the mean annual value of the considered variable. For non-additive variables (aridity index *AI*) the deviation (%) of the mean seasonal value from the mean annual value is shown. For additive variables (total precipitation *P*) the deviation (%) of the cumulative (3 month) seasonal value from the average among the cumulative values for the four seasons is shown. Thin grey lines represent the borders of the four main landscape regions of Germany (from north to south): North German Plain, Central Uplands, South German Scarplands and Alpine Foreland. Catchments' borders are not shown for clarity

conditions in winter (i.e., country-wide positive trends of the aridity index and negative trends of soil moisture), runoff coefficients mostly increase in the Alpine Forelands and Southern Scarplands. On the other hand, runoff coefficients tend to decrease in the North Plain despite an increase of the volume of rainfall events, and both negative and positive trends are detected in the Central Uplands (Figure 2.9, *rc.winter*). Event time scales also reveal varied patterns of change across the country (Figure 2.10, *ts.winter*).

Finally, catchments featuring land use changes larger than 2% of their surface area (represented with dots and triangles in Figures 2.9 and 2.10) exhibit deviations from regionally consistent trends (i.e., climate-induced trends) only in a few cases. For example, a very strong negative trend of the event time scales is detected in autumn for a catchment in the Central Uplands with land use change between 2 and 4% (green circle in Figure 2.10, *ts.autumn*), although there are no apparent differences in rainfall, snowmelt, soil moisture and hydro-climatic trends compared to other catchments from the same region (see the green ellipse representing 95% confidence level, Figure 2.10, *ts.autumn*).

## 2.5 Discussion and Conclusions

An automated time-series-based event separation procedure consisting of available base flow separation, runoff event identification and rainfall attribution methods and of a novel iterative procedure for the adjustment of thresholds needed to identify and separate single-peak components of multiple-peak events was proposed. This procedure was explicitly developed with the goal of facilitating large scale investigation of temporal dynamics of the event runoff response in catchments characterized by diverse morphological attributes and subject to different climatic forcing (the whole of Germany was used as a case study). Five different base flow separation methods were tested. The simple smoothing approach (Institute of Hydrology, 1980) proved to be superior in identifying the starting point of potential runoff events (i.e., troughs) and performed consistently in a wide range of catchments. The other investigated methods (Chapter 2.4.1.1) had problems in lowland catchments with high groundwater contribution and in the Alpine Foreland catchments, where base flow rises in spring due to snowmelt. In fact, according to them streamflow of lowland

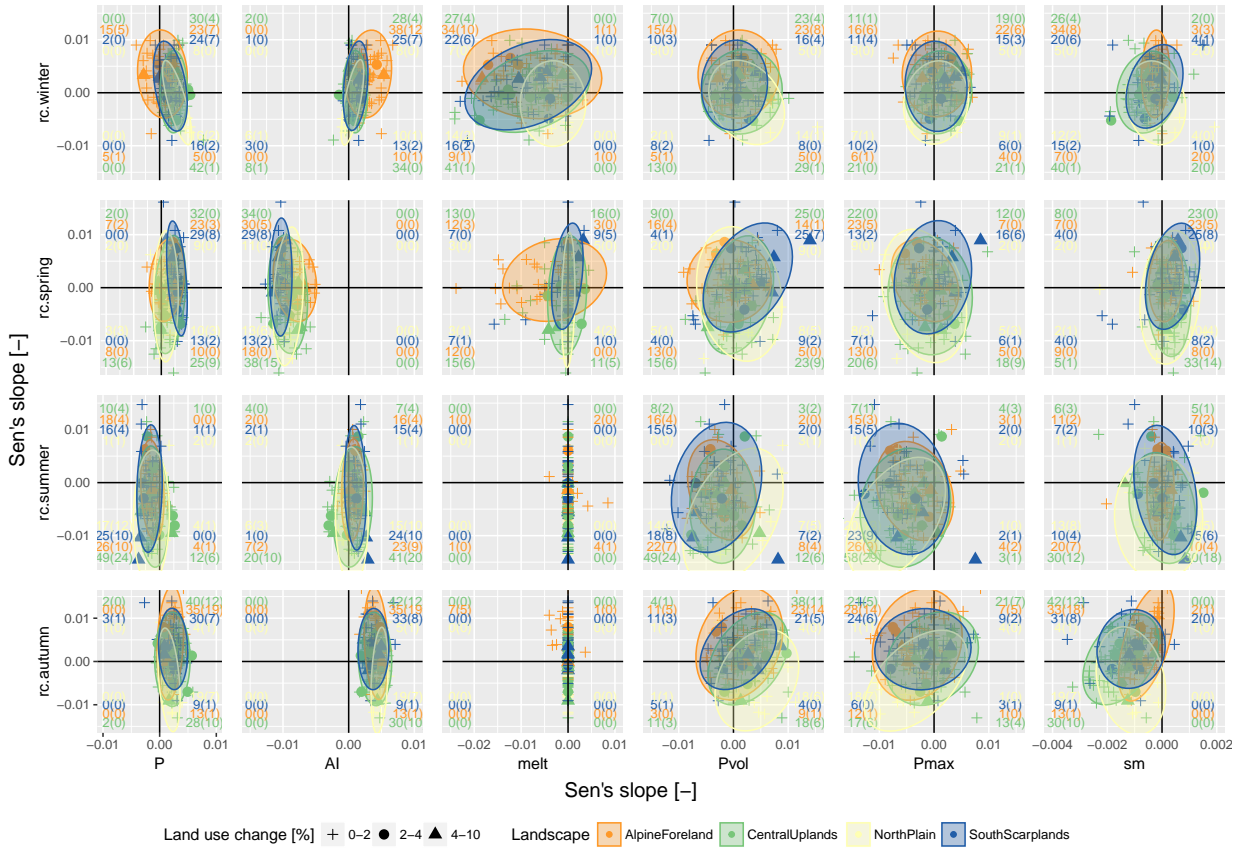


Figure 2.9: Long-term changes of the event runoff coefficient. Seasonal trends of  $rc$  in the period 1951-2013 were plotted against seasonal trends of rainfall properties (volume of rainfall events  $Pvol$ , maximum intensity of rainfall events  $Pmax$ ) and hydro-climatic variables (total precipitation amount  $P$ , aridity index  $AI$ , soil moisture  $sm$ , contribution of snow melt  $melt$ ). Trends were quantified by means of the relative Sen's slope that can be interpreted as the mean change per year in percent of the long-term mean value of the considered variable. Each marker represents a catchment belonging to a specific natural region differentiated by color. The marker's shape indicates the relative change of land use in the catchment from 1990-2012. Color-coded ellipses represent 95% confidence interval of seasonal trends for each natural region. The number of catchments in each quadrant was recorded in the corner of respective quadrant and color-coded according to a specific natural region. The number of catchments with significant trends of event runoff coefficient ( $\alpha = 0.1$ ) was noted in brackets for each quadrant and color-coded according to a specific natural region.

rivers and summer discharge of pre-alpine catchments always have a share of quick flow, thus making an automated separation of runoff events impossible (Merz et al., 2006).

No overlapping rainfall or snowmelt was found for a small portion (ca. 1%) of the identified runoff events. These were mostly small events observed in small and middle-sized catchments. The occurrence of local rainfall events not recorded at any station is a possible reason for this discrepancy, but uncertainty linked to the modeling of melting processes cannot be excluded as well. It is worth to note that, if the minimum peak discharge for quick flow to qualify as a runoff event is set to a value higher than the currently used 10% of the base flow, the above mentioned problem disappears.

The number of sampled events affects the reliability of the distribution equality test used in the iterative procedure to objectively identify suitable separation thresholds. The proposed method is consequently limited by the availability of relatively long hydro-climatic time series. Moreover, the approach is based on the assumption that single-peak and multiple-peaks events have significantly different distributions of event runoff coefficients. Therefore, the method must be applied with care to catchments where runoff is strongly smoothed or event-to-event variability of runoff response is very low.

In this study we used hydro-climatic time series of daily resolution to identify rainfall-runoff events. Daily resolution might limit event identification, especially in small catchments where events are often shorter than 1 day. However, only 13 study catchments have catchment area less than 100

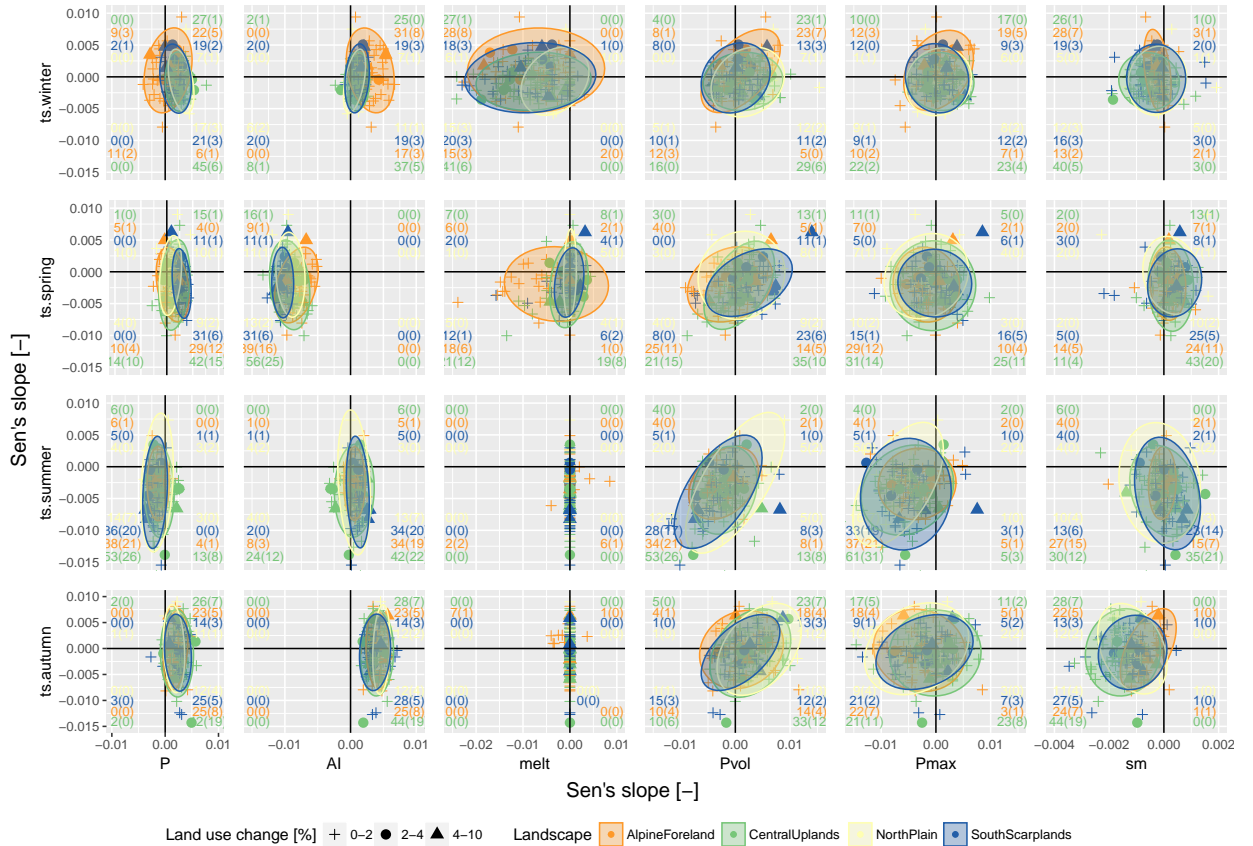


Figure 2.10: Long-term changes of the event time scale. Seasonal trends of  $ts$  in the period 1951-2013 were plotted against seasonal trends of rainfall properties (volume of rainfall events  $Pvol$ , maximum intensity of rainfall events  $Pmax$ ) and hydro-climatic variables (total precipitation amount  $P$ , aridity index  $AI$ , soil moisture  $sm$ , contribution of snow melt  $melt$ ). Trends were quantified by means of the relative Sen's slope that can be interpreted as the mean change per year in percent of the long-term mean value of the considered variable. Each marker represents a catchment belonging to a specific natural region differentiated by color. The marker's shape indicates the relative change of land use in the catchment from 1990-2012. Color-coded ellipses represent 95% confidence interval of seasonal trends for each natural region. The number of catchments in each quadrant was recorded in the corner of respective quadrant and color-coded according to a specific natural region. The number of catchments with significant trends of event runoff coefficient ( $\alpha = 0.1$ ) was noted in brackets for each quadrant and color-coded according to a specific natural region.

$\text{km}^2$ , while most analyzed catchments are mesoscale basins. In addition, the analysis of event dynamics at multiple temporal scales requires long time series. These are not available with finer resolution in a large number of locations. Therefore, we believe that using daily data is suitable for this data set in the context of the objectives of our study. Moreover, daily data can be considered sufficient to represent event characteristics selected for this study as they are based on volumetric ratios of rainfall and runoff (e.g., runoff coefficient, time scale). Event characteristics based on timing of event might be indeed affected by coarse resolution of the available data, which in fact might be the reason why for event rise time no clear drivers were identified among tested variables (Figure 2.6,  $rt$ ).

Although there is no certainty about the real nature (i.e., single- or multiple-peak) of runoff events (Hewlett and Hibbert, 1967), the proposed iterative procedure enabled the identification and attribution of more than 220,000 rainfall-runoff events and consistently addressed the issue of multiple-peak events refinement in catchments characterized by various runoff regimes and different climatic and physiographic properties, thus allowing for a country-wide analysis of the event runoff response.

The study of the event-to-event variability of runoff event characteristics at this large scale unveiled the existence of different runoff generation mechanisms in Germany. The dominance of the rainfall/ snowmelt event volume compared to its intensity as a driver of event runoff coefficients indicates that Dunnian processes prevail in the studied catchments. This is in line with what found

by Merz et al. (2006); Graeff et al. (2012) and Seibert et al. (2016), who reported similar results for several mesoscale European catchments. Event runoff generation through infiltration excess as the result of intensive rainfall seems to be only possible in small mountainous catchments in the Western part of the country where intensive rainfall events are common. Rainfall intensity was identified as an important driver of runoff response in single mountainous catchments also by previous studies (e.g., Blume et al., 2007; Graeff et al., 2012). A particularly strong relation between event runoff coefficients and volume of rainfall events exist in the Central Uplands and South German Scarplands (Figure 2.6), indicating that in these regions event-fed saturation is possible (i.e., a single rainfall event can lead to partial or full catchment saturation and thus cause increase of the event runoff coefficient) (Berghuijs et al., 2016b). For drier hilly and lowland catchments with higher storage capacity pre-event saturation (i.e., catchment saturation caused by a sequence of antecedent rainfall or snowmelt events) is instead the main mechanism of event runoff generation, as it is here unlikely that a single rainfall/ snowmelt event will lead to catchment saturation. These catchments show a characteristic gradual increase of the event runoff coefficient with increasing soil moisture content (i.e., a very slow transition between “dry” and “wet” states) (Figure 2.7a, low parameter  $b$ ). These findings are similar to those of Norbiato et al. (2009), who showed that the difference between mean runoff coefficients of “dry” and “wet” states was minimal in the catchments with highly permeable aquifers. On the contrary, in the Central Uplands and mountainous Alpine catchments with poor-developed soils the event runoff coefficient increases rapidly as soil saturation rises (Figure 2.7a, high parameter  $b$ ), marking a clear transition between two functioning types. A threshold-like dependence between event runoff coefficients and antecedent soil moisture might be an indicator of a critical switch in the catchment behavior, in correspondence of which the hydrologic connectivity and its characteristic pattern change (James and Roulet, 2007; Graeff et al., 2012). Our results also indicate that, unlike antecedent soil moisture and pre-event base flow, the amount of rainfall in the 10 days preceding runoff events do not well represent the wetness state of German catchments (Figure 2.6). Taking into account the strong seasonality of the event runoff coefficients (Figure 2.8), antecedent rainfall computed during a longer time range (30-60 days) might be a more suitable proxy of wetness state (Merz and Blöschl, 2009a). Similarly to Gaál et al. (2012) we found that the time scale of runoff events depends on properties of rainfall events (Figure 2.6,  $ts$ ). Weaker correlation in the Alpine Foreland catchments indicates that the time scale of rainfall events is instead strongly altered by the storage capacity and mechanisms of water release of these catchments. Our results also suggest that the event rise time may be governed by the spatial distribution of rainfall within the basin, which was not characterized by the basin-averaged rainfall characteristics we used here.

The seasonal analysis of rainfall-runoff event characteristics and their potential drivers confirms that event runoff response is directly defined by the properties of rainfall events (i.e., volume or intensity) only in the western part of the Central Uplands and in the South German Scarplands (Figure 2.8), while in the rest of the country seasonal event characteristics are defined by the seasonality of the water balance components (i.e., ratio of precipitation and evapotranspiration) and contribution of snowmelt (Figure 2.8). Interestingly, the analysis shows conflicting seasonality of total precipitation amount (Figure 2.8,  $P$ ) and runoff generating precipitation (Figure 2.8,  $P_{vol}$  and  $P_{int}$ ) in the Western part of Germany. Furthermore, in the Northeast German Plain and Alpine Foreland the maximum of the runoff generating rainfall occurred in summer and spring (Figure 2.8,  $P_{vol}$ ), while event runoff coefficients (Figure 2.8,  $rc$ ) were higher in winter, indicating a crucial role of pre-event saturation compared to event-fed saturation for runoff generation processes in these regions. Alpine Foreland catchments noticeably exhibit almost no seasonality of event characteristics (Figure 2.8). This can be explained by a seasonal change of the main drivers of runoff, e.g., very wet conditions during winter, a strong contribution of snowmelt in spring/summer and intensive rainfall events in the summer/autumn period.

Interestingly, while Merz and Blöschl (2009a) showed that in Austria the seasonality of event runoff coefficients follows the seasonal pattern of soil moisture, these seem to be shifted in Germany (Figure 2.8,  $sm$ ). The difference is possibly due to the existence of a pronounced winter runoff regime in most of Germany (Beurton and Thieken, 2009) versus the spring and summer runoff regime of Austria triggered by snow and glaciers melt from the Alps (Merz and Blöschl, 2009a). On the other



hand, the long event time scales for German catchments during spring revealed by our analysis can be explained (similarly to Austria, see Gaál et al. (2012)) by melting in mountainous regions (Figure 2.8, *melt*), while in winter high values might be linked to long rainfall events with large volumes (Figure 2.8, *Pvol*) resulting from westerly wind dynamics and Atlantic cyclones influences (Beurton and Thieken, 2009).

The pronounced seasonality of event characteristics and drivers defines their season-specific long-term changes (Figure 2.9-2.10). Seasonal indicators of wetness state (i.e., aridity index and soil moisture) and snowmelt contribution especially display marked trends. Melt contribution is clearly shrinking, whereas the total volume of precipitation mostly increases (Figure 2.9). According to Blöschl et al. (2017), season-specific changes might be the result of changes in seasonal dynamic of melting or in precipitation type (from solid to liquid). There is no clear consistency between trends of runoff event characteristics and a single hypothesized driver (Figure 2.9-2.10), but hints of consistency can be identified when several potential drivers are considered together. Changes in total precipitation amount alone do not explain the magnitude of changes in event characteristics (Figure 2.9-2.10). However, snowfall-to-rain transition can be a driving force of runoff response change even when no trends in total precipitation exist (Dumanski et al., 2015). Our findings hint at the existence of a complex interplay between changes in volume of rainfall events, soil moisture and snowmelt contribution. In catchments where storage capacity is limited (e.g., Central Uplands, South Scarplands) and infiltration excess or event-fed saturation dominates, a more pronounced influence of rainfall volume changes on event characteristics is noticeable in most seasons (Figure 2.9). On the contrary, changes of the seasonal wetness state define trends in the North Plain catchments characterized by large subsurface storages. Moderate changes of land use in most catchments (less than 2% of their surface area) might explain the observed overwhelming role played by climatic characteristics in driving the non-stationarity of the runoff response. In fact, Martin et al. (2012) reported that the effect of urbanization on runoff response can be detected only if more than 15% of the catchment area has been modified. Interestingly, land use change mostly impacts event time scale and rise time, whereas no clear effects on normalized event peak and runoff coefficient are observed. Difficulties to attribute changes of the hydrological response to land use modifications were also reported by Sawicz et al. (2014), who found only minor evidence of a consistent relation between land use change and long-term trends of runoff signatures derived from water balance.

In this study we exploit observed temporal dynamics of runoff event characteristics derived from readily available hydrological and meteorological time series to provide insights on regional processes of runoff generation. By proposing an iterative procedure to objectively adjust separation thresholds our study allows for comparison of event characteristics on multiple temporal and at large spatial scales. Temporal dynamics of event characteristics reveal underlying regional patterns of dominant runoff generation processes. Climatic and landscape drivers of these patterns are examined in detail in a companion study by Tarasova et al. (2018a). Regional heterogeneity in runoff generation processes also defines patterns of response to changes of rainfall event characteristics and water balance components. Generally, catchments dominated by infiltration excess and event-fed saturation (Figure 2.9, Central Uplands and South Scarplands) are more vulnerable to changes of rainfall characteristics. In these catchments flow paths vary greatly among events and eventually lead to erratic patterns of water and nutrients delivery to streams. Observed changes of rainfall characteristics are instead buffered by the available catchment storage in catchments where event runoff generation depends on pre-event saturation (Figure 2.9, North Plain and Alpine Foreland). Here evapotranspiration might play a much more important role as it affects available storage. Their characteristic gradual switching from “dry” to “wet” states might shape more constant flow paths and thus results in a more persistent supply of water and nutrients to streams. Identifying temporal dynamics of the hydrologic response and highlighting regional diversities of runoff generation processes is therefore directly relevant for the management of water resources, the mitigation of human impacts on water quality of rivers and on their aquatic ecosystems, as well as for adaptation to changing flood hazard.

## 2.6 Supporting Information

This Supporting Information give details on the test of distribution equality used in the iterative procedure of multiple-peak event refinement described in the Chapter 2.3.1.4. Moreover additional information on the long-term trends of event characteristics is presented.

### 2.6.1 Test of the distribution equality

Considerable differences in event characteristics between single-peak and multiple-peak events were previously indicated by Mei and Anagnostou (2015) and Tang and Carey (2017). Therefore, we assumed that the single-peak and multiple-peak events have significantly different distributions of event runoff coefficients and we composed the empirical distribution of runoff coefficients of potentially single events derived from multiple-peak events and the reference distribution of single-peak events in order to decide if the current separation thresholds were suitable for the study catchment. To assess the equality of the two distributions and hence the suitability of the chosen thresholds we applied a non-parametric Kolmogorov-Smirnov test of the equality (Haan, 1977) at 5% significance level. The size of the samples used to estimate the distributions is crucial for the equality test (Haan, 1977). To avoid accepting the hypothesis when it is in fact wrong we restricted the application of the test to the sample sizes complying with the following rule of thumb:

$$(n_1 * n_2)/(n_1 + n_2) \geq 4 \quad (2.1)$$

where  $n_1$  and  $n_2$  are sample sizes of the reference single-peak event group and of the group of potentially single events.

### 2.6.2 Long-term trends of the event characteristics

Changes of the event runoff response in terms of event rise time and normalized peak discharge and their relation with the long-term evolution of hydro-climatic characteristics and land use are analyzed in Figures 2.11-2.12. To emphasize the regional patterns the results are grouped according to the four major natural regions of Germany: North German Plain, Central Uplands, South German Scarplands and Alpine Foreland (respectively yellow, green, blue and red markers and ellipses in Figures 2.11-2.12). Evidences of consistency between detected changes of event characteristics and their possible drivers (Merz et al., 2012) are investigated by plotting the relative Sen's slope of long-term seasonal trends in event characteristics versus trends in hydro-climatic variables (total precipitation amount  $P$ , aridity index  $AI$ , soil moisture  $sm$ ), properties of rainfall (events' volume  $Pvol$ , maximum rainfall intensity  $Pmax$ ) and snowmelt contribution ( $melt$ ) (Figure 2.11-2.12). The relative Sen's slope can be interpreted as the mean change per year in percent of the long-term mean value of the considered variable within the analyzed period (1951-2013). The significance of trends was defined at significance level for Kendall's  $p$ -value. If there is evidence of trend consistency between two variables the points in Figure 2.11-2.12 appear either in the top right and bottom left quadrants (if the variables are directly proportional), or in the two remaining quadrants (if the variables are inversely proportional). If points are dispersed along the  $y$ -axis but constrained within a limited range on the  $x$ -axis, there is no evidence of consistency in trends.

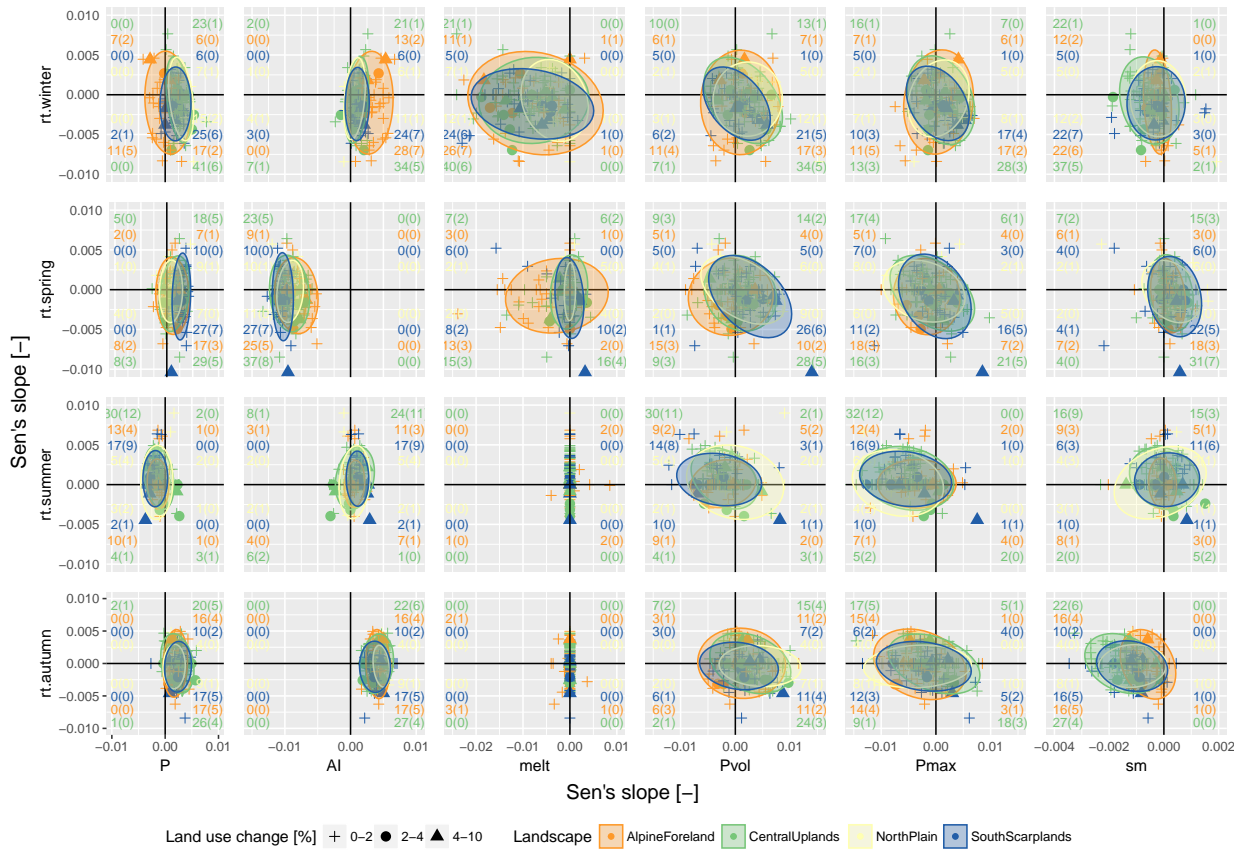


Figure 2.11: Long-term changes of the event rise time. Seasonal trends of  $rt$  in the period 1951-2013 were plotted against seasonal trends of rainfall properties (volume of rainfall events  $Pvol$ , maximum intensity of rainfall events  $Pmax$ ) and hydro-climatic variables (total precipitation amount  $P$ , aridity index  $AI$ , soil moisture  $sm$ , contribution of snow melt  $melt$ ). Trends were quantified by means of the relative Sen's slope that can be interpreted as the mean change per year in percent of the long-term mean value of the considered variable. Each marker represents a catchment belonging to a specific natural region differentiated by color. The marker's shape indicates the relative change of land use in the catchment from 1990-2012. Color-coded ellipses represent 95% confidence interval of seasonal trends for each natural region. The number of catchments in each quadrant was recorded in the corner of respective quadrant and color-coded according to a specific natural region. The number of catchments with significant trends of event runoff coefficient ( $\alpha = 0.1$ ) was noted in brackets for each quadrant and color-coded according to a specific natural region.

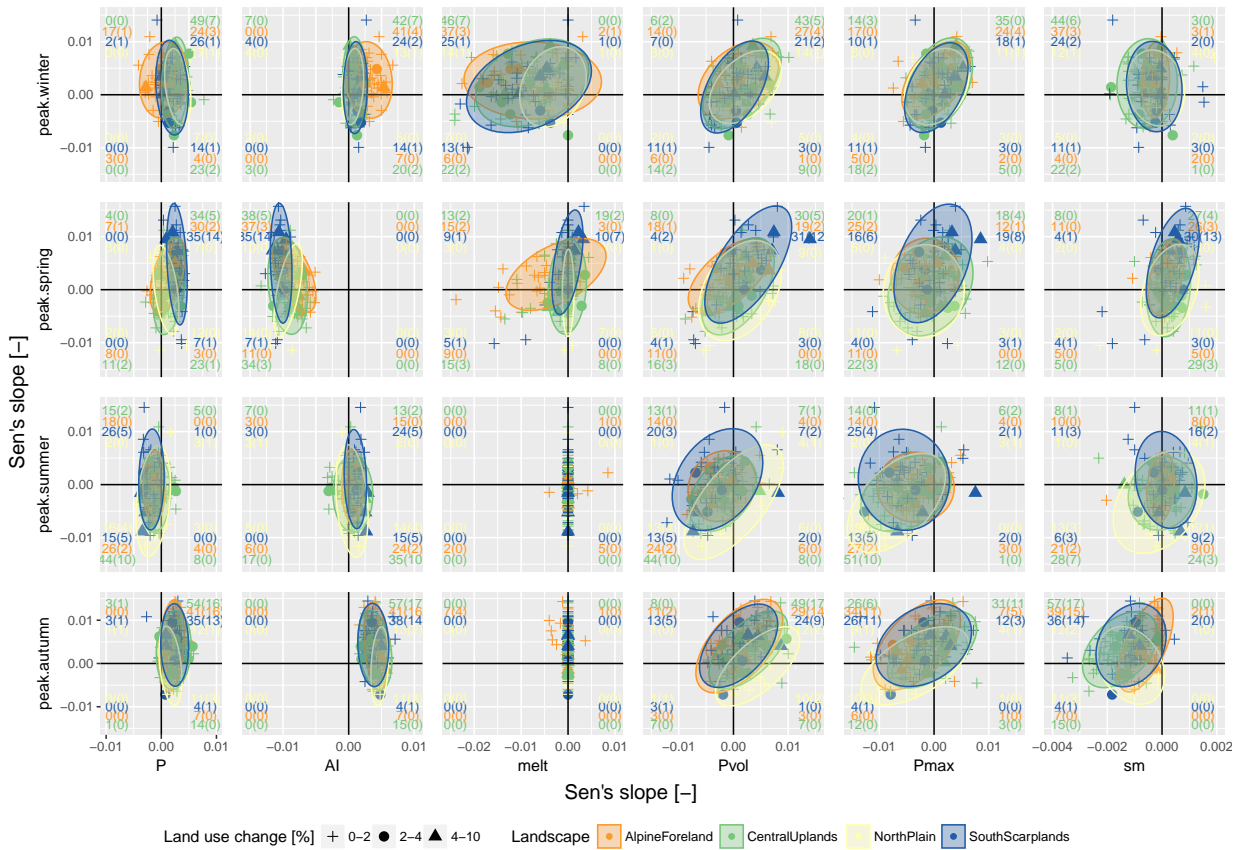


Figure 2.12: Long-term changes of the normalized event peak discharge. Seasonal trends of *peak* in the period 1951-2013 were plotted against seasonal trends of rainfall properties (volume of rainfall events *Pvol*, maximum intensity of rainfall events *Pmax*) and hydro-climatic variables (total precipitation amount *P*, aridity index *AI*, soil moisture *sm*, contribution of snow melt *melt*). Trends were quantified by means of the relative Sen's slope that can be interpreted as the mean change per year in percent of the long-term mean value of the considered variable. Each marker represents a catchment belonging to a specific natural region differentiated by color. The marker's shape indicates the relative change of land use in the catchment from 1990-2012. Color-coded ellipses represent 95% confidence interval of seasonal trends for each natural region. The number of catchments in each quadrant was recorded in the corner of respective quadrant and color-coded according to a specific natural region. The number of catchments with significant trends of event runoff coefficient ( $\alpha = 0.1$ ) was noted in brackets for each quadrant and color-coded according to a specific natural region.

---

### 3 Exploring Controls on Rainfall-Runoff Events: Regional Patterns and Spatial Controls of Event Characteristics in Germany

This Chapter presents a formatted version of the original paper: **Tarasova, L.**, Basso, S., Poncelet, C., and Merz, R. (2018). Exploring controls on rainfall-runoff events: 2. Regional patterns and spatial controls of event characteristics in Germany. *Water Resources Research*, 54 (10), 7688–7710. <https://doi.org/10.1029/2018WR022588>, with permission from Wiley (Copyright 2018 Wiley).

**Own contribution:** The manuscript was drafted by Larisa Tarasova, who also prepared catchment descriptors, separated rainfall-runoff events, performed the analysis and interpreted the results under supervision of Stefano Basso and Ralf Merz. Carine Poncelet has prepared the hydrometeorological data.

**Acknowledgment and Data:** The financial support of the German Research Foundation (DFG) in terms of the research group FOR 2416 “Space-Time Dynamics of Extreme Floods (SPATE)” and Helmholtz Centre for Environmental Research – UFZ is gratefully acknowledged. We thank Charles Luce, Beverly Wemple, Alberto Montanari and three anonymous reviewers for their valuable suggestions and critiques that helped to improve the manuscript. For providing the discharge data for Germany, we are grateful to: LfU, Baden-Württemberg Office of Environment, Measurements and Environmental Protection (LUBW), Brandenburg Office of Environment, Health and Consumer Protection (LUGV), Saxony State Office of Environment, Agriculture and Geology (SMUL), Saxony-Anhalt Office of Flood Protection and Water Management (LHW), Thüringen State Office of Environment and Geology (TLUG), Hessian Agency for the Environment and Geology (HLUG), Rhineland Palatinate Office of Environment, Water Management and the Factory Inspectorate (LUWG), Saarland Ministry for Environment and Consumer Protection (MUV), Office for Nature, Environment and Consumer Protection North Rhine-Westphalia (LANUV NRW), Lower Saxony Office for Water Management, Coast Protection and Nature Protection (NLWKN), Water and Shipping Management of the Fed. Rep (WSV), the European Water Archive (EWA) and the GRDC (<http://www.bafg.de/GRDC>). Our thanks go to Luis Samaniego and Matthias Zink for the simulations of the mHM (<http://www.ufz.de/index.php?en=41160>). Climatic data can be obtained from the DWD (<ftp://ftp-cdc.dwd.de/pub/CDC/>). Soil and geology data are provided by the BGR (<http://www.bgr.bund.de>) or retrieved from Harmonized World Soil Dataset (HWSD) (<http://webarchive.iiasa.ac.at/Research/LUC/>). Land use data is available as CORINE2000 dataset (<http://www.eea.europa.eu/data-and-maps/>). The digital elevation model can be obtained from SRTM (<http://www.cgiar-csi.org/data/>).

#### Abstract

This study unveils regional patterns of rainfall-runoff event characteristics in Germany and identifies their spatial controls. Characteristics describing mean value, variability and seasonality of event runoff coefficient, time scale, rise time, and of the occurrence of multiple-peak events are derived for a set of 196,073 rainfall-runoff events observed in 401 mesoscale German catchments. Multi-objective performances of various variable selection methods are used to identify hydrologically-relevant variables from a comprehensive set of 115 descriptors of climate, topography, geomorphology, soil, land use, hydrogeology and geology for every catchment. Results show that although event characteristics have relatively clear regional patterns due to the dominance of climatic controls at regional scale, subsurface properties (i.e., catchment storage) play a considerable role for the prediction of event runoff response. Compared to other tested variable selection methods the application of a backward elimination procedure allows for the most accurate prediction of spatial patterns and regionalized values of event characteristics identifying soil depth, hydraulic permeability and frequency, size and seasonality of wet spells as hydrologically-relevant catchment descriptors. Climatic and hydrogeological descriptors outperform other generic groups of catchment descriptors. The hydrological interpretation of the emergent regional pattern of event characteristics, their variability and seasonality provides insight on archetypical catchment behaviors and their controls.

### 3.1 Introduction

Understanding why certain functioning behaviors occur in given river basins sheds light on the origin of similarity and dissimilarity among catchments and is the key for understanding hydrological processes at catchment scale (Sawicz et al., 2011). Event hydrographs are among the most detailed signatures of how catchments behave, revealing aspects of their internal states and dynamics (Blöschl et al., 2013b). Analyzing the immediate response of catchments to rainfall inputs allows for deeper insights into the properties of triggering rainfall events, runoff generation mechanisms and routing processes (Merz et al., 2006; Blume et al., 2007). Exemplary hydrological behaviors of two contrasting catchments are displayed in Figure 3.1. A drier catchment with infrequent but sometimes substantial rainfall events is shown on the left side. The subsurface storage capacity is small and vegetation is sparse. Direct runoff is only generated in smaller parts of the catchment. Hence sharp event hydrographs with lower on average but variable event runoff coefficients are expected. The catchment on the right side represents instead a wetter densely vegetated catchment with frequent rainfall events and substantial subsurface storage. Such catchment structure may determine smooth event hydrographs with long rise time and time scale. Depending on the frequency of rainfall, event hydrographs with multiple peaks may be observed. Larger on average but less variable runoff coefficients result from larger saturated areas and low variability of soil moisture conditions. In both cases inter-event drying of soils due to evapotranspiration and vertical percolation into deeper subsurface layers control the antecedent soil moisture and therefore impose a feedback on the variability of event characteristics. Moreover, if rainfall and evaporation have strong seasonality, event characteristics may mirror this seasonality as well (Merz and Blöschl, 2009a). Furthermore, topography, vegetation cover, soil properties, hydrogeological settings and many other physical attributes also shape runoff generation and hence event runoff characteristics (Gaál et al., 2012). Hence, event hydrographs may also summarize patterns of catchment response emerged from complex co-evolution of climate, topography, soil and vegetation, thus standing out as valuable hydrological signatures of catchment behaviors Blöschl et al. (2013b).

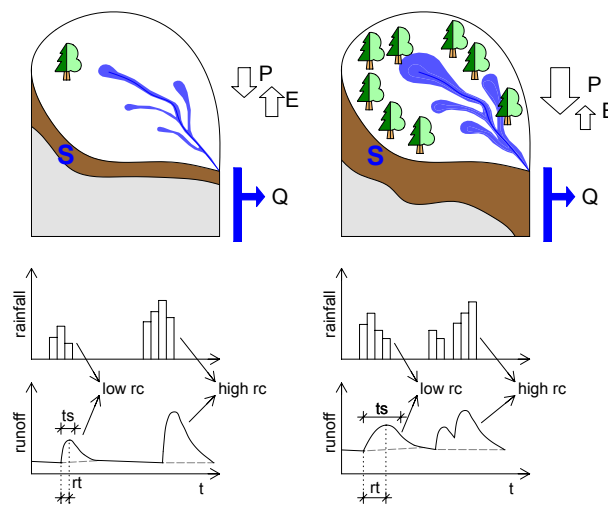


Figure 3.1: Example of two contrasting catchments with different climatic conditions ( $P$  – annual precipitation,  $E$  – annual potential evaporation, physical characteristics (storage capacity, vegetation) (upper panel) and hydrological response (lower panel). The extents of pre-event saturated areas (dark blue areas) represent typical runoff generation conditions in each catchment. The hydrological response of each catchment is presented for two different rainfall events (middle panel). Each event can be described by the event characteristics  $rc$  (event runoff coefficient [-]),  $ts$  (event time scale [days]),  $rt$  (event rise time [-]) (lower panel)

Although the concept of event runoff dates back to the work of Sherman (1932), analyzing event runoff generation processes is still an active research field in hydrology. Many of the studies published in the literature, either based on field measurements (e.g., Weiler and McDonnell, 2004; Tromp-Van Meerveld and McDonnell, 2006; Scherrer et al., 2006; dos Santos et al., 2016; Ries et al., 2017) or hydrological modelling (e.g., Vivoni et al., 2007; Frei et al., 2010; Sinha et al., 2016; Ala-aho et al., 2017), focus on runoff generation at small scales, such as irrigation plots, hillslopes

or single catchments. These studies point to a great variability of the factors controlling runoff generation during rainfall events, but results are site and scale specific.

In order to investigate catchment-scale generation of event runoff, individual events separated from continuous streamflow time series (Blume et al., 2007) are attributed to their rainfall triggers and characterized by means of dimensionless variables (e.g., event runoff coefficient, time scale and rise time) (Merz and Blöschl, 2009a; Gaál et al., 2012). Links among event characteristics and climate and landscape features are then searched to provide insights on the physical drivers of the event runoff response.

However, a limited number of studies exist that analyze event characteristics of large samples of river basins. A countrywide study of several hundred Austrian catchments ranging from high alpine snow-dominated to drier lowland catchments by Merz and Blöschl (2009a) showed that climate imposes a first-order control on the event runoff coefficient, whereas land use, soil types and geological classes have minor importance. Norbiato et al. (2009) reported that although climatic descriptors (e.g., long-term mean annual precipitation) are the most important explanatory variables of the spatial variability of event runoff coefficients in alpine Italian catchments, also geology (i.e., permeability index) plays an important role in drier catchments. Differences among event runoff coefficients observed in 17 alpine Swiss catchments are instead primarily explained by topographic characteristics, drainage density and geology (Gottschalk and Weingartner, 1998). Finally, although event time scales are primarily a function of climate processes in most Austrian catchments (Gaál et al., 2012), they were also found to be a byproduct of geological structure, soil type and geomorphological properties in some cases.

Despite these studies provide a deeper insight on runoff controls in several catchments, they all focus on the alpine region and therefore their results may be difficult to generalize for other landscapes and climates. The presence in alpine environments of a clear topographically-induced precipitation gradient coinciding with changes of subsurface storage capacity and land use is likely to result in strong links of event characteristics with climatic or topographical variables. A wider and more heterogeneous set of catchments and climate types is required for more comprehensive analyses and sound results. Additionally, not only characteristic values but also variability and seasonality of event runoff coefficients and time scales should be examined as hydrological signatures, since they might help to clarify the role played by catchment storage capacity.

Identification of the settings that determine certain runoff responses usually involves the analysis of landscape and climate descriptors of the considered catchments. The choice of the set of catchment descriptors to be used in the analysis is a somehow subjective matter, often influenced by data availability and by the researchers' perspectives on what are the relevant variables. An examination of 42 manuscripts published from 1989 to 2009 revealed the use of 66 unique climatic variables, 72 topographic and geomorphologic characteristics, 15 land use classes and 98 soil properties (Ssegane et al., 2012a). The most frequently used variables were catchment area, mean elevation and mean annual precipitation. The least used were soil properties, although their importance is widely recognized (Oudin et al., 2010). The hydrological relevance of the selected descriptors is then normally tested by the strength of their link with signatures of runoff behavior and is quantified by means of different methods ranging from empirical inference (e.g., Sawicz et al., 2011) to bivariate correlations (e.g., Merz and Blöschl, 2009a; Gaál et al., 2012), stepwise regression models (e.g., Ssegane et al., 2012a) and cluster similarity (e.g., Di Prinzio et al., 2011; Ley et al., 2011; Razavi and Coulibaly, 2013). It is worth to notice that a-priori choice of catchment descriptors may significantly affect the conclusions of the studies (Ssegane et al., 2012a). Reducing the dimensionality of the available set of catchment descriptors by means of multivariate analysis (e.g., Principal Component and Canonical Component Analysis) and variable selection methods (e.g., Olden and Poff, 2003; Di Prinzio et al., 2011) has the purpose of minimizing their redundancy and identifying relevant catchment descriptors able to characterize regional hydrologic behaviors (Ssegane et al., 2012b). The performance measures used by the variable selection methods largely depends on the scope of the application (i.e., process understanding, identification of homogeneous hydrological regions, regionalization). Studies aiming at process understanding often opt for simple one-dimensional correlation approaches applied to small sets of subjectively pre-defined catchment descriptors (Ssegane et al., 2012b). This causes discrepancies among studies

and may undermine accurate predictions (Olden and Poff, 2003), thus leading to fragmented and contradictory information regarding spatial controls of runoff response.

The purpose of this study is to analyze regional patterns of runoff response in the whole of Germany using event characteristics as hydrological signatures, and to identify their spatial controls. Specifically, we address the following research questions:

- What are the spatial controls of event characteristics in a wide range of catchments encompassing different landscape and climatic regions?
- Which generic group of catchment descriptors (e.g., climate, topography, soil properties, land use or hydrogeology) is the most informative for understanding spatial variability and predicting event characteristics? Which variable selection method is appropriate for identification of relevant catchment descriptors?
- Can emergent regional patterns of event characteristics be explained from a hydrological point of view, and do they provide inference regarding dominant runoff generation mechanisms?

In this work we apply the concept of comparative hydrology. As Sivapalan (2009) suggested: “Instead of attempting to reproduce the response of individual catchments, research should advance comparative hydrology, aiming to characterize and learn from the similarities and differences between catchments in different places, and interpret these in terms of underlying climate-landscape-human controls.” To do so, we analyze event characteristics (Chapter 3.3.1) from 196,073 rainfall-runoff events separated from hydro-climatic time series observed in 401 German catchments using the event separation method described in Tarasova et al. (2018b) (Chapter 3.3.2). To reduce the effect of subjective pre-defined choices of hydrologically-relevant climate and landscape characteristics we select them from the widest possible set of catchment descriptors belonging to generic groups usually adopted in regional studies (Chapter 3.2) by means of different variable selection methods (Chapter 3.3.4.2) and performance measures (Chapter 3.3.4.3 and 3.4.3.2). Controlling climate and landscape characteristics are assumed to be those which allow for reproducing spatial clustering of catchments with similar event characteristics (Di Prinzio et al., 2011) and for predicting values of event characteristics in a regionalization experiment. In Chapter 3.5.3 we merge and interpret the results of the performed data-based analysis of emergent regional patterns of event characteristics and their spatial controls with the findings of the companion study of Tarasova et al. (2018b) on temporal dynamics of event runoff response, and illustrate archetypical catchment structures and behaviors from a hydrological point of view.

In light of the discussion above, we believe that runoff event characteristics are a valuable fingerprint of catchment behavior that synthesizes internal states and dynamics of a catchment (Blöschl et al., 2013b). Analyzing their spatio-temporal patterns might provide more insight into similarities and dissimilarities of catchments’ response to rainfall, and hence help to improve regionalization approaches based on physical similarity and regional conceptual rainfall-runoff modeling, where the choice of model structure is challenged by simplicity and appropriate representation of the dominant runoff processes in the study area (Fenicia et al., 2008). Moreover, understanding regional heterogeneities of the runoff response and of its drivers might provide insights on the heterogeneity of flood generation processes and on the physical controls of flood hazard (Rogger et al., 2013).

## 3.2 Data and study area

The study area is the whole of Germany. The western part of the country is influenced by maritime climate with prevailing westerly circulation patterns. Their influence decreases toward the East, where a more continental climate dominates. The orographic effect of the Central Uplands and the Alps plays an important role in shaping spatial patterns of precipitation (Figure 3.2b). Germany has four major landscape regions (Figure 3.2a): the North German Plain, Central Uplands, South German Scarplands and Alpine Forelands. The North German Plain was formed by glacial and periglacial geomorphologic processes which resulted in a very flat landscape with porous permeable aquifers (Figure 3.2c). The eastern part of the lowlands has multiple lakes left behind during



glaciers' retreat, while the western part is intensively used for agricultural purposes (Figure 3.2d). The Central Uplands belong to the oldest mountains in Europe and exhibit a wide variety of forms due to the long-term effects of different erosion processes. Different types of aquifers (e.g., fractured, karstic) and aquitards can be found here (Figure 3.2c). The South German Scarplands, adjacent to the Upper Rhine and Main Valley (Figure 3.2a), are characterized by escarpments. Exposure of limestone due to the uplift led to considerable karstification (e.g., in the Black Forest). The Alpine Forelands were shaped during the Ice Age and comprise different geologic formations (Figure 3.2c). The south boundary of the Alpine Foreland is a narrow strip of the Bavarian Alps, which are part of the Northern Limestone Alps with karstic aquifers (Figure 3.2c) and several lakes of glacial origin (Figure 3.2a). Catchments of the Alpine Foreland drain through the Danube to the Black Sea. All other German catchments drain either to the North or to the Baltic Sea.

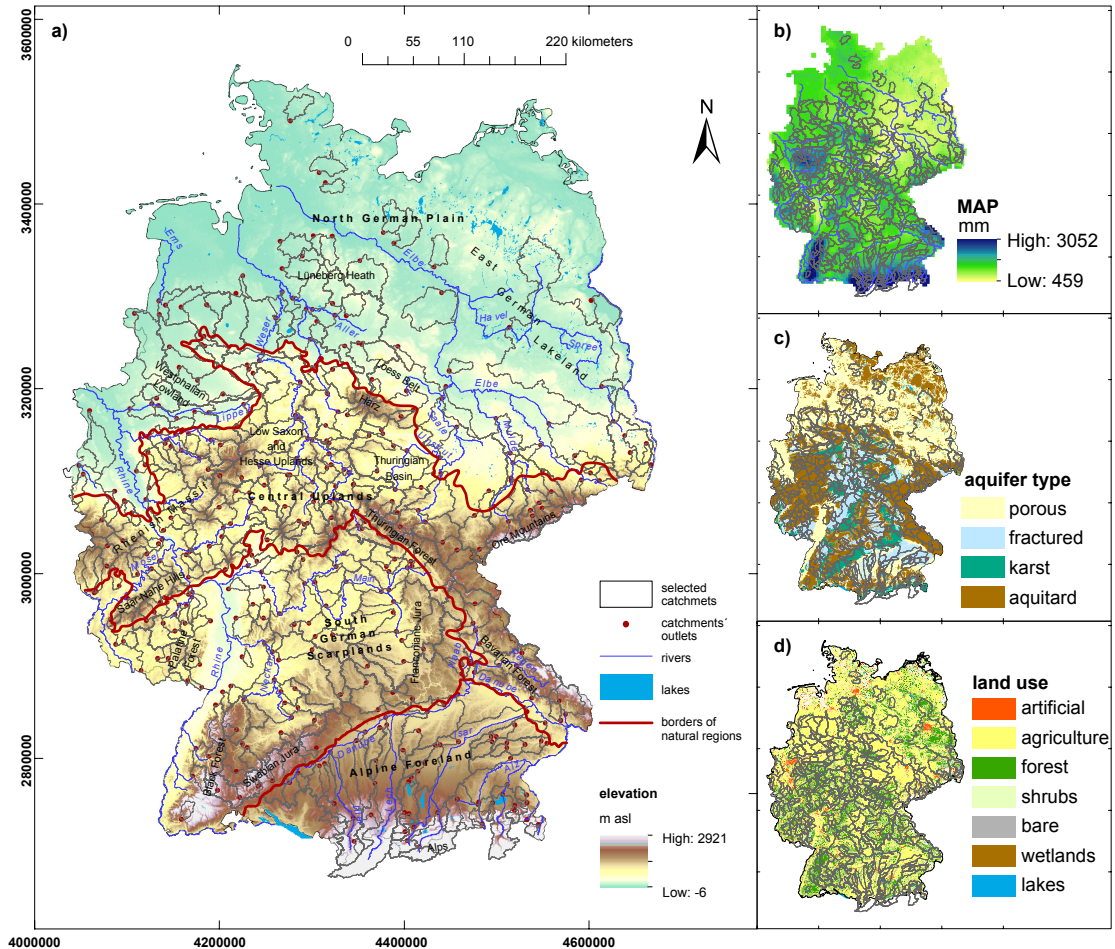


Figure 3.2: The study area is the whole of Germany, which is divided into four main landscape units (the North German Plain, Central Uplands, South German Scarplands and Alpine Foreland region). The names of smaller natural regions of Germany are also indicated. 401 catchments where daily flows are not affected by anthropogenic modifications were selected based on data availability. Elevation (a), mean annual precipitation (b), aquifer type (c) and land use (d) are indicated by the color of the background

All river catchments where runoff observations are available but flows are reported to be disturbed by large reservoirs or control gates (Lehner et al., 2011) were removed from the dataset. Moreover, catchments were removed from the dataset if visual examination revealed obvious flow disturbances and if for them the performance (i.e., Kling-Gupta Efficiency (KGE)) of a simple hydrological model modèle du Génie Rural à 6 paramètres Journalier (GR6J) was less than  $KGE = 0.7$  (Ponzelet et al., 2017). 401 German catchments were finally selected based on these criteria. The area of the selected catchments ranges from 31 to 23,700 km<sup>2</sup>, with a median value of 476 km<sup>2</sup>. Event separation was performed on the observed discharge data for the time period from 1979 to 2002 (22 years). Information about irrigation and groundwater abstraction was not available at catchment scale. According to the Federal Institute for Geosciences and Natural Resources (BGR),

groundwater abstraction countrywide accounts for about 12% of the annual recharge (48 km<sup>3</sup>), and only 2000 km<sup>2</sup> of agricultural areas (mostly in the North-East of the country) are irrigated (Siebert et al., 2013). This makes daily losses of streamflow due to anthropogenic withdrawals irrelevant for the purposes of rainfall-runoff analysis, as they do not affect the dynamics of rainfall-runoff events at daily scale.

Apart from observed daily runoff time series, daily precipitation time series obtained from the REGNIE dataset (Rauthe et al., 2013) provided by the DWD, and snowmelt time series simulated by the mHM model (Samaniego et al., 2010; Kumar et al., 2013) and provided by Zink et al. (2017) were used in this study.

A wide range of catchment descriptors (CDs) representing climate, topography, geomorphology, land use, soil physical and soil water properties, hydrogeology and geology of every study catchment (Table 3.1) was acquired and examined to identify potential spatial drivers of event characteristics. These generic groups of descriptors are typically used for regionalization studies (Oudin et al., 2010; Ssegane et al., 2012b; Blöschl et al., 2013b). Time-varying attributes were aggregated by computing their mean or median values for every catchment (e.g., mean annual precipitation). Categorical data (e.g., land use) were transformed to continuous variables, by deriving percent of catchment area covered by specific land uses. The resolution of gridded data layers and the map scale of vector data are summarized in Table 3.1 for each generic group of catchment descriptors. The potential relevance of each group for event runoff response is presented in Table 3.2. A comprehensive list of the catchment descriptors used in this study, their relevance for event runoff response and data quality of respective layers is reported in the Supporting Information (Chapter 3.6, Table 3.3).

### 3.3 Methods

#### 3.3.1 Event characteristics as hydrological signatures

Every rainfall-runoff event examined in this study is described by means of four event characteristics described below and in Table 3.2. These characteristics provide information on short-term runoff dynamics which might point at the nature of rainfall partitioning and storage in the catchment as well as indicate dominant processes of water release from the river basin. Inter-catchment differences of these characteristics thus provide essential information about spatial differences in dominant runoff generation processes.

The event runoff coefficient ( $rc$ ) [dimensionless] is defined as the ratio between the volumes of the quick component [mm] of a particular runoff event and the respective rainfall and/or snowmelt event [mm]. It characterizes the portion of rainfall immediately contributing to event runoff and the portion that is instead stored in the subsurface or evaporatranspired from the catchment.

The runoff event time scale ( $ts$ ) [days] is the ratio between quick runoff volume [mm] and peak discharge [mm/day] (Gaál et al., 2012), and characterizes the shape of the hydrograph and the duration of events. The event time scale is an indicator of catchment flashiness and of the importance of fast runoff generation processes, such as overland flow or fast subsurface storm flow. Fast-reacting catchments will have small event time scales, while catchments with slower runoff generation processes tend to have larger time scales.

The relative importance of fast and slow runoff generation processes within one event can be described by the event rise time ( $rt$ ) [dimensionless], which is the ratio of the duration [days] from the beginning of the event till the day when peak discharge is observed (Bell and Om Kar, 1969) and the overall duration of the event in days. It shows how fast the peak is reached. When an event with mixture of runoff generation processes occurs, event rise can be an indicator of relative importance of fast components.

Abundance or absence of multiple-peaks (*multi*) in the event hydrographs provides information on the typical recurrence interval of rainfall and snowmelt events in a given catchment and is an important indicator of possible event-fed saturation of the catchment.

In this study we use 11 metrics describing mean values, variability and seasonality of these four event characteristics (Table 3.2) that comply with the guidelines for hydrological signatures proposed by McMillan et al. (2017), i.e. they are characterized by identifiability, robustness, consistency, representativeness and discriminatory power. The metrics were derived for each catchment

Table 3.1: Metadata of catchment descriptors (CDs)

Group of CDs, data source, resolution and map scale	Description	Number of continuous CDs	Number of categorical CDs
Climate; DWD <sup>a</sup> (1-8 km raster data)	Climatic settings (mean annual precipitation, air temperature, evaporation) and their seasonality; characteristics of wet spells (mean volume of precipitation events, their seasonality and variation) and dry spells (maximum and median duration)	12	-
Topography and geomorphology; SRTM (30 m raster data)	Basin area, topographical (elevation, slope, aspect, topographic wetness index) and geomorphological characteristics of the catchment (drainage density, length and slope of the main channel, number of junctions)	9	-
Land use; European Environmental Agency (EEA) (100 m raster data)	Percent of catchment area covered by specific land cover groups (artificial surfaces, agricultural surfaces, different types of forest, shrub and herbaceous vegetation, open surfaces, wetlands and water bodies)	-	9
Soil physical properties; HWSD (0.4-1km raster data); BGR (1:1000000 map scale for vector data)	Texture properties of topsoil and subsoil (percent of clay, sand, silt and gravel), morphological properties of soil (e.g., bulk density), soil depth, soil type (based on soil genesis)	11	8
Soil water properties; BGR (400 m raster data); Zink et al. (2017) (4 km raster data)	Soil properties affecting soil water movement such as available water content, field capacity, presence and location of impermeable layers within the soil column, the ability of soil to drain water and characteristics of soil wetness (mean annual soil moisture state)	2	16
Hydrogeology; BGR (1 km raster data; 1:200000 map scale)	Hydrogeological settings (hydrostratigraphic units, consolidation, yield, recharge) and hydraulic properties of upper aquifer (hydraulic conductivity)	1	21
Geology; BGR (1:200000 and 1:1000000 map scale)	Geologic setting of the catchment (rock origin and types of geological formation)	-	26

<sup>a</sup> Web links of the data sources are provided in the Acknowledgement and Data Chapter. The source of data for each individual catchment descriptor is provided in Table 3.3

from a large sample of rainfall-runoff events separated from continuous daily time series (Chapter 3.3.2), thus singling out possible short-term errors in streamflow and rainfall observations (identifiable) and reducing the effect of extreme events occurred (robust). Event characteristics used in this analysis are dimensionless and do not require scaling (consistent). Moreover, they refer to catchment-scale behavior and are not sensitive to exact gauge location (representative). Finally, the chosen event characteristics have high discriminatory power as their differences directly imply the difference in partitioning, storage and transport of precipitation water (Norbiato et al., 2009; Gaál et al., 2012).

### 3.3.2 Event separation

To derive event characteristics continuous hydro-climatic time series were separated into rainfall-runoff events by using the time-series-based method presented by Tarasova et al. (2018b), which consists of the following steps:

- i Base and quick flows are separated using a simple smoothing algorithm introduced by Institute of Hydrology (1980);

- ii Rainfall and snowmelt events are attributed to quick flow events if they occurred within the season-specific median lag time of the catchment (Mei and Anagnostou, 2015);
- iii Thresholds used to distinguish multiple-peak events from overlapping single-peak events are identified by iteratively comparing the reference distribution of runoff coefficients of single-peak events with the one obtained for single-peak components of multiple-peak events (Tarasova et al., 2018b).

### 3.3.3 Identifying regions of homogeneous event runoff response

By identifying groups of catchments with similar event characteristics we aim to understand spatial patterns of event runoff response. Catchments exhibiting similar event runoff response were clustered using a data-driven classification method, (i.e., unsupervised artificial neural networks). This technique, also known as Self-Organizing Maps (SOM), was previously used for catchment classification (e.g., Di Prinzio et al., 2011; Ley et al., 2011) and proved to outperform standard linear procedures (Razavi and Coulibaly, 2013). The SOM is a non-linear technique, which is able to compress high-dimensional data into a low-dimensional output space while preserving the most essential information (Kohonen, 2001). The size of the SOM is user-defined, and was set to the desired number of clusters in this study. The number of clusters was chosen after comparing the SOM quality of different neuron sizes. To avoid misclassification the clustering was repeated 100 times and the probability of a catchment to be assigned to a specific cluster was assessed.

### 3.3.4 Linking event characteristics and catchment descriptors

To understand spatial controls of event runoff response, event characteristics were related to catchment descriptors. The flowchart of the methodology used for understanding spatial controls of event runoff response in study catchments is presented in Figure 3.3. We used the widest possible set of descriptors, encompassing generic groups typically used in regionalization studies (Chapter 3.2). First, the strengths of the relationships among individual event characteristics and catchment descriptors were examined using bivariate correlation analysis (Chapter 3.3.4.1). Since catchment descriptors are likely to show complex inter-correlations due to the co-evolution of climate and landscape, further multivariate analyses were applied. Different variable selection methods were utilized to identify highly informative and non-redundant catchment descriptors (Chapter 3.3.4.2) and to reduce the impact of subjective pre-defined choices of climate and landscape characteristics in the identification of the main controls on event characteristics. The variable selection methods were evaluated through two independent approaches. First, we adopted the hypothesis of Di Prinzio et al. (2011) and Ssegane et al. (2012b), namely that catchment classification using hydrologically-relevant catchment descriptors would display the highest similarity to the reference clustering obtained by using event characteristics. Following this hypothesis, we analyzed which selection of CDs is superior in reproducing spatial patterns of event characteristics (Chapter 3.3.4.3). In a second approach, we assessed each set of the CDs by its ability to predict event characteristics in a regionalization experiment using multiple regression models. Additionally, the value of each generic group of CDs (e.g., climate, geology, land use) for catchment classification was examined in a similar fashion.

**3.3.4.1 Correlation analysis** A simple descriptive statistical analysis was used as starting point for understanding the relationships among event characteristics and catchment descriptors. In particular, pair-wise correlations between individual event characteristics and catchment descriptors were calculated based on Spearman-rank correlation coefficient and summarized in a matrix. To explore these interactions the correlation matrix was re-arranged and displayed as a heatmap, which was used to highlight the groups of catchment descriptors that had similar effect on event characteristics.

Table 3.2: Summary of the rainfall-runoff event characteristics, the metrics used to describe them in this study and the generic groups of catchment descriptors that are supposed to control them

Description and metrics	Implication	Possible controlling catchment descriptors
<b>Event runoff coefficient (<math>rc</math>):</b> shows how much of rainfall (snowmelt) becomes event runoff		
Mean value ( $rc.mean$ ) [dimensionless]	Inference about dominant runoff generation process	Wetness conditions (climate, soil water); subsurface storage and flow conditions (soil, soil water, hydrogeology, geology); infiltration capacity (soil, land use); interception (land use)
Coefficient of variation ( $rc.cv$ ) [dimensionless]	Variability: sensitivity of runoff response to wetness state and natural variability of climatic forcing	Variability of precipitation events (climate); variability of wetness conditions (climate); subsurface storage (soil, geology)
Ratio of summer and winter medians ( $rc.sum2win$ ) [dimensionless]	Seasonality: origin of variability and inference about the nature of its drivers	Seasonality of precipitation events (climate); seasonality of wetness conditions (climate); seasonal cycle of vegetation (land use)
<b>Event time scale (<math>ts</math>):</b> it shows event duration and shape of the hydrograph		
Mean value ( $ts.mean$ ) [dimensionless]	Inference about fast and slow runoff generation mechanisms (Gaál et al., 2012)	Characteristics of precipitation events (climate); subsurface storage (soil, geology); interception (land use); drainage network (topology, geomorphology)
Coefficient of variation ( $ts.cv$ ) [dimensionless]	Variability: sensitivity of runoff response to wetness state and natural variability of climatic forcing	Variability of precipitation events (climate); variability of wetness conditions (climate); subsurface storage (soil, geology)
Ratio of summer and winter medians ( $ts.sum2win$ ) [dimensionless]	Seasonality: origin of variability and inference about the nature of its drivers	Seasonality of precipitation events (climate); seasonality of wetness conditions (climate); seasonal cycle of vegetation (land use)
<b>Event rise time (<math>rt</math>):</b> it shows location of the peak within event (hydrograph's skew)		
Mean value ( $rt.mean$ ) [dimensionless]	Related to time of concentration and travel time (Bell and Om Kar, 1969) and dominance of fast/ slow runoff components	Drainage network (topology, geomorphology); wetness conditions (climate, soil water); subsurface storage (soil, geology); infiltration capacity (soil, land use)
Coefficient of variation ( $rt.cv$ ) [dimensionless]	Variability: sensitivity of runoff response to wetness state and natural variability of climatic forcing	Variability of wetness conditions (climate); subsurface storage (soil, geology)
Ratio of summer and winter medians ( $rt.sum2win$ ) [dimensionless]	Seasonality: origin of variability and inference about the nature of its drivers	Seasonality of precipitation events (climate); seasonality of wetness conditions (climate); seasonal cycle of vegetation (land use)
<b>Occurrence of multiple-peak events (<math>multi</math>):</b> single-peak or multiple-peak structure of event hydrograph		
Fraction of multiple-peak events among all events ( $multi$ ) [dimensionless]	Inference about possible runoff generation processes	Characteristics of precipitation events (climate); wetness conditions (climate, soil water); subsurface storage (soil, geology); snowmelt occurrence (climate, topography)
Ratio of summer and winter medians ( $multi.sum2win$ ) [dimensionless]	Seasonality: origin of variability and inference about the nature of its drivers	Seasonality of characteristics of precipitation events (climate); seasonality of wetness conditions (climate)

**3.3.4.2 Variable selection methods** We have tested the three independent methods described below to reduce the dimensionality of data and select only highly informative and non-redundant catchment descriptors:

- Information Gain (IG) – The information gain method compares pairs of correlated explanatory variables based on their relevance (i.e., mutual information between variable and response), redundancy (i.e., mutual information between variables) and conditional redun-

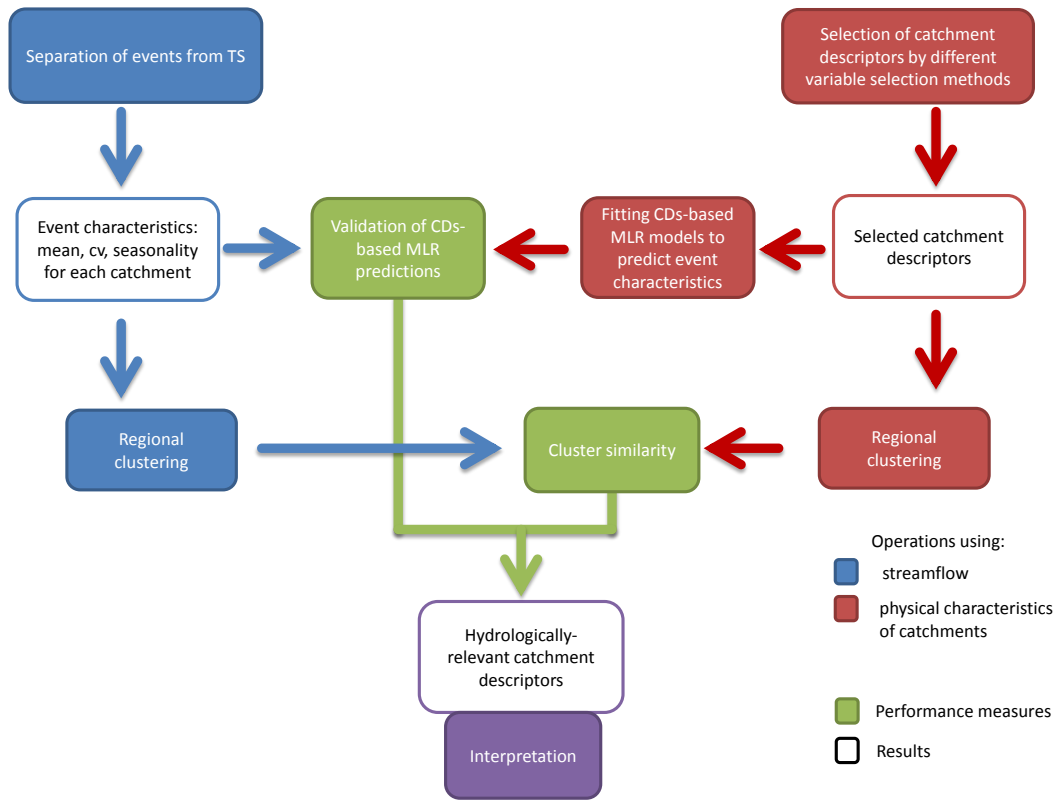


Figure 3.3: Flowchart of the methodology used to identify hydrologically-relevant catchment descriptors based on their predictive power and their ability to reproduce observed spatial patterns of event characteristics. TS – time series; CD – catchment descriptor; MLR – multiple-regression models

dancy (i.e., the increase of mutual information between previously selected variables and the response conditioned on the currently analyzed variable) (Brown, 2009). The variable with the highest information gain is retained (Ssegane et al., 2012a). In this study, the information gain was computed for the catchment descriptors exhibiting correlation coefficient higher than 0.7 with any other catchment descriptor. The IG for predicting each event characteristics was computed separately, and the average IG was then used to select the catchment descriptors to retain.

- **Principal Component Analysis (PCA)** – The Principal Component Analysis is a statistical technique that uses orthogonal transformation to translate original correlated variables into uncorrelated Principal Component (PC) (Haan, 1977), thus revealing the underlying structure of data. The first PC explains the larger part of the variance of data; each following component is orthogonal to the preceding one and contributes less to the total variance. The PCA is often applied in hydrology to reduce data dimensionality (e.g., Razavi and Coulibaly, 2013) and select informative and non-redundant catchment descriptors (e.g., Olden and Poff, 2003), without however establishing physical relationship between explanatory and response variables (Ssegane et al., 2012a,b). Significant principal components were identified in this study by using a broken-stick method based on eigenvalues from random data (Frontier, 1976; Jackson, 1993). Since PCs are a linear combination of the original variables, the relative contribution of each catchment descriptor to each PC is known and can be compared to the expected average contribution calculated as  $C = \frac{1}{n} * \sum_{i=1}^m Eig_i$ , where  $Eig_i$  is the eigenvalue of each PC (i.e., the variance of the dataset in the direction  $i$ ),  $n$  is the number of the original variables, and  $m$  is the number of the significant PCs considered. Catchment descriptors whose contributions to the significant PCs are higher than the expected average were selected for further analysis.
- **Backward Elimination (BE)** – The approach is similar to the backward elimination procedure used for stepwise regression model selection. However, the tool to select catchment descrip-

tors was catchment clustering instead of multiple regression analysis. Initially, a benchmark value of a metric of cluster similarity (i.e., Adjusted Rand Index (ARI)) (see Chapter 3.6.1) was calculated by using all available catchment descriptors and the reference clustering obtained from event characteristics. In a second step the deletion of each catchment descriptor was tested and the ARI was re-calculated. The catchment descriptor, whose deletion loss determined the largest improvement of the ARI, was eliminated from the subset and the benchmark ARI was updated. The procedure was repeated until no more improvement could be achieved.

**3.3.4.3 Performance of variable selection methods** The performance of the three variable selection methods (Chapter 3.3.4.2) and of each single (i.e., one at a time of the seven) generic groups of catchment descriptors (Table 3.1) was assessed according to the following criteria:

- **Cluster similarity** – Alternative catchment classifications were performed through SOM using all CDs and various subsets of the. The ARI (Hubert and Arabie, 1985) was adopted as a measure of the similarity between the reference classification based on event characteristics and each alternative classification. The ARI is an adjusted version of the Rand Index (Rand, 1971) that can assume negative values and is equal to 1 in case of random clustering with the same number of objects in each class (see Chapter 3.6.1). ARI has higher discriminatory power than the original Rand Index and is also less sensitive to the number of classes (Di Prinzio et al., 2011). To avoid the effect of misclassification the mean ARI of 100 independent classifications was used instead of the ARI of a single realization (Sawicz et al., 2011).
- **Predictive potential** – The effectiveness of the variable selection methods and individual generic groups of catchment descriptors was assessed in terms of the predictive performance of stepwise regression models. A regression model expresses the relation between dependent variables (i.e., event characteristics) and independent variables (i.e., catchment descriptors). The regression model is constructed by means of a multiple regression analysis comprising, model selection, estimation of model parameters and assessment of errors (Haan, 1977). The Akaike Information Criterion (AIC) (Akaike, 1974) was used for combined forward and backward stepwise model selection. The performance of the selected model was assessed by averaging the normalized Root Mean Squared Error (nRMSE) between predicted and observed values of each event characteristic using “leave-one-out” cross-validation procedure. Here we use cross-validation performance rather than statistics of model fit as an assessment criterion since good performance in terms of the latter can be erroneous due to model over-fit (Jobson, 1991). Two predictive performance measures were calculated: the performance of a general model for all 401 German catchments and the performance of specific models for each cluster catchments exhibiting of similar event runoff response (Chapter 3.3.3). The frequency with which every CD was selected as an explanatory variable for the regression model was recorded in order to identify hydrologically-relevant catchment descriptors.

## 3.4 Results

### 3.4.1 Event characteristics and their spatial patterns

In this study a total number of 196,073 events of various magnitudes and occurrence time during the period 1979-2002 were separated from continuous hydro-climatic time series in 401 mesoscale German catchments. An example of event separation for 6 representative catchments with contrasting runoff regime is presented in Figure 3.10. The spatial distribution of mean value, variability and seasonality of event characteristics obtained from the separated rainfall-runoff events is displayed in Figure 3.4, which provides a first glimpse on the variability of event runoff response in Germany.

High event runoff coefficients are typical of mountainous regions of the Central Uplands (e.g., Harz, Ore Mountains, Thuringian Forest, and Rhenish Massif), the South German Scarplands (e.g., Black Forest, Swabian Jura) and the Alps (Figure 3.4a). The smallest runoff coefficients are

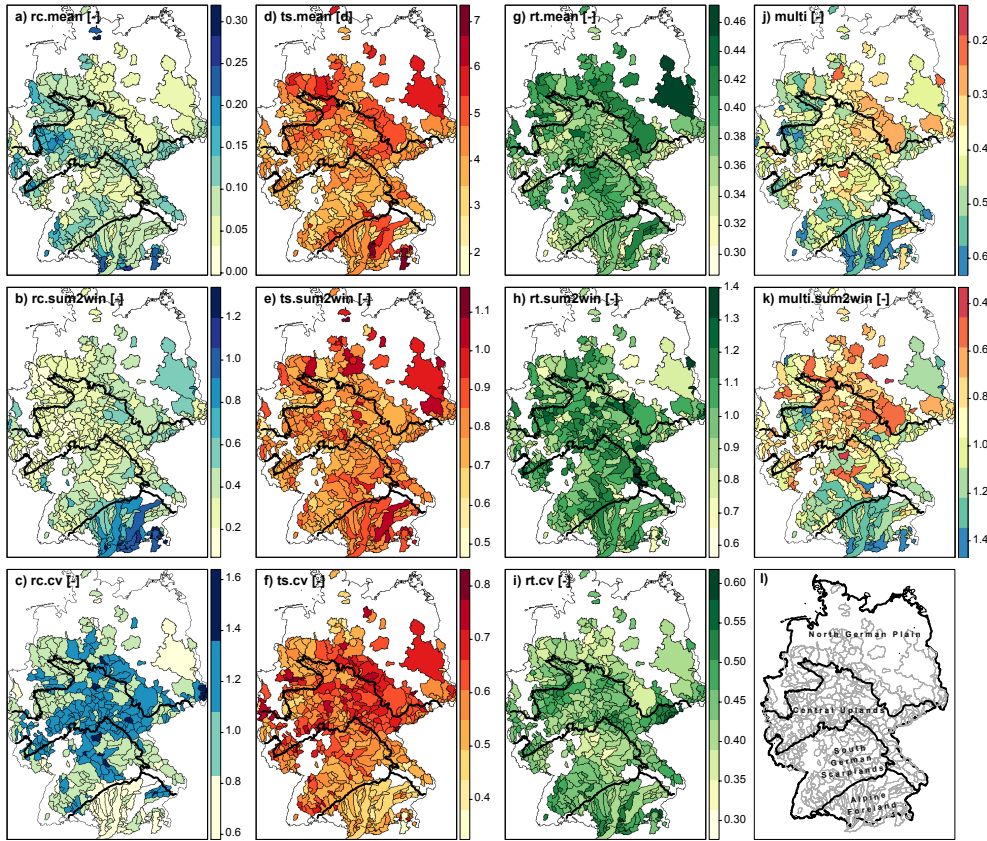


Figure 3.4: Spatial distribution of event characteristics: metrics describing a-c) event runoff coefficients ( $rc$ ), d-f) event time scale ( $ts$ ), g-i) event rise time ( $rt$ ) and j-k) fraction of multiple-peak events ( $multi$ ) are displayed, together with the; l) main natural regions of Germany. The top row (a, d, g, j) displays the average ( $mean$ ) of the respective event characteristics, the middle row (b, e, h, k) shows the ratio between summer and winter median values ( $sum2win$ ), whereas the bottom row (c, f, i) shows the coefficient of variation ( $cv$ ) of the considered event characteristic. Solid black lines represent the borders of the main natural regions of Germany (Figure 3.2a)

found for catchments in the Palatine Forest located in the Upper Rhine Scarplands. In the lowlands, the wet western part of the North German Plain (see Figure 3.2b) is associated with higher mean and lower variability of event runoff coefficients (Figure 3.4c), while the drier eastern part has very low mean and generally highly variable runoff coefficients. Similarly, dry catchments of the Main basin exhibit highly variable runoff coefficients. Three regions with different seasonality of the runoff coefficients emerge (Figure 3.4b). Higher winter event runoff coefficients occur in the Central Uplands, especially in their western part. The lowland catchments, especially in the eastern part (e.g., the Loess belt), have weaker seasonality characterized by slightly higher runoff coefficients in winter than in summer. No seasonal variability is observed in the Alpine Foreland. Long event time scales are typical of catchments where runoff is strongly smoothed by the effect of lakes (e.g., the Spree and Havel catchments in the eastern part of the North German Plain; the Amper and Alz catchments in the Alpine Foreland) (Figure 3.4d). Larger catchments tend to have longer event time scale as well. Also in the Thuringian Forest and the Harz Mountains events have on average also long time scales, especially in summer when snowmelt occurs. In the lowlands of the Loess Belt region events typically have long time scale. A clear difference is identified between Alpine Foreland catchments with melt-dominated headwaters in the Alps and flatter catchments of the lower Alpine Foreland. Small event time scales are instead typical of the South German Scarplands (e.g., the Neckar River). The small mountainous catchments of the Central Uplands also have high variability and seasonality of the event time scale (Figure 3.4e, f). Short and variable event rise times in mountainous catchments contrast with long rise times characterized by little variability in lowland catchments (Figure 3.4g, i). Longer summer rise times are observed in almost all catchments (Figure 3.4h). Multiple-peak events are very frequent in the Alpine Foreland especially in summer, when snowmelt plays an important role in runoff generation (Figure 3.4j, k). Also in other mountainous regions



(e.g., the Black and Bavarian Forests and the Rhenish Massif) summer multiple-peak events are frequent. On the contrary, in lowland catchments of the western part of the North German Plain multiple-peak events occur in winter. Finally, multiple events are extremely rare in the eastern part of the North German Plain.

### 3.4.2 Regions with homogeneous event runoff response

Clustering of the derived event characteristics (Figure 3.5a) has reveals generally clear regional patterns of event runoff response in Germany (e.g., catchments of the Loess Belt, Rhenish Massif, Black Forest and Ore Mountains are clustered together respectively). On the other hand, there are also evidences of regional inhomogeneity of runoff response (e.g., the runoff response of several catchments of the Alpine Foreland is similar to that of catchments in the North German Plain; catchments of the South Scarplands are split among several clusters).

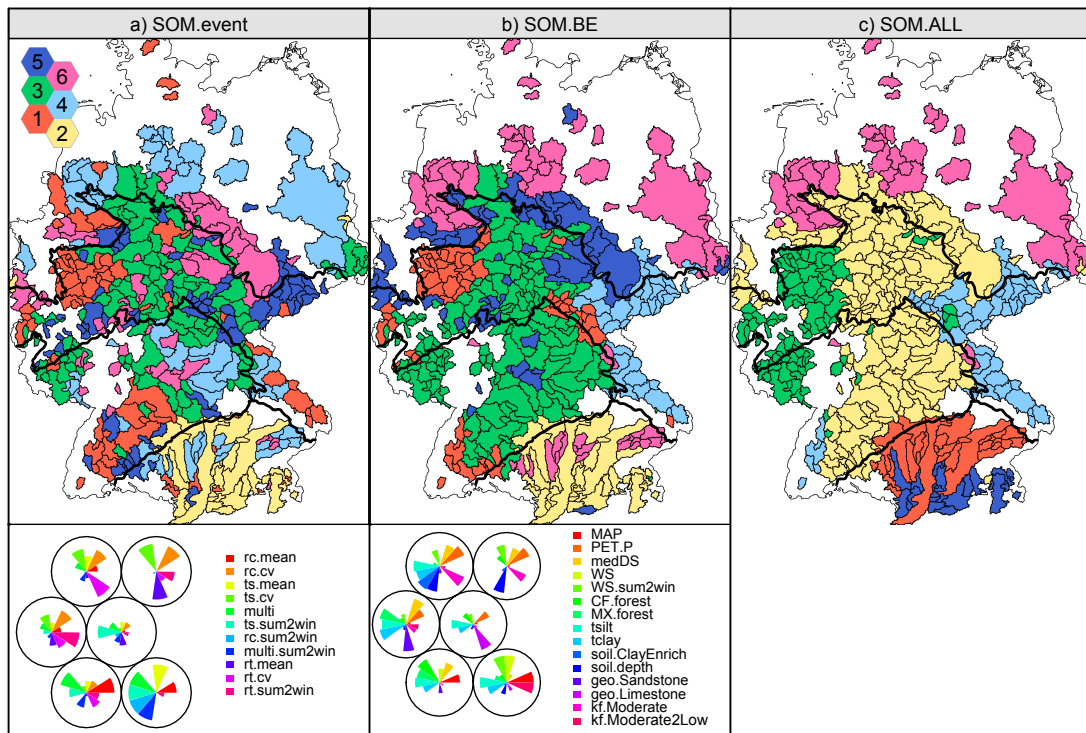


Figure 3.5: Linking event characteristics and catchment descriptors (CDs) through catchment classification: a) reference classification obtained by using Self-Organizing Maps based on event characteristics (SOM.event); b) alternative classification based on the CDs selected by the BE method (SOM.BE); c) alternative classification using all CDs (SOM.ALL). The hexagonal topology of the output layer with cluster numbering is depicted in the top left corner of the figure. The bottom panel represents the hexagonal topology of the output layer with node weight vectors derived from normalized values of the original variables. Solid black lines represent the borders of the main natural regions of Germany (Figure 3.2a)

Cluster 1 (Figure 3.5a) consists of the western mountainous catchments (the Rhenish Massif, Black Forest, Swabian Jura) and the Bavarian Forest catchments. Catchments of this cluster are characterized by very high and slightly variable runoff coefficients with higher values in winter, moderate and slightly variable time scales with shorter events in summer and very short rise times especially in winter. Multiple-peak events are very frequent, especially in winter.

Cluster 2 includes most of the catchments of the Alpine Foreland and the Alps, excluding small flat catchments in the lower reaches of Danube tributaries (Figure 3.5a). For these catchments very long event time scales and high runoff coefficients are typical, and events often exhibit multiple-peaks. There is almost no seasonality and variability of event characteristics, although multiple-peak events are more frequent in summer.

The catchments of the lower Central Uplands (with the exception of those belonging to their mountain ranges) are aggregated into Cluster 3 (Figure 3.5a). Here runoff coefficients and rise times

are moderate but variable, while both average values and variability of time scales are moderate. In winter runoff coefficients and time scales are higher, while rise times are shorter. Multiple-peak events are rare and usually occur in winter.

The lowland catchments of the North German Plain, flat lowland catchments of the Danube basin, and dry hilly catchments of the Main basin constitute Cluster 4 (Figure 3.5a). In this cluster runoff coefficients are small, have low variability and much higher values in winter. Time scales are rather long and show almost no variability and no seasonality. Rise times are moderately long with almost no variability or seasonality. There are almost no multiple-peak events in catchments of this cluster.

Cluster 5 refers to the eastern part of the Central Uplands (the Ore Mountains and Thuringian Forest) (Figure 3.5a), where event runoff coefficients and time scales are relatively high and variable, while rise times are short and variable. Runoff coefficients, time scales and rise times are much higher in winter. Infrequent multiple-peak events occur mostly in winter.

Finally, Cluster 6 (Figure 3.5a) combines catchments in the transition zone between lowlands and uplands (e.g., the Loess Belt and Thüringen Basin), and noncontiguous catchments in the Rhine Valley. Very low on average but very variable runoff coefficients and time scales with much larger values in winter are typical of these catchments. Rise times are very long and variable with shorter values in winter. There are almost no multiple-peak events.

### 3.4.3 Linking event characteristics and catchment descriptors

**3.4.3.1 Correlation analysis** Relationships among event characteristics and catchment descriptors were first investigated by means of simple correlation analyses. Figure 6 summarizes the results of these analyses by means of a heatmap. Strong inter-correlation among catchment descriptors, indicated by the prevalence of intense colors, was detected. Metrics related to event runoff coefficients and the fraction of multiple-peak events, show strong correlations with climatic (e.g., mean annual precipitation *MAP*, mean volume of precipitation events *WS*) and topographical (e.g., elevation, slope) descriptors. The event time scales mostly correlates with soil physical (e.g., the fraction of silt or sand in the subsoil) and soil water (e.g., soil drainage ability) properties, while the event rise times shows complex relationships with different groups of CDs, including climatic (e.g., dryness index *PET.P*, temperature *MAT*), soil physical (e.g., bulk density of the topsoil *tbulk*) and soil water (available water content *awc*) properties. The seasonality of the event characteristics, especially the runoff coefficient (*rc.sum2win*), is affected by the seasonality of precipitation (i.e., high correlation with seasonality of precipitation amount *P.sum2win* and volume of wet spells, *WS.sum2win*). Finally, the variability of the event characteristics (*rc.cv*, *ts.cv* and *rt.cv*) is higher in catchments with small subsurface storage, indicated by a high fraction of aquifers with low hydraulic conductivity (*kf.Low2ExtremelyLow*), aquitards (*aquitard*), silty subsoils (*ssilt*) and low groundwater yield (*Yless150*) (Figure 3.6).

The identified correlation among catchment descriptors can negatively impact the predictive power and stability of regression models (Jobson, 1991) that use them as explanatory variables to predict characteristics of runoff events. Therefore, variables selection methods were applied with the goal of selecting only highly informative and non-redundant catchment descriptors.

**3.4.3.2 Performance of variable selection methods and generic groups of CDs** We applied three different variable selection methods (IG, PCA and BE) to identify sets of highly informative and non-redundant catchment descriptors controlling event characteristics out of all the available descriptors. Variable selection methods were evaluated by considering how well the spatial clustering of event characteristics was reproduced by clustering driven by the selected sets of CDs (Figure 3.5 and 3.7a), and how well multiple regression models estimated from the selected sets of CDs predicted event characteristics (Figure 3.7b, c). In a similar fashion, we examined performances of clustering and regression models which only use a single generic group of CDs (e.g. geology or climate) to understand the value of each of them. As a baseline we considered the performance obtained by using all available CDs.

Different numbers of catchment descriptors (from 15 for the BE to 84 for the IG methods) were

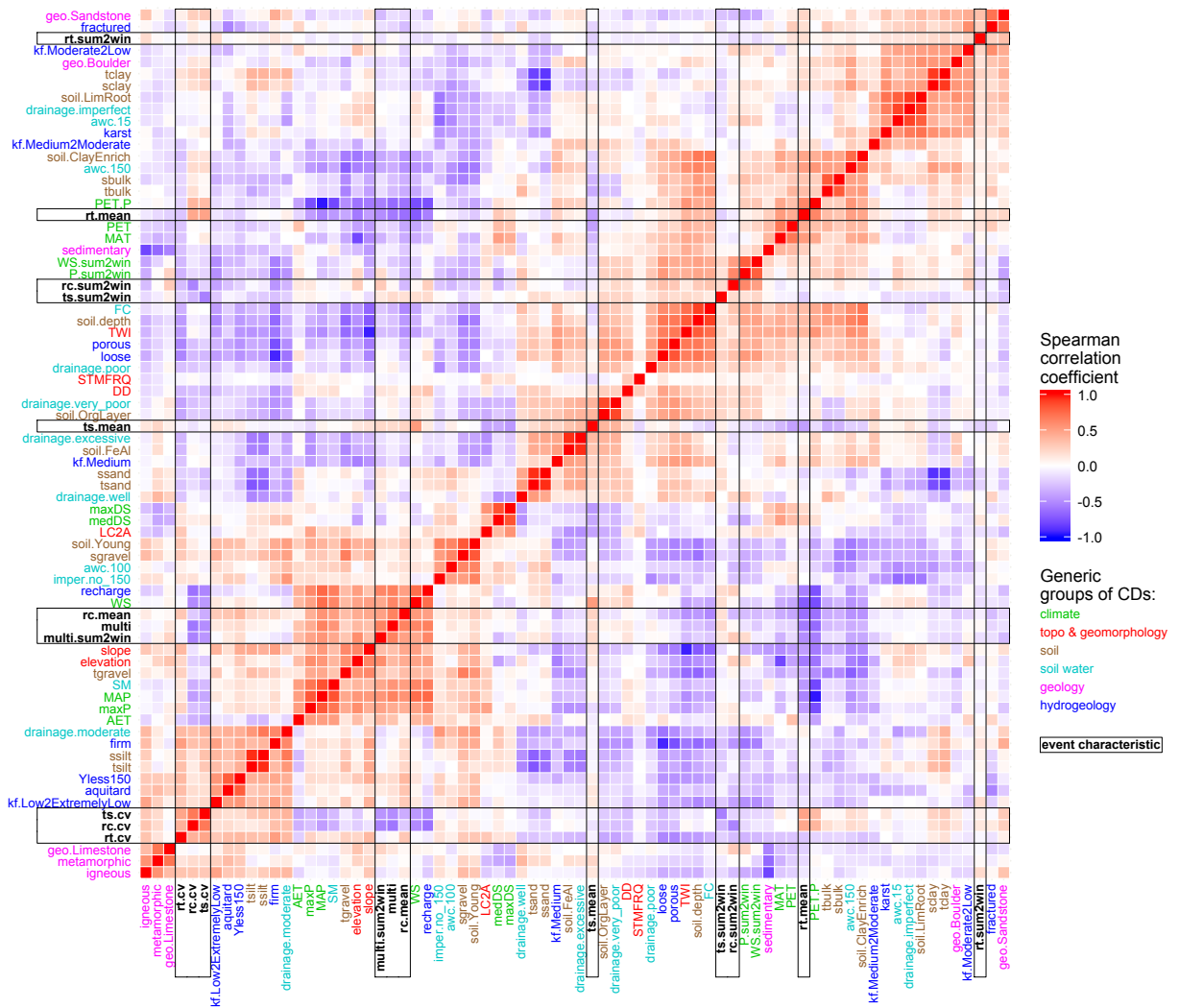


Figure 3.6: Heatmap of the correlations among event characteristics and catchment descriptors (CDs). The CDs are color-coded according to their generic group. Only the principal CDs identified through the PCA are shown (for details refer to Chapter 3.3.4.2). A detailed description of the CDs is available in Table 3.10

selected by the examined variable selection methods (Figure 3.7a, Table 3.3). Only seven CDs (catchment area *area*, agricultural land cover *agri*, groundwater recharge *recharge* and 4 geological classes, see Table 3.3) have never been chosen.

In terms of cluster similarity, the BE method (Figure 3.5b) outperformed the PCA and IG methods (Figure 3.7a). This result was expected since the BE method was designed to reproduce clustering of the event characteristics. Both the PCA and IG methods provided selections of catchment descriptors that are able to reproduce the observed patterns of event characteristics slightly worse than by considering all catchment descriptors (Figure 3.7a).

In terms of prediction potential of stepwise regression models only the PCA selection method is comparable to considering all CDs, while the IG and BE methods perform slightly worse (i.e., they exhibited higher errors, see Figure 3.7b). When regression models are estimated for each individual cluster of catchments (i.e., smaller but more homogeneous sets of catchments are used for model estimation and subsequent prediction of event characteristics) the model selected from all available CDs has the poorest performance (Figure 3.7c). Apparently, high inter-correlation of the CDs together with smaller sample size of catchments lead to biased model selection and multicollinearity. The BE selection method performs slightly better than the other variable selection methods. However, compared to other event characteristics the prediction of metrics of runoff coefficient is still challenging similar to all other variable selection methods (Figure 3.7b, c).

Single generic groups of catchment descriptors show variable performances. The performances in terms of cluster similarity of climatic and hydrogeological CDs are comparable to the performance

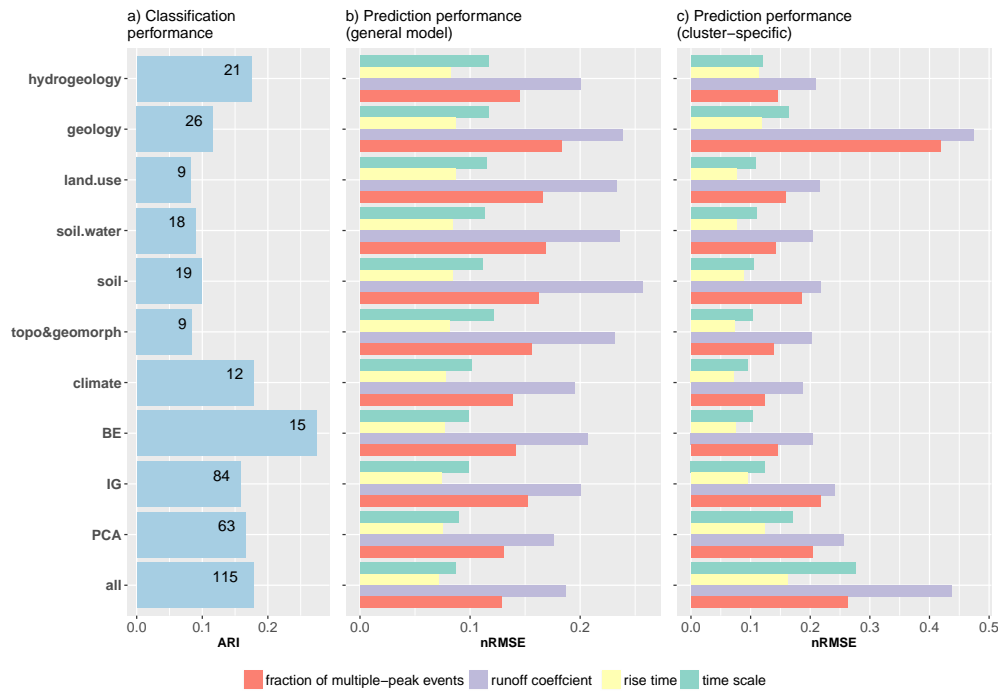


Figure 3.7: Summary of the variable selection performance: a) classification performance based on cluster similarity evaluated by means of the ARI between the reference and alternative classifications. The numbers on the bars indicates the number of CDs selected for catchment classification; b) prediction performance of stepwise regression models (normalized root mean square error (nRMSE) of “leave-one-out” cross-validation procedure) for each event characteristic; c) prediction performance of cluster-specific stepwise regression models (nRMSE) for each event characteristic

of all CDs and of the set of CDs selected by PCA and IG methods (Figure 3.7a). The group of climatic descriptors performs better than other groups for regionalization of event characteristics using general regression model (Figure 3.7). Hydrogeological and geological characteristics perform better than soil physical and soil water properties, land use, topography and geomorphology for reproducing spatially coherent patterns of event characteristics (Figure 3.7a). However, our analysis shows that geological variables, as well as land use and soil characteristics perform quite poorly for regionalization of event characteristics. Cluster-specific regression models selected from climatic, topographical and soil water descriptors show the best performance and outperform models estimated from the whole set of available CDs (Figure 3.7c).

**3.4.3.3 Dominant controls of event characteristics within homogenous regions** According to the best-performing variable selection method (i.e., the backward elimination method, BE) the emerged regional patterns of event characteristics can be described by using a set of 15 catchment descriptors which includes indicators of catchment wetness (e.g., mean annual precipitation *MAP*, dryness index *PET.P*), climate seasonality (e.g., seasonality of precipitation events *WS.sum2win*), catchment storage (e.g., soil depth), soil hydraulic conditions (e.g., texture of the subsoil *tsilt*, presence of clay layer in the subsoil *soil.ClayEnrich*), presence of karst systems (e.g., presence of limestone *geo.limestone*) and hydraulic properties of aquifers (e.g., hydraulic conductivity of upper aquifer *kf.Moderate2Low*) (Figure 3.5b).

The importance of each of these 15 CDs to explain the variability of all selected CDs and to reproduce event characteristics in each cluster of catchments is presented in Figure 3.8. The height of the bars shows the contribution provided by each single CD for explaining the variability of the selected CD dataset. CDs which contribute above average (horizontal dashed lines) are referred as the principal (Razavi and Coulibaly, 2013). Hatched bars show CDs that are most frequently selected by regression models (Ssegane et al., 2012a) used for prediction of event characteristics within each homogeneous cluster. Wetness conditions (e.g., *PET.P*), the texture properties subsurface soil (e.g., *tsilt* and *tclay*) and storage properties defined by soil depth and hydraulic conductivity (e.g.,

*soil.depth* and *kf.Moderate2Low*) are frequently selected as explanatory variables of cluster-specific regression models and constitute the principal CDs in all clusters (Figure 3.8). Climatic variables are instead the most informative for spatially dispersed Cluster 6 (Figure 3.8f). Land use and descriptors of geological settings appear to have less explanatory power, accounting only for a small portion of the variability of the selected CDs dataset. Only for Cluster 3 (i.e., Central Uplands) land cover seems to play an important role.

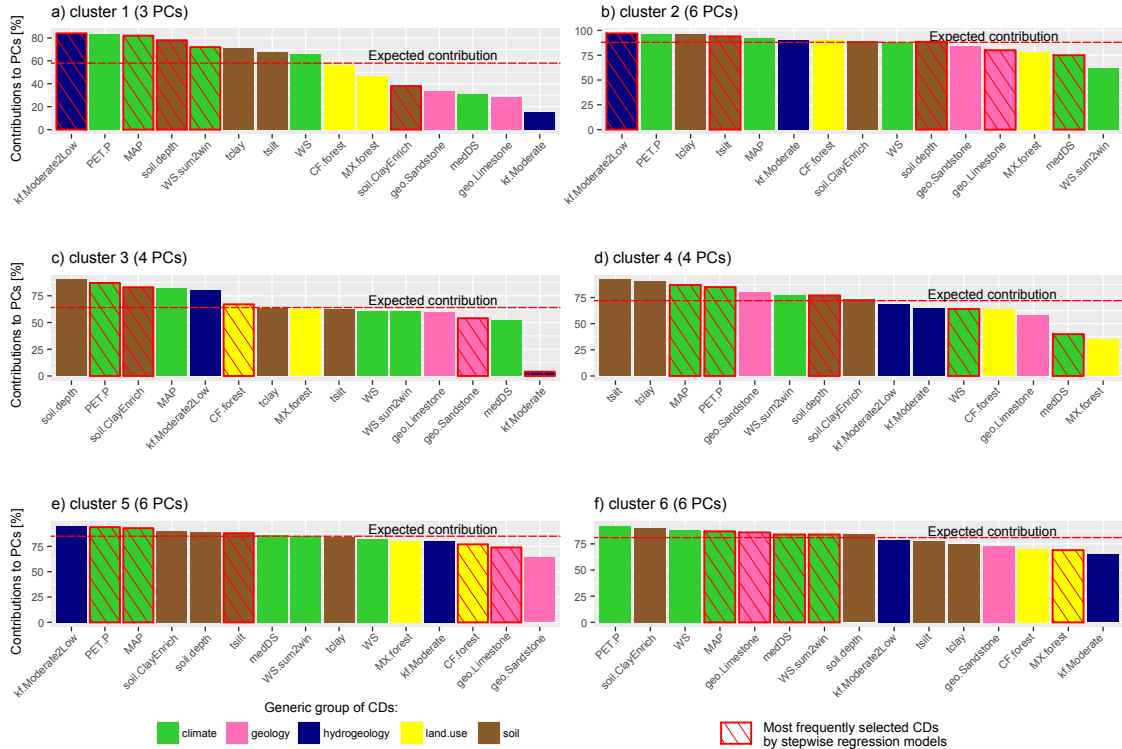


Figure 3.8: Contribution (%) of individual catchment descriptor CDs (selected through the BE method based on cluster similarity) to the significant Principal Components (PCs) of each cluster. The CDs that contributed above the average expected contribution were referred as the principal CDs (Razavi and Coulibaly, 2013). Cluster numbering refers to topology of the SOM output layer (see Figure 3.5). Hatched bars indicate the most informative explanatory descriptors defined as the variables most frequently selected by regression models for prediction of event characteristics within the cluster (Ssegane et al., 2012a)

### 3.5 Discussion and Conclusions

#### 3.5.1 Regions of homogeneous event runoff response

Clear regional patterns of event runoff response are visible in Germany due to the dominant role of climatic conditions. However, exceptions that provide an insight on the role played by other controls exist. For example, despite considerable differences in elevation and precipitation amounts (Figure 3.2a, b), the flatter catchments of the Alpine Foreland show event runoff response more similar to catchments of the North German Plains (Figure 3.5a, cluster 4) than to their snow-dominated neighbors with headwaters in the Alps (Figure 3.5a, cluster 2). The reason of this similarity is to be found in soil and hydrogeological properties of the Alpine Foreland catchments: deep soils, permeable porous aquifers provide large subsurface storage, analogously to lowland catchments of the North Plain. On the other hand, the strong dominance of Atlantic cyclones in Western Germany (Hofstätter et al., 2016) attenuates differences in topography and geology among western catchments (Figure 3.5a, cluster 1) and results in distinct behaviors of otherwise similar western and eastern catchments. For example, the mountain regions of the Ore Mountains (the Eastern Central Uplands) and the Black Forest (the South German Scarplands) have different event characteristics (Figure 3.5a, cluster 1 and 5) despite similar geologic formations and elevation ranges. The behavior of catchments in the Black Forest is rather similar to those in

the Rhenish Massif (the Western Central Uplands), which have much lower elevation and different hydrogeological settings.

### 3.5.2 Linking event characteristics and catchment descriptors

In order to identify catchment descriptors that embody the spatial controls of event characteristics we searched for CDs a) whose spatial clustering is the most similar to clustering based on event characteristics and which b) have the highest predictive power in estimating event characteristics with multiple regression models in a regionalization experiment. We avoided subjective a-priori choices of catchment descriptors by employing several variable selection methods and two different performance criteria. Our results show that the variables selected by the best performing method (BE) do not necessarily have very high correlation with event characteristics (Figure 3.5b and 3.6). The BE method selected only 15 catchment descriptors (which is much less than the other variable selection methods did) (Figure 3.7a), performed better in terms of cluster similarity and comparable in terms of predictive performance. Selected CDs belong to five different generic groups of descriptors: climate, soil, land use, hydrogeology and geology. Thus, we found several pivotal controls but, differently from other studies, we could not identify one dominant driver, probably due to the heterogeneity of the study region and to the varied scale of influence of different physical processes. At national scale climate and hydrogeological settings are the two primary controls on hydrological similarity. In fact, catchment classification based on climatic or hydrogeological CDs alone provides clusters similar to those obtained by the classifying catchments based on event characteristics (Figure 3.7a).

Differently from the results of Gottschalk and Weingartner (1998), topographic CDs were not explicitly required to reproduce the observed patterns of event characteristics. However, clusters with similar event characteristics organized themselves according to dominant landscape units (i.e., high range mountains, medium range mountains, hills, plains). Combinations of climatic descriptors, soil properties and land use (e.g., forested areas) are essentially substitutes for topographic features. Compared to climate, soil and hydrogeological properties, land use descriptors can predict event characteristics of the studied mesoscale catchments only to a limited extent (Figure 3.7-3.8). Abundance of agricultural areas in Germany leads to low variability of the adopted land use descriptor. Hence, its explanatory and discriminative power is low in this study. Our results confirmed the findings of Merz and Blöschl (2009a) and Gaál et al. (2012) about the irrelevance of catchment size as spatial control of event characteristics for mesoscale catchments ( $>10 \text{ km}^2$ ). For smaller catchments, however, the effect might still be considerable as reported by Cerdan et al. (2004). Geological classes that were not selected by any of tested methods are confined to the specific regions and therefore probably are not informative for prediction at regional scale. The poor explanatory power of the groundwater recharge descriptor can be explained by deficiencies of its derivation. Indeed, it was obtained by Jankiewicz et al. (2005) based on water balances of 106 German catchments and then interpolated countrywide by using slope, drainage, land use, depth of groundwater table and effective field capacity.

In summary, our findings reveal that when all the available catchment descriptors are used the performance in terms of cluster similarity and predictive potential of cluster-specific models is lower than the one obtained by only using the selected CDs. The application of a backward elimination procedure to select relevant catchment descriptors promises accurate prediction of spatial patterns and regionalized values of event characteristics. Hence, prior identification of hydrologically-relevant catchment descriptors is essential for improving the performance of regionalization methods based on physical similarity.

### 3.5.3 Hydrological interpretation of the emerged regional pattern of event characteristics and their spatial controls

In this Chapter a hydrological interpretation of the findings of our data-based analysis is presented. The spatial analysis of event runoff characteristics reveals the existence of six clusters of different event runoff behavior in Germany (Figure 3.5a), which can be effectively explained

by 15 catchment descriptors (Figure 3.5b). In Figure 3.9 we generalize the findings by showing for each cluster an archetypical catchment, where the mean values of the 15 CDs are visualized (Figure 3.9, legend bottom panel) together with cluster typical event runoff characteristics, such as the cumulative distribution function of event runoff coefficients, the typical shape of the runoff hydrograph (inferred from values of event time scale and rise time) and the relationships of event runoff coefficients with event rainfall volume and soil moisture (top of each cluster panel). We also visualize some hydrological reasoning resulting from the analysis. We assume that saturation excess is the primary runoff generation mechanism since for most of the analyzed catchments only a limited relationship between event runoff coefficient and rainfall intensity was observed (Tarasova et al., 2018b), thus implying that infiltration excess plays only a minor role. Therefore, the higher the event runoff coefficient the higher the portion of catchment area that contributes to runoff. Accordingly, the lower quartile of the typical cumulative distribution of event runoff coefficients for each cluster (Figure 3.9, upper panel) represents the portion of catchment area that permanently contributes to runoff generation (i.e., the permanently saturated region). Adopting the formulation of Rogger et al. (2013), the upper quartile of the distribution of runoff coefficients indicates the spatial extent of the variably saturated region, whereas the difference between lower and upper quartiles provides information on the modality of increase of the variably saturated area. Since our lumped approach does not allow for explicitly identifying which parts of a catchment contribute to runoff, we plotted the runoff contributing portion of the catchment around the riparian areas in Figure 3.9. Characteristic time scales and rise times provide inference about the importance of fast and slow interflow for event runoff generation. Accordingly, we plotted arrows of various thicknesses, indicating the relative contribution of fast and slow interflow and base flow in the different clusters. Finally, the importance of snowmelt for runoff generation can be inferred from the seasonality of time scale and the occurrence of multiple-peak events. Crucial physical attributes of catchments and key hydrological processes occurring in each cluster are discussed in the following.

**Cluster 1. Small storage, in-phase seasonality of soil moisture and rainfall** According to its typical cumulative distribution of event runoff coefficients (Figure 3.9a, upper panel), the lower quartile is much lower than the median, indicating that only a small portion of the catchment area permanently contributes to runoff generation. On the contrary, the upper quartile is very high, indicating that the spatial extent of the variably saturated region encompasses most of the catchment area. A substantial difference between the lower and upper quartiles of the distribution of runoff coefficients denotes an instantaneous increase of the saturated area (Rogger et al., 2013). The fast interflow component plays a dominant role in event runoff generation for the fast-reacting catchments of this cluster. Melt is relatively important as well.

In this cluster runoff coefficients strongly depend on the volume of single rainfall events (Figure 3.9a, middle panel) (Tarasova et al., 2018b), implying possible event-fed saturation (Berghuijs et al., 2016b). According to the findings reported in the companion study of Tarasova et al. (2018b), this is the only region where a high correlation between event runoff coefficient and precipitation intensity exists, thus implying that infiltration excess is a possible runoff generation mechanism as well. Moreover, there is a distinct non-linear relationship between runoff coefficient and antecedent soil moisture (Figure 3.9a, middle panel), which indicates two distinct functioning states for catchments of this cluster (Grayson et al., 1997).

These catchments are characterized by small subsurface storage (i.e., shallow soils (Struthers and Sivapalan, 2007) and impermeable bedrock (Pfister et al., 2017)) (Figure 3.9a, lower panel). Small storage, high annual precipitation and volume of rainfall events explain the large extent of the variably saturated region in these catchments. The presence of impermeable bedrock implies the possible existence of bedrock depressions which must be filled to trigger the generation of subsurface flow (Tromp-Van Meerveld and McDonnell, 2006). Large fractions of clay and silt in the topsoil provide the condition for runoff generation caused by infiltration excess, as hypothesized above based on the detected relation between runoff coefficients and intensity of rainfall events. Corresponding seasonality of soil moisture and rainfall (i.e., substantial precipitation falls during the winter season when evapotranspiration is low and soils are wet) is another indicator of a

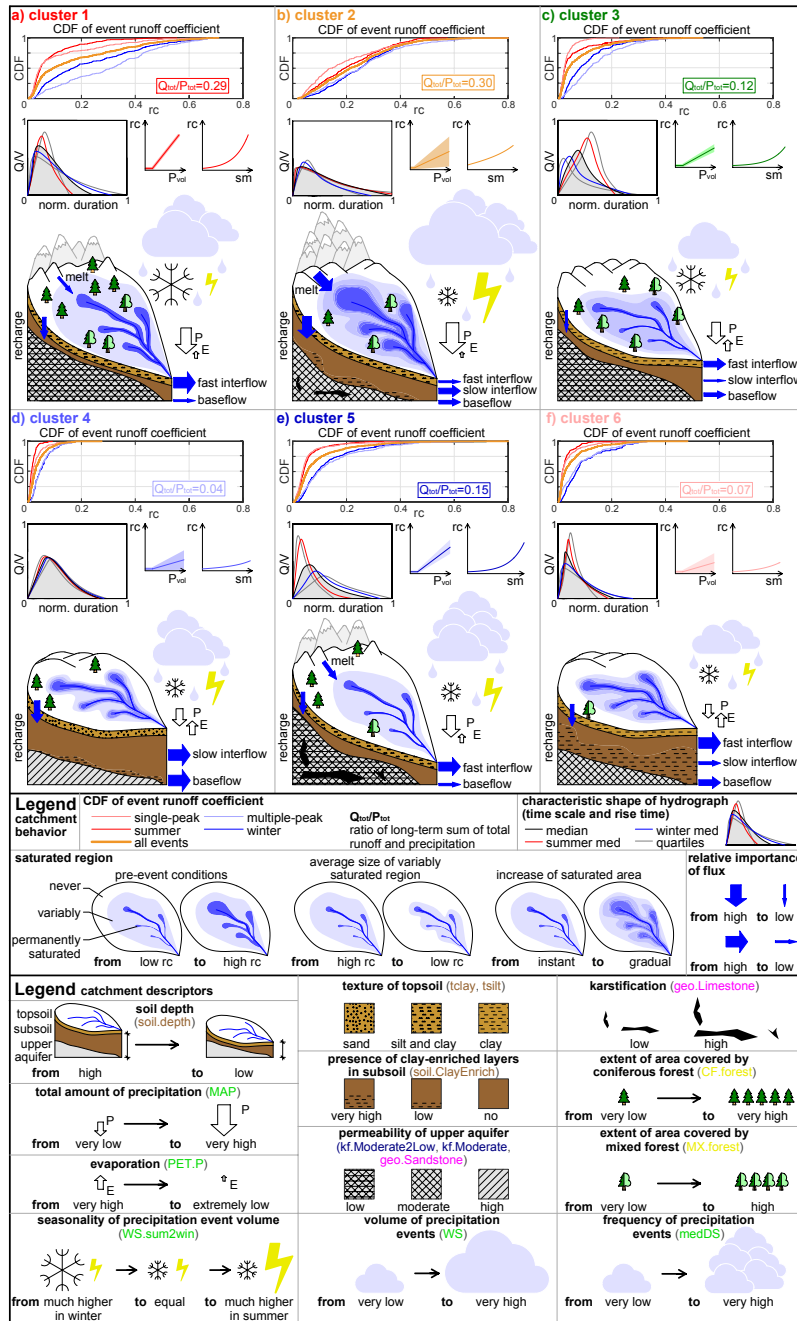


Figure 3.9: Archetypal behaviors of catchments from the identified clusters (Figure 3.5a). The cumulative distribution function of event runoff coefficients for a representative catchment (Figure 3.10) of respective cluster (upper panel of each cluster) informs about runoff coefficients for “dry” and “wet” states (and thus on the extent of the variably and permanently saturated regions) and about the character of change between the states (i.e., distinct switch or gradual increase). Typical shapes of hydrographs and their variability and seasonality (middle panel) are derived from cumulative distributions of event time scales and rise times. Typical relationships between runoff event coefficient ( $rc$ ) and both volume of precipitation event ( $Pvol$ ) and antecedent soil moisture ( $sm$ ) are schematically represented as well (middle panel). Typical catchment properties are presented using CDFs selected by the best-performing variable selection method. The thickness of the blue arrows indicates the relative importance of the hypothesized fluxes. The texture of the topsoil is represented based on the proportion of silt and clay. The thickness of the subsoil is related to the descriptor of soil depth. The presence of duplex subsoil structure with one of the horizons enriched with clay is inferred from the abundance of Luvisol soil type (*soil.ClayEnrich*). The permeability of the upper aquifer is derived from the two classes of the descriptor of hydraulic conductivity (*moderate* and *from moderate to low*) and from the presence of sandstone, which can be interpreted as an indicator of low conductivity. The presence of limestone is perceived as an indicator of possible karstification. Land cover is presented in terms of abundance of coniferous and mixed forests. The volume of precipitation events (symbolized by the size of clouds) is approximated as the mean volume of wet spells, while the frequency of the events (number of clouds) is derived from the median duration of dry spells. The seasonality of precipitation (relative sizes of snowflakes and flashes of lightning) is derived from the ratio between the mean volumes of summer and winter precipitation. General climatic conditions (i.e., precipitation and evaporation, represented with white arrows) are inferred from mean annual precipitation and dryness index.



pronounced threshold behavior in this cluster (Sivapalan et al., 2005).

**Cluster 2. Spatially variable storage, seasonal influence of melt, large rainfall events and soil moisture** The lower quartile of the distribution of runoff coefficients is relatively high (Figure 3.9b, upper panel), indicating that a substantial portion of the catchment area permanently contributes to runoff generation. The upper quartile is very high, denoting large spatial extent of the variably saturated area. The increase between quartiles is almost linear, indicating a gradual filling of the catchment's variably saturated region (Rogger et al., 2013). A mixture of runoff generation processes occurs in these catchments. However, snowmelt and fast components of runoff generation are pivotal especially in summer. In this cluster runoff coefficients are largely independent from the volume of single rainfall events (Figure 3.9b, middle panel), implying that event-fed saturation is unlikely to occur (Tarasova et al., 2018b). A near-linear increase of runoff coefficients with increasing antecedent soil moisture indicates a gradual transition from "dry" to "wet" states. Due to variable landscape conditions catchments (Figure 3.9b, lower panel) of this cluster have variable subsurface storage capacity. Spatial variability of soil depth and porosity (i.e., presence of clay-enriched subsoil layers) explains the gradual and linear increase of the saturated area, as the regions with shallow soils will be saturated first (Struthers and Sivapalan, 2007). Very high annual precipitation and event volumes determine the existence of a large variably saturated area (Rogger et al., 2013). Processes driving runoff generation appear to be seasonally interchangeable in this cluster: in spring and early summer melt processes dominate, large rainfall events occur in late summer and autumn, while soil moisture is very high in winter due to low evapotranspiration. Although existent, threshold processes are in this cluster essentially averaged by the seasonal and spatial interchange of different runoff generation mechanisms.

**Cluster 3. Spatially variable storage, in-phase seasonality of soil moisture and rainfall** Only a relatively small portion of the catchment area contributes to runoff generation, since the lower and the upper quartiles of the distribution of runoff coefficients are fairly low (Figure 3.9c, upper panel). The difference between quartiles, sizable but much smaller than in cluster 1, indicates a more gradual filling of the variably saturated area (Rogger et al., 2013). Fast interflow is especially important in winter, but generally a mixture of processes occurs. In this cluster runoff coefficients weakly depend on the volume of single rainfall events (Figure 3.9c, middle panel), implying possible although infrequent event-fed saturation (Berghuijs et al., 2016b), as the volume of precipitation events is rather moderate (Figure 3.9c, lower panel). Moreover, there is a non-linear relationship between runoff coefficient and antecedent soil moisture (Figure 3.9c, middle panel) (Tarasova et al., 2018b) which reveals two distinct functioning states for catchments of this cluster (Grayson et al., 1997). It is worth to note that the transition between these two states seems to be less pronounced than in cluster 1 (Figure 3.9a, middle panel). Similar to cluster 1 these catchments have relatively shallow soils and impermeable bedrock, which imply small subsurface storage (Figure 3.9c, lower panel). However, due to the presence of diverse landscape forms varying from low-range mountains to hilly and flatter areas the soil depth is more variable and the expansion of the variably saturated region might occur more gradually (Rogger et al., 2013). Possible threshold behaviors in this cluster might be strengthened by the in-phase seasonality of soil moisture and rainfall (Sivapalan et al., 2005).

**Cluster 4. Very large storage, evaporation-controlled soil moisture** Only a very small portion of the catchment area contributes to runoff generation, as indicated by the very small values of the lower and upper quartiles of the distribution of runoff coefficients (Figure 3.9d, upper panel). Their difference is also very small, thus denoting a gradual filling of the catchment's variably saturated region (Rogger et al., 2013). Slow interflow is the dominant runoff generation process. Absence of variability and seasonality of time scale and rise time (Figure 3.9d, middle panel) highlights the catchment's ability to effectively filter the variability of the climatic inputs. In this cluster runoff coefficients are largely independent from the volume of single rainfall events (Figure 3.9d, middle panel), implying that event-fed saturation is unlikely to occur. There is a

very gradual increase of runoff coefficients with increasing soil moisture (Tarasova et al., 2018b). These catchments are characterized by very large subsurface storage provided by deep permeable soils and aquifers (Figure 3.9d, lower panel). The gradual increase of event runoff coefficients and hence the increase of the variably saturated region is probably controlled by the variability of groundwater interactions in the riparian zone of the catchment, because the subsurface storage (i.e., soil depth) appears to be uniformly distributed in space and therefore cannot explain a gradual increase of the variably saturated region. High evapotranspiration control inter-event drying of sandy topsoil, which have poor water-holding capacity. Since rainfall events are typically small, their frequency and especially the intensity of inter-event evapotranspiration define the extent of the variably saturated region and the event runoff response (Berghuijs et al., 2016b). In this cluster threshold processes seem to affect catchment behavior only to a very limited extent.

**Cluster 5. Small storage, frequent small rainfall events, antiphase seasonality of soil moisture and rainfall** The low value of the lower quartile in cluster 4 (Figure 3.9e, upper panel) resembles the one observed in cluster 1 and cluster 3 and indicates a small extent of the permanently saturated area. The value of the upper quartile is higher than in cluster 3 but lower than in cluster 1, revealing an intermediate extent of the variably saturated region and a rapid increase of the area contributing to event runoff generation (Figure 3.9e, upper panel). A mixture of runoff generation processes occurs, but fast components play an important role especially in summer. Flashy summer hydrographs indicate that snowmelt contributes to runoff generation only to a limited extent during this season.

In this cluster runoff coefficients weakly depend on the volume of single rainfall events (Figure 3.9e, middle panel), implying that event-fed saturation is rather unlikely (Berghuijs et al., 2016b). Similar to cluster 1 and 3, there is a distinct non-linear relationship between runoff coefficient and antecedent soil moisture (Figure 3.9e, middle panel) (Tarasova et al., 2018b), revealing two distinct functioning states of the catchment (Grayson et al., 1997).

These catchments are characterized by small subsurface storage (i.e., shallow soils). Possible karstification (Figure 3.9e, lower panel) might be an additional source of threshold processes in this cluster (Hartmann et al., 2013). Small but very frequent rainfall events together with a relatively low dryness index indicate that runoff generation is controlled by the sequence of rainfall events which modify the extent of the variably saturated region (Berghuijs et al., 2016b). Differently from cluster 4, drying of soil moisture through evapotranspiration plays a minor role in this cluster as indicated by the low ratio between overall evapotranspiration and precipitation amounts. The effect of threshold processes observed in the catchment might be weakened by the antiphase seasonality of soil moisture and large summer rainfall events (Sivapalan et al., 2005).

**Cluster 6. Duplex (layered) subsoil structure, evaporation-controlled soil moisture** Similar to cluster 4, the lower and upper quartiles of the distribution of runoff coefficients (Figure 3.9f, upper panel) are very small in this cluster, indicating that only a very small portion of the catchment area contributes to runoff generation. The difference between quartiles is also very small and denotes a gradual filling of the catchment's variably saturated region (Rogger et al., 2013).

In this cluster runoff coefficients are largely independent from the volume of single rainfall events (Figure 3.9f, middle panel), implying that event-fed saturation is unlikely to occur. There is a very gradual increase of runoff coefficients with increasing soil moisture (Tarasova et al., 2018b). Fast interflow is the dominant runoff generation process, especially in winter.

These catchments are characterized by large subsurface storage provided by deep soils and permeable aquifers (Figure 3.9f, lower panel). However, the subsoil of these catchments typically has a pronounced duplex (layered) structure set by the presence of clay-enriched layers (i.e., Luvisols) (FAO, 2006; Western et al., 2004). Such structure of the subsoil entails high spatial variability of the available subsurface storage and determines a gradual increase of the variably saturated region (Rogger et al., 2013) and the respective event runoff coefficients (Figure 3.9f, upper panel). It restricts the depth of subsurface flow as well. Very small rainfall events with long dry spells and intense evapotranspiration control the inter-event drying of the topsoil, which constitutes the dominant control of event runoff response (Berghuijs et al., 2016b). However, high silt and clay

contents in the topsoil of this cluster might buffer the drying effect compared to sandy topsoil of cluster 4. Interestingly, intra-cluster predictability of event characteristics was dependent on the portion of catchment covered by mixed forest (Figure 3.8f), supporting the hypothesis that evapotranspiration-driven drying of soils is a major control for this cluster. Finally, threshold processes seem to affect catchment behavior only to a very limited extent.

### 3.5.4 Concluding remarks: event characteristics as hydrological signatures

In this study we adopt event characteristics of separated rainfall-runoff events as hydrological signatures of catchment behavior and analyze their regional pattern and spatial controls to shed light on the heterogeneity of runoff generation processes. Linking observed event characteristics and their temporal dynamics (Tarasova et al., 2018b) with event runoff generation mechanisms (Berghuijs et al., 2016b) and the concept of threshold processes in catchments (e.g., Grayson et al., 1997; Zehe and Sivapalan, 2009; Struthers and Sivapalan, 2007; Tromp-Van Meerveld and McDonnell, 2006; Rogger et al., 2013) allowed us to develop archetypes of distinct catchment behaviors (Figure 3.9) that are supported by a set of objectively selected hydrologically-relevant catchment descriptors.

Rainfall-runoff events appear to be a representative unit of runoff dynamics, which not only reflects rainfall as the main driver, but also provides insights on the catchment sensitivity to pre-event state (i.e., variability of available storage capacity). Pre-event catchment state (i.e., soil moisture) is largely affected by evapotranspiration-controlled drying, thus temporal dynamics (i.e., variability) of the event runoff response displays as well the effect of inter-event evapotranspiration.

In fact, strong relations between event characteristics and wetness state allow for direct inference concerning the role of storage in catchment functioning. This makes dynamic event characteristics advantageous compared to long-term water-balance-based signatures (e.g., long-term ratio of runoff and precipitation  $Q_{tot}/P_{tot}$ , see Figure 3.9, upper panels), which assume no net change in storage (Olden and Poff, 2003) and therefore rather refers to long-term partition of precipitation into runoff and evaporation (i.e., they essentially relate to the dryness index defined as the ratio of long-term potential evaporation and precipitation) and do not necessarily capture differences in catchment functioning (see e.g. cluster 1 and 2 in Figure 3.9, having similar  $Q_{tot}/P_{tot}$  but different cumulative distributions of event runoff coefficients and runoff generation mechanisms).

Identified archetypes of catchment behavior are largely explained by characteristics of subsurface storage (e.g., soil depth, permeability, texture) and climatic attributes (e.g., duration of dry spells, volume of wet spells, dryness index). The identified controls of event runoff response and hydrologically-homogeneous regions can provide useful information for selecting relevant physical catchment descriptors for regionalization of hydrological metrics and improving the realism of conceptual hydrological models by deriving regionally-coherent and physically-informed model parameters for the whole of Germany. Although selected catchment descriptors might vary in different settings and other regions, it is likely that descriptors expressing properties of subsurface storage, rainfall dynamics and evapotranspiration will define event runoff response elsewhere. Land use might control dissimilarity of catchment behaviors within regions with relatively homogeneous climatic conditions and subsurface structure where evapotranspiration-controlled drying of soil moisture largely defines pre-event wetness state.

The identified cluster-specific dominant drivers of event runoff response have important implications for understanding controls on threshold processes at catchment scale and their effects on the predictability of catchment response and flood hazard (Zehe and Blöschl, 2004; Rogger et al., 2013). Moreover, the derived catchment archetypes provide information on the sensitivity of certain catchments to possible changes. For example, catchments dominated by event-fed saturation with an instant increase of the variably saturated region are vulnerable to change of rainfall volumes, whereas changes of temperature and frequency of rainfall events will be decisive in catchments where the event runoff response is controlled soil moisture resulting from evapotranspiration. In such catchments changes of land use might impose pronounced modifications of the event runoff response as well. Finally, changes in the seasonality of rainfall, soil moisture and snowmelt can additionally affect the emergence or intensity of non-linear catchment behaviors.

### 3.6 Supporting Information

This Supporting information presents additional information in Table 3.3 on the catchment descriptors used in this study and selected by different variable selection methods (grey filling of the corresponding cells). An example of the event separation is presented in Figure 3.10. Moreover, Chapter 3.6.1 gives details on Adjusted Rand Index used as the measure of similarity between two catchment classifications.

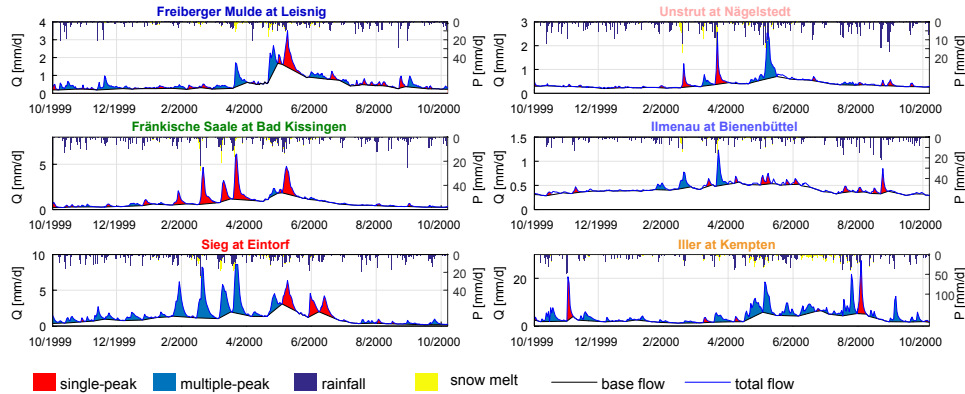


Figure 3.10: Examples of event separation and rainfall attribution for the hydrological year 1999-2000. The six catchments shown exemplify the behaviors of the six clusters of catchments identified in Germany (Figure 3.5a). The colors used for the catchments' names match those of the clusters in Figure 3.5a.

Table 3.3: Summary of catchment descriptors (CDs)

Group	Label	Units	Description	Relevance for runoff generation	Source and resolution of raster data or map scale for vector data	IG	PCA	BE
Climate	MAP	mm	Long-term mean annual precipitation	Climatic conditions	REGNIE DWD (Rauthe et al., 2013), 1x1 km raster			
	MAT	°C	Long-term mean annual temperature aggregated from daily fields interpolated by external drift kriging (Zink et al., 2017)	Climatic conditions	DWD, 8x8 km raster			
	PET	mm	Long-term mean annual temperature-based potential evapotranspiration (Oudin et al., 2005)	Climatic conditions	Temperature from DWD, 8x8 km raster			
	AET	mm	Long-term mean annual actual evapotranspiration simulated by mHM model (Samaniego et al., 2010; Kumar et al., 2013)	Climatic conditions	(Zink et al., 2017), 4x4 km raster			
	PET.T	-	Aridity index (Budyko, 1974) as ratio of mean annual potential evaporation and mean annual precipitation	Approximate long-term water balance	DWD, 8x8 km raster			

Continued on next page

Continued from previous page

Group	Label	Units	Description	Relevance for runoff generation	Source and resolution of raster data or map scale for vector data	IG	PCA	BE
	P.sum2win	-	Ratio of long-term summer precipitation and winter precipitation	Seasonality of climatic conditions	REGNIE DWD (Rauthe et al., 2013), 1x1 km raster			
	maxP	mm/day	Long-term mean maximum daily precipitation	Extremeness of climatic conditions	REGNIE DWD (Rauthe et al., 2013), 1x1 km raster			
	WS	mm	Median volume of wet spells (minimum 1 dry day between two spells)	Indicates average magnitude of precipitation events	REGNIE DWD (Rauthe et al., 2013), 1x1 km raster			
	WS.cv	-	Coefficient of variation of volume of wet spells (minimum 1 dry day between two spells)	Indicates variability of precipitation events	REGNIE DWD (Rauthe et al., 2013), 1x1 km raster			
	WS.sum2-win	mm	Ratio of median volume of summer and winter wet spells (minimum 1 dry day between two spells)	Indication seasonality of precipitation events	REGNIE DWD (Rauthe et al., 2013), 1x1 km raster			
	medDS	days	Long-term median duration of dry spells (minimum 1 wet day between dry spells)	Indicates frequency of precipitation event occurrence	REGNIE DWD (Rauthe et al., 2013), 1x1 km raster			
	maxDS	days	Mean of yearly maximum dry spells (minimum 1 wet day between dry spells)	Extremeness of climatic conditions	REGNIE DWD (Rauthe et al., 2013), 1x1 km raster			
Topography & geomorphology	elevation	m asl	Median elevation	Related to the long-term precipitation and temperature, hence to soil moisture and snow processes as well (Blöschl et al., 2013b)	DEM, SRTM, 30x30 m raster			
	slope	%	Median slope	Provides information on partition of surface and subsurface runoff generation mechanisms (Blöschl et al., 2013b)	DEM, SRTM, 30x30 m raster			
	aspect	°	Median aspect	Indicates the prevailing orientation of slopes	DEM, SRTM, 30x30 m raster			

Continued on next page

Continued from previous page

Group	Label	Units	Description	Relevance for runoff generation	Source and resolution of raster data or map scale for vector data	IG	PCA	BE
	TWI	-	Mean topographic wetness index (Beven and Kirkby, 1979) defined as $\ln(\text{area}/\text{slope})$	Defines location of possible saturation zones	DEM, SRTM, 30x30 m raster			
	area	km <sup>2</sup>	Area	First-order indicator of catchment storage (Blöschl et al., 2013b)	DEM, SRTM, 30x30 m raster			
	DD	km/km <sup>2</sup>	Drainage density	Indicator of water availability, infiltration characteristics of topsoil and drainage ability of underlying geological formation (Blöschl et al., 2013b)	DEM, SRTM, 30x30 m raster			
	LC2A	km/km <sup>2</sup>	Length of main channel to catchment area	Indicates the shape of the catchment (elongated vs. fan-shaped), affects the shape of event hydrograph (Dyck and Peschke, 1995)	DEM, SRTM, 30x30 m raster			
	slope.ch	%	Mean slope of main channel	Affects the shape of event hydrograph (Dyck and Peschke, 1995)	DEM, SRTM, 30x30 m raster			
	STMFRQ	number/km <sup>2</sup>	Number of stream junctions over catchment area (Institute of Hydrology, 1980)	Indicator of catchment shape that influences the shape of event hydrograph (Dyck and Peschke, 1995)	DEM, SRTM, 30x30 m raster			
Land use	shrub	%	Percent of the catchment covered with shrubs and herbaceous vegetation	Defines interception, infiltration capacity and evapotranspiration	CORINE 2000, EEA, 100x100 m raster			
	open.space	%	Percent of the catchment covered with little or no vegetation, and open spaces	Defines interception, infiltration capacity and evapotranspiration	CORINE 2000, EEA, 100x100 m raster			
	agri	%	Percent of the catchment covered with agricultural areas	Defines interception, infiltration capacity and evapotranspiration	CORINE 2000, EEA, 100x100 m raster			
	wetland	%	Percent of the catchment covered with wetlands	Defines additional catchment storage and smoothing of response	CORINE 2000, EEA, 100x100 m raster			
	artificial	%	Percent of the catchment covered with artificial surfaces	Defines infiltration capacity and evapotranspiration	CORINE 2000, EEA, 100x100 m raster			
	BL.forest	%	Percent of the catchment covered with broad-leaved forest	Defines interception, infiltration capacity and evapotranspiration	CORINE 2000, EEA, 100x100 m raster			
	CF.forest	%	Percent of the catchment covered with coniferous forest	Defines interception, infiltration capacity and evapotranspiration	CORINE 2000, EEA, 100x100 m raster			

Continued on next page

Continued from previous page

Group	Label	Units	Description	Relevance for runoff generation	Source and resolution of raster data or map scale for vector data	IG	PCA	BE
	MX.forest	%	Percent of the catchment covered with mixed forest	Defines interception, infiltration capacity and evapotranspiration	CORINE 2000, EEA, 100x100 m raster			
	lake	%	Percent of the catchment covered with lakes	Defines additional catchment storage and smoothing of response	CORINE 2000, EEA, 100x100 m raster			
Soil physical properties	ssilt	%	Mean fraction of silt in subsoil (30-100 cm)	Defines soil hydraulic characteristics	HWSD, 1x1 km raster			
	ssand	%	Mean fraction of sand in subsoil (30-100 cm)	Defines soil hydraulic characteristics	HWSD, 1x1 km raster			
	sclay	%	Mean fraction of clay in subsoil (30-100 cm)	Defines soil hydraulic characteristics	HWSD, 1x1 km raster			
	sgravel	%	Mean fraction of gravel in subsoil (30-100 cm)	Defines soil hydraulic characteristics	HWSD, 1x1 km raster			
	tsilt	%	Mean fraction of silt in topsoil (0-30 cm)	Defines soil hydraulic characteristics	HWSD, 1x1 km raster			
	tsand	%	Mean fraction of sand in topsoil (0-30 cm)	Defines soil hydraulic characteristics	HWSD, 1x1 km raster			
	tclay	%	Mean fraction of clay in topsoil (0-30 cm)	Defines soil hydraulic characteristics	HWSD, 1x1 km raster			
	tgravel	%	Mean fraction of gravel in topsoil (0-30 cm)	Defines soil hydraulic characteristics	HWSD, 1x1 km raster			
	sbulk	kg/dm <sup>3</sup>	SOTWIS bulk density (Engelen et al., 2005) of subsoil (30-100 cm)	Indicates subsoil material (mineral material has higher bulk density than organic matter) and compaction of subsoil	HWSD, 1x1 km raster			
	tbulk	kg/dm <sup>3</sup>	SOTWIS bulk density (Engelen et al., 2005) of topsoil (0-30 cm)	Indicates topsoil material (mineral material has higher bulk density than organic matter) and compaction of topsoil	HWSD, 1x1 km raster			
	soil.depth	dm	Mean soil depth	Indicates available subsurface storage and possible depth of subsurface flow	BÜK1000, BGR, 250x250 m raster			
	soil.	%	Percent of catchment with one of the 8 soil groups based on the classification of World Reference Base for Soil Resources (FAO, 2006):  soil.OrgLayer: soils with thick organic layers  soil.Antropo: soils with strong human influence	Classification of soil types based on their genesis  Peat soils, mainly occur in the lowlands. Presence of organic matter indicates soil ability for water retention (FAO, 2006)  Diverse soils modified by human activity (FAO, 2006)	BÜK1000, BGR, map scale 1:1000000			

Continued on next page

Continued from previous page

Group	Label	Units	Description	Relevance for runoff generation	Source and resolution of raster data or map scale for vector data	IG	PCA	BE
			<p>soils.LimRoot: soils with limited rooting due to shallow permafrost or stoniness</p> <p>soil.Water: soils influenced by water, either flood and tides or groundwater-affected</p> <p>soil.FeAl: soils set by Fe/Al chemistry</p> <p>soil.OrgAccum: soils with accumulation of organic matter</p> <p>soil.ClayEnrich: soils with a clay-enriched subsoil</p> <p>soil.Young: relatively young soils with little profile development</p>	<p>Very shallow soils over continuous rock and extremely gravelly soils, common in mountainous regions (FAO, 2006)</p> <p>Wetland soils that are saturated by groundwater for substantial time or genetically young alluvial soils (FAO, 2006)</p> <p>Develop in humid temperate and boreal regions with flat and hilly landscape and under coniferous forest (FAO, 2006)</p> <p>Presence of organic matter indicates soil ability for water retention (FAO, 2006)</p> <p>Reveals structure of soil profile (uniform/duplex) and defines depth of lateral flow (Western et al., 2003). Presence of finer texture indicates soil ability for water retention. Most common in flat and gently sloping landscapes with pronounced dry and wet season (FAO, 2006)</p> <p>Weakly developed soils in unconsolidated materials, typical for mountainous regions and extensively eroding lands (FAO, 2006)</p>				
Soil water properties	awc.	%	<p>Percent of catchment with one of the 6 classes of available water content (FAO, 2006):</p> <p>awc.150: 150 [mm/m]</p> <p>awc.125: 125 [mm/m]</p> <p>awc.100: 100 [mm/m]</p> <p>awc.75: 75 [mm/m]</p> <p>awc.50: 50 [mm/m]</p> <p>awc.15: 15 [mm/m]</p>	<p>Soil moisture characteristic, shows the amount of water available for plants (difference between field capacity and permanent wilting point) (sandy soils have lower awc than clayey soils) (FAO, 2006)</p>	HWSD, 1x1 km raster			

Continued on next page



Continued from previous page

Group	Label	Units	Description	Relevance for runoff generation	Source and resolution of raster data or map scale for vector data	IG	PCA	BE
	FC	mm	Mean effective field capacity in rooting zone	Soil moisture characteristic, shows total amount of water in the root zone after initial percolation (FAO, 2006)	BÜK1000, BGR, 250x250 m raster			
	imper.	%	Percent of catchment with one of the 4 classes. Indicates the presence and the location (depth from the surface) of an impermeable layer within the soil profile:  imper.40: impermeable layer within 40 cm  imper.no_150: no impermeable layer within 150 cm  imper.40_80: impermeable layer between 40 and 80 cm  imper.80_150: impermeable layer between 80 and 150 cm	Defines soil profile (uniform/ duplex/ gradational) (Western et al., 2004), thus indicating possible depth of lateral flow  Implies duplex soil profile and possibility of near surface lateral flow  Implies uniform soil profile and possibility of very deep lateral flow  Implies duplex soil profile and possibility of shallow lateral flow  Implies gradational soil profile and possibility of deep lateral flow	HWSD, 1x1 km raster			
	drainage.	%	Percent of catchment with one of the 6 classes. Soil drainage classes are based on the guidelines from (FAO, 2006): drainage.excessive drainage.well drainage.moderate drainage.imperfect drainage.poor <b>drainage.very_poor</b>	Reflect how fast does soil drain (coarse textured soils drain faster than the fine textured soils) (FAO, 2006)	HWSD, 1x1 km raster			
	SM	-	Long-term mean annual soil moisture within entire soil column simulated by mHM model (Samaniego et al., 2010; Kumar et al., 2013)	Average soil moisture characteristic of the catchment	(Zink et al., 2017), 4x4 km raster			

Continued on next page

Continued from previous page

Group	Label	Units	Description	Relevance for runoff generation	Source and resolution of raster data or map scale for vector data	IG	PCA	BE
Hydro-geology	recharge	mm/a	<p>Mean groundwater recharge from water balance for 1961-1990. The recharge is estimated as the difference between total precipitation, actual evapotranspiration and volume of direct runoff. Total runoff is separated into direct and base flow by the empirical method of (Kille, 1970). Base flow index of 106 gauges is interpolated to the ungauged grids using multiple regression model. Slope, drainage density, land use, effective field capacity and depth of ground water table are chosen as explanatory variables (Jankiewicz et al., 2005)</p>	Portion of rainfall that contributes to generation of slow runoff generation component	HAD, BGR, 1x1 km raster			
	Y.	%	<p>Percent of catchment with one of 5 groundwater yield classes. Measured yield of groundwater wells is regionalized using hydrogeological and geological information about aquifers:</p> <p>Yless150: yield less than 150 m<sup>3</sup>/d                      Yless500: yield less than 500 m<sup>3</sup>/d                      Y500-1300: yield from 500 m<sup>3</sup>/d to 1300 m<sup>3</sup>/d                      Y1300-4000: yield from 1300 m<sup>3</sup>/d to 4000 m<sup>3</sup>/d                      Ymore4000: yield more than 4000 m<sup>3</sup>/d</p>	Characterizes the subsurface storage of a catchment; depends on aquifers material and aquifer extent	HAD, BGR, map scale 1:200,000			
	kf.	%	<p>Percent of catchment with one of the 11 classes of permeability:</p> <p>kf.VeryHigh2High (&gt;10<sup>-3</sup> m/s)                      kf.High (10<sup>-2</sup>-10<sup>-3</sup> m/s)                      kf.Medium (10<sup>-3</sup>-10<sup>-4</sup> m/s)</p>	Hydraulic characteristics of subsurface	HÜK200, BGR, map scale 1:200,000			

Continued on next page

Continued from previous page

Group	Label	Units	Description	Relevance for runoff generation	Source and resolution of raster data or map scale for vector data	IG	PCA	BE
			kf.Medium2Moderate (10 <sup>-3</sup> -10 <sup>-5</sup> m/s) kf.Moderate (10 <sup>-4</sup> -10 <sup>-5</sup> m/s) kf.Moderate2Low (10 <sup>-4</sup> -10 <sup>-6</sup> m/s) kf.Low (10 <sup>-5</sup> -10 <sup>-7</sup> m/s) kf.Low2ExtremelyLow (<10 <sup>-5</sup> m/s) kf.VeryLow (10 <sup>-7</sup> -10 <sup>-9</sup> m/s) kf.ExtremelyLow (<10 <sup>-9</sup> m/s) kf.variable Percent of catchment with upper aquifer built with firm material Percent of catchment with upper aquifer built with loose material Percent of the catchment with aquitard Percent of the catchment with porous aquifer Percent of the catchment with karst aquifer Percent of the catchment with fractured aquifer	Indicates relatively impermeable aquifers  Indicates relatively permeable aquifers  Indicates impermeable subsurface formations and accordingly poor subsurface storage  Indicates highly permeable aquifers and accordingly high subsurface storage  Indicates presence of the karstification and therefore possible very variable permeability  Indicates possible variable permeability of upper aquifer	HÜK200, BGR, map scale 1:200,000 HÜK200, BGR, map scale 1:200,000 HÜK200, BGR, map scale 1:200,000 HÜK200, BGR, map scale 1:200,000 HÜK200, BGR, map scale 1:200,000 HÜK200, BGR, map scale 1:200,000			
firm		%						
loose		%						
aquitard		%						
porous		%						
karst		%						
fractured		%						
Geology	geo.	%	Percent of catchment with one of the 23 groups of geologic formation of bedrock: geo.Limestone-SandstoneMarlstone: bedrock formed by limestone, sandstone and marlstone geo.Impactite: bedrock formed by impactites geo.Peat: bedrock formed by peats geo.RiparianClay: bedrock formed by riparian clays geo.Aeolian: bedrock formed by aeolian depositions	It is related to storage characteristics as the type of geologic formation has a specific drainage characteristics (Blöschl et al., 2013a)	GÜK1000, BGR, map scale 1:1000000			

Continued on next page

Continued from previous page

Group	Label	Units	Description	Relevance for runoff generation	Source and resolution of raster data or map scale for vector data	IG	PCA	BE
			geo.Volcanic: bedrock formed by volcanic rocks geo.Plutonite: bedrock formed by plutonite geo.Slate: bedrock formed by slate geo.Quartzite: bedrock formed by quartzite geo.Dolomite-Marlstone: bedrock formed by dolomite and marlstone geo.Metamorph: bedrock formed by metamorphic rocks geo.Greywacke; bedrock formed by greywacke, siltstone and sandstone geo.Limestone: bedrock formed by limestone geo.Claystone-Siltstone: bedrock formed by claystone and siltstone geo.Sandstone-Conglomerate: bedrock formed by sandstone, claystone, conglomerate and partly by bituminous coal geo.Sandstone: bedrock formed by sandstone geo.ClaySilt: bedrock formed by clay and silt geo.Boulder: bedrock formed by boulder clay and till geo.SandGravelLoam: bedrock formed by sand, gravel and partly loam geo.SandClayCoal: bedrock formed by sand, clay and brown coal geo.Sand: bedrock formed by sand geo.Gravel: bedrock formed by gravel					

Continued on next page

Continued from previous page

Group	Label	Units	Description	Relevance for runoff generation	Source and resolution of raster data or map scale for vector data	IG	PCA	BE
	igneous	%	Percent of catchment with geological formation with igneous origin	It is related to storage characteristics as the type of geologic formation has a specific drainage characteristics (Blöschl et al., 2013b)	HÜK200, BGR, map scale 1:200,000			
	metamorph	%	Percent of catchment with geological formation with metamorphic origin	It is related to storage characteristics as the type of geologic formation has a specific drainage characteristics (Blöschl et al., 2013b)	HÜK200, BGR, map scale 1:200,000			
	sediment	%	Percent of catchment with geological formation with sedimentary origin	It is related to storage characteristics as the type of geologic formation has a specific drainage characteristics (Blöschl et al., 2013b)	HÜK200, BGR, map scale 1:200,000			

### 3.6.1 Adjusted Rand Index

The Adjusted Rand Index (ARI) (Hubert and Arabie, 1985) was used as a measure of similarity between the reference and each alternative classification. The ARI is expressed as follows:

$$ARI = \frac{N(a + d) - [(a + b)(a + c) + (b + d)(c + d)]}{N^2 - [(a + b)(a + c) + (b + d)(c + d)]} \quad (3.1)$$

where  $N$  is total number of catchment pairs;  $a$  is number of pairs, which belong to the same cluster according to both methods;  $b$  is number of pairs placed in one group by the first method, but not according to the second method;  $c$  is an opposite situation of  $b$ ; and  $d$  is a number of pairs, which do not belong to the same cluster according to both methods.

---

## 4 A Process-Based Framework to Characterize and Classify Runoff Events: The Event Typology of Germany

This Chapter presents a formatted version of the original paper: **Tarasova, L.**, Basso, S., Wendi, D., Viglione, A., Kumar, R., and Merz, R. A Process-Based Framework to Characterize and Classify Runoff Events: the Event Typology of Germany. *Water Resources Research*, 56(5), 1-24. <https://doi.org/10.1029/2019WR026951>, with permission from the authors (Copyright 2020 CC BY).

**Own contribution:** The manuscript was drafted by Larisa Tarasova, who also developed the proposed framework for event characterization and classification, prepared the data, performed the analysis and interpreted the results under supervision of Stefano Basso and Ralf Merz. Dadiyorto Wendi has constructed cross recurrence plots and performed recurrence quantification analysis. Alberto Viglione contributed to the derivation of indicators for the proposed framework. Rohini Kumar has provided simulated snowmelt and soil moisture for this study.

**Acknowledgement and Data:** The financial support of the German Research Foundation (“Deutsche Forschungsgemeinschaft”, DFG) in terms of the research group FOR 2416 “Space-Time Dynamics of Extreme Floods (SPATE)”, the Austrian Science Fund (“Fonds zur Förderung der wissenschaftlichen Forschung”, FWF) in terms of subproject I 3174 and the Helmholtz Centre for Environmental Research — UFZ is gratefully acknowledged. We thank Charles Luce, the Associate Editor and three anonymous reviewers for their valuable comments that helped to improve the original manuscript. For providing the discharge data for Germany, we are grateful to: LfU, LUBW, LUGV, SMUL, LHW, TLUG, HLUG, LUWG, MUV, LANUV NRW, NLWKN, WSV, EWA and GRDC prepared by BfG (<http://www.bafg.de/GRDC>). The simulations of the mHM model are available at <http://www.ufz.de/index.php?en=41160>. Climatic data can be obtained from DWD ([https://opendata.dwd.de/climate\\_environment/CDC/](https://opendata.dwd.de/climate_environment/CDC/)). CRP toolbox for MATLAB is available at <http://tocsy.pik-potsdam.de/CRPtoolbox/>. A Data Set S1 of classified events can be found at Zenodo repository (<https://zenodo.org/record/3575024>). The manuscript and Supporting Information provide all the information needed to replicate the results.

### Abstract

This study proposes a new process-based framework to characterize and classify runoff events of various magnitudes occurring in a wide range of catchments. The framework uses dimensionless indicators that characterize space-time dynamics of precipitation events and their spatial interaction with antecedent catchment states, described as snow cover, distribution of frozen soils and soil moisture content. A rigorous uncertainty analysis showed that the developed indicators are robust and regionally consistent. Relying on covariance- and ratio-based indicators leads to reduced classification uncertainty compared to commonly used (event-based) indicators based on absolute values of metrics such as duration, volume and intensity of precipitation events. The event typology derived from the proposed framework is able to stratify events that exhibit distinct hydrograph dynamics even if streamflow is not directly used for classification. The derived typology is therefore able to capture first-order controls of event runoff response in a wide variety of catchments. Application of this typology to about 180,000 runoff events observed in 392 German catchments revealed six distinct regions with homogeneous event type frequency that match well regions with similar behavior in terms of runoff response identified in Germany. The detected seasonal pattern of event type occurrence is regionally consistent and agrees well with the seasonality of hydroclimatic conditions. The proposed framework can be a useful tool for comparative analyses of regional differences and similarities of runoff generation processes at catchment scale and their possible spatial and temporal evolution.

## 4.1 Introduction

Understanding event runoff generation processes at catchment scale is crucial for gaining insights about event-to-event variability of runoff response and solutes export from catchments (McGlynn and McDonnell, 2003). This knowledge is instrumental in a wide variety of applications ranging from hydrologically-sound flood frequency predictions (Merz and Blöschl, 2008a) to the derivation of effective indicators for water quality assessment at management (i.e., catchment) scale (Minaudo et al., 2019). In a changing world, understanding generation processes of runoff events is pivotal for elucidating mechanisms behind intensification and shifts in the seasonality of river flows (Blöschl et al., 2017), trends in long-term flood series (Slater and Wilby, 2017), and possible changes in the magnitude of flood hazard in the future (Turkington et al., 2016). Therefore, the development of a general framework for understanding and comparing typical runoff event generation processes and event runoff response at large (i.e., from catchment to regional) scales is an important task. Such a framework would be a valuable tool to link a wide variety of event runoff generation processes to individual catchment responses at the event time scale. It would also enable a detailed analysis of the transformation of dominant processes from small to large runoff events, thus unveiling possible differences between processes responsible for the occurrence of unexpected extreme and ordinary events (e.g., Rogger et al., 2012; Smith et al., 2018).

Classification frameworks are essential for reducing information into a manageable amount of classes by grouping together similar objects, and are widely used in hydrological science (e.g., Wagener et al., 2007; Sivakumar and Singh, 2012; Sawicz et al., 2014; Knoben et al., 2018). Process-based classification of hydrological events, such as river floods and hydrological droughts, also gained momentum in the last decades (e.g., Merz and Blöschl, 2003a; van Loon and van Lanen, 2012) as it provides a basis for understanding the observed variety of hydrological behaviors and their causes. Large scale studies dealing with process-based classification of hydrological events usually focus on large runoff events (e.g., maximum annual floods). Applications at regional (e.g., Hirschboeck, 1987; Diezig and Weingartner, 2007; Nied et al., 2014; Sikorska et al., 2015), country-wide (Merz and Blöschl, 2003a; Berghuijs et al., 2016b), continental (Berghuijs et al., 2019) and even global scales (Stein et al., 2019) exist. A comprehensive overview of existing causative flood classification approaches is given by Tarasova et al. (2019). Yet, a consistent framework for process-based characterization and classification of runoff events that, beside flood events, analyzes a wide range of runoff magnitudes and is suitable for varied catchment sizes is still lacking.

Although the above mentioned flood classifications could theoretically be used to sort generation processes of a larger sample of runoff events (i.e., including small events), they mostly adopt spatially and temporally lumped characteristics of precipitation events (e.g., catchment- and event-averaged amount of rainfall), often neglect pre-event wetness states, and are therefore unsuitable to capture the spatio-temporal interactions of rainfall and soil moisture (Tarasova et al., 2019). This is, however, known to be a key driver of runoff generation. For example, Von Freyberg et al. (2014) found that only a small fraction (1-26%) of the total catchment area generates streamflow during rainfall events in a small pre-alpine catchment. Similarly, McGlynn and McDonnell (2003) showed that contribution from riparian zones dominates runoff for smaller events, while hillslope runoff generation increases for larger events in a New Zealand catchment. According to Seo et al. (2012) and Mei et al. (2014), space-time dynamics might also be crucial to correctly mimic magnitude and timing of flood events.

In recent decades, high-resolution observed and simulated hydrometeorological data sets became available (e.g., Zink et al., 2017), thus providing tools to analyze variations of runoff generation processes at catchment scale and their drivers (Woods and Sivapalan, 1999; Viglione et al., 2010a). This advances aim to bridge the gap between small scale studies that investigate runoff generation processes by means of detailed observations (e.g., Tromp-Van Meerveld and McDonnell, 2006; Jencso et al., 2009; Rinderer et al., 2019) and large scale studies which offer predictions of future changes of these processes purely based on modeling approaches (e.g., Gosling et al., 2017; Donnelly et al., 2017).

Another drawback of most existing flood classification frameworks is the use of classification thresholds that are only valid for specific regions. This limits the transferability of the frameworks to

other regions and hinders their application at larger (e.g., global) scales. To overcome this issue, Stein et al. (2019) introduced thresholds expressed as catchment-specific percentiles of the considered indicators. However, the application of percentiles might be less justified when a wider sample of runoff events is considered and variability of indicators based on absolute values (e.g., maximum precipitation intensity and volume of precipitation events) are much higher than for samples that include only maximum annual flood events. Therefore, it is important to develop a framework that relies primarily on dimensionless indicators and is transferable across climatic conditions and to catchments and events of different sizes (Tarasova et al., 2019).

The quality of data-based characterization and classification schemes largely depends on the quality of the available data and the robustness of the applied classification methods with respect to several aspects of uncertainty (Tarasova et al., 2019). In fact, classification results are sensitive to the uncertainty of input data from different sources (e.g., different observed temperature or precipitation data (Kampf and Lefsky, 2016), various soil moisture and snowmelt simulations (Stein et al., 2019)), to the choice of indicators used to characterize event types, and to the values of thresholds applied to attribute events to different classes (Sikorska et al., 2015; Stein et al., 2019). All these aspects must be examined to provide a robust characterization framework and guidelines for selection of input data, indicators and their corresponding thresholds.

Finally, existing automated event classification frameworks (e.g., Sikorska et al., 2015; Stein et al., 2019) utilized pre-defined classification trees, whose structures were devised based on hydrological reasoning about possible runoff generation processes. The underlying assumption is that similar hydrometeorological and catchment state conditions within an individual catchment (i.e., the blocks of the classification tree) result in similar hydrological responses (Sikorska et al., 2015). Although this assumption is rarely tested (Tarasova et al., 2019), proving its soundness would confirm the validity of the classification and lay the foundation for transferring classification results to ungauged locations.

This study aims to amend gaps and limitations of the existing classification frameworks discussed above. First, we propose a new multi-layer framework (Chapter 4.3.1) for process-based characterization of runoff events of various sizes (i.e., a large numbers of events are analyzed in addition to peaks over thresholds or events with large magnitude and recurrence intervals). The proposed framework relies on a set of transferable dimensionless indicators which describe the nature of the inducing meteorological event, its spatio-temporal dynamics and the interaction of precipitation and catchment wetness state, and does not use streamflow data. We test the effects of the uncertainty of input data and chosen indicators, as well as their sensitivity to the choice of classification thresholds, and compared their performance to that of traditional indicators relying on absolute values and lumped characteristics of inducing events and catchment states (Chapter 4.3.3 and 4.4.1). By using the proposed characterization framework, we then derive an event typology for Germany (Chapter 4.3.2). We investigate the adequacy of the hypothesized runoff generation processes by testing whether the derived event types group events with similar hydrograph dynamics (Chapter 4.3.4). Finally, we examine spatial and temporal (seasonal) patterns of event type occurrence in a wide set of German catchments (Chapter 4.3.5), and thus reveal spatial heterogeneity and temporal variability of dominant catchment-scale streamflow generation processes across Germany (Chapter 4.5).

## 4.2 Data and study area

The event classification is performed on the set of 183,955 runoff events occurred in 392 German catchments (Figure 4.1) during the course of 22 years (1979 -2002) of observations reported by Tarasova et al. (2018a). Catchment sizes range from 36 km<sup>2</sup> to 23,843 km<sup>2</sup>. The median area of catchments in the data set is 494 km<sup>2</sup>. Runoff events were identified from continuous hydroclimatic time series using the procedure illustrated in Tarasova et al. (2018b). First we separated base and quick flows using a simple smoothing algorithm (Institute of Hydrology, 1980). Then we attributed precipitation to each quick flow event if it occurred within the seasonal lag time of the respective catchment (Mei and Anagnostou, 2015). Finally, we identified single-peak components of multiple-peak events by using a set of iteratively adjusted refinement thresholds. The iterative



procedure is based on an equality test between the two distributions of event runoff coefficients derived from a reference single-peak and a refined single-peak event groups. For a detailed description of the event separation procedure we refer the reader to Tarasova et al. (2018b).

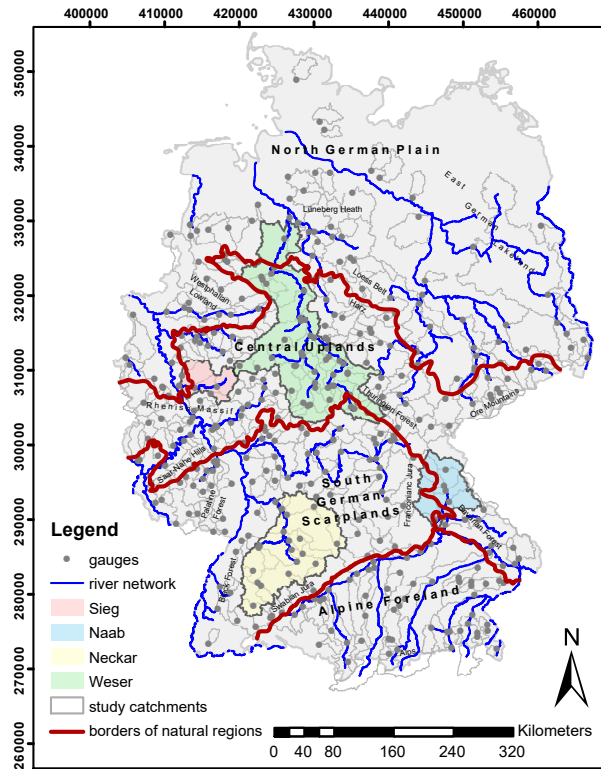


Figure 4.1: Study catchments (thin black outline) and four test river basins: the Sieg, Naab, Neckar and Weser Rivers. Grey points indicate location of gauging stations. Red lines indicate the borders of four main German natural regions: the North German Plain, Central Uplands, South German Scarplands and Alpine Forelands.

The initial rainfall-runoff event attribution described above essentially defines the lag time from the starting point of the considered runoff event backwards within which rainfall events are searched at each individual location (i.e., gauge). However, inducing events (i.e., precipitation) in the headwaters might start earlier than the observed streamflow reactions at the outlet of large river networks (Diederer et al., 2019). Therefore, precipitation events considered for the same runoff event at upstream and downstream locations might differ when the start of the precipitation event lays inside the search distance defined by the lag time for the upstream location, but is outside of this distance for the downstream location (see Chapter 4.7.1 and Figure 4.10 for a visual explanation). To remedy this issue in the case of nested catchments, individual runoff events were organized along the river network they belong to and the starting points of runoff events at downstream locations were adjusted in a way that the earliest starting date among upstream locations was assigned to all the downstream locations. These starting dates of runoff events were then used to search for the corresponding precipitation event for each individual catchment according to the seasonal median lag time as described above (see also Figure 4.10b). The search time range backwards was bounded by the starting date of the precipitation event at the upstream location. The above described procedure ensures that no precipitation is accidentally discarded in larger catchments, and allows for characterizing nested catchments consistently. We used the identified beginning and end dates of the attributed precipitation event to subset daily gridded products of hydrometeorological variables and compute event-based indicators according to the proposed characterization framework.

We used daily gridded rainfall data (1 km grid) from the REGNIE data set (Rauthe et al., 2013) provided by the DWD, and snowmelt and soil moisture time series (on a 4 km grid) simulated by the mHM (Samaniego et al., 2010; Kumar et al., 2013) along with air temperature interpolated using external drift kriging (Zink et al., 2017). For uncertainty analysis and robustness check

we additionally used a precipitation data set interpolated by means of external drift kriging (as reported in Zink et al. (2017)), a temperature data set interpolated by using the inverse distance method, 100 equifinal realizations (i.e., 100 different simulations resulted from using 100 different representative parameter sets) of the mHM model (Zink et al., 2017), as well as simulations of the alternative distributed regionally-calibrated hydrological model "The SAme Like The Others" (SALTO) (Merz et al., 2020), which has a structure similar to the conceptual Hydrologiska Byråns Vattenbalansavdelning (HBV) model (Bergström, 1995).

The uncertainty analysis (Chapter 4.3.3) was performed in 75 catchments (19% of all study catchments) belonging to four large river basins in Germany (i.e., the Sieg, Naab, Neckar and Weser Rivers, Figure 4.1). Overall it considered 38,289 individual runoff events (21% of all runoff events in the data set). The size of catchments ranges from 218 to 2825 km<sup>2</sup> for the Sieg River (4 catchments, 2462 events), from 588 to 5096 km<sup>2</sup> for the Naab River (7 catchments, 2937 events), from 135 to 12,670 km<sup>2</sup> for the Neckar River (19 catchments, 10,711 events) and from 36 to 21,583 km<sup>2</sup> for the Weser River (45 catchments, 22,179 events). The selected catchments represent the whole range of catchments sizes and hydroclimatic conditions in the German data set.

Similarity of hydrograph dynamics for each event pair in each individual catchment (Chapter 4.3.4) was calculated for events that are at least 5 days long (see Chapter 4.7.3). In total 100,750 events (55% of all runoff events) were analyzed through this procedure.

## 4.3 Methods

### 4.3.1 A process-based framework for characterization of runoff events

Here we propose a multi-layer framework for process-based characterization of runoff events based on a consistent set of indicators which capture space-time dynamics of rainfall and snowmelt, spatial organization of antecedent catchment wetness states, snow cover and soil freezing conditions as well as the spatial interaction of precipitation and soil moisture within catchments (Figure 4.2a). The idea underlying this characterization approach is that runoff events can be categorized by a set of indicators, each describing a single aspect of the transformation of rainfall into runoff. For example, one indicator characterizes the spatial extent of the precipitation field during the event, while another describes the temporal evolution of the precipitation rate during the event. The set of observed runoff events is split at each layer based on crisp predefined thresholds (e.g., Brunner et al., 2018) applied to the layer-specific dimensionless indicators (Table 4.1), and runoff events are labeled accordingly (Figure 4.2a). The combination of states categorized at each layer composes the overall character of runoff generation processes during a given event.

In the proposed framework streamflow data are not utilized for characterization, but only used to define start and end date of the events (see Chapter 4.2). In addition, we used streamflow data to validate the proposed classification (Chapter 4.3.4) by analyzing the similarity of event hydrographs of the derived event types (Chapter 4.3.2).

In the first layer of the characterization framework, we analyzed the nature of the meteorological inducing event. An event was considered a pure snowmelt (*Snowmelt*) event if the volumetric ratio of catchment-averaged event snowmelt and total precipitation is larger than a prescribed threshold value (i.e., 0.95). Such high threshold value was selected to identify events that are solely triggered by melting processes and where the contribution of rainfall is minimal. This choice as well as the choice of later described thresholds is unavoidably subjective. The sensitivity of all thresholds was therefore examined in a thorough uncertainty analysis (see Chapter 4.3.3 and 4.4.1). Similarly to snowmelt events, we used the volumetric ratio between catchment-averaged event rainfall and total precipitation to identify purely rainfall events (Table 4.1, Figure 4.2a). Among their mixtures (i.e., when the volumetric portion of both rainfall and snowmelt in the total precipitation event volume was higher than 0.05, *Mixture of Rainfall and Snowmelt*), *Rain-on-snow* events were identified by using the spatial covariance of pre-event snow water equivalent and event rainfall volume normalized by the product of their average values (Table 4.1). Spatial covariance was calculated as a grid-wise covariance of two gridded variables for a certain time step (i.e., in this case positive values of spatial covariance indicate that, within a catchment more rainfall fell on the areas where more snow water equivalent was accumulated before the beginning of the event).

*Rain-on-ice* (e.g., Wendi et al., 2019) occurs when rain falls on frozen surfaces (e.g., frozen soils) and was here distinguished from rainfall events using the spatial covariance of event-averaged rainfall volume and pre-event degree of soil freezing ( $SF_0$ ) defined as  $SF_0 = \sum_{i=0}^n |T_i|$ , where  $T$  is air temperature ( $^{\circ}\text{C}$ ) of a snow-free pixel and  $n$  is the number of days with air temperature below  $-2^{\circ}\text{C}$  during the 5 days preceding the start of a rainfall event (Flerchinger et al., 2004).

We also considered the temporal organization of the inducing event by analyzing the coefficient of variation in time of the catchment-averaged precipitation rate and the ratio of maximum intensity to total volume of the inducing event (rainfall, snowmelt or mixture depending on the nature of the inducing event) (Table 4.1). For this ratio-based indicator the classification threshold was set to its mean value (i.e., 0.5). When the ratio of maximum intensity to total volume of the inducing event is higher than 0.5, it indicates that more than 50% of event precipitation volume occurred in a single time step. Therefore, with regard to their temporal organization events can be intensity-dominated or volume-dominated (Figure 4.2a), essentially corresponding to different runoff generation mechanisms (i.e., infiltration-excess and saturation-excess) (Horton, 1933; Dunne, 1978).

Moreover, we analyzed the space-time organization of the inducing event using the coefficient of variation in space of precipitation volume and event-averaged spatial covariance of precipitation fields between consecutive time steps (Table 4.1). Using these two indicators, an event can be characterized as *Local Steady*, *Local Unsteady*, *Extensive Steady* and *Extensive Unsteady* (Figure 4.2a). For a *Local* event precipitation volume is unevenly distributed in the catchment and mostly concentrated in a small portion of it, thus possibly hinting towards local runoff generation. For an *Extensive* event, precipitation volume is instead evenly distributed in the catchment, thus possibly suggesting extensive runoff generation. For a *Steady* event, daily precipitation volume mostly occurs in the same part of the catchment during consecutive days of a wet spell, with higher likelihood of having saturated areas in this part of the catchment. On the contrary, the location of the daily precipitation volumes during consecutive days of a wet spell varies (i.e., the centroid of the precipitation moves) for an *Unsteady* event, thus suggesting that different portions of the catchment are wetted.

The second characterization layer sorts events according to their corresponding pre-event catchment wetness state (Figure 2a). We labeled event conditions as *Wet* or *Dry* based on catchment-averaged antecedent soil moisture. By using simulated soil moisture we inevitably introduce model-specific bias into the characterization framework. Simulated soil moisture essentially shows the current state of the soil moisture storage unit according to accounting schemes that are widely used in computational hydrology (e.g., Bergström, 1995). If the non-linear storage-discharge relationship used in the model differs in different catchments (e.g., Figure 4.11), using percentiles of soil moisture as threshold to define wet and dry states might be inappropriate. To properly account for the non-linear behavior of the soil moisture storage reservoir, we used the measure of maximum curvature  $\kappa$  (see e.g., Rogger et al., 2013) of a fitted exponential function that describes the non-linear relation between event runoff coefficient ( $rc$ ) and antecedent soil moisture ( $sm$ ) (Tarasova et al., 2018b, and Figure 4.11) as a classification threshold. For soil moisture states below the point of maximum curvature, event runoff coefficients tend to increase slowly with increasing soil moisture (representing dry catchment states), while beyond this point event runoff coefficients increase rapidly with soil moisture (representing wet catchment states) (Rogger et al., 2013). Curvature at each point of the function  $rc = f(sm)$  is calculated as  $\kappa = \frac{f(sm)''}{[1+(f(sm)')^2]^{\frac{3}{2}}}$  and its maximum value is calculated for each catchment in the data set. More details on the threshold used to define the wetness state of a catchment are provided in Chapter 4.7.2.

We also characterized the spatial interaction between inducing event and antecedent catchment wetness state. We used the spatial coefficient of variation as an indicator of *Uniform* or *Patchy* spatial organization of the soil moisture (Table 4.1), and in case of detected spatial inhomogeneity, the spatial covariance of event precipitation volume and pre-event soil moisture state (Table 4.1) was used to detect spatial overlapping of saturated areas and area wetted by the current precipitation event. In terms of spatial interaction each event can be characterized as *Uniform*, *Patchy Overlap* or *Patchy No Overlap* (Figure 4.2a).

For all covariance-based indicators we set the threshold at zero, because positive values of spatial covariance correspond to the occurrence of spatial overlap of the investigated hydrometeorological variables. For indicators based on the temporal coefficient of variation the threshold was set to 1 (i.e., the case when the mean is equal to the standard deviation) for all catchments. The spatial coefficient of variation instead showed dependence on catchment size, with larger catchments always having higher values of the spatial coefficient of variation compared to smaller ones. Therefore, we selected the 2<sup>nd</sup> quartile (i.e., the median) as threshold for the indicators based on the spatial coefficient of variation (Table 4.1).

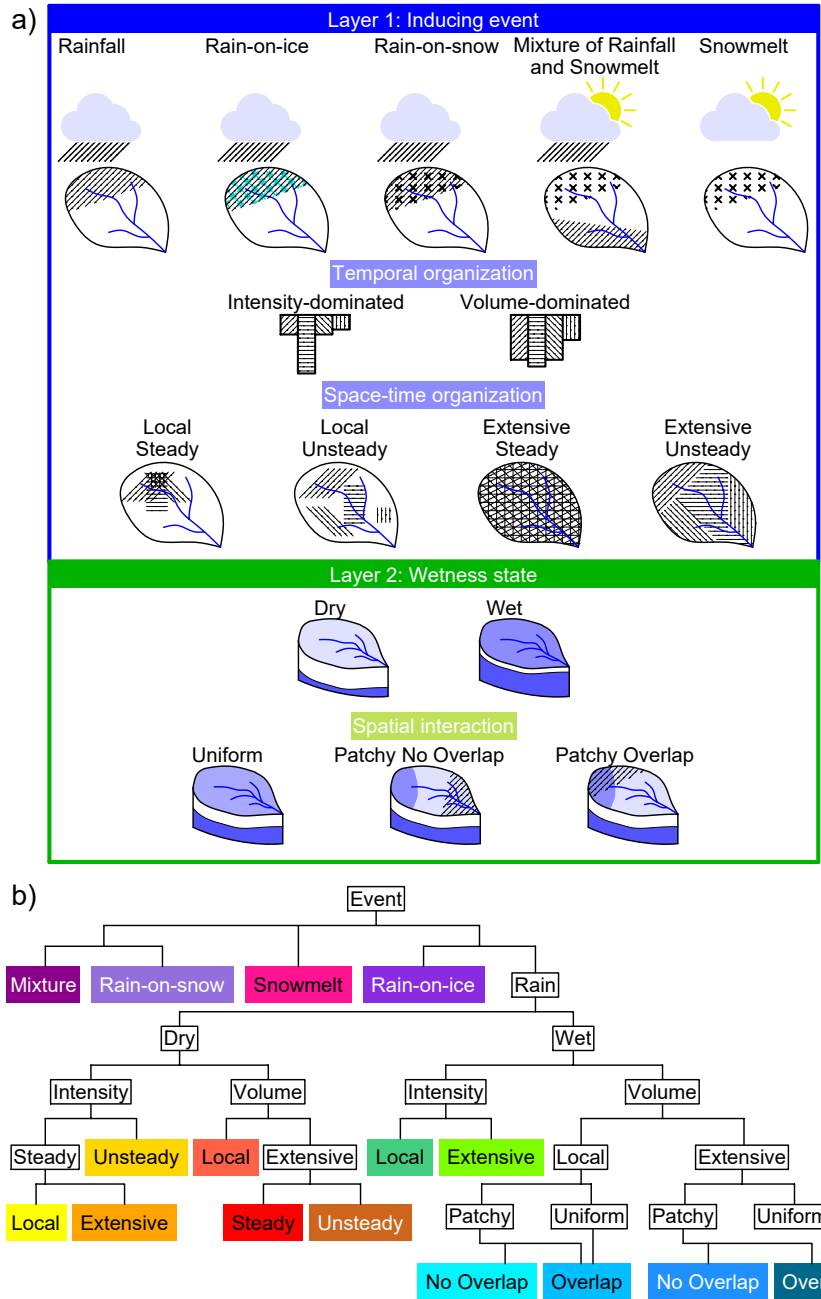


Figure 4.2: a) A multi-layer framework for process-based characterization and categorization of runoff events. Indicators and categorization thresholds used for each layer of the framework are summarized in Table 4.1; b) A decision tree to perform hierarchical classification of runoff events. The amount of possible combinations (i.e., event types) was reduced by lumping together hydrologically similar (i.e., by hypothesizing possible runoff generation processes at catchment scale that correspond to each type of runoff events, see Table 4.2) and rarely occurring combinations.

Table 4.1: Indicators for each characterization layer and alternative indicators used for robustness check of the proposed characterization framework

Layer	Selected indicator (dimensionless)	Expression	Selected thresholds and their possible intervals	Alternative indicators and their units	Thresholds and intervals for alternative indicators	Performed split
a) Inducing event	Ratio of event snowmelt volume and total event precipitation volume	$\frac{M_{x,y,t}}{P_{x,y,t}}$	0.95; [0, 1]	Absolute values of snowmelt volume (mm)	$Q_1^a; (0, +\infty)$	<i>Snowmelt</i> vs. any other type of inducing event <i>Rainfall</i> or <i>Rain-on-ice</i> vs. <i>Mixture</i> or <i>Rain-on-snow</i> <i>Rain-on-snow</i> vs. <i>Mixture</i>
	Ratio of event rainfall volume and total event precipitation volume	$\frac{R_{x,y,t}}{P_{x,y,t}}$	0.95; [0, 1]	Absolute values of rainfall volume (mm)	$Q_1; (0, +\infty)$	
	Normalized spatial covariance of event-averaged snow cover and rainfall	$\frac{cov_{x,y}(SWE_t, R_t)}{SWE_{x,y,t} * R_{x,y,t}}$	0; $(-\infty, +\infty)$	Extent of snow covered areas (-)	0.5; (0, 1)	
	Normalized spatial covariance of pre-event level of soil freezing and event rainfall volume	$\frac{cov_{x,y}(SF(t_0), R_t)}{SF_{x,y,t} * R_{x,y,t}}$	0; $(-\infty, +\infty)$	Portion of overlap of areas with frozen soils and rainfall field (-)	0.25; (0, 1)	
Temporal organization	Temporal coefficient of variation of precipitation rate	$\frac{\sqrt{var_t(P_{x,y,t})}}{P_{x,y,t}}$	1; (0, +∞)	Duration of precipitation event (days)	$Q_2; (0, +\infty)$	<i>Volume-dominated</i> vs. <i>Intensity-dominated</i>
	Ratio of maximum precipitation rate and total precipitation volume	$\frac{max(P_{x,y,t}(t))}{P_{x,y,t}}$	0.5; (0, 1]	Maximum precipitation rate (mm/d)	$Q_3; (0, +\infty)$	
Space-time organization	Spatial coefficient of variation of precipitation event volume	$\frac{\sqrt{var_{x,y}(P_t)}}{P_{x,y,t}}$	$Q_2; (0, +\infty)$	Extent of precipitation field (-)	0.5; (0, 1)	<i>Local</i> vs. <i>Extensive</i>
	Mean normalized spatial covariance of precipitation rates between consecutive time steps	$\frac{1}{t+1} \sum_t \frac{cov_{x,y}(P(t), P(t+1))}{P_{x,y,t} * P_{x,y,t}}$	0; $(-\infty, +\infty)$	Portion of overlap of precipitation fields during consecutive time steps (-)	0.25; (0, 1)	
b) Wetness state	Catchment-averaged antecedent soil moisture	$SM_{x,y}(t_0)$	$max(\kappa)^b; [0, 1]$	30-day antecedent rainfall and snowmelt index (mm)	$Q_2^a; (0, +\infty)$	<i>Wet</i> vs. <i>Dry</i>
Spatial interaction of precipitation and soil moisture	Spatial coefficient of variation of antecedent soil moisture	$\frac{\sqrt{var_{x,y}(SM_{t_0})}}{SM_{x,y,t}}$	$Q_2; (0, +\infty)$	Extent of wet areas (-)	0.5; (0, 1)	
	Normalized spatial covariance of precipitation event volume and antecedent soil moisture	$\frac{cov_{x,y}(SM(t_0), P(t))}{SM_{x,y,t} * P_{x,y,t}}$	0; $(-\infty, +\infty)$	Portion of overlap of wet areas and precipitation field (-)	0.25; (0, 1)	<i>Patchy No Overlap</i> vs. <i>Patchy Overlap</i>

Note Input data is raster-based and for each grid  $(x, y)$  and time step  $t$  during an event the following variables are provided: event rainfall rate  $R(x, y, t)$  (mm/d); event snowmelt rate  $M(x, y, t)$  (mm/d); total event precipitation rate (i.e., sum of rainfall and snowmelt rates)  $P(x, y, t)$  (mm/d); snow water equivalent  $SWE(x, y, t)$  (mm). Antecedent soil moisture  $SM(x, y, t_0)$  (-) and antecedent degree of soil freezing  $SF(x, y, t_0)$  ( $^{\circ}C$ ) (see Chapter 4.3.1) are only provided for the pre-event time step  $t_0$ . As an example of notation catchment-averaged (in space) rainfall rate  $R$  variable for time step  $t$ , is noted as  $R_{x,y}(t)$ , while event-averaged (in time) raster of event rainfall volumes is referred as  $R_t(x, y)$ .  $R_{x,y,t}$  is a catchment-averaged variable corresponding to the event rainfall total volume precipitated in a catchment. All other variables are noted in the same fashion. Here we adopt the notation of analytical framework of Viglione et al. (2010b), that quantifies space-time dynamics of runoff events and refer to spatial covariance as  $cov_{x,y}$ . Similarly, we indicate spatial and temporal variances as  $var_{x,y}$  and  $var_t$ . All covariance-based indicators are normalized by the product of the average values of the corresponding variables.

<sup>a</sup>  $Q_1, Q_2, Q_3$  are quartile of a variable that correspond to the 25<sup>th</sup> percentile, median and 75<sup>th</sup> percentile respectively.

<sup>b</sup>  $\kappa$  is the curvature of a non-linear function that describes the relation between event runoff coefficients and simulated soil moisture (see Chapter 4.3.1 for details).

### 4.3.2 Hierarchical event classification: the event typology of Germany

A goal of this study is to investigate the occurrence of different runoff generation processes, their spatial patterns and seasonality in Germany. The combination of states categorized at each layer of the proposed characterization framework (e.g., *Rain.Intensity.Local.Steady.Dry.Uniform*; Chapter 4.3.1) thoroughly describes the runoff generation process occurring during a given event. Not every possible combination occurred for each catchment in the data set (e.g., almost all rain-on-snow events are volume-dominated events occurring on wet conditions). Therefore, we reduced the amount of possible combinations of mechanisms by hypothesizing plausible runoff generation processes at catchment scale (Table 4.2), and lumping together similar and rarely occurring combinations during the hierarchical classification (Figure 4.2b).

The classification tree derived in this study is referred in the following as event typology for Germany (Figure 4.2b, Table 4.2). Notice that the complexity of the characterization framework can be adapted for the specific task at hand, for instance if a certain sample size is required for each event type (e.g., for deriving mixed distributions for flood frequency analysis) (e.g., House and Hirschboeck, 1997), or if certain characteristics are crucial despite their rarity (as in the case of sediment transport by intensity-dominated events (Basso et al., 2015)).

Table 4.2: Event types and corresponding hypothesized runoff generation processes at catchment scale

Event type	Hypothesized runoff generation processes
<i>Snowmelt</i>	Radiation-induced snowmelt (usually <i>Wet.Volume.Steady</i> )
<i>Rain-on-ice</i>	Frozen soils prevent infiltration of rainfall (usually <i>Wet.Intensity.Uniform</i> )
<i>Rain-on-snow</i>	Several possible ways of runoff generation ranging from situations when snowpack prevents infiltration of rainfall or instead either stores substantial portion of rainfall water or is degraded due to rainfall-induced snowmelt (usually <i>Wet.Volume.Extensive.Steady.Uniform</i> )
<i>Mixture of Rainfall and Snowmelt</i>	Radiation-induced snowmelt and simultaneous in time but not in space rainfall (usually <i>Wet.Volume.Local.Unsteady</i> )
<i>Rain.Wet.Intensity.Local</i>	Local runoff generation; pre-event saturation or infiltration excess; possible connectivity <sup>a</sup>
<i>Rain.Wet.Intensity.Extensive</i>	Extensive runoff generation; pre-event saturation or infiltration excess; possible connectivity
<i>Rain.Wet.Volume.Local.No.Overlap</i>	Local runoff generation, event-fed saturation, possible connectivity
<i>Rain.Wet.Volume.Local.Overlap</i>	Local runoff generation, pre-event saturation, established connectivity
<i>Rain.Wet.Volume.Extensive.No.Overlap</i>	Extensive runoff generation, event-fed saturation, possible connectivity
<i>Rain.Wet.Volume.Extensive.Overlap</i>	Extensive runoff generation, pre-event saturation, established connectivity
<i>Rain.Dry.Intensity.Local.Steady</i>	Local runoff generation; possible infiltration excess or event-fed saturation; no connectivity
<i>Rain.Dry.Intensity.Unsteady</i>	Local runoff generation; possible infiltration excess; no connectivity
<i>Rain.Dry.Intensity.Extensive.Steady</i>	Possible extensive runoff generation; possible event-fed saturation and infiltration excess; possible event-induced connectivity
<i>Rain.Dry.Volume.Local</i>	Local event-fed saturation; no connectivity
<i>Rain.Dry.Volume.Extensive.Steady</i>	Extensive event fed-saturation; possible event-induced connectivity
<i>Rain.Dry.Volume.Extensive.Unsteady</i>	Extensive runoff generation; possible pre-event saturation; possible event-induced connectivity

*Note* Due to the small number of events induced by snowmelt, rain-on-ice, rain-on-snow and mixtures of rainfall and snowmelt compared to pure rainfall-induced events, no further splitting was performed (see Figure 4.2b), but their most frequent attributes are noted in brackets.

<sup>a</sup> Here by connectivity we refer to a catchment state when a direct linkage between runoff source areas and the stream is established (Jencso et al., 2009; Rinderer et al., 2019).

### 4.3.3 Uncertainty analysis and robustness check of the proposed framework

The proposed characterization framework (Chapter 4.3.1) relies heavily on the quality of the observed and simulated input data. Therefore, we performed a rigorous uncertainty analysis and robustness check. We analyzed two different uncertainty aspects in the case of 75 test catchments belonging to four river basins that represent the variety of climatic conditions, catchment characteristics and sizes in the data set (see Chapter 4.2). First we quantified the input data uncertainty by measuring the discrepancy (defined as the portion of inconsistently categorized events among all events) in the characterization obtained at each layer when varying one of the following components:

- *Input data source (interpolation method)*: we used two Germany-wide gridded precipitation products (i.e., Rauthe et al., 2013; Zink et al., 2017) that were produced through different interpolation methods of station observations. The test was performed at 4 km resolution due to the coarser resolution of the precipitation product provided by Zink et al. (2017). In a similar fashion we analyzed effects on the results of the characterization due to different interpolation methods applied in the considered temperature data sets. In both cases only the interpolation method differed while the amount of data was not altered.
- *Data resolution*: the original spatial resolution of observed and simulated data used for event characterization was upscaled by a factor of 2 (i.e., we analyzed the effect of a coarser spatial resolution).
- *Parameter set*: we used snowmelt and soil moisture data simulated by 100 different representative parameter sets (i.e., 100 equifinal realizations of parameters in terms of streamflow efficiency for major German river catchments) of the mHM model (Samaniego et al., 2010; Kumar et al., 2013; Zink et al., 2017).
- *Model structure and calibration technique*: we used simulated snowmelt and soil moisture of two regionally-calibrated distributed conceptual hydrological models, namely the mHM and SALTO (Merz et al., 2020) models. The comparison was performed at 8 km resolution due to the coarser resolution of the latter model outputs. Both models were driven by the same input data.

In a second step we focused on the uncertainty of the categorization itself (i.e., the results of binary splits) evaluating the robustness of thresholds and selected indicators by means of Monte Carlo experiments similar to the procedure described by Sikorska et al. (2015):

- *Thresholds uncertainty*: we performed a Monte Carlo experiment by substituting the former crisp thresholds (e.g., the original value of the threshold for the temporal coefficient of variation of the precipitation rate, which was equal to 1, see Table 4.1) with random variables with probability density functions defined as truncated normal distributions (Sikorska et al., 2015). The distribution was bounded at 0 for all thresholds since negative values are physically not possible for ratio- and coefficient of variation-based indicators. For covariance-based indicators negative values are possible, but disagree with the intended meaning of the indicators (i.e., spatial coincidence) and therefore these thresholds were bounded at 0 as well. The experiment was run 10,000 times and every time a new value for each threshold was sampled randomly and used to perform the categorization based on the proposed multi-layer framework. Different from Sikorska et al. (2015), we analyzed the uncertainty at every characterization layer separately, since our framework is envisaged in a way that overcompensation through other thresholds is not possible (i.e., once attributed to a group within a characterization layer, an event cannot change its attribution). In this way we were able to quantify robustness of each layer of the proposed framework.
- *Uncertainty of indicator choice*: We chose alternative indicators for each characterization layer that potentially allows for similar stratification of events and that were previously used for causative classification of river flood events (Tarasova et al., 2019). In particular, we

compared ratio-based indicators with their counterparts based on absolute values (e.g., ratio of snowmelt and rainfall is substituted by their absolute values) (Table 4.1). Covariance-based indicators were instead compared with indicators based on the portion of overlap (e.g., instead of normalized spatial covariance of precipitation volume and antecedent soil moisture, the portion of overlapping precipitation fields and wet areas are used). In the same fashion, indicators that were based on the spatial coefficient of variation are tested (e.g., instead of the spatial coefficient of variation of precipitation volumes we used extent of the precipitation field relative to the catchment area) (Table 4.1). For indicators of catchment-averaged wetness state we used the antecedent precipitation and snowmelt index (Kohler and Linsley, 1951), which is often used as a substitute of soil moisture (Keller et al., 2018). To avoid possible biases in the application of these absolute indicators in a wide set of catchments their thresholds were defined as catchment-specific percentiles (Stein et al., 2019). First, we compared the results of categorization using these alternative indicators and the original indicators. In the following step, we performed analysis of their *threshold uncertainty* using a Monte Carlo experiment as described above for the original indicators.

#### 4.3.4 Validation of the derived event typology: similarity of hydrograph dynamics of event types

The validity of the hypothesized runoff generation processes (Table 4.2) cannot be verified at catchment scale (i.e., we cannot observe these processes at this scale). However, if a set of indicators used for event characterization is able to capture distinct runoff generation processes, similarly classified events should exhibit similar hydrological response (Sikorska et al., 2015). The proposed framework is essentially runoff-free (i.e., runoff data are used only for identifying beginning and end of events and in the regional calibration of the hydrological models which provide soil moisture and snow cover datasets). Therefore, we can validate the derived event typology (Chapter 4.3.2; Figure 4.2b) by testing if the identified event types group events with distinct hydrological response, which is comprehensively described by event hydrographs (Blöschl et al., 2013b).

To quantify and compare dynamics of event hydrographs within each study catchment we used Cross Recurrence Plot (CRP) and recurrence quantification analysis (Marwan et al., 2007). CRPs aim to describe the degree of similarity/dissimilarity between (non-linear and non-monotonic) time series of complex environmental systems and their recurring patterns. They were successfully applied in several disciplines of environmental sciences (e.g., Eroglu et al., 2016; Aceves-Fernandez et al., 2012).

The CRP similarity quantification method is based on the time delay embedded phase space representation of time series, in our case event discharge hydrographs (Wendi et al., 2019). Essentially, every point of an event hydrograph (i.e., streamflow at every time step  $Q(t)$ , Figure 4.3a) is represented in the  $m$ -dimensional phase space (e.g., a 3-dimensional phase space on Figure 4.3b) by plotting the original values of event hydrograph separated by the time delay  $\tau$  and connecting these points as a trajectory (Figure 4.3b). Time delay embedding provides an opportunity to account for the multidimensional relationships between different points in time within the events. This means that temporal evolution of discharge including effect of antecedent conditions is accounted for (Wendi et al., 2019).

Streamflow hydrographs are compared to each other based on the Euclidean distance of their phase space trajectories (Figure 4.3b). In phase space domain two event hydrographs that have similar temporal dynamics of streamflow have very close trajectories (Figure 4.3b, top panel). Instead the trajectories of two hydrographs with disparate streamflow dynamics are far away from each other in the phase space domain (Figure 4.3b, bottom panel). CRP is finally used to visualize the aforementioned similar trajectories corresponding to their time of similarity occurrence (Figure 4.3c). These are trajectories within the user-defined distance range/radius ( $\varepsilon$ ), and when the condition is met it is indicated as value 1 or otherwise 0 on a CRP. A CRP is a 2-dimensional binary matrix with  $x$  and  $y$  - axis representing the time of two compared events. When two identical event hydrographs are compared (even if they are time shifted) a single diagonal line appears on the CRP and indicates the time when two trajectories are similar (Figure 4.3c, top panel). Instead, when



two dissimilar hydrographs are compared the line on the CRP plot becomes non-existent and/or not diagonal (Figure 4.3c, bottom panel).

The resulting patterns within a CRP (Figure 4.3c) can be quantified by Recurrence Quantification Analysis (RQA), which is essentially used as a similarity measure between two event hydrographs. The chosen measure, called determinism (DET) (see Chapter 4.7.1, Figure 4.3c), intrinsically varies between 0 and 1 and defines a range from low to high (or identical) similarity in the dynamics of the two times series (Marwan, 2010). It is worth to note that CRP and RQA can effectively compare pairs of event hydrographs regardless of their possibly different duration (Wendi et al., 2019).

For detailed information on construction of CRP and performing RQA we refer the reader to the work of Wendi et al. (2019). The parameterization of CRP used in this study is described in Chapter 4.7.3.

To use DET as a similarity metric of hydrograph dynamics of event types, we calculated DET for each event pair in every catchment separately. Once events were classified, we calculated the average hydrograph similarity  $DET_{intra}$  among event pairs belonging to the same type (e.g., *Rain-on-snow*) in each individual study catchment. Similarly, we calculated the similarity  $DET_{inter}$  between event pairs belonging to different types (e.g., *Rain-on-snow* and *Rain-on-ice*). In each catchment,  $DET_{intra}$  shows how similar events of the same type are while  $DET_{inter}$  shows how similar are events classified into different types. If  $DET_{intra} > DET_{inter}$ , streamflow dynamics of events that are classified into the same type are more similar than those of events that are classified into different types. Fulfillment of this condition would support our assumption that the different hypothesized runoff generation processes (Figure 4.2b, Table 4.2) determine distinct streamflow dynamics.

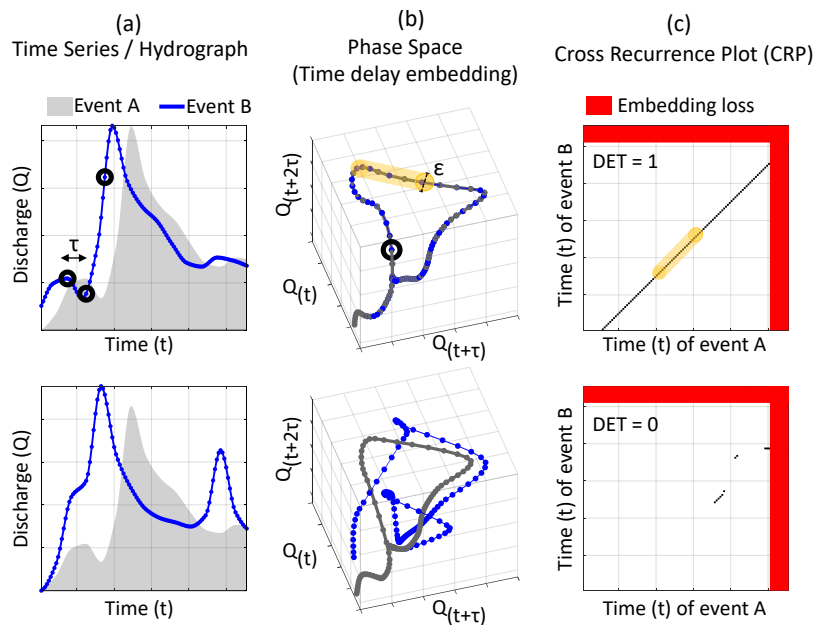


Figure 4.3: Cross recurrence plot (CRP) illustration for quantifying similarity of runoff dynamics between (a) event hydrographs (Event A and B). Top panels illustrate how two identical hydrographs with different time of occurrence (blue line and shaded area in top panel (a)) are compared in their 3-dimensional phase space where the axis correspond to the original hydrograph values separated by the time delay  $\tau$  and  $2\tau$  (top panel (b)) and CRP (top panel (c)). The bottom panels illustrate the same comparison, but for two hydrographs with different runoff dynamics. Any identical or similar piece of the phase space trajectory which falls within the distance range/radius ( $\epsilon$ ) (displayed in yellow in the top panel) is converted into a diagonal line in the CRP. These diagonal lines thus summarize the similarity of runoff dynamics between the compared hydrographs. Two perfectly identical runoff dynamics (top) have a  $DET$  of 1, while dissimilar dynamics yield low  $DET$  values (in our example  $DET = 0$ ). Portion of CRP shaded in red indicate the information loss resulted from the time delay embedding method.

### 4.3.5 Exemplary application of derived event typology in Germany

The event typology derived in Chapter 4.3.2 was applied to classify runoff events for the set of German catchments (see Chapter 4.2). Here our goal was to analyze spatial patterns of event type occurrence, their seasonality in Germany, and to obtain typical runoff characteristics for each event type.

To identify regions with similar event type occurrence, we clustered all catchments in the data set according to their distribution of event type occurrences. A simple k-mean clustering approach (Hartigan and Wong, 1979) was used. The number of clusters was determined using silhouette index (Rousseeuw, 1987).

We analyzed the seasonality of the dominant event types by defining the most frequent type within the whole study period in a particular season (i.e., for summer (June-August), autumn (September-November), winter (December-February) and spring (March-May)) and catchment. Additionally we evaluated inter-annual variability of event type occurrence for each season using a variability measure for categorical variables (Kader and Perry, 2007):

$$u_2 = 1 - \sum_{i=1}^j \left( \frac{k_i}{n} \right)^2 \quad (4.1)$$

where  $u_2$  is called coefficient of unalikeability (Perry and Kader, 2005), which is a measure of categorical variability for a variable that has  $j$  number of categories (i.e., number of possible event types),  $n$  observations (i.e., total number of events in a certain season for the whole observation period) and  $k_i$  number of objects (i.e., events) within a category (i.e., event type). Essentially, the coefficient of unalikeability defines how often the category of observations varies and can be interpreted as a portion of possible comparisons (i.e., event pairs) which are unlike (Kader and Perry, 2007). When one event type dominates in a certain season the value of  $u_2$  is close to 0. When several event types are equally dominant for a certain season  $u_2$  increases towards the maximum value of 1.

For each classified event, we derived typical event runoff characteristics that describe event runoff response. Here we considered: event runoff coefficient (dimensionless), time scale (days), rise time (dimensionless), peak discharge (mm/day) and total volume of runoff event (mm). These runoff event characteristics are fundamentally different from the indicators of the proposed framework and can be used to shed light on event runoff response (see e.g., Tarasova et al., 2018b) among different event types. The event runoff coefficient is a volumetric ratio between event runoff and event precipitation. It characterizes which portion of precipitation is stored and which portion instead contributes to event runoff. The event time scale is a ratio between event volume and peak discharge (Gaál et al., 2012). It is related to both the shape and duration of the event hydrograph. Shorter event time scales are expected when fast runoff generation processes (i.e., overland flow, fast subsurface stormflow) dominate, while longer time scales indicate the dominance of slow runoff components. The event rise time characterizes the duration (in days) from the beginning of the event till the day when peak discharge is observed (Bell and Om Kar, 1969) normalized by the overall duration of the event in days. Therefore it indicates how fast the peak discharge is reached. The peak discharge and total runoff event volume characterize the magnitude of the event. Since these characteristics depend on size, landscape and climatic settings of each catchment (Tarasova et al., 2018a), we scaled them to obtain zero mean and unit variance for their samples in each catchment and thus make them comparable across settings.

## 4.4 Results and Discussion

### 4.4.1 Uncertainty analysis and robustness check of the proposed framework

We performed an uncertainty analysis and robustness check for four test river basins (75 catchments in total) to evaluate possible regional inhomogeneity in the uncertainty of the results of the proposed characterization framework (Figure 4.4). We quantified the uncertainty as the portion of discrepancy (i.e., portion of events that is differently categorized) for each catchment among cases

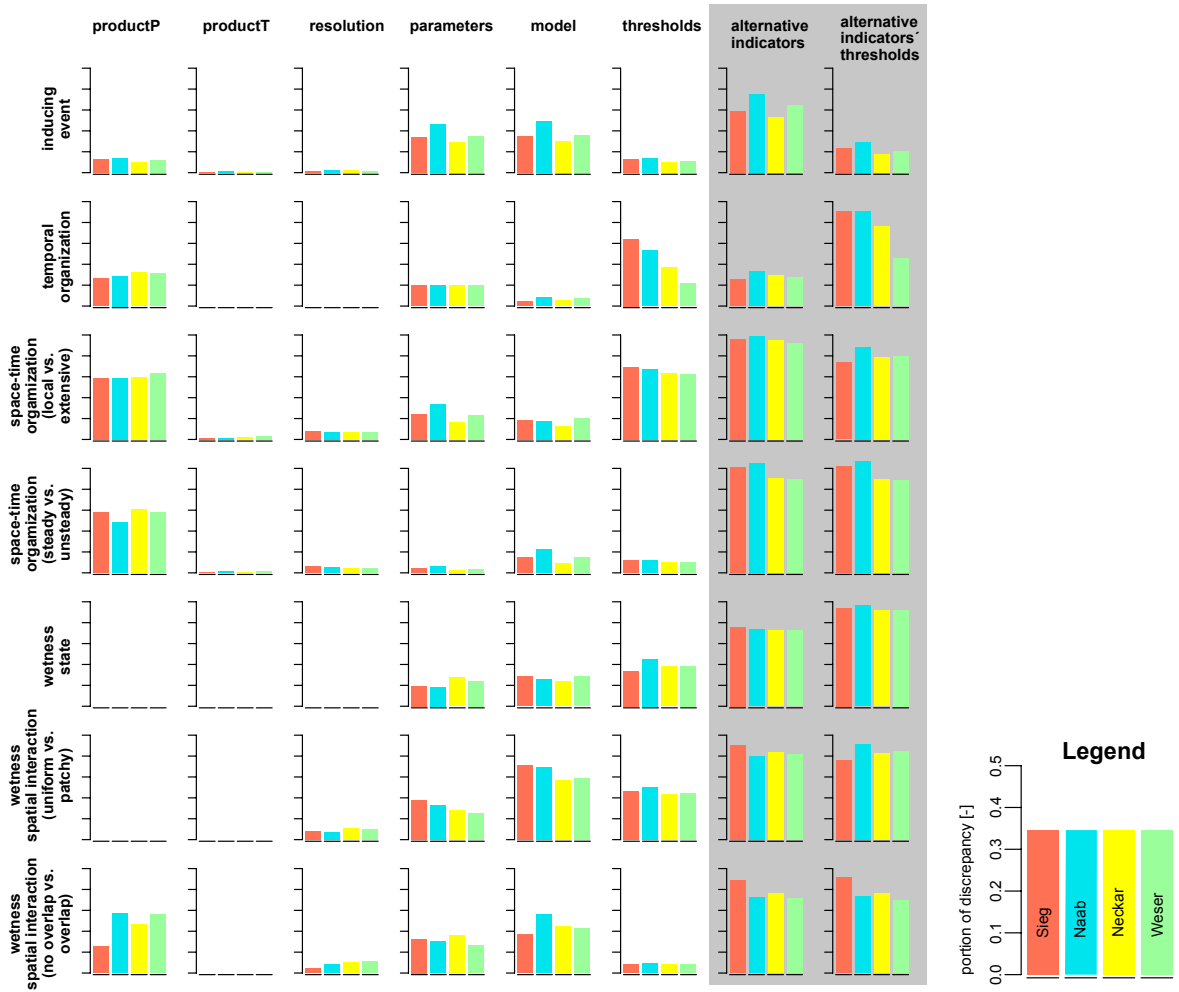


Figure 4.4: Quantification of input uncertainty and robustness of the characterization framework for four test river basins (75 catchments in total): the Sieg, Naab, Neckar and Weser Rivers. Categorization discrepancy (i.e., portion of all events that is differently categorized) was calculated for each layer of the framework (i.e., inducing event, temporal organization, spatial organization, space-time organization, wetness state and spatial interaction; see rows of the Figure). The portion of discrepancy may vary from 0 to 1. High discrepancy indicates that categorization results are highly sensitive to the specific choice of the tested feature (i.e., input data, thresholds or indicators). Different features were examined (see columns of the Figure): different precipitation (*productP*) and, temperature (*productT*) products, original spatial resolution of products upscaled by a factor of 2 (*resolution*), set of 100 different soil moisture and snow water equivalent realizations simulated by 100 equifinal parameter sets of the mHM model (*parameters*), simulations of soil moisture and snow water equivalent from the alternative SALTO model instead of the original mHM run (*model*). We performed the robustness test for thresholds (*thresholds*) by means of a Monte Carlo experiment, where values of thresholds were randomly sampled from distributions assigned to the respective indicators (see Table 4.1). We averaged the categorization discrepancy over 10,000 Monte Carlo runs. The grey background highlights categorization discrepancy when alternative indicators listed in Table 4.1 (*alternative indicators*) were used instead of the original indicators. The robustness test for their thresholds (*alternative indicators thresholds*) shows average categorization discrepancy of 10,000 Monte Carlo runs.

that use different input data, thresholds or indicators.

The choice of the precipitation product (i.e., the method used to interpolate data from rainfall gauges) (Figure 4.4, *productP*) greatly affects categorization of events in terms of the space-time organization, while their temporal organization and the nature of inducing events are only slightly affected. These results are somehow expected, as interpolation methods largely decide the spatial organization of precipitation (i.e., the data used in the space-time organization layer). However, given the large density of rain gauges in Germany, different interpolation methods are likely to provide similar results in terms of catchment-averaged precipitation rates (i.e., data used in the inducing event and temporal organization layers, Table 4.1). Increasing availability of radar data, which are believed to accurately detect the spatial structure of rainfall events (Rabiei and Haberlandt, 2015), might improve consistency also for what concerns the space-time organization of events. Conversely, the choice of the temperature product (i.e., interpolation model) (Figure 4.4,

*productT*) and the spatial resolution of input data (Figure 4.4, *resolution*) do not affect classification results in the examined catchments.

Parametric uncertainty has minor effects on event characterization (Figure 4.4, *parameters*). In case of wetness state characterization, the visible stability of the performance is an outcome of the choice made to define the classification threshold specifically for each model simulation. We set the threshold equal to the simulated soil moisture value that corresponds to the point of maximum curvature of the catchment-specific function describing the relation between soil moisture simulated by a specific model parameter set and observed event runoff coefficients (see Chapter 4.3.1). Except for the spatial organization of pre-event catchment states, the uncertainty linked to different hydrological models is comparable with the effect of parametric uncertainty of the initially selected model (Figure 4.4, *parameters* and *model*).

There is also no evidence of regional differences in the framework, save for the temporal organization layer. Indicators of temporal organization in the Sieg and Naab River basins seem to be sensitive to variations of their thresholds. A similar pattern of discrepancy is observed for the original and alternative indicators, signaling that the problem probably does not lie in the indicators themselves. However, we could not identify the exact reason of this discrepancy.

Covariance- and ratio-based indicators proved to be less sensitive to the choice of specific thresholds than indicators based on coefficient of variations (Figure 4.4, *thresholds*). Generally, the choice of indicators plays a crucial role for the characterization results, except for the temporal organization of inducing events (Figure 4.4, *alternative indicators*). According to the Monte Carlo experiment, the tested alternative indicators (which are based on absolute values and use catchment-specific percentiles of these values as thresholds) are less stable than the original indicators (Figure 4.4, *alternative indicators' thresholds*). This means that selecting quartiles as thresholds, even if it supports regional homogeneity of classification rules for indicators based on absolute values (Stein et al., 2019), makes characterization results very sensitive to the choice of thresholds. In fact, this behavior also emerges for the original (i.e., dimensionless) indicators in the space-time organization layer (*Local* vs. *Extensive*), where a quartile of the spatial coefficient of variation was used as threshold to avoid biases due to threshold selection in catchments of different sizes. This resulted in the larger threshold sensitivity compared to other dimensionless indicators, which do not use thresholds based on quartiles (Figure 4.4, *thresholds*).

#### 4.4.2 Validation of the derived event typology: similarity of hydrograph dynamics of event types

The results of the recurrence quantification analysis averaged for all catchments in the data set show distinct differences in the event hydrographs generated during wet and dry conditions (Figure 4.5a, red pixels in the lower right corner). Events that occurred during dry conditions tend to have more diverse intra-type dynamics than events occurred during wet conditions (i.e., wet events have lower  $DET_{intra}$  values on the diagonal of the matrix than the dry ones, Figure 4.5a). This can be explained by the fact that during wet cases a larger portion of catchment is contributing to runoff generation than during dry cases, thus resulting in more homogeneous runoff generation conditions.

Generally, *Local* rainfall events show much more variability in runoff dynamics (i.e., on average lower values of DET, Figure 4.5a) compared to their *Extensive* counterparts, indicating that the exact location of rainfall in the catchment for *Local* events might be the dominant control of a particular event runoff dynamic in both dry and wet cases.

Inter and intra type similarities are comparable for events that are generated during dry conditions, indicating that events generated during dry conditions have somewhat similar dynamics which are not affected by the space-time properties of rainfall events. This phenomenon is consistently observed in most of the catchments (i.e., low coefficient of variation of DET values in the lower left corner, Figure 4.5b). On the contrary a clear difference among intensity- and volume-dominated events can be observed for events generated during wet conditions (i.e., large differences between  $DET_{intra}$  and  $DET_{inter}$  values for *Rain.Wet.Intensity* and *Rain.Wet.Volume* than compared to their dry counterparts, Figure 4.5a).

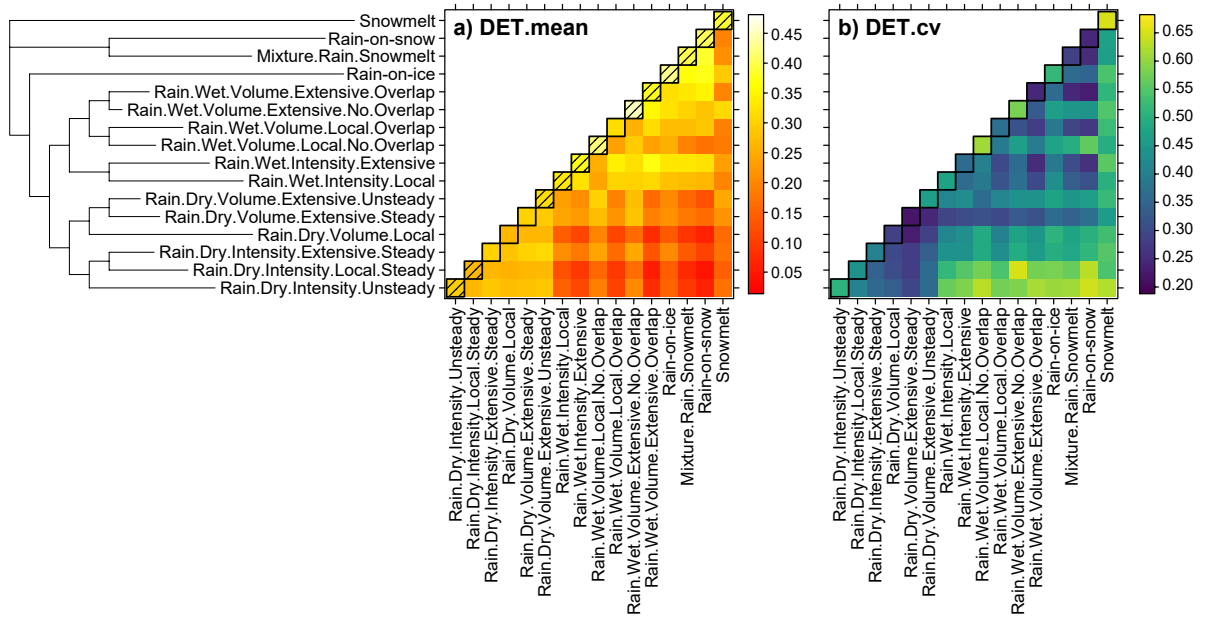


Figure 4.5: Matrix of intra-type and inter-type value of determinism ( $DET$ , see Chapter 4.3.4, 4.7.3 and Wendi et al. (2019)), which measures the similarity of hydrograph dynamics of event pair ( $DET = 0$  corresponds to a low similarity in the dynamics): a) mean and b) coefficient of variation of the average values of  $DET_{intra}$  and  $DET_{inter}$  for all catchments. The diagonal shows  $DET_{intra}$  (black outline), horizontal and vertical bars show  $DET_{inter}$ . Events of a certain type exhibit more similar runoff dynamics compared to other event types if the value on the diagonal is higher than the values of the corresponding horizontal and vertical bars (these conditions are indicated by hatched squares). The matrix of coefficient of variations shows the variability of  $DET_{intra}$  (diagonal values, black outline) and  $DET_{inter}$  (values on horizontal and vertical bars) in the set of study catchments. The hierarchical classification tree corresponds to the decision tree in Figure 4.2b.

Interestingly, very distinct characteristics also distinguish runoff events that are generated when there is high or low spatial interaction between rainfall and wet areas (i.e., most of rainfall occurs in the parts of catchment that is respectively wet or dry) as the  $DET_{inter}$  between *Overlap* and *No Overlap* events is rather low (i.e., dark orange colors, Figure 4.5a), while the corresponding  $DET_{intra}$  of these types are very high (i.e., light yellow colors on the diagonals, Figure 4.5a). *Rain-on-ice* events have a very specific dynamics that is to some extent similar to *Rain-on-snow* and *Mixture of Rainfall and Snowmelt* events. Pure *Snowmelt* events have even more specific hydrograph dynamics that does not match any other event type, as evidenced by the presence of light yellow colors (i.e., high  $DET$ ) only in the diagonal of Figure 4.5a. However, in some catchments the variability of runoff dynamics within *Snowmelt* event type can be higher than on average for the whole data set (Figure 4.5b). Interestingly, there is more resemblance between *Rain.Wet.Volume.Extensive.Overlap* and events that involve snowmelt (i.e., *Rain-on-snow* and *Mixture of Rain and Snowmelt*) compared to other rainfall-induced events (i.e., yellow colors of  $DET_{inter}$  between these types, Figure 4.5a), indicating that the runoff generation conditions in these cases (despite the differences in the nature of the inducing event itself) are controlled by similar space-time dynamics of inducing event and wetness state of the catchment. This appears to be consistent for most of the analyzed catchments in the data set (i.e., low values of coefficient of variation of  $DET_{inter}$  for these three event types, Figure 4.5b).

#### 4.5 Exemplary application of event typology in Germany

In this Section we applied the event typology (Figure 4.2b, Table 4.2) derived for the set of German catchments for investigating the spatial distribution of event type occurrence, the seasonal variations of the dominant event types in Germany and their runoff characteristics. These are exemplary applications, which are reported and discussed here to give a taste of the possible uses of such a typology.

### 4.5.1 Spatial patterns of event types

To analyze spatial patterns of event types in Germany, all catchments in the data set were clustered according to the frequency of occurrence of their event types. We identified six clusters (Figure 4.6a) with distinct distributions of event types (Figure 4.6b). The resulting spatial clustering of catchments resembles the one obtained by using event runoff characteristics (i.e., mean, variability and seasonality of event runoff coefficient, time scale and rise time) that is in turn comparable to the spatial variability of catchment and climatic descriptors (see Figure 3.5).

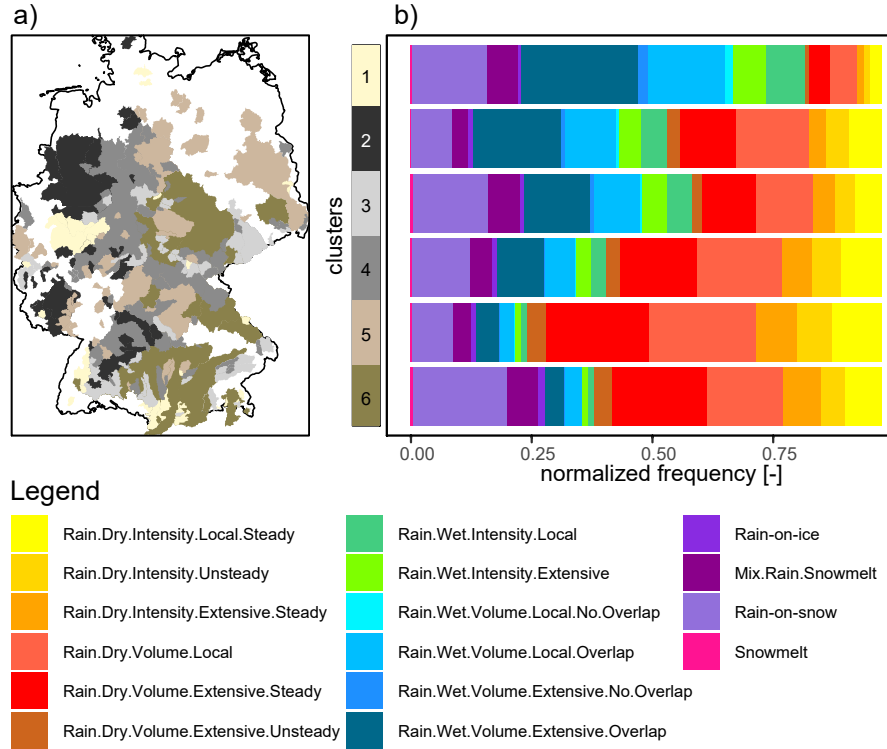


Figure 4.6: Regional pattern of event type frequency in Germany: a) spatial distribution of six homogeneous clusters in terms of frequency of event types; b) frequency of event types per cluster for all events.

The first cluster mostly consists of mountainous catchments of the Alpine Foreland, Black Forest and Rhenish Massif (Figure 4.6a). Here almost 25% of events are either *Rain-on-snow* or *Mixture of Rainfall and Snowmelt* (Figure 4.6b). A big portion of rainfall events occurs during wet conditions and only less than 25% of events occurs during dry conditions. This can be explained by the fact that this cluster largely corresponds to the group of catchments with small subsurface storage and in-phase seasonality of soil moisture and rainfall (i.e., substantial rainfall amount falls during the cold season when evaporation is low and soils are wet) (Tarasova et al., 2018a). This explains the high portion of rainfall events on wet conditions (Figure 4.6, green and blue colors). Around 5% of all events are volume-dominated rainfall events in wet conditions, when most of rainfall occurs on less saturated soil (i.e., events categorized as *No Overlap*). This indicates that the corresponding runoff events might be the result of event-fed saturation in these catchments. Cluster 2 combines wet lowland catchments of the western North German Plain, mid-range catchments of the western Central Uplands and the South German Scarplands. Here the role of events involving snow, especially *Rain-on-snow* events, is lower than in the previous cluster as the elevations are limited. More than 40% of rainfall event occurs during wet conditions due to in-phase seasonality of rainfall and soil moisture (Tarasova et al., 2018a). Volume-dominated rainfall events clearly prevail during both dry and wet conditions. Event-fed saturation during wet conditions when large portions of catchments are active and contribute to runoff generation is probably a rare situation in these catchments as only a small portion of events is categorized as *No Overlap* events. However, during dry conditions when the distribution of active runoff generation zones is

very heterogeneous, local event-fed saturation is the most frequent runoff generation mechanism (i.e., there is abundance of *Rain.Dry.Volume.Local* and *Rain.Dry.Volume.Extensive.Steady* event types).

Cluster 3 encompasses mountainous catchments of the eastern Central Uplands (i.e., the Harz, Ore Mountains and Thuringian Forest) and the Alpine Forelands. Similarly to Cluster 1 almost 25% of events are associated with *Rain-on-snow* and *Mixtures of Rainfall and Snowmelt*. However, rainfall events are distributed almost equally between dry and wet conditions indicating large variability in the extent of area that actively contributes to streamflow generation in these catchments compared to Cluster 1. Almost 25% of all events are generated by means of localized event-fed saturation during dry conditions when the connectivity among active runoff generation areas is poor (*Rain.Dry.Volume.Local* and *Rain.Dry.Volume.Extensive.Steady* events). During wet conditions both extensive and local runoff generations are almost exclusively controlled by the spatial interaction between soil moisture state and rainfall amounts (i.e., *Rain.Wet.Volume.Local.Overlap* and *Rain.Wet.Volume.Extensive.Overlap* prevail among events occurring in a wet catchment state).

The fourth cluster combines the catchments of the central parts of the North German Plain, the hilly catchments of the Central Uplands and South German Scarplands and the lower Alpine Foreland. A larger portion of rainfall events occurs during dry conditions indicating that generally only small portions of catchments contribute to streamflow generation. As in all other regions in Germany, during wet conditions (that are usually in the cold period of the year) volume-dominated events prevail. However, in this cluster both local and extensive volume-dominated rainfall events are only generated when there is strong interaction with soil moisture (i.e., pre-event saturation is necessary for runoff generation).

The fifth cluster consists of the dry lowland catchments in the east of the North German Plain and the South German Scarplands. Here, only a small portion of events belongs to *Rain-on-snow* or *Mixture of Rainfall and Snowmelt* types. Only few rainfall events occur during wet conditions, as seasonality of soil moisture and rainfall is not synchronized. Around 25% of all events are intensity-dominated rainfall events with prevailing local runoff generation and possible infiltration excess. Most of volume-dominated rainfall events during dry conditions have local character (i.e., large portion of *Rain.Dry.Volume.Local*) possibly indicating very spatially heterogeneous runoff generation patterns that largely depend on the intensity of inter-event evaporation controlling pre-event soil moisture state.

The sixth cluster covers a large portion of the Alpine Forelands, as well as Loess Belt catchments that drain mid-range Mountains of the Central Uplands (e.g., the Harz, Thuringian Forest). For this cluster, *Rain-on-snow* and *Mixtures of Rainfall and Snowmelt* events play an important role as their portion is the largest compared to other clusters. The portion of rainfall events during wet conditions is rather small because rainfall and soil moisture are not seasonally synchronized. Steady rainfall events during dry conditions are very frequent, potentially indicating the occurrence of orographic slow-moving storms, which are mainly volume-dominated but can occasionally have an intensity-dominated structure. Almost 20% of all rainfall events are intensity-dominated indicating that infiltration excess is a possible runoff generation mechanism in these catchments. The above mentioned evidences of similarity among regions with homogeneous event type frequency and archetypical catchment behavior in terms of event runoff response (as reported in Tarasova et al., 2018a) indicate that on one hand the similarity of event runoff response might be controlled by the occurrence of similar event types, and on the other hand that catchments with similar physiographic and climatic conditions are likely to have similar distribution of event type frequency.

#### 4.5.2 Seasonality of dominant event types

Event type occurrence naturally varies throughout the year (Figure 4.7). In large parts of Germany *Rain-on-snow* and *Mixture of Rainfall and Snowmelt* are the two most typical event types in winter (Figure 4.7a). However, in the western part of the North German Plain, where snowfalls seldom occur, extensive steady rainfall on wet conditions is the most common winter event type. In spring the situation changes and extensive steady rainfalls on wet conditions dominate the whole

Western part of Germany, indicating the dominance of Western cyclones and resulting synoptic precipitation (Hofstätter et al., 2016). Similar rainfall events also prevail in the Eastern part of Germany, but the catchment wetness state is generally lower (Figure 4.7a). The Southern part of Germany (i.e., the Alpine Forelands and Bavarian Forest) and the eastern part of the Central Uplands are still dominated by Rain-on-snow events in spring (Figure 4.7a), as snowpack is still present in areas with higher elevation. In summer, the character of precipitation changes, leading to dominance of local volume-dominated rainfall events on dry conditions. The frequent occurrence of intensity-dominated events in the Eastern part of Germany indicates the importance of convective precipitation for runoff event generation in warm periods of the year. In autumn, increased precipitation in mountainous catchments of the Alpine Foreland, Black Forest and Rhenish Massif leads to abundance of rainfall events on wet conditions. Lower catchments still remain dry, but rainfall events mostly have extensive coverage. The transformation from dry to wet state in most of the catchments and the change from local to extensive rainfall events in autumn lead to increased variability of event type occurrence (Figure 4.7b). Similarly, the variability is high in spring when event types change from events which involve snow to rainfall-induced events. The variability of event type occurrence is lower in summer when rainfall events on dry conditions dominate. Except for the western part of the North German Plain, where air temperature is fluctuating around critical values for snowfall, the lowest variability is observed in winter when the bulk of events results from processes which involve snow (Figure 4.7b).

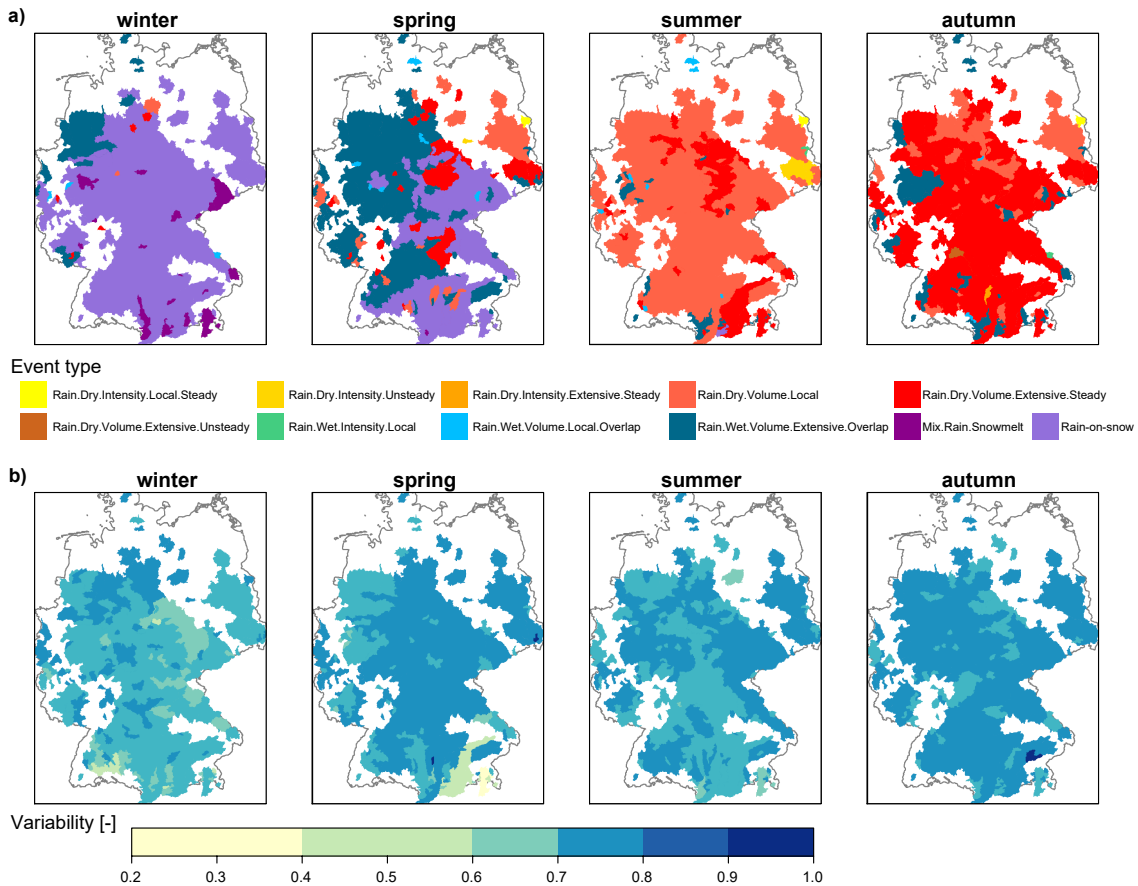


Figure 4.7: Seasonality of event types in Germany: a) dominant type (i.e., most frequent type in the season) and b) variability of event type occurrence for each season defined as coefficient of unalikeability (see Chapter 4.3.5 and Kader and Perry (2007)). This metric defines the portion of all event pairs in the season that are unalike. When one event type dominates in a certain season the value of the coefficient of unalikeability is close to 0. When several event types are equally dominant for a certain season the value of the coefficient increases towards the maximum value of 1.



### 4.5.3 Runoff characteristics of event types

Here, we analyzed five runoff event characteristics (i.e., event runoff coefficient, time scale, rise time, peak discharge and total event volume; see Chapter 4.3.5) of the derived event types. These characteristics describe short-term runoff dynamics, which might shed light on the nature of precipitation partitioning and storage in the catchments and indicate principal mechanisms of water release during events (Tarasova et al., 2018b). In addition to the set of all events, sub-samples of larger (i.e., runoff events with peak discharge higher than the 3<sup>rd</sup> quartile) and smaller (i.e., runoff events with peak discharge smaller than the 3<sup>rd</sup> quartile) events are also considered in this analysis with the purpose to investigate possible differences among runoff generation mechanisms of small and large events.

Generally, the majority of all runoff events in Germany and especially of small events results from rainfall events occurring during dry soil moisture conditions (Figure 4.8a, c; warm colors). Rainfall during wet conditions (indicated by green and blue palette), and especially *Rain-on-snow* and *Mixtures of Rainfall and Snowmelt* (violet colors), are much more common among larger events (Figure 4.8b). Only a small portion of events was classified as *Rain-on-ice* and pure *Snowmelt* event types (Figure 4.8a), indicating that these are rare runoff generation processes in Germany. Nonetheless, a portion of larger events are generated by these processes (Figure 4.8b) indicating that rare processes might still be responsible for generation of large flood events (e.g., Stein et al., 2019).

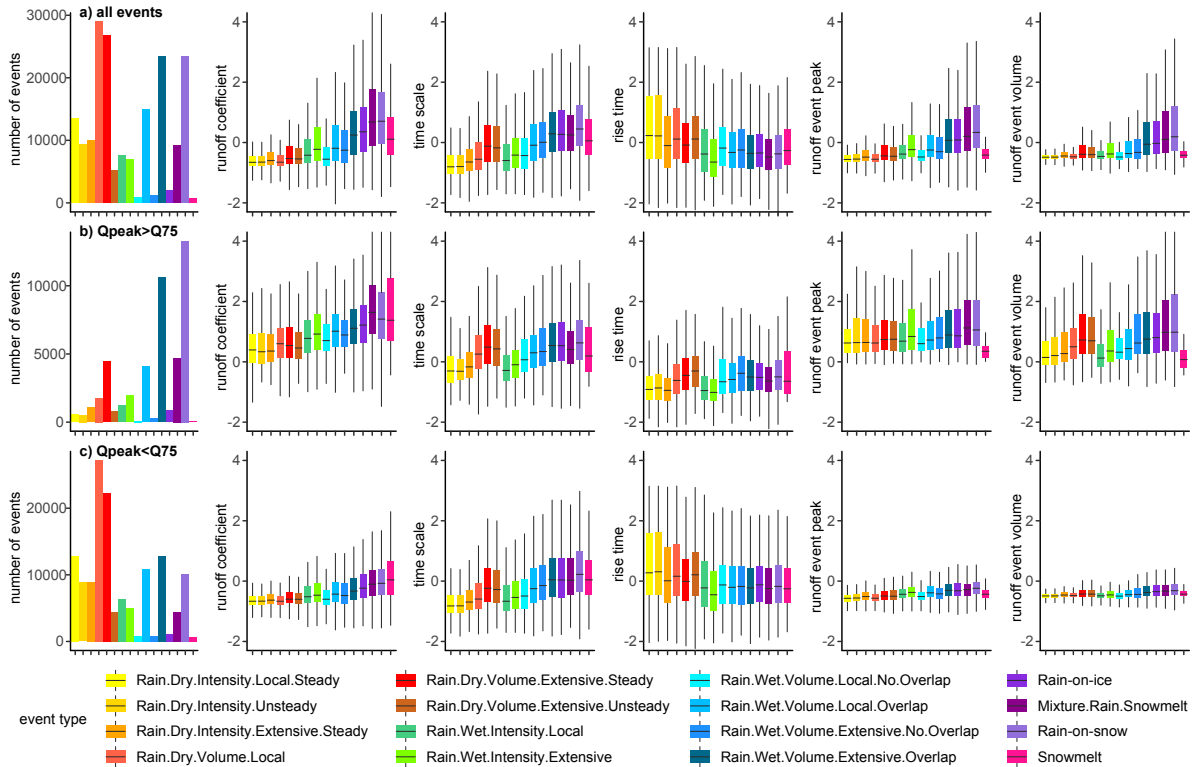


Figure 4.8: Hydrological response of event types in terms of their runoff event characteristics (i.e., event runoff coefficient, time scale, rise time, peak discharge and volume): a) all events; b) events with  $Q_{peak} > Q_{75}$ ; c) events with  $Q_{peak} < Q_{75}$ . Runoff event characteristics are standardized by scaling all events to zero mean (by subtracting the mean of the sample from the original values) and unit variance (by dividing them by the standard deviation) for each catchment to make them comparable. Legend shows color coding of event types that is also valid for Figure 4.9.

A clear increase of event runoff coefficients is observed from dry rainfall events to wet rainfall events (Figure 4.8) indicating that a substantial portion of rainfall is stored during dry conditions. The highest runoff coefficients are observed for *Rain-on-ice* and events which involve snow (i.e.,

*Mixtures of Rainfall and Snowmelt, Rain-on-snow and Snowmelt*). These event types are often characterized by very wet conditions (Table 4.2). Moreover, frozen soils and snow cover might also hinder infiltration of rain water, which then immediately contributes to runoff. When events of all sizes are considered a very similar pattern is revealed for peak discharges and runoff event volumes (Figure 4.8a). Interestingly, when only larger events are considered smaller runoff volumes are typical for intensity-dominated rainfall events, but there are little differences between event runoff volumes of extensive rainfall events during wet conditions (dark blue colors) and all events which involve snow. This can be explained by the fact that these events are indeed similar in terms of space-time organization of the precipitation events and wetness state of the catchments (Figure 4.5a).

Differences in peak discharges among event types for larger events almost vanish compared to the case when all events are considered. However, volume, intensity and duration of the corresponding precipitation events (Figure 4.9b) indicate distinct differences among event types even for large events. Intensity-dominated rainfall events on dry conditions are characterized by higher precipitation intensities than their counterparts with wet conditions. Similarly, volume-dominated rainfall events on dry conditions have higher precipitation event volume than their counterparts with wet conditions (Figure 4.9b), but show little difference in the event runoff volumes (Figure 4.8b), likely because the storage available in dry conditions is of the order of the difference between rainfall amounts of the two states.

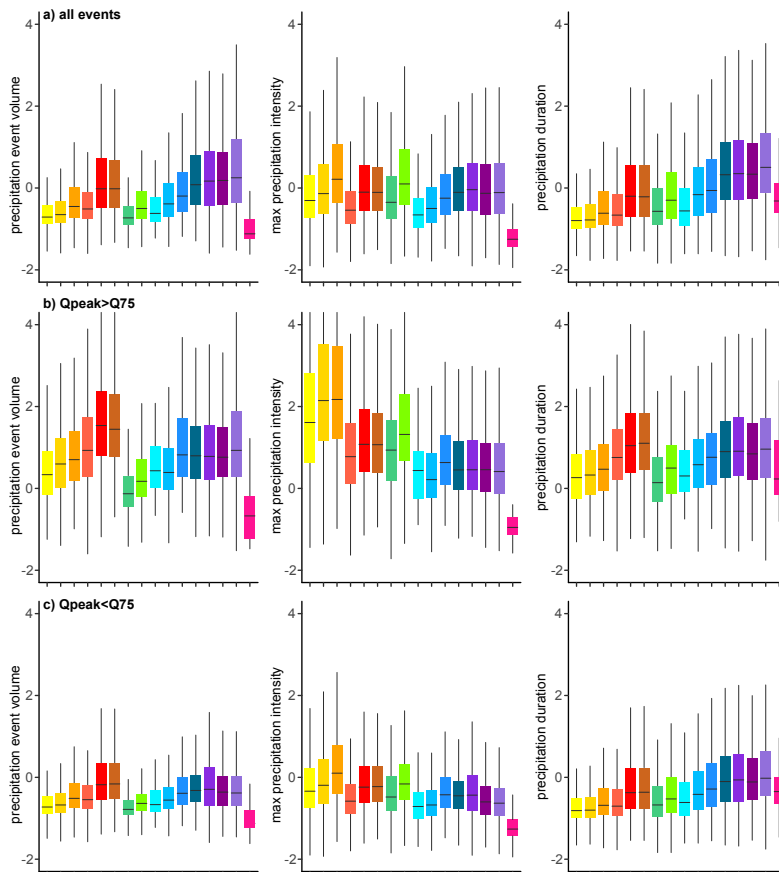


Figure 4.9: Precipitation properties of event types that were not used for event characterization (i.e., maximum precipitation intensity, total volume of precipitation event, duration of precipitation event): a) all events; b) events with  $Q_{peak} > Q_{75}$ ; c) events with  $Q_{peak} < Q_{75}$ . Maximum precipitation intensity, total volume of rainfall and duration of precipitation events are standardized by scaling all events to zero mean (by subtracting the mean of the sample from the original values) and unit variance (by dividing them by the standard deviation) for each catchment to make them comparable. The color-coding of this Figure corresponds to the color key in Figure 4.8.

The event time scale of intensity-dominated rainfall events (yellow and green palette) is smaller than the one of their volume-dominated counterparts (red and blue palette) (Figure 4.8). These

differences are especially distinct for larger events (Figure 4.8b). Event time scale of *Rain-on-snow* and *Mixtures of Rainfall and Snowmelt* are usually longer than for rainfall events (Figure 4.8a, c), but this tendency is less pronounced for larger events (Figure 4.8b).

When events of different magnitudes are considered together (Figure 4.8a), no clear differences in event rise time are detectable (Figure 4.8a). However, for larger magnitudes intensity-dominated rainfall events seem to have shorter rise time than volume-dominated ones (Figure 4.8b), showing that when runoff is generated by intensity-dominated events fast flow paths can be activated.

Distinct runoff characteristics of event types are valuable features for constructing event type-based design hydrographs (e.g., Brunner et al., 2018). The above-mentioned disparate runoff and precipitation characteristics of event types provide useful information on how runoff characteristics might change in the future given the expected change in precipitation properties (e.g., if intense rainfall events become more frequent in the future (Kendon et al., 2014)).

## 4.6 Conclusions and Outlook

A new process-based framework for characterizing runoff events and deriving event typologies was proposed. The indicators used in the framework categorize runoff events based on space-time dynamics of observed precipitation and simulated snowmelt and soil moisture and their mutual interactions within river catchments. A rigorous uncertainty analysis shows that the indicators of the proposed characterization framework are robust and regionally consistent. The adoption of dimensionless covariance- and ratio-based indicators reduces classification uncertainty compared to commonly used indicators relying on absolute values of metrics such as rainfall volume, duration or intensity. This indicates that the proposed characterization framework is a reliable tool that could be used for regional studies on runoff generation processes and for investigating their temporal evolution in the past as well as in the future.

The analysis of cross recurrence plots showed that the event typology derived in this study proves able to stratify events with distinct hydrograph dynamics, even though streamflow was not directly used for classification. This indicates that the derived event typology effectively captures first-order controls of event runoff response in a wide variety of catchments. Application of the derived event typology to a country-wide dataset from Germany revealed six distinct regions characterized by different dominant event types, which match well with the corresponding regions exhibiting similar runoff response. Unveiled seasonal patterns of event type occurrence show high spatial coherence that agrees with the seasonality of hydroclimatic conditions prevailing across Germany. These are valuable findings for regionalization of hydrological signatures and prediction of the seasonal character of the runoff response in ungauged locations.

The proposed framework, which allows for a consistent characterization and comparison of runoff events of various sizes and recurrence intervals in a wide range of German catchments, is expected to perform similarly well in regions where hydrometeorological data of comparable quality in terms of density of observations, spatial and temporal resolution of the input data is available.

Instead, application of the framework to regions with extremely pronounced seasonality (e.g., snow- or monsoon-dominated river regimes) might not be trivial, since the very definition of runoff event in these areas differs from the one adopted for temperate climates (e.g., a runoff event can last several months making computation of temporal and spatial organization of the corresponding inducing event and wetness state ambiguous using the proposed indicators).

Thanks to the adaptive structure of the proposed characterization framework, the complexity of derived event typologies can be adapted to specific applications or adjusted in case of known problems in the reliability or availability of input data. The characterization framework and the derived event typology can be further applied for understanding regional differences of runoff and flood events and detect temporal changes of the dominant flood generation processes. This might help explain previously detected disparate trends in unstratified floods. The same approach could be also applied for disentangling the variability of solutes and particulates exports from catchments during different runoff event conditions (as recently suggested by Karwan et al. (2018) and Knapp et al. (2020)), thus providing additional insights on variability of water quality metrics observed in streams.

## 4.7 Supporting Information

### 4.7.1 Rainfall-runoff event attribution in nested river networks

Initial rainfall-runoff event attribution was performed using seasonal median lag time as proposed by Mei and Anagnostou (2015). This lag time is used to set distance backwards from the starting point of considered runoff event within which rainfall event is searched at each individual location (i.e., catchment) (Figure 4.10a). However, in the headwaters, inducing events (i.e., precipitation) might start much earlier than observable streamflow reactions at the outlet of large river networks (Diederer et al., 2019). Therefore, the precipitation event considered for the same runoff event at upstream and downstream location might be different when the start of the precipitation event lays inside of the search distance defined by lag time for the upstream location, but is outside of this distance for the downstream location (Figure 4.10b). To remedy this issue in the case of nested catchments, individual runoff events were organized along the river network they belong to and the starting points of runoff events at downstream locations are adjusted in a way that the earliest starting date among all upstream locations is assigned to the corresponding downstream location. This starting date of runoff events was then used to search for the corresponding precipitation event for each individual catchment according to seasonal median lag time as described above (Figure 4.10b). The search time range backwards was bounded by the starting date of the precipitation event at the upstream location. The above described procedure ensures that no precipitation is accidentally discarded in larger catchments, and allows for characterizing nested catchments consistently.

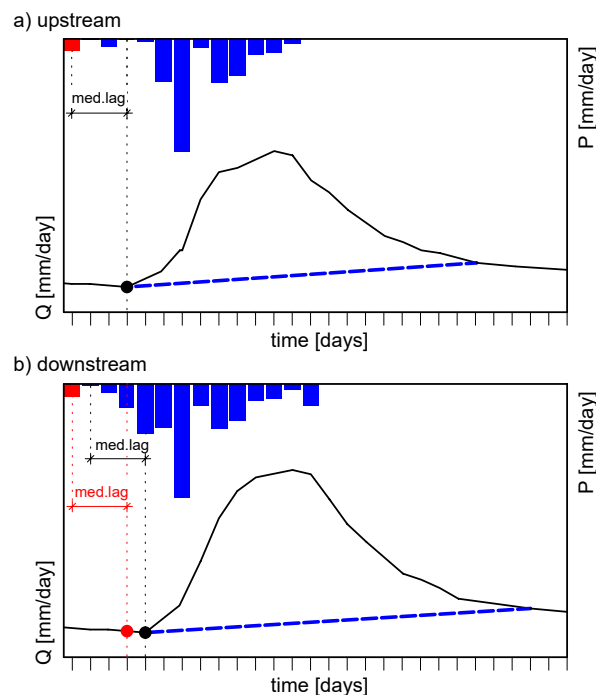


Figure 4.10: Attribution of rainfall-runoff events at upstream and downstream locations on the example of the River Kyll: a) at the upstream location using seasonal median lag time as a searching distance; b) at the downstream location using seasonal median lag time as a searching distance from the starting point of local runoff event (black color; compared to the upstream location the first precipitation pulse does not contribute to the considered runoff event) and from the corrected starting that corresponds to the runoff event starting date at the upstream location date (red color; similar to the upstream location the first precipitation pulse contributes to the considered runoff event).

### 4.7.2 Definition of the threshold for catchment wetness state

The second characterization layer sorts events according to their corresponding pre-event catchment wetness state (see Chapter 4.3.1 and Figure 4.2a). We labeled event conditions as *Wet* or *Dry* based on catchment-averaged antecedent soil moisture. By using simulated soil moisture we

inevitably introduce model-specific bias into the characterization framework. Simulated soil moisture essentially shows the current state of the soil moisture storage unit according to accounting schemes that are widely used in computational hydrology (e.g., Bergström, 1995). If the non-linear storage-discharge relationship differs in different catchments (Figure 4.11a), using percentiles of soil moisture as threshold to define wet and dry state might be inappropriate. To properly account for the non-linear behavior of the soil moisture storage reservoir, we use the measure of maximum curvature (Rogger et al., 2013) of a fitted exponential function that describes the non-linear relation between event runoff coefficient ( $rc$ ) and antecedent soil moisture ( $sm$ ) (Tarasova et al., 2018b, and Figure 4.11b) as a classification threshold. For soil moisture states below the point of maximum curvature, event runoff coefficients tend to increase slowly with increasing soil moisture (representing dry catchment states), while beyond this point event runoff coefficients increase rapidly with soil moisture (representing wet catchment states) (Figure 4.11). Curvature at each point of the function  $rc = f(sm)$  is calculated as  $\kappa = \frac{|f(sm)''|}{[1+(f(sm)')^2]^{\frac{3}{2}}}$  and its maximum value is calculated for each catchment in the data set.

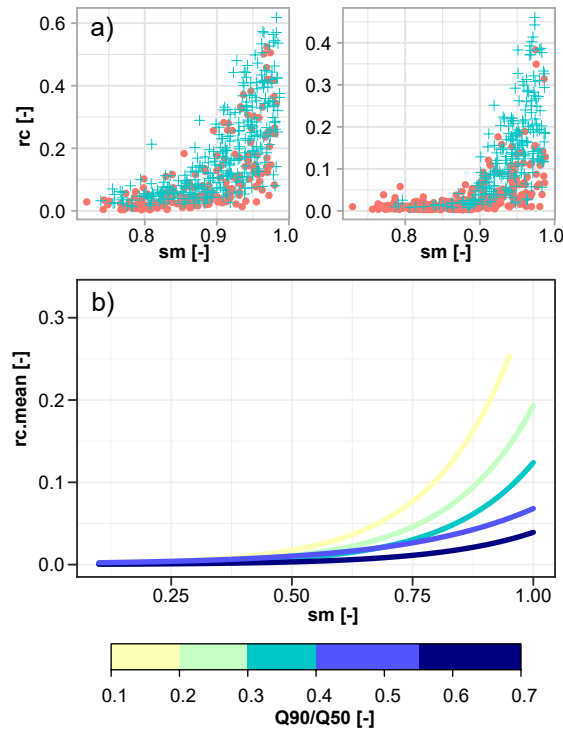


Figure 4.11: Soil moisture as non-linear control of event runoff coefficient: a) Relationship between the observed event runoff coefficients and pre-event soil moisture simulated by the mHM model on example of the Lippe at Haltern and Ems at Einen and the fitted exponential function as described in Tarasova et al. (2018b). Circles correspond to single-peak events. Crosses correspond to multiple-peak events; b) the average of the observed event runoff coefficients corresponding to different simulated soil moisture conditions is presented for selected catchments as an exponential function of simulated soil moisture fitted to them as described in Tarasova et al. (2018b). The lines are color coded according to subsurface storage index defined as the ratio between Q90 and Q50 (ratio between daily discharges which is exceeded 90% of the time and the median flow). The Figure is modified from Tarasova et al. (2018b) with the permission from Wiley.

### 4.7.3 Cross Recurrence Plots and Recurrence Quantification Analysis

CRP is essentially a visualization in a form of pointwise similarity of two dynamical systems (see Figure 4.3c), with matrix elements (i.e., recurrence points  $CR_{i,j}$ ) corresponding to times when two phase space trajectories are similar (similarity distance is defined by threshold  $\varepsilon$ ):

$$CR_{i,j}(\varepsilon) = \begin{cases} 1, & |\vec{x}_i - \vec{y}_j|_2 < \varepsilon \\ 0, & \text{otherwise} \end{cases} \quad i = 1, \dots, N, j = 1, \dots, M \quad (4.2)$$

where  $N$  and  $M$  are the number of measured points in the compared phase space trajectories  $\vec{x}_i$  and  $\vec{y}_i$ .

Three parameters are required to construct a CRP. These are the two parameters for the time delay embedding, namely, the embedding dimension  $m$  and the time delay  $\tau$ , as well as the phase space distance threshold  $\varepsilon$ .

To balance embedding losses that result from the constructing of the high-dimensional phase space trajectories with time delay  $\tau$ , only events with duration longer than 5 days can be considered. This was supported by interpolating each event time series into 8 points per day (3-hourly) using shape preserving piecewise cubic interpolation method. The shortest possible  $\tau = 12$  [hours] was therefore selected as time delay. We used  $m = 3$  [-] embedding dimensions since an initial sensitivity analysis showed that the results did not vary considerably when a higher number of dimensions was used. Our choice of distance radius or threshold parameter is based on 10<sup>th</sup> percentile of all Euclidian distances in the phase space of every pairwise comparison. That said, the procedure is to first calculate the Euclidean distance matrix between two events, and then use the 10<sup>th</sup> percentile of all distances as threshold to define CRP points. Further we only choose the points within this threshold that happen to be local minima of the distances in reference to each compared vector point in phase space (i.e., every row in the distance matrix), and that consequent local minima have to be at least distanced of two discrete time points, in our case 6 hours minimum. This method of further filtering CRP points with local minima and their minimum distance in addition to threshold parameter  $\varepsilon$  avoids CRP pitfalls when noise might be present in the time series (Wendi et al., 2019). When two identical time series are compared the CRP pattern will be a single diagonal line (e.g., top panels of Figure 4.3). Thus, diagonal lines within the CRP matrix are an indicator of similarity between two dynamical systems (Wendi et al., 2019).

The resulting patterns within a CRP can be quantified by RQA which is essentially used as a similarity measure between two runoff event hydrographs. The selected RQA measure determinism (DET) describes the similarity (or dissimilarity) of two dynamical systems using the distribution of connected recurrence points that form diagonal lines, over all the points within the CRP (Wendi et al., 2019):

$$DET = \frac{\sum_{l=l_{min}}^N lP(l)}{\sum_{i,j}^N CR_{i,j}} \quad (4.3)$$

where  $P(l) = \{l_i; i = 1, \dots, N_l\}$  is the relative frequency of the lengths  $l$  of diagonal structures,  $N_l$  is the total number of those diagonal lines in the CRP, and  $l_{min}$  is the minimum length of diagonal lines in this case defined as the minimum of two connecting points. This quantification based on the fraction of diagonal lines among all recurrence points ( $CR_{i,j}$ ) considers the influence of scattered single recurrence points that occur by chance. DET varies between 0 and 1 and defines a range from low to high similarity in the dynamics of the two times series (Marwan, 2010).

---

## 5 Conclusions and Perspectives

The main results described in previous Chapters summarized here and potential future applications and areas of research are presented.

### 5.1 Conclusions

The main goal of this thesis was to enable automated identification of rainfall-runoff event from continuous hydrometeorological time series, to deepen the understanding of large scale controls of runoff event characteristics and to develop a framework for event characterization and classification that is able to distinguish events governed by different runoff generation processes.

The proposed automated time-series-based event separation algorithm (Chapter 2) with novel iterative procedure for the adjustment of thresholds needed to identify and separate single-peak components of multiple-peak events enabled the identification and attribution of more than 220,000 rainfall-runoff events in 185 German catchments for the period 1951-2013 and consistently addressed the issue of multiple-peak events refinement in catchments characterized by various runoff regimes and different climatic and physiographic properties, thus allowing for a country-wide analysis of the event runoff response at different temporal scales.

Temporal dynamics (i.e., event-to-event variability, seasonality and long term changes) of runoff event characteristics (e.g., event runoff coefficient, time scale, rise time, peak discharge) derived from identified events reveal clear patterns of event runoff response in Germany (Chapter 2). In mountainous catchments with poor storage event runoff response is strongly controlled by the characteristics of rainfall. A distinct switch between *Dry* and *Wet* states occurs in these catchments. A weak relation between rainfall and runoff event properties is instead observed in lowland and hilly catchments with substantial storage, where a gradual transformation between functioning states occurs and the response is driven by pre-event saturation. The seasonality of runoff event characteristics is governed by the contribution of snowmelt and the seasonality of the aridity index rather than of rainfall properties. Long-term changes of total precipitation amount alone do not explain season-specific long-term changes of runoff event characteristics that are rather consistent with changes of seasonal indicators of the wetness state. The effects of land use changes are detectable only in a few cases and display themselves mostly in the characteristic response time of catchments (Tarasova et al., 2018b).

Long-term aggregates of runoff event characteristics (i.e., their mean values, variability and seasonality in each catchment) are essential hydrological signatures of catchment behavior. Their regional patterns and relationship with climatic and catchment descriptors provide valuable information spatial controls of event runoff response in Germany (Chapter 3). Although runoff event characteristics have relatively clear regional patterns due to the dominance of climatic controls at regional scale, subsurface properties (i.e., catchment storage) also play a considerable role for the prediction of event runoff response. Compared to other tested variable selection methods the application of the proposed backward elimination procedure based on SOM allows for the most accurate prediction of spatial patterns and regionalized values of runoff event characteristics identifying soil depth, hydraulic permeability and frequency, size and seasonality of wet spells as hydrologically-relevant catchment descriptors (Tarasova et al., 2018a).

Linking the findings on temporal dynamics of runoff event characteristics (Chapter 2) and their spatial controls (Chapter 3) with hypothesized runoff generation mechanisms and the concept of threshold processes in catchments (e.g., Rogger et al., 2013) allowed us to develop archetypes of distinct catchment behaviors in Germany (Figure 3.9). The identified controls of event runoff response and hydrologically-homogeneous regions can provide useful information for selecting relevant physical catchment descriptors for various hydrological applications (e.g., regionalization of hydrological metrics). Although selected catchment descriptors might vary in different settings and other regions, it is likely that descriptors expressing properties of subsurface storage, rainfall dynamics and evapotranspiration will define event runoff response elsewhere. Land use might control dissimilarity of catchment behaviors within regions with relatively homogeneous climatic conditions and subsurface structure where evapotranspiration-controlled drying of soil moisture

largely defines the pre-event wetness state (Tarasova et al., 2018a).

These advances were the basis for development of a new process-based framework for characterizing runoff events and deriving event typologies (Chapter 4). The indicators of the proposed framework categorize runoff events based on space-time dynamics of observed precipitation and simulated snowmelt and soil moisture and their mutual interactions within river catchments. A rigorous uncertainty analysis showed that the indicators of the proposed characterization framework are robust and regionally consistent. Dimensionless covariance- and ratio-based indicators used in the proposed framework reduces classification uncertainty compared to commonly used indicators relying on absolute values of metrics such as rainfall volume, duration or intensity and allow consistent classification of runoff events of various magnitudes and recurrences. The validation procedure based on CRPs showed that the event typology derived in this thesis is able to stratify events with distinct hydrograph dynamics in most of study catchments, even though streamflow was not directly used for classification (Tarasova et al., 2020). This indicates that the derived event typology effectively captures first-order controls of event runoff response in a wide variety of German catchments.

## 5.2 Outlook

The proposed framework for process-based event characterization and classification developed and presented in this thesis proved robust and allowed consistent classification of runoff events in different catchments encompassing a variety of climatic and physio-geographic settings in Germany. Therefore, application of the proposed frameworks provides several interesting research avenues. Some examples of application are discussed below.

**Implications for flood frequency analysis and prediction of flood characteristics** Flood events exhibit a wide variety of process controls that determine their time of occurrence, duration, extent and severity. However, the different generating mechanisms and characteristics of flood events are often ignored in statistical analyses (Merz and Blöschl, 2003a). In fact, a principal hypothesis of extreme value statistics is that observations are homogeneous and originate from the same distribution (Gumbel, 1941). However, flood events observed in a catchment might be non-identically distributed (due to their different origins) and non-stationary (because of the natural climatic variability or human interventions) (Hirschboeck, 1987; Merz et al., 2014). Joint analysis of floods that are generated by different processes may result in uncertain predictions of flood estimates (Potter, 1958). Classifying flood events using the proposed framework can help address these issues.

Deriving event-type-based mixed distributions can help in improving at-site frequency estimates (e.g., Hirschboeck et al., 2000; Alila and Mtiraoui, 2002). Application of process-based event classification for prediction of flood characteristics might also play a crucial role for strengthening the hydrological basis of flood estimation and prediction procedures and aid shifting from statistical flood frequency analysis to flood frequency hydrology (Merz and Blöschl, 2008a,b; Viglione et al., 2013). Derivation of event-type-based compound distributions for at-site flood frequency analysis can be used by practitioners to improve design flood values, as utilization of event types is recommended in Germany's and USA's guidelines for estimating flood probabilities (DWA, 2012; England et al., 2018).

The robustness of flood estimates directly depends on the length of the available observations (Merz and Blöschl, 2008a). Additional causal information on flood generation mechanisms introduced through classification of flood events from relatively short time series using the proposed framework might be a valuable substitute for the information accumulated from the long unstratified flood event series (e.g., Merz and Blöschl, 2003b). This can improve the robustness of predictions in the places where the observations of streamflow started recently and only short time series are at hand.

Regional flood frequency analysis can also benefit from stratifying flood samples, either through the identification of homogeneous regions with same dominant flood generation mechanisms (see Chapter 4.5.1) or through the regionalization of event-type-specific distribution parameters and moments (Tarasova et al., 2019). Physical characteristics of catchments (e.g., climate, soil type,



land use) are known to be poor regional predictors of flood moments (Merz and Blöschl, 2009a), event-type-based regional flood frequency analysis might be a key to improve them (e.g., Jarrett and Costa, 1988).

Developed event separation procedure and classification framework that apart from flood events considers also a wide variety of runoff events of different magnitudes allows to increase the size of event sample for flood estimations. By relaxing the assumptions of the traditional extreme value theory and postulating that extremes emerge from ordinary events, the metastatistical approaches (Zorretto et al., 2016) can account for the full distribution of the runoff events and not only flood events (Miniussi et al., 2020). Coupling of metastatistical approaches with the proposed event classification framework provides a unique opportunity not only to include a large sample of events but also additional causal information to improve the accuracy and the robustness of the flood frequency predictions.

Runoff events of different types have pronounced differences in runoff event characteristics (e.g., event time scales that corresponds to the relationship between event runoff volume and peak discharge, see Chapter 4.5.3). Therefore, event typology can be also used to derive event-type specific synthetic hydrographs (e.g., Brunner et al., 2018) that are constructed based on volume-peak dependences for each individual event type. Accounting for event-type specific volume-peak dependences might help to improve flood estimates especially in nonstationary conditions and therefore contribute to more efficient design of hydraulic structures and flood protection measures (Brunner et al., 2019).

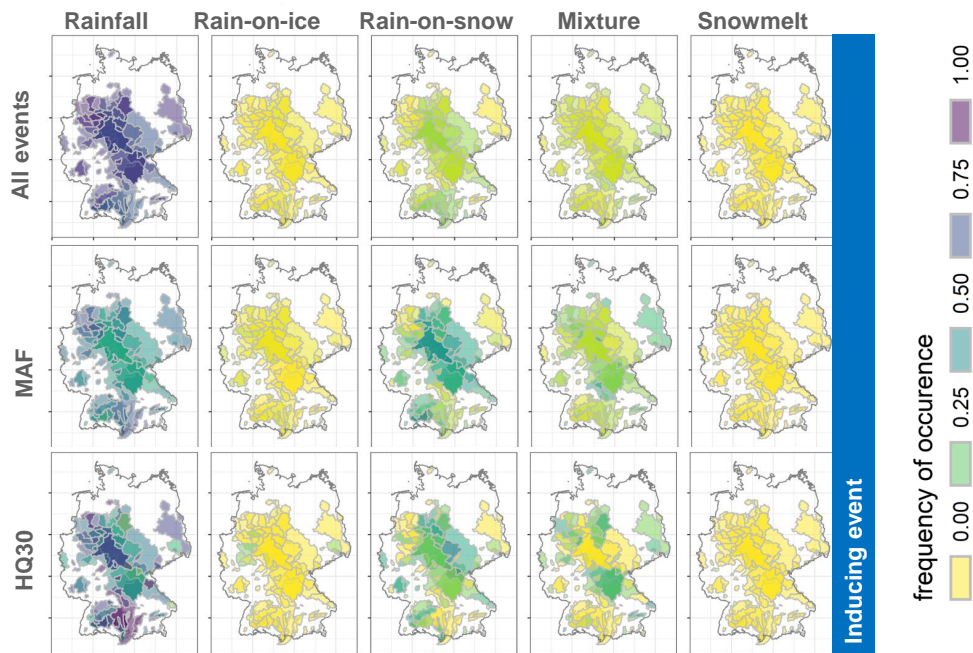


Figure 5.1: Frequency of occurrence of different states within the first layer (i.e., *Inducing event*) of event characterization framework proposed in Chapter 4.3.1. The frequency of occurrence is calculated as the ratio between the number of events attributed to each category of *Inducing event* (see Figure 4.2a and Table 4.1) and the number of all events in the sample. Three different event samples are considered: all events identified by event separation procedure; maximum annual floods (MAF); and flood events with the estimated return period of at least 30 years (HQ30). All three event samples were obtained from the continuous hydrometeorological time series for the period 1951-2013 (see data reported in Tarasova et al., 2018b) and classified according to the framework proposed by Tarasova et al. (2020). A similar procedure can be performed for other layers of the proposed framework (e.g., *Temporal organization*, *Space-time organization of inducing event* or *Wetness state*)

**Implications for understanding the origins of upper tail flood events** Another interesting avenue that can be examined using the proposed event classification framework is understanding the origins of upper tail flood events (Villarini and Smith, 2010) and the emergence of unpredictable flood events (e.g., Smith et al., 2018). It was noted by Rogger et al. (2012) based on the field evidences from two Austrian catchments that there are distinct differences between generation processes of ordinary runoff events and extreme floods. Smith et al. (2018) came to similar conclusions reporting

that hydro-climatic drivers of upper tail flood events in the continental US are very different from the annual floods implying that extreme flood events are in fact different from ordinary ones. On the other hand, Miniussi et al. (2020) has showed that considering all runoff events instead of only flood events allows more accurate and robust predictions of the latter implying that extremes originate from ordinary events (Zorzetto et al., 2016). The proposed framework is a well-suited tool to examine similarities and differences among small and large events. By analyzing dominant generation mechanisms of different event samples it is possible to examine transformation of processes from small to large events and to detect regional differences in these transformations (e.g., Figure 5.1).

**Evolution of event types** Our limited understanding of regional flood generation mechanisms hampers attribution of historical flood changes and curbs reliability of future flooding predictions (Kundzewicz et al., 2014). Furthermore, observed discrepancy in changes of extreme precipitation and extreme floods poses a challenge for understanding past and future flood changes (Berghuijs et al., 2019). Changes of event types can provide essential information on future flood hazard, and help to detect changes when no significant trends in classical flood characteristics (e.g., peak discharge) are recognizable (Blöschl et al., 2017). Therefore, proposed event classification framework might be a valuable tool for understanding and detecting possible changes or nonstationarities in flood event series, the emergence of new event types and their implications for estimation. Variations of event types can be analyzed for historic time series (e.g., Kampf and Lefsky, 2016; Vormoor et al., 2015; Kemter et al., 2020; Sikorska-Senoner and Seibert, 2020) and for future runoff time series generated using projections generated by climatic models (e.g., Turkington et al., 2016). It would allow to answer the question whether a particular event type has become more frequent over a number of decades instead of merely examining the magnitudes of all events in a lumped way (Tarasova et al., 2019).

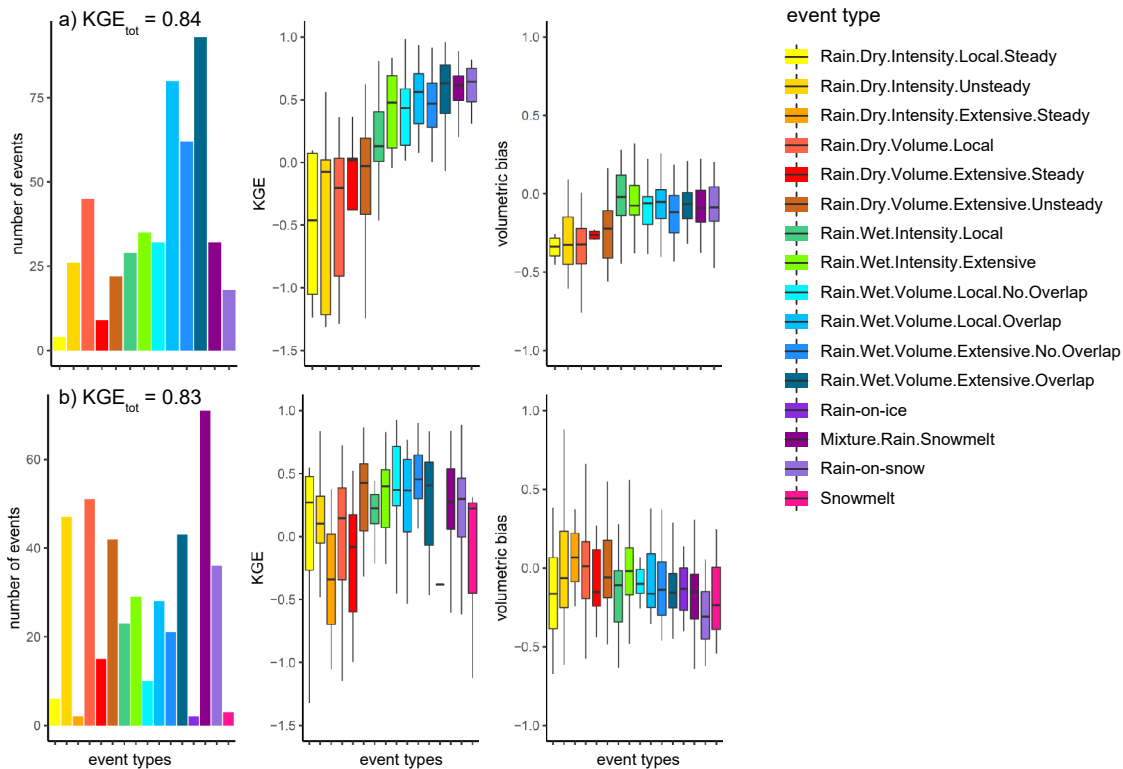


Figure 5.2: Event-type-based diagnostic of the SALTO hydrological model (Merz et al., 2020) using two different performance measures (Kling-Gupta Efficiency (KGE) and volumetric bias) calculated event-wise for two mesoscale catchments (a) the River Sülz at Hoffnungsthal, 224 km<sup>2</sup> and b) the River Freiberger Mulde at Berthelsdorf, 246 km<sup>2</sup>) for the period 1979-2002.  $KGE_{tot}$  refers to a value of KGE calculated for the whole study period without event stratification. Event types are assigned to the events according to the hierarchical classification tree derived in Chapter 4, Figure 4.2b

**Event types as a diagnostic tool for hydrological models** Event-type-based evaluation of model performance can pinpoint particular deficiencies of hydrological models at use and enhance their prediction and forecasting skill (e.g., Cullmann et al., 2008). The ability of state-of-the-art conceptual hydrological models to represent streamflow dynamics of specific event types can be tested using the developed event separation procedure and event classification framework. Comparing the performance of the models in reproducing different event types provides an opportunity to decipher which event types are especially difficult to simulate. This might hint on possible limitations of current deterministic models and on the predictability of certain event types (e.g., Figure 5.2). This additional process-informed evaluation of model performance increase the chance of selecting a physically-sound model structure and parametrization for a particular region (Kirchner, 2009) and hence increases the chances of producing more robust predictions in the uncertain future.

**Event-driven solutes export at catchment scale** The proposed event classification framework can be also used for disentangling the variability in the mobilization and delivery of solutes and particulates to the streams during different event conditions (e.g., Karwan et al., 2018). Due to different generation mechanisms events of different types are expected to be responsible for different concentration-discharge patterns (i.e., mobilization or dilution) in the long-term (e.g., Minaudo et al., 2019) and at the event time scale (e.g., Knapp et al., 2020). Therefore, deciphering event type controls on the export patterns of solutes and particulates might help in defining appropriate water quality monitoring and management strategies at the catchment scale.

---

## References

- Aceves-Fernandez, M. A., Ramos-Arreguín, J. M., Pedraza-Ortega, J. C., Sotomayor-Olmedo, A., and Tovar-Arriaga, S. (2012). Finding Trends of Airborne Harmful Pollutants by Using Recurrence Quantification Analysis. *American Journal of Environmental Engineering*, 1(1):10–14.
- Ajami, H., Sharma, A., Band, L. E., Evans, J. P., Tuteja, N. K., Amirthanathan, G. E., and Bari, M. A. (2017). On the non-stationarity of hydrological response in anthropogenically unaffected catchments: an Australian perspective. *Hydrology and Earth System Sciences*, 21(1):281–294.
- Akakike, H. (1974). A new look at the statistical model identification. *IEEE Transactions Automatic Control*, 19:716–723.
- Ala-aho, P., Soulsby, C., Wang, H., and Tetzlaff, D. (2017). Integrated surface-subsurface model to investigate the role of groundwater in headwater catchment runoff generation: A minimalist approach to parameterisation. *Journal of Hydrology*, 547:664–677.
- Alila, Y. and Mtiraoui, A. (2002). Implications of heterogeneous flood-frequency distributions on traditional stream-discharge prediction techniques. *Hydrological Processes*, 16(5):1065–1084.
- Andréassian, V., Parent, E., and Michel, C. (2003). A distribution-free test to detect gradual changes in watershed behavior. *Water Resources Research*, 39(9):1–11.
- Babovic, V. (2005). Data mining in hydrology. *Hydrological Processes*, 19(7):1511–1515.
- Basso, S., Frascati, A., Marani, M., Schirmer, M., and Botter, G. (2015). Climatic and landscape controls on effective discharge. *Geophysical Research Letters*, 42(20):8441–8447.
- Bell, F. C. and Om Kar, S. (1969). Characteristic response times in design flood estimation. *Journal of Hydrology*, 8(2):173–196.
- Berghuijs, W. R., Harrigan, S., Molnar, P., Slater, L. J., and Kirchner, J. W. (2019). The Relative Importance of Different Flood-Generating Mechanisms Across Europe. *Water Resources Research*, 55(6):4582–4593.
- Berghuijs, W. R., Hartmann, A., and Woods, R. A. (2016a). Streamflow sensitivity to water storage changes across Europe. *Geophysical Research Letters*, 43(5):1980–1987.
- Berghuijs, W. R., Woods, R. A., Hutton, C. J., and Sivapalan, M. (2016b). Dominant flood generating mechanisms across the United States. *Geophysical Research Letters*, 43(9):4382–4390.
- Bergström, S. (1995). The HBV model. In Singh, V., editor, *Computer Models of Watershed Hydrology*. Water Resources Publications, Highlands Ranch, Colorado.
- Beurton, S. and Thielen, A. H. (2009). Seasonality of floods in Germany. *Hydrological Sciences Journal*, 54(1):62–76.
- Beven, K. J. and Kirkby, M. J. (1979). A physically based, variable contributing area model of basin hydrology. *Hydrological Sciences Bulletin*, 24(1):43–69.
- Blöschl, G., Hall, J., Parajka, J., Perdigão, R. A., Merz, B., Arheimer, B., Aronica, G. T., Bilibashi, A., Bonacci, O., Borga, M., Čanjevac, I., Castellarin, A., Chirico, G. B., Claps, P., Fiala, K., Frolova, N., Gorbachova, L., Gül, A., Hannaford, J., Harrigan, S., Kireeva, M., Kiss, A., Kjeldsen, T. R., Kohnová, S., Koskela, J. J., Ledvinka, O., Macdonald, N., Mavrova-Guirguinova, M., Mediero, L., Merz, R., Molnar, P., Montanari, A., Murphy, C., Osuch, M., Ovcharuk, V., Radevski, I., Rogger, M., Salinas, J. L., Sauquet, E., Šraj, M., Szolgay, J., Viglione, A., Volpi, E., Wilson, D., Zaimi, K., and Živković, N. (2017). Changing climate shifts timing of European floods. *Science*, 357(6351):588–590.

- Blöschl, G., Nester, T., Komma, J., Parajka, J., and Perdigão, R. A. (2013a). The June 2013 flood in the Upper Danube Basin, and comparisons with the 2002, 1954 and 1899 floods. *Hydrology and Earth System Sciences*, 17(12):5197–5212.
- Blöschl, G., Sivapalan, M., Wagener, T., Viglione, A., and Savenije, H. (2013b). *Runoff Prediction in Ungauged Basins: synthesis across Processes, Places and Scales*. Cambridge University Press, Cambridge, UK.
- Blume, T., Zehe, E., and Bronstert, A. (2007). Rainfall-runoff response, event-based runoff coefficients and hydrograph separation. *Hydrological Sciences Journal*, 52(5):843–862.
- Bonell, M., McDonnell, J. J., Scatena, F. N., Seibert, J., Uhlenbrook, S., and van Lanen, H. A. (2006). HELPing FRIENDs in PUBs: Charting a course for synergies within international water research programmes in gauged and ungauged basins. *Hydrological Processes*, 20(8):1867–1874.
- Brown, G. (2009). A new perspective for information theoretic feature selection. *Journal of Machine Learning Research*, 5(1):49–56.
- Brunner, M. I., Hingray, B., Zappa, M., and Favre, A. C. (2019). Future Trends in the Interdependence Between Flood Peaks and Volumes: Hydro-Climatological Drivers and Uncertainty. *Water Resources Research*, 55(6):4745–4759.
- Brunner, M. I., Sikorska, A. E., Furrer, R., and Favre, A. C. (2018). Uncertainty Assessment of Synthetic Design Hydrographs for Gauged and Ungauged Catchments. *Water Resources Research*, 54(3):1493–1512.
- Budyko, M. (1974). *Climate and Life*. Academic, New York, NY.
- Capell, R., Tetzlaff, D., Hartley, A. J., and Soulsby, C. (2012). Linking metrics of hydrological function and transit times to landscape controls in a heterogeneous mesoscale catchment. *Hydrological Processes*, 26(3):405–420.
- Cerdan, O., Le Bissonnais, Y., Govers, G., Lecomte, V., Van Oost, K., Couturier, A., King, C., and Dubreuil, N. (2004). Scale effect on runoff from experimental plots to catchments in agricultural areas in Normandy. *Journal of Hydrology*, 299(1-2):4–14.
- Chapman, T. (1999). A comparison of algorithms for streamflow recession and baseflow separation. *Hydrological Processes*, 13:701–714.
- Chapman, T. and Maxwell, A. (1996). Baseflow Separation - Comparison of Numerical Methods with Tracer Experiments. In *Hydrology and Water Resources Symposium*, number 96/05, pages 539–545.
- Collischonn, W. and Fan, F. M. (2013). Defining parameters for Eckhardt’s digital baseflow filter. *Hydrological Processes*, 27(18):2614–2622.
- Cullmann, J., Krauß, T., and Philipp, A. (2008). Enhancing flood forecasting with the help of processed based calibration. *Physics and Chemistry of the Earth*, 33(17-18):1111–1116.
- Di Prinzio, M., Castellarin, A., and Toth, E. (2011). Data-driven catchment classification: Application to the pub problem. *Hydrology and Earth System Sciences*, 15(6):1921–1935.
- Diederer, D., Liu, Y., Gouldby, B., Diermanse, F., and Vorogushyn, S. (2019). Stochastic generation of spatially coherent river discharge peaks for continental event-based flood risk assessment. *Natural Hazards and Earth System Sciences*, 19(5):1041–1053.
- Diezig, R. and Weingartner, R. (2007). Hochwasserprozessstypen—schlüssel zur hochwasserabschätzung. *Wasser und Abfall*, 4(1-2):18–26.

- Donnelly, C., Greuell, W., Andersson, J., Gerten, D., Pisacane, G., Roudier, P., and Ludwig, F. (2017). Impacts of climate change on European hydrology at 1.5, 2 and 3 degrees mean global warming above preindustrial level. *Climatic Change*, 143(1-2):13–26.
- dos Santos, J. C. N., de Andrade, E. M., Guerreiro, M. J. S., Medeiros, P. H. A., de Queiroz Palácio, H. A., and de Araújo Neto, J. R. (2016). Effect of dry spells and soil cracking on runoff generation in a semiarid micro watershed under land use change. *Journal of Hydrology*, 541:1057–1066.
- Dumanski, S., Pomeroy, J. W., and Westbrook, C. J. (2015). Hydrological regime changes in a Canadian Prairie basin. *Hydrological Processes*, 29(18):3893–3904.
- Dunne, T. (1978). Field studies of hillslope flow processes. In Kirkby, M., editor, *Hillslope Hydrology*, pages 227–293. John Wiley&Sons.
- DWA (2012). Ermittlung von Hochwasserwahrscheinlichkeiten. Technical Report Merkblatt M-552, Deutscher Verband für Wasser- und Abfallwirtschaft.
- Dyck, S. and Peschke, G. (1995). *Grundlagen der Hydrologie*. VEB Verlag für Bauwesen, Berlin, Germany.
- Eckhardt, K. (2005). How to construct recursive digital filters for baseflow separation. *Hydrological Processes*, 19(2):507–515.
- Engelen, V. V., Batjes, N., and Huting, J. (2005). Harmonized Global Soil Resources Database. Technical report, World Soil Information and Food and Agriculture Organization, Wageningen.
- England, J., Cohn, T., Faber, B., Stedinger, J., Thomas, W.O., J., Veilleux, A., Kiang, J., and Mason, R.R., J. (2018). *Guidelines for Determining Flood Flow Frequency Bulletin 17C*. U.S. Geological Survey, Reston, Virginia.
- Eroglu, D., McRobie, F. H., Ozken, I., Stemler, T., Wyrwoll, K. H., Breitenbach, S. F., Marwan, N., and Kurths, J. (2016). See-saw relationship of the Holocene East Asian-Australian summer monsoon. *Nature Communications*, 7(12929):1–7.
- FAO (2006). World Reference Base for soil resources - A framework for international classification, correlation and communication. Technical Report 103, International Union of Soil Sciences, ISRIC - World Soil Information and Food and Agriculture Organization of the United Nations, Rome.
- Fenicia, F., McDonnell, J. J., and Savenije, H. H. (2008). Learning from model improvement: On the contribution of complementary data to process understanding. *Water Resources Research*, 44(6):1–13.
- Flerchinger, G. N., Lehrsch, G. A., and McCool, D. K. (2004). Freezing and Thawing - Processes. In *Encyclopedia of Soils in the Environment*, volume 4, pages 104–110.
- Frei, S., Lischeid, G., and Fleckenstein, J. H. (2010). Effects of micro-topography on surface-subsurface exchange and runoff generation in a virtual riparian wetland - A modeling study. *Advances in Water Resources*, 33(11):1388–1401.
- Frontier, S. (1976). Étude de la décroissance des valeurs propres dans une analyse en composantes principales: Comparaison avec le moddle du bâton brisé. *Journal of Experimental Marine Biology and Ecology*, 25(1):67–75.
- Gaál, L., Szolgay, J., Kohnová, S., Parajka, J., Merz, R., Viglione, A., and Blöschl, G. (2012). Flood timescales: Understanding the interplay of climate and catchment processes through comparative hydrology. *Water Resources Research*, 48(4):1–21.

- Gosling, S. N., Zaherpour, J., Mount, N. J., Hattermann, F. F., Dankers, R., Arheimer, B., Breuer, L., Ding, J., Haddeland, I., Kumar, R., Kundu, D., Liu, J., van Griensven, A., Veldkamp, T. I., Vetter, T., Wang, X., and Zhang, X. (2017). A comparison of changes in river runoff from multiple global and catchment-scale hydrological models under global warming scenarios of 1 C, 2 C and 3 C. *Climatic Change*, 141(3):577–595.
- Gottschalk, L. and Weingartner, R. (1998). Distribution of peak flow derived from a distribution of rainfall volume and runoff coefficient, and a unit hydrograph. *Journal of Hydrology*, 208(3-4):148–162.
- Graeff, T., Zehe, E., Blume, T., Francke, T., and Schröder, B. (2012). Predicting event response in a nested catchment with generalized linear models and a distributed watershed model. *Hydrological Processes*, 26(24):3749–3769.
- Grayson, R. B., Western, A. W., Chiew, F. H., and Blöschl, G. (1997). Preferred states in spatial soil moisture patterns: Local and nonlocal controls. *Water Resources Research*, 33(12):2897–2908.
- Gumbel, E. (1941). The return period of flood flows. *The Annals of Mathematical Statistics*, 12:163–190.
- Haan, C. (1977). *Statistical Methods in Hydrology*. The Iowa State University Press, Ames, IA.
- Hartigan, J. A. and Wong, M. A. (1979). Algorithm AS 136: A K-Means Clustering Algorithm. *Applied Statistics*, 28(1):100.
- Hartmann, A., Weiler, M., Wagener, T., Lange, J., Kralik, M., Humer, F., Mizyed, N., Rimmer, A., Barberá, J. A., Andreo, B., Butscher, C., and Huggenberger, P. (2013). Process-based karst modelling to relate hydrodynamic and hydrochemical characteristics to system properties. *Hydrology and Earth System Sciences*, 17(8):3505–3521.
- Hewlett, J. D. and Hibbert, A. R. (1967). Factors affecting the response of small watersheds to precipitation in humid areas. In Sopper, W. and Lull, H., editors, *Forest hydrology*, pages 275–290. Pergamon Press, New York.
- Hirschboeck, K., Ely, L., and Maddox, R. (2000). Hydroclimatology of Meteorologic Floods. In *Inland Flood Hazards*, pages 39–72.
- Hirschboeck, K. K. (1987). Hydroclimatically-defined mixed distributions in partial duration flood series. In *Hydrologic Frequency Modeling: Proceedings of the International Symposium on Flood Frequency and Risk Analyses, 14-17 May 1986, Louisiana State University, Baton Rouge, U.S.A.*, pages 199–212.
- Hirschboeck, K. K. (2009). Future Hydroclimatology and the Research Challenges of a Post-Stationary World. *Journal of Contemporary Water Research & Education*, 142(1):4–9.
- Hofstätter, M., Chimani, B., Lexer, A., and Blöschl, G. (2016). A new classification scheme of European cyclone tracks with relevance to precipitation. *Water Resources Research*, 52(9):7086–7104.
- Horton, R. (1933). The role of infiltration in the hydrologic cycle. *Transactions of the AGU*, 14:446–460.
- House, P. K. and Hirschboeck, K. K. (1997). Hydroclimatological and Paleohydrological Context of Extreme Winter Flooding in Arizona, 1993. In *Storm-Induced Geological Hazards: Case Histories From the 1992-1993 Winter Storm in Southern California and Arizona*, Geological Society of America Reviews in Engineering Geology, 11, pages 1–24.
- Hubert, L. and Arabie, P. (1985). Comparing partitions. *Journal of Classification*, 2(1):193–218.

- Institute of Hydrology (1980). Low Flow Studies. Technical Report 2, Institute of Hydrology, Wallingford.
- Jackson, D. A. (1993). Stopping rules in principal components analysis: A comparison of heuristical and statistical approaches. *Ecology*, 74(8):2204–2214.
- James, A. L. and Roulet, N. T. (2007). Investigating hydrologic connectivity and its association with threshold change in runoff response in a temperate forested watershed. *Hydrological Processes*, 21(25):3391–3408.
- James, P. M. (2007). An objective classification method for Hess and Brezowsky Grosswetterlagen over Europe. *Theoretical and Applied Climatology*, 88(1-2):17–42.
- Jankiewicz, P., Neumann, J., Duijnsveld, W. H., Wessolek, G., Wycisk, P., and Hennings, V. (2005). Abflusshöhe - Sickerwasserrate - Grundwasserneubildung - Drei Themen im Hydrologischen Atlas von Deutschland. *Hydrologie und Wasserbewirtschaftung*, 49(1):2–13.
- Jarrett, R. D. and Costa, J. E. (1988). Evaluation of the Flood Hydrology in the Colorado Front Range Using Precipitation, Streamflow, and Paleoflood Data for the Big Thompson River Basin. *United States Geological Survey*, pages 1–37.
- Jencso, K. G., McGlynn, B. L., Gooseff, M. N., Wondzell, S. M., Bencala, K. E., and Marshall, L. A. (2009). Hydrologic connectivity between landscapes and streams: Transferring reach- and plot-scale understanding to the catchment scale. *Water Resources Research*, 45(4):1–16.
- Jobson, J. (1991). *Applied multivariate data analysis. Regression and Experimental Design*. Springer, New York, NY.
- Kader, G. D. and Perry, M. (2007). Variability for categorical variables. *Journal of Statistics Education*, 15(2).
- Kampf, S. K. and Lefsky, M. A. (2016). Transition of dominant peak flow source from snowmelt to rainfall along the Colorado Front Range: Historical patterns, trends, and lessons from the 2013 Colorado Front Range floods. *Water Resources Research*, 52(1):407–422.
- Karwan, D. L., Pizzuto, J. E., Aalto, R., Marquard, J., Harpold, A., Skalak, K., Benthem, A., Levia, D. F., Siegert, C. M., and Aufdenkampe, A. K. (2018). Direct Channel Precipitation and Storm Characteristics Influence Short-Term Fallout Radionuclide Assessment of Sediment Source. *Water Resources Research*, 54(7):4579–4594.
- Keller, L., Rössler, O., Martius, O., and Weingartner, R. (2018). Delineation of flood generating processes and their hydrological response. *Hydrological Processes*, 32(2):228–240.
- Kemter, M., Merz, B., Marwan, N., Vorogushyn, S., and Blöschl, G. (2020). Joint Trends in Flood Magnitudes and Spatial Extents Across Europe. *Geophysical Research Letters*, 47(7):1–8.
- Kendall, M. (1975). *Rank Correlation Methods*. Griffin, London, UK.
- Kendon, E. J., Roberts, N. M., Fowler, H. J., Roberts, M. J., Chan, S. C., and Senior, C. A. (2014). Heavier summer downpours with climate change revealed by weather forecast resolution model. *Nature Climate Change*, 4(7):570–576.
- Kille, K. (1970). Das Verfahren MoMNQr, ein Beitrag zur Berechnung der mittleren langjährigen Grundwasserneubildung mit Hilfe der monatlichen Niedrigwasserabflüsse. *Sonderheft Hydrogeologie Hydrogeochemie*, 89-9.
- Kirchner, J. W. (2009). Catchments as simple dynamical systems: Catchment characterization, rainfall-runoff modeling, and doing hydrology backward. *Water Resources Research*, 45:1–34.



- Knapp, J. L. A., Freyberg, J. V., Studer, B., Kiewiet, L., and Kirchner, J. W. (2020). Concentration-discharge relationships vary among hydrological events, reflecting differences in event characteristics. *Hydrology and Earth System Sciences Discussions*.
- Knoben, W. J., Woods, R. A., and Freer, J. E. (2018). A Quantitative Hydrological Climate Classification Evaluated With Independent Streamflow Data. *Water Resources Research*, 54(7):5088–5109.
- Kohler, M. and Linsley, R. (1951). Predicting the runoff from storm rainfall. *Weather Bureau Research Paper No. 34*.
- Kohonen, T. (2001). *Self-Organizing Maps*. Springer, Berlin, Germany.
- Koskelo, A. I., Fisher, T. R., Utz, R. M., and Jordan, T. E. (2012). A new precipitation-based method of baseflow separation and event identification for small watersheds (<50 km<sup>2</sup>). *Journal of Hydrology*, 450-451:267–278.
- Kumar, R., Livneh, B., and Samaniego, L. (2013). Toward computationally efficient large-scale hydrologic predictions with a multiscale regionalization scheme. *Water Resources Research*, 49(9):5700–5714.
- Kundzewicz, Z. W., Kanae, S., Seneviratne, S. I., Handmer, J., Nicholls, N., Peduzzi, P., Mechler, R., Bouwer, L. M., Arnell, N., Mach, K., Muir-Wood, R., Brakenridge, G. R., Kron, W., Benito, G., Honda, Y., Takahashi, K., and Sherstyukov, B. (2014). Le risque d’inondation et les perspectives de changement climatique mondial et régional. *Hydrological Sciences Journal*, 59(1):1–28.
- Lehner, B., Liermann, C. R., Revenga, C., Vörösmarty, C., Fekete, B., Crouzet, P., Döll, P., Endejan, M., Frenken, K., Magome, J., Nilsson, C., Robertson, J. C., Rödel, R., Sindorf, N., and Wisser, D. (2011). High-resolution mapping of the world’s reservoirs and dams for sustainable river-flow management. *Frontiers in Ecology and the Environment*, 9(9):494–502.
- Ley, R., Casper, M. C., Hellebrand, H., and Merz, R. (2011). Catchment classification by runoff behaviour with self-organizing maps (SOM). *Hydrology and Earth System Sciences*, 15(9):2947–2962.
- Lutz, S. R., Mallucci, S., Diamantini, E., Majone, B., Bellin, A., and Merz, R. (2016). Hydro-climatic and water quality trends across three Mediterranean river basins. *Science of the Total Environment*, 571:1392–1406.
- Marchi, L., Borga, M., Preciso, E., and Gaume, E. (2010). Characterisation of selected extreme flash floods in Europe and implications for flood risk management. *Journal of Hydrology*, 394(1-2):118–133.
- Martin, E. H., Kelleher, C., and Wagener, T. (2012). Has urbanization changed ecological streamflow characteristics in Maine (USA)? *Hydrological Sciences Journal*, 57(7):1337–1354.
- Marwan, N. (2010). How to avoid potential pitfalls in recurrence plot based data analysis. *International Journal of Bifurcation and Chaos*, 21(4):1003–1017.
- Marwan, N., Romano, M., Thiel, M., and Kurths, J. (2007). Recurrence plots for the analysis of complex systems. *Physics Reports*, 438:237–329.
- McDonnell, J. J. (1990). A Rationale for Old Water Discharge Through Macropores in a Steep, Humid Catchment. *Water Resources Research*, 26(11):2821–2832.
- McGlynn, B. L. and McDonnell, J. J. (2003). Quantifying the relative contributions of riparian and hillslope zones to catchment runoff. *Water Resources Research*, 39(11).

- McGlynn, B. L., McDonnell, J. J., Seibert, J., and Kendall, C. (2004). Scale effects on headwater catchment runoff timing, flow sources, and groundwater-streamflow relations. *Water Resources Research*, 40(7):1–14.
- McMillan, H., Westerberg, I., and Branger, F. (2017). Five guidelines for selecting hydrological signatures. *Hydrological Processes*, 31(26):4757–4761.
- Mei, Y. and Anagnostou, E. N. (2015). A hydrograph separation method based on information from rainfall and runoff records. *Journal of Hydrology*, 523:636–649.
- Mei, Y., Anagnostou, E. N., Stampoulis, D., Nikolopoulos, E. I., Borga, M., and Vegara, H. J. (2014). Rainfall organization control on the flood response of mild-slope basins. *Journal of Hydrology*, 510:565–577.
- Merz, B., Aerts, J., Arnbjerg-Nielsen, K., Baldi, M., Becker, A., Bichet, A., Blöschl, G., Bouwer, L. M., Brauer, A., Cioffi, F., Delgado, J. M., Gocht, M., Guzzetti, F., Harrigan, S., Hirschboeck, K., Kilsby, C., Kron, W., Kwon, H. H., Lall, U., Merz, R., Nissen, K., Salvatti, P., Swierczynski, T., Ulbrich, U., Viglione, A., Ward, P. J., Weiler, M., Wilhelm, B., and Nied, M. (2014). Floods and climate: Emerging perspectives for flood risk assessment and management. *Natural Hazards and Earth System Sciences*, 14(7):1921–1942.
- Merz, B., Vorogushyn, S., Uhlemann, S., Delgado, J., and Huntecha, Y. (2012). HESS Opinions: "More efforts and scientific rigour are needed to attribute trends in flood time series". *Hydrology and Earth System Sciences*, 16(5):1379–1387.
- Merz, R. and Blöschl, G. (2003a). A process typology of regional floods. *Water Resources Research*, 39(12):1–20.
- Merz, R. and Blöschl, G. (2003b). Regionalisation of flood risk in Austria. In *Hydrological Risk: recent advances in peak river flow modelling, prediction and real-time forecasting. Assessment of the impacts of land-use and climate changes*, Bologna, Italy.
- Merz, R. and Blöschl, G. (2008a). Flood frequency hydrology: 1. Temporal, spatial, and causal expansion of information. *Water Resources Research*, 44(8):1–17.
- Merz, R. and Blöschl, G. (2008b). Flood frequency hydrology: 2. Combining data evidence. *Water Resources Research*, 44(8):1–16.
- Merz, R. and Blöschl, G. (2009a). A regional analysis of event runoff coefficients with respect to climate and catchment characteristics in Austria. *Water Resources Research*, 45(1):1–19.
- Merz, R. and Blöschl, G. (2009b). Process controls on the statistical flood moments - A data based analysis. *Hydrological Processes*, 23(5):675–696.
- Merz, R., Blöschl, G., and Parajka, J. (2006). Spatio-temporal variability of event runoff coefficients. *Journal of Hydrology*, 331(3-4):591–604.
- Merz, R., Parajka, J., and Blöschl, G. (2011). Time stability of catchment model parameters: Implications for climate impact analyses. *Water Resources Research*, 47(2):1–17.
- Merz, R., Tarasova, L., and Basso, S. (2020). Parameter's Controls of Distributed Catchment Models—How Much Information is in Conventional Catchment Descriptors? *Water Resources Research*, 56(2):1–18.
- Milly, P. C., Betancourt, J., Falkenmark, M., Hirsch, R. M., Kundzewicz, Z. W., Lettenmaier, D. P., and Stouffer, R. J. (2008). Climate change: Stationarity is dead: Whither water management? *Science*, 319(5863):573–574.

- Minaudo, C., Dupas, R., Gascuel-Oudou, C., Roubéix, V., Danis, P. A., and Moatar, F. (2019). Seasonal and event-based concentration-discharge relationships to identify catchment controls on nutrient export regimes. *Advances in Water Resources*, 131.
- Miniussi, A., Marani, M., and Villarini, G. (2020). Metastatistical Extreme Value Distribution applied to floods across the continental United States. *Advances in Water Resources*, 136.
- Mizukami, N., Clark, M. P., Newman, A. J., Wood, A. W., Gutmann, E. D., Nijssen, B., Rakovec, O., and Samaniego, L. (2017). Towards seamless large-domain parameter estimation for hydrologic models. *Water Resources Research*, 53(9):8020–8040.
- Nied, M., Pardowitz, T., Nissen, K., Ulbrich, U., Hundecha, Y., and Merz, B. (2014). On the relationship between hydro-meteorological patterns and flood types. *Journal of Hydrology*, 519:3249–3262.
- Norbiato, D., Borga, M., Merz, R., Blöschl, G., and Carton, A. (2009). Controls on event runoff coefficients in the eastern Italian Alps. *Journal of Hydrology*, 375(3-4):312–325.
- Olden, J. D. and Poff, N. L. (2003). Redundancy and the choice of hydrologic indices for characterizing streamflow regimes. *River Research and Applications*, 19(2):101–121.
- Oudin, L., Hervieu, F., Michel, C., Perrin, C., Andréassian, V., Anctil, F., and Loumagne, C. (2005). Which potential evapotranspiration input for a lumped rainfall-runoff model? Part 2 - Towards a simple and efficient potential evapotranspiration model for rainfall-runoff modelling. *Journal of Hydrology*, 303(1-4):290–306.
- Oudin, L., Kay, A., Andréassian, V., and Perrin, C. (2010). Are seemingly physically similar catchments truly hydrologically similar? *Water Resources Research*, 46(11):1–15.
- Perry, M. and Kader, G. (2005). Variation as unalikeability. *Teaching Statistics*, 27(2):58–60.
- Petrow, T., Zimmer, J., and Merz, B. (2009). Changes in the flood hazard in Germany through changing frequency and persistence of circulation patterns. *Natural Hazards and Earth System Science*, 9(4):1409–1423.
- Pfister, L., Martínez-Carreras, N., Hissler, C., Klaus, J., Carrer, G. E., Stewart, M. K., and McDonnell, J. J. (2017). Bedrock geology controls on catchment storage, mixing, and release: A comparative analysis of 16 nested catchments. *Hydrological Processes*, 31(10):1828–1845.
- Poncelet, C., Merz, R., Merz, B., Parajka, J., Oudin, L., Andréassian, V., and Perrin, C. (2017). Process-based interpretation of conceptual hydrological model performance using a multinational catchment set. *Water Resources Research*, 53(8):7247–7268.
- Potter, W. (1958). Upper and low frequency curves for peak rates of runoff. *Transactions American Geophysical Union*, 39:100–105.
- Rabiei, E. and Haberlandt, U. (2015). Applying bias correction for merging rain gauge and radar data. *Journal of Hydrology*, 522:544–557.
- Rand, W. M. (1971). Objective criteria for the evaluation of clustering methods. *Journal of the American Statistical Association*, 66(336):846–850.
- Rauthe, M., Steiner, H., Riediger, U., Mazurkiewicz, A., and Gratzki, A. (2013). A Central European precipitation climatology - Part I: Generation and validation of a high-resolution gridded daily data set (HYRAS). *Meteorologische Zeitschrift*, 22(3):235–256.
- Razavi, T. and Coulibaly, P. (2013). Classification of Ontario watersheds based on physical attributes and streamflow series. *Journal of Hydrology*, 493:81–94.

- Ries, F., Schmidt, S., Sauter, M., and Lange, J. (2017). Controls on runoff generation along a steep climatic gradient in the Eastern Mediterranean. *Journal of Hydrology: Regional Studies*, 9:18–33.
- Rinderer, M., van Meerveld, H. J., and McGlynn, B. L. (2019). From Points to Patterns: Using Groundwater Time Series Clustering to Investigate Subsurface Hydrological Connectivity and Runoff Source Area Dynamics. *Water Resources Research*, 55(7):5784–5806.
- Rinderer, M., van Meerveld, I., Stähli, M., and Seibert, J. (2016). Is groundwater response timing in a pre-alpine catchment controlled more by topography or by rainfall? *Hydrological Processes*, 30(7):1036–1051.
- Rodríguez-Blanco, M., Taboada-Castro, M., and Taboada-Castro, M. (2012). Rainfall–runoff response and event-based runoff coefficients in a humid area (northwest Spain). *Hydrological Sciences Journal*, 57(3):445–459.
- Rogger, M., Pirkl, H., Viglione, A., Komma, J., Kohl, B., Kirnbauer, R., Merz, R., and Blöschl, G. (2012). Step changes in the flood frequency curve: Process controls. *Water Resources Research*, 48(5):1–15.
- Rogger, M., Viglione, A., Derx, J., and Blöschl, G. (2013). Quantifying effects of catchments storage thresholds on step changes in the flood frequency curve. *Water Resources Research*, 49(10):6946–6958.
- Rousseeuw, P. J. (1987). Silhouettes: A graphical aid to the interpretation and validation of cluster analysis. *Journal of Computational and Applied Mathematics*, 20:53–65.
- Samaniego, L., Kumar, R., and Attinger, S. (2010). Multiscale parameter regionalization of a grid-based hydrologic model at the mesoscale. *Water Resources Research*, 46(5):1–25.
- Sawicz, K., Wagener, T., Sivapalan, M., Troch, P. A., and Carrillo, G. (2011). Catchment classification: Empirical analysis of hydrologic similarity based on catchment function in the eastern USA. *Hydrology and Earth System Sciences*, 15(9):2895–2911.
- Sawicz, K. A., Kelleher, C., Wagener, T., Troch, P., Sivapalan, M., and Carrillo, G. (2014). Characterizing hydrologic change through catchment classification. *Hydrology and Earth System Sciences*, 18(1):273–285.
- Scherrer, S., Naef, F., Faeh, A. O., and Cordery, I. (2006). Formation of runoff at the hillslope scale during intense precipitation. *Hydrology and Earth System Sciences Discussions*, 3(4):2523–2558.
- Seibert, S. P., Jackisch, C., Ehret, U., Pfister, L., and Zehe, E. (2016). Exploring the interplay between state, structure and runoff behaviour of lower mesoscale catchments. *Hydrology and Earth System Sciences Discussions*, pages 1–51.
- Sen, P. (1968). Estimates of the regression coefficient based on Kendall’s tau. *Journal of American Statistical Association*, 63:1379–1389.
- Seo, Y., Schmidt, A. R., and Sivapalan, M. (2012). Effect of storm movement on flood peaks: Analysis framework based on characteristic timescales. *Water Resources Research*, 48(5):1–12.
- Sherman, P. (1932). Streamflow from rainfall by the unit-graph method. *Engineering News Records*, 108:501–505.
- Siebert, S., Henrich, V., Frenken, L., and Burke, J. (2013). Global Map of Irrigation Areas. Technical Report 5, Rheinische Friedrich-Wilhelms-University, Bonn, Germany / Food and Agriculture Organization of the United Nations, Rome, Italy.
- Sikorska, A. E., Viviroli, D., and Seibert, J. (2015). Flood-type classification in mountainous catchments using crisp and fuzzy decision trees. *Water Resources Research*, 51(10):7959–7976.

- Sikorska-Senoner, A. E. and Seibert, J. (2020). Flood-type trend analysis for alpine catchments. *Hydrological Sciences Journal*.
- Sinha, S., Rode, M., and Borchardt, D. (2016). Examining runoff generation processes in the Selke catchment in central Germany: Insights from data and semi-distributed numerical model. *Journal of Hydrology: Regional Studies*, 7:38–54.
- Sivakumar, B. and Singh, V. P. (2012). Hydrologic system complexity and nonlinear dynamic concepts for a catchment classification framework. *Hydrology and Earth System Sciences*, 16(11):4119–4131.
- Sivapalan, M. (2009). The secret to 'doing better hydrological science': Change the question! *Hydrological Processes*, 23(9):1391–1396.
- Sivapalan, M., Blöschl, G., Merz, R., and Gutknecht, D. (2005). Linking flood frequency to long-term water balance: Incorporating effects of seasonality. *Water Resources Research*, 41(6):1–17.
- Slater, L. J. and Wilby, R. L. (2017). Measuring the changing pulse of rivers. *Science*, 357(6351):552.
- Smakhtin, V. U. (2001). Low flow hydrology: A review. *Journal of Hydrology*, 240(3-4):147–186.
- Smith, J. A., Cox, A. A., Baeck, M. L., Yang, L., and Bates, P. (2018). Strange Floods: The Upper Tail of Flood Peaks in the United States. *Water Resources Research*, 54(9):6510–6542.
- Soulsby, C., Neal, C., Laudon, H., Burns, D. A., Merot, P., Bonell, M., Dunn, S. M., and Tetzlaff, D. (2008). Catchment data for process conceptualization: simply not enough? *Hydrological Processes*, 22(12):2057–2061.
- Ssegane, H., Tollner, E. W., Mohamoud, Y. M., Rasmussen, T. C., and Dowd, J. F. (2012a). Advances in variable selection methods I: Causal selection methods versus stepwise regression and principal component analysis on data of known and unknown functional relationships. *Journal of Hydrology*, 438-439:16–25.
- Ssegane, H., Tollner, E. W., Mohamoud, Y. M., Rasmussen, T. C., and Dowd, J. F. (2012b). Advances in variable selection methods II: Effect of variable selection method on classification of hydrologically similar watersheds in three Mid-Atlantic ecoregions. *Journal of Hydrology*, 438-439:26–38.
- Stein, L., Pianosi, F., and Woods, R. (2019). Event-based classification for global study of river flood generating processes. *Hydrological Processes*, pages 1514–1529.
- Stieglitz, M., Shaman, J., McNamara, J., Engel, V., Shanley, J., and Kling, G. W. (2003). An approach to understanding hydrologic connectivity on the hillslope and the implications for nutrient transport. *Global Biogeochemical Cycles*, 17(4).
- Struthers, I. and Sivapalan, M. (2007). A conceptual investigation of process controls upon flood frequency: Role of thresholds. *Hydrology and Earth System Sciences*, 11(4):1405–1416.
- Su, C.-H., Costelloe, J. F., Peterson, T. J., and Western, A. W. (2016). On the structural limitations of recursive digital filters for base flow estimation. *Water Resources Research*, 52(6):4745–4764.
- Tang, W. and Carey, S. K. (2017). HydRun: A MATLAB toolbox for rainfall–runoff analysis. *Hydrological Processes*, 31(15):2670–2682.
- Tarasova, L., Basso, S., Poncelet, C., and Merz, R. (2018a). Exploring Controls on Rainfall-Runoff Events: 2. Regional Patterns and Spatial Controls of Event Characteristics in Germany. *Water Resources Research*, 54(10):7688–7710.

- Tarasova, L., Basso, S., Wendi, D., Viglione, A., Kumar, R., and Merz, R. (2020). A Process-Based Framework to Characterize and Classify Runoff Events: The Event Typology of Germany. *Water Resources Research*, 56(5):1–24.
- Tarasova, L., Basso, S., Zink, M., and Merz, R. (2018b). Exploring Controls on Rainfall-Runoff Events: 1. Time Series-Based Event Separation and Temporal Dynamics of Event Runoff Response in Germany. *Water Resources Research*, 54(10):7711–7732.
- Tarasova, L., Merz, R., Kiss, A., Basso, S., Blöschl, G., Merz, B., Viglione, A., Plötner, S., Guse, B., Schumann, A., Fischer, S., Ahrens, B., Anwar, F., Bárdossy, A., Bühler, P., Haberlandt, U., Kreibich, H., Krug, A., Lun, D., Müller-Thomy, H., Pidoto, R., Primo, C., Seidel, J., Vorogushyn, S., and Wietzke, L. (2019). Causative classification of river flood events. *Wiley Interdisciplinary Reviews: Water*, 6(4):e1353.
- Tetzlaff, D., Carey, S. K., McNamara, J. P., Laudon, H., and Soulsby, C. (2017). The essential value of long-term experimental data for hydrology and water management. *Water Resources Research*, 53(4):2598–2604.
- Tromp-Van Meerveld, H. J. and McDonnell, J. J. (2006). Threshold relations in subsurface stormflow: 2. The fill and spill hypothesis. *Water Resources Research*, 42(2):1–11.
- Trudeau, M. and Richardson, M. (2015). Change in event-scale hydrologic response in two urbanizing watersheds of the Great Lakes St Lawrence Basin 1969–2010. *Journal of Hydrology*, 527:1174–1188.
- Turkington, T., Breinl, K., Ettema, J., Alkema, D., and Jetten, V. (2016). A new flood type classification method for use in climate change impact studies. *Weather and Climate Extremes*, 14:1–16.
- van Loon, A. F. and van Lanen, H. A. J. (2012). A process-based typology of hydrological drought. *Hydrology and Earth System Sciences*, 16:1915–1946.
- Viglione, A., Chirico, G. B., Komma, J., Woods, R., Borga, M., and Blöschl, G. (2010a). Quantifying space-time dynamics of flood event types. *Journal of Hydrology*, 394(1-2):213–229.
- Viglione, A., Chirico, G. B., Woods, R., and Blöschl, G. (2010b). Generalised synthesis of space-time variability in flood response: An analytical framework. *Journal of Hydrology*, 394(1-2):198–212.
- Viglione, A., Parajka, J., Rogger, M., Salinas, J. L., Laaha, G., Sivapalan, M., and Blöschl, G. (2013). Comparative assessment of predictions in ungauged basins - Part 3: Runoff signatures in Austria. *Hydrology and Earth System Sciences*, 17(6):2263–2279.
- Villarini, G. and Smith, J. A. (2010). Flood peak distributions for the eastern United States. *Water Resources Research*, 46(6):1–17.
- Vivoni, E. R., Entekhabi, D., Bras, R. L., and Ivanov, V. Y. (2007). Controls on runoff generation and scale-dependence in a distributed hydrologic model. *Hydrology and Earth System Sciences*, 11(5):1683–1701.
- Vogel, R. M. and Kroll, C. N. (1992). Regional geohydrologic-geomorphic relationships for the estimation of low-flow statistics. *Water Resources Research*, 28(9):2451–2458.
- Von Freyberg, J., Radny, D., Gall, H. E., and Schirmer, M. (2014). Implications of hydrologic connectivity between hillslopes and riparian zones on streamflow composition. *Journal of Contaminant Hydrology*, 169:62–74.

- Vormoor, K., Lawrence, D., Heistermann, M., and Bronstert, A. (2015). Climate change impacts on the seasonality and generation processes of floods – Projections and uncertainties for catchments with mixed snowmelt/rainfall regimes. *Hydrology and Earth System Sciences*, 19(2):913–931.
- Wagener, T., Sivapalan, M., Troch, P., and Woods, R. (2007). Catchment Classification and Hydrologic Similarity. *Geography Compass*, 1(4):901–931.
- Weiler, M. and McDonnell, J. (2004). Virtual experiments: A new approach for improving process conceptualization in hillslope hydrology. *Journal of Hydrology*, 285(1-4):3–18.
- Wendi, D., Merz, B., and Marwan, N. (2019). Assessing Hydrograph Similarity and Rare Runoff Dynamics by Cross Recurrence Plots. *Water Resource Research*, 55:1–23.
- Western, A. W., Zhou, S. L., Grayson, R. B., McMahon, T. A., Blöschl, G., and Wilson, D. J. (2004). Spatial correlation of soil moisture in small catchments and its relationship to dominant spatial hydrological processes. *Journal of Hydrology*, 286(1-4):113–134.
- Wittenberg, H. (1999). Baseflow recession and recharge as nonlinear storage processes. *Hydrological Processes*, 13(5):715–726.
- WMO (2008). Manual on Low-flow Estimation and Prediction. Technical Report 1029, World Meteorological Organization.
- Woods, R. and Sivapalan, M. (1999). A synthesis of space-time variability in storm response: Rainfall, runoff generation, and routing. *Water Resources Research*, 35(8):2469–2485.
- Ye, S., Li, H. Y., Huang, M., Ali, M., Leng, G., Leung, L. R., wen Wang, S., and Sivapalan, M. (2014). Regionalization of subsurface stormflow parameters of hydrologic models: Derivation from regional analysis of streamflow recession curves. *Journal of Hydrology*, 519:670–682.
- Yue, S., Pilon, P., Phinney, B., and Cavadias, G. (2002). The influence of autocorrelation on the ability to detect trend in hydrological series. *Hydrological Processes*, 16:1807–1829.
- Zehe, E. and Blöschl, G. (2004). Predictability of hydrologic response at the plot and catchment scales: Role of initial conditions. *Water Resources Research*, 40(10):1–21.
- Zehe, E. and Sivapalan, M. (2009). Threshold behaviour in hydrological systems as (human) geo-ecosystems: Manifestations, controls, implications. *Hydrology and Earth System Sciences*, 13(7):1273–1297.
- Zink, M., Kumar, R., Cuntz, M., and Samaniego, L. (2017). A high-resolution dataset of water fluxes and states for Germany accounting for parametric uncertainty. *Hydrology and Earth System Sciences*, 21(3):1769–1790.
- Zorzetto, E., Botter, G., and Marani, M. (2016). On the emergence of rainfall extremes from ordinary events. *Geophysical Research Letters*, 43(15):8076–8082.





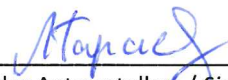
**Eidesstattliche Erklärung / Declaration under Oath**

Ich erkläre an Eides statt, dass ich die Arbeit selbstständig und ohne fremde Hilfe verfasst, keine anderen als die von mir angegebenen Quellen und Hilfsmittel benutzt und die den benutzten Werken wörtlich oder inhaltlich entnommenen Stellen als solche kenntlich gemacht habe.

*I declare under penalty of perjury that this thesis is my own work entirely and has been written without any help from other people. I used only the sources mentioned and included all the citations correctly both in word or content.*

13.05.2020

Datum / Date



Unterschrift des Antragstellers / Signature of the applicant



# Larisa Tarasova

## *Curriculum Vitae*

### Personal Data

Date of Birth 29.06.1990  
Place of Birth Kalinin, USSR  
Sex Female  
Citizenship Russian

### Work Experience

April 2016–present **Doctoral Researcher**,  
*Department Catchment Hydrology, Helmholtz Centre for Environmental Research – UFZ, Halle (Saale), Germany.*

April 2015–March 2016 **Student Assistant**,  
*Department Catchment Hydrology, Helmholtz Centre for Environmental Research – UFZ, Halle (Saale), Germany.*

October 2014–July 2015 **Tutor**,  
*Faculty of Civil Engineering and Geodetic Science, Leibniz University of Hannover, Hannover, Germany.*

September 2009–June 2010 **Student Assistant**,  
*Department of Inorganic Chemistry, Peoples' Friendship University of Russia, Moscow, Russia.*

### Education and Training

October 2013– **M.Sc. in Water Resources and Environmental Management**,  
*Faculty of Civil Engineering and Geodetic Science, Leibniz University of Hannover, Hannover, Germany.*

September 2015 **Master thesis**: Hydrological modeling in the data-scarce glacierized catchment of the Gunt River, Tajik Pamir

September 2012–June 2013 **Chinese studies**,  
*Xiamen University; Nanjing Normal University, China.*

September 2007–June 2012 **B.Sc. in Ecology and Environmental Engineering,**  
*Peoples' Friendship University of Russia, Moscow, Russia.*

2012 **Bachelor thesis:** Prediction of water mineralization in the Dalai Lake (China) under different water use scenarios

June–July 2011 **Internship,**  
*Ivankovskaya Research Laboratory, Institute of Water Problems, Russian Academy of Science, Moscow, Russia.*

September 2000–June 2007 **Secondary and High School Diploma,**  
*Mathematics Secondary and High School #17, Tver, Russia.*

## Skills

Languages English | Proficient  
 German | Proficient  
 Chinese | Intermediate  
 Russian | Mother tongue

Programming R, MATLAB  
 GIS ArcGIS  
 Writing LaTeX

## Scientific Publications

**Tarasova, L.,** Basso, S., Wendi, D., Viglione, A., Kumar, R., Merz, R. (2020): A Process-Based Framework to Characterize and Classify Runoff Events: the Event Typology of Germany, *Water Resour. Res.*, 56(5)

Merz, R., **Tarasova, L.,** Basso, S., (2020): Parameter's controls of distributed catchment models – How much information is in conventional catchment descriptors?, *Water Resour. Res.*, 56(2)

**Tarasova, L.,** Merz, R., Kiss, A., Basso, S., Blöschl, G., Merz, B., Viglione, A., Plötner, S., Guse, B., Schumann, A., Fischer, S., Ahrens, B., Anwar, F., Bárdossy, A., Bühler, P., Haberlandt, U., Kreibich, H., Krug, A., Lun, D., Müller-Thomy, H., Pidoto, R., Primo, C., Seidel, J., Vorogushyn, S., Wietzke, L., (2019): Causative classification of river flood events, *Wiley Interdiscip. Rev.-Water* 6 (4)

**Tarasova, L.,** Basso, S., Zink, M., Merz, R., (2018): Exploring controls on rainfall-runoff events: 1. Time-series-based event separation and temporal dynamics of event runoff response in Germany, *Water Resour. Res.*, 54(10)

**Tarasova, L.,** Basso, S., Poncelet, C., Merz, R., (2018): Exploring controls on rainfall-runoff events: 2. Regional patterns and spatial controls of event characteristics in Germany, *Water Resour. Res.*, 54(10)

Müller, C., Musolff, A., Strachauer, U., Brauns, M., **Tarasova, L.**, Merz, R., Knöller, K., (2018): Tomography of anthropogenic nitrate contribution along a mesoscale river, *Sci. Total Environ.* 615, 773 - 783

**Tarasova, L.**, Knoche, M., Dietrich, J., Merz, R., (2016): Effects of input discretization, model complexity, and calibration strategy on model performance in a data-scarce glacierized catchment in Central Asia, *Water Resour. Res.* 52 (6)

Polyakova, I.N., Egorova, O.A., Sergienko, V.S., **Tarasova, L.**, Davydov, V.V., (2011). Crystal and molecular structure of 2-[(4-nitrophenyl)carbonyl]cyclohex-1-ene-1-yl 4-nitrobenzoate. *Crystallography Reports*, 56: 270

---

## Oral Presentations

- Joint Workshop on Event Identification and Characterization, TU Wien, Vienna, Austria, 2018
- SYSTEM-RISK Conference, Potsdam, 2019

---

## Poster Presentations

- EGU, Vienna, Austria, 2019, 2017
- Gordon Seminar and Conference, New Hampshire, USA, 2019
- IUGG, Montreal, Canada, 2019
- HIGRADE Conference, Leipzig, 2019
- Tag der Hydrologie, Dresden, 2018

---

## Awards

- 2018 WRR Editors' Choice Award for paper Tarasova et al. "Exploring controls on rainfall-runoff events: 2. Regional patterns and spatial controls of event characteristics in Germany"
- Top Downloaded Paper Award 2018-2019 for paper Tarasova et al. "Causative classification of river flood events"
- Best Poster Award (3<sup>rd</sup> Prize), HIGRADE Conference, Leipzig, 2019
- President's Award for Talented Youth (Moscow, 2006; 2007)
- Russian National Contest in Ecology, Winner (2004, 2005, 2006, 2007)
- International Award for Young Scientists (Saint Petersburg, 2006)

Halle, 13.05.2020 